

**REFINERY WASTEWATER TREATMENT AND  
VALUE ADDITION USING *RHODOCOCCUS  
OPACUS*- A HYDROCARBONCLASTIC  
OLEAGINOUS BACTERIUM**

*A Thesis*

*Submitted in partial fulfillment of the requirement for the degree of*

**DOCTOR OF PHILOSOPHY**

by

**Tanushree Paul**



**Centre for the Environment  
Indian Institute of Technology Guwahati  
Guwahati 781039, Assam, India.**

**February 2021**

***Dedicated to My Parents and  
My Grand Parents***



# Indian Institute of Technology Guwahati

## Centre for the Environment



### Statement

I, hereby declare that the content embodied in this thesis entitled “Refinery wastewater treatment and value addition using *Rhodococcus opacus*-a hydrocarbonoclastic oleaginous bacterium” is the result of investigations carried out by me at the Centre for the Environment, Indian Institute of Technology Guwahati, Guwahati, India, under the supervision of **Professor Kannan Pakshirajan Sir (Supervisor)** and **Professor G. Pugazhenti Sir (Supervisor)**.

In keeping with the general practice of reporting scientific observations, due acknowledgements have been made wherever the work described is based on the findings of other investigators.

Tanushree Paul.

Date: 16<sup>th</sup> February 2021

Tanushree Paul

**Indian Institute of Technology Guwahati**  
**Centre for the Environment**



**Certificate**

It is certified that the work described in this thesis entitled “Refinery wastewater treatment and value addition using *Rhodococcus opacus*-a hydrocarbonoclastic oleaginous bacterium” by Tanushree Paul for the award of degree of Doctor of Philosophy is an authentic record of the results obtained from the research work carried out under our supervision at the Centre for the Environment, Indian Institute of Technology Guwahati, Guwahati, India, and this work has not been submitted elsewhere for any degree.

**Dr. Kannan Pakshirajan**

Professor

(Thesis Supervisor)

Department of Biosciences  
and Bioengineering

IIT Guwahati, Guwahati 781039

Assam, India

**Dr. G. Pugazhenth**

Professor

(Thesis Supervisor)

Department of Chemical  
Engineering

IIT Guwahati, Guwahati 781039

Assam, India

## Acknowledgements

There are no words to express my gratitude towards the two most important persons in my life, my pillar of strength and support, to whom this thesis is dedicated, my parents. I really want to express my heartfelt gratitude to my Grandparents, who always believed my true potential. I want to thank Almighty, as I feel blessed to have such wonderful and supportive guardian. I thank God for providing me the courage, health and well-being to perform the task during my entire thesis work.

I would like to express my sincere gratitude to my research supervisors, **Professor Kannan Pakshirajan Sir** (Department of Biosciences and Bioengineering, IIT Guwahati) and **Professor G. Pugazhenti Sir** (Department of Chemical Engineering, IIT Guwahati) for their constant motivation, support, trust and efforts for designing my work. Their constant encouraging words, guidance and faith on me helped me to complete my research work. I am blessed to be a part of their research group. I really feel, valuable suggestions and guidance is the key that drives a researcher to proceed towards the right direction and follow the correct path. Words are not enough to show my gratitude towards Professor Kannan Pakshirajan Sir, for giving me this opportunity and trusting my capabilities, without whom this PhD work would have been certainly impossible.

I would also like to extend my gratitude to my Doctoral committee members. **Dr. Senthilkumar Sivaprakasam Sir** (Chairman, Doctoral committee), **Professor Chandan Das Sir** (member) and **Professor Ajaikumar B. Kunmakkara Sir** (member). Their constructive criticism has always helped me to improve my work and proceed towards the right direction, pertaining to the PhD thesis. I would also like to thank present Head of the Centre for the Environment Professor Mihir Kumar Purkait Sir and past HoC's Professor Gopal Das Sir and Professor Vikash Kumar Dubey Sir, who always helped me during my

initial days of my PhD, under whose administration I was able to carry out my research work in a collegial environment.

I owe my sincere thanks to Centre for the Environment, Department of Biosciences and Bioengineering, Department of Chemical Engineering and Central Instrument Facility, IIT Guwahati for providing the necessary facilities to fulfill the PhD thesis objectives.

I would also like to acknowledge Professor S. K. Deb (Department of Civil Engineering) for his constant support and encouragement during my entire PhD work which really kept me motivated.

I am grateful to each and every member of the interview panel for selecting me during my PhD interview (2015). I would also like to acknowledge technical officers of the centre for the Environment Partha Protim Bakal Sir, Deepmoni Deka ma'am and all the staff members (Mr. Rajiv Kumar Gogoi, Mr. Kaustubh Rakshit, Mr. Mridul Das) for their healthy support in this endeavour.

I am thankful to my seniors Dr. M. Gopi Kiran, Dr. Arindam Sinharoy and Dr. Lalit Goswami, who taught me important aspects during my PhD tenure. I would also like to thank Dr. Divya Baskaran and Dr. Arnab Ghosh for their constant support and help. My heartfelt thanks to the past and present lab members Dr. Madhavi Singh, Dr. Vibha Sinha, Dr. Tejas Namboodiri, Mr. Arun Sakthivel, Dr. Arul Manikandan, Miss Kakali Goswami, Miss Preeti Singh, Mr. Iyyappan J, Mr. Ajaykumar Venugopal, Mr. Dipak Kumar Kanaujiya and Mr. Manoj Kumar.

I really acknowledge MHRD and our institute for providing fellowship throughout the PhD program. Special thanks to the academic people, library facilities, computer center, centre staff and Core I-IV people for their necessary support in every aspect. I would also like

to thank each and every website from where I have acquired beneficial information. Also, I would like to acknowledge all the staff members, security bhaiyya and didi, hospital facilities, mess, general stores and all kinds of campus facilities for their friendly and kind support throughout my stay in the campus. I cannot thank enough to my batch mates (July-2015) whose support and help made my stay in the campus comfortable and friendly.

I would also like to pay gratitude to each and everyone who supported me (knowingly and unknowingly) in completing this work. I am grateful to The Lord Maa Kamakhya and Lord Jagannath for blessing me and giving me enough strength to overcome the difficult and challenging situations throughout these years of hard work.

Date: 16<sup>th</sup> February 2021

Tanushree Paul

**Abstract**

Petroleum refineries generate a huge amount of wastewater containing recalcitrant hydrocarbons which needs to be treated before it could be discharged into the environment. In addition to hydrocarbons, other major pollutants present in the wastewater are sulfides, phenols etc. It may also contain some hemotoxic, teratogenic and carcinogenic compounds like BTEX and PAH which are considered as recalcitrant and highly toxic. Also, due to the expected depletion of fossil fuel sources in the near future, increasing attention is paid to the development of alternative sources of energy.

The main objective of this study is treatment of refinery wastewater and value addition using *Rhodococcus opacus*, which is based on its capability to degrade complex hydrocarbons and accumulate lipids inside. Initial experiments were carried out with *R. opacus* to optimize the different parameters involved in treating the wastewater. The effect of three media constituents viz.  $\text{NH}_4\text{Cl}$ ,  $\text{KH}_2\text{PO}_4$ , and  $\text{Na}_2\text{HPO}_4$  and three physicochemical parameters i.e., pH, agitation and temperature on refinery wastewater treatment by *R. opacus* were studied employing Plackett Burman experimental design. From the obtained results, it was observed that variation in the levels of these parameters did not show any significant effect on the wastewater treatment efficiency indicating the robust nature of *R. opacus* in treating the wastewater.

Following the optimization study, experiments using batch shake flasks were performed for utilizing refinery wastewater containing complex hydrocarbons as the sole substrate for lipid-rich biomass production by *Rhodococcus*. The effect of different initial chemical oxygen demand (COD) concentrations of the wastewater in the range  $2.5\text{-}4.5\text{ g L}^{-1}$  was examined on biomass growth, COD utilization, and lipid production by *R. opacus*. Almost complete utilization (96.8%) of COD present in the wastewater was achieved for an initial COD concentration of  $2.5\text{ g L}^{-1}$  and the value decreased to 90% and 75% for  $3.5\text{ g L}^{-1}$  and  $4.5\text{ g L}^{-1}$  COD concentrations, respectively. Moreover, a maximum lipid production of  $1.3\text{ g L}^{-1}$  was obtained for an initial COD concentration of  $3.5\text{ g L}^{-1}$ . The results of COD utilization by the bacterium were further fitted to substrate utilization kinetic models reported in the literature, which matched well with the Logistic model. Modified Gompertz model best fitted the kinetic data on biomass growth and lipid production by the bacterium. Whereas *R. opacus* biomass-specific growth was found to be inhibited at a high COD concentration of the wastewater, the

Haldane model predicted the experimental specific growth rate values with a very high determination of coefficient ( $R^2$ ) value of more than 0.99. All these results suggest that refinery wastewater can serve as the sole substrate for lipid-rich biomass production by *R. opacus*, thereby adding value to the wastewater treatment process.

Refinery wastewater treatment and lipid-rich biomass production by *R. opacus* were then carried out using a bioreactor operated under different modes batch, fed-batch and sequential batch (SBR). A maximum biomass concentration of  $1.5 \text{ g L}^{-1}$  along with a high lipid accumulation of  $0.83 \text{ g L}^{-1}$  (55%, w/w) of biomass obtained in the batch bioreactor experiments. Moreover, a maximum COD removal of 86% was achieved in the batch experiments confirming that *R. opacus* could efficiently degrade the toxic hydrocarbons present in refinery wastewater for its metabolism and growth. In fed-batch experiments with the bioreactor, the maximum biomass growth, COD removal and lipid accumulation values were  $2.3 \text{ g L}^{-1}$ , 95%, and  $1.8 \text{ g L}^{-1}$ , respectively. Approximately, 78% (w/w) of lipids were accumulated in *R. opacus* biomass under the fed-batch operation mode, which is higher than the value obtained in the batch bioreactor experiments. In SBR mode of operation performed for a total cycle period of 18 h (HRT) the maximum biomass concentration, lipid production, and COD removal efficiency values were  $1.87 \text{ g L}^{-1}$ ,  $1.23 \text{ g L}^{-1}$  (66% w/w), and 87 %, respectively.

Under continuous (CSTR) operating mode of the bioreactor at different hydraulic retention time (HRT) (8, 16 and 24 h), more than 95% of COD was removed for an optimum HRT of 16 h (dilution rate  $0.06 \text{ h}^{-1}$ ). Maximum accumulated lipid content in the biomass of  $1.1 \text{ g L}^{-1}$  (64%, w/w),  $2.35 \text{ g L}^{-1}$  (81%, w/w), and  $2.16 \text{ g L}^{-1}$  (80%, w/w) were obtained at 8, 16, and 24 h HRT, respectively.

A bubble column reactor (BCR) with *R. opacus* was studied for producing lipid-rich biomass using refinery wastewater as the substrate under different HRTs viz. 48h, 24h, 16h, and 12h HRT. During the continuous wastewater treatment using BCR, a very high chemical oxygen demand (COD) removal efficiency of 97% was obtained along with  $2.4 \text{ g L}^{-1}$  of biomass and  $1.33 \text{ g L}^{-1}$  lipid yield in 48h HRT. The biomass concentration was minimum ( $1.26 \text{ g L}^{-1}$ ) at 12 h HRT and the lipid concentration was observed to be 1.33, 1.1, 0.91,  $0.79 \text{ g L}^{-1}$  at 48h, 24h, 16h, and 12h HRT, respectively.

Bioreactor operated under continuous mode with cell-recycle using a tubular ceramic membrane was evaluated in this study. The tubular ceramic membrane for cell separation

and recycle, was prepared locally available inorganic precursors. Thus, a novel strategy involving continuous bioreactor operation with cell recycle for refinery wastewater treatment and water reuse was demonstrated. The continuous cell recycle system proved efficient in terms of complete removal of chemical oxygen demand (COD) (99%) and high lipid production (86%, w/w) at a hydraulic retention time (HRT) of 16 h (dilution rate of  $0.06 \text{ h}^{-1}$ ). Toxicity assessment of the permeate water carried out following three different methods, viz. seed germination, brine shrimp lethality and MTT assays established reuse potential of the treated wastewater. By performing seed germination assay, a GI of 73.63% with the permeate water obtained following the cell recycle step proved that the treated wastewater is free from any harmful phyto-toxic agents. The results of brine shrimp lethality assay as well correlated with the results of toxicity assessment by seed germination assay. However, the results of MTT assay were inconsistent and found to be invalid for wastewater toxicity assessment. Similar to the results of toxicity assessment of treated wastewater using continuous bioreactor with cell recycle, the treated water from the two-stage STMBR showed a high GI value of 82.02%.

A novel strategy involving two-stage submerged tubular membrane bioreactor (STMBR) was effectively employed for COD removal from refinery wastewater. The membrane performance was evaluated on the basis of flux, COD removal along with biomass growth as well as lipid accumulation inside the bioreactor. Characteristics of the foulants formed during the membrane operation were analyzed in order to gain insight into the membrane fouling phenomenon and its role in improving the process efficiency. The results of continuous experiments with the STMBR carried out at 16 HRT revealed a maximum COD removal of 84% was achieved with an average flux of  $0.4 \times 10^{-3} \text{ m}^3/\text{m}^2\text{s}$ . In order to further enhance the COD removal efficiency, two STMBRs were connected in series for treatment which yielded complete COD removal along with  $2.98 \text{ g L}^{-1}$  biomass growth and  $2.3 \text{ g L}^{-1}$  lipid concentration.

Finally, response surface method was employed to examine and optimize hydrothermal liquefaction of lipid-rich *R. opacus* biomass for bio-oil production. A maximum bio-oil yield of 25.53% (w/w) was obtained at 215 °C temperature, 125 minutes treatment time, and 0.25 biomass/water ratio. The bio-oil had a high heating value (HHV) of 20.73 MJ/Kg and contained a very low amount of water-soluble products. Gas chromatography-mass spectroscopy (GC-MS) analysis of the bio-oil

revealed the presence of a variety of compounds, mainly aldehydes, ketones, and fatty acid, whereas the water-soluble product contained mainly alcohols and phenolic compounds. Further analysis of the aqueous phase obtained as a byproduct revealed its potential for reuse as a supplement for microbial growth owing to the presence of nutritional compounds. FTIR spectra of bio-oil revealed the presence of C-H bonds due to alkanes as the predominant functional group present in the product.

This study thus demonstrated that the lipid-rich *R. opacus* biomass grown on cheaply available refinery wastewater is highly suited for potential bio-oil production. Moreover, novel strategies based on bioreactor and its operations, biomass separation using low-cost ceramic membrane, refinery wastewater treatment and bio-oil production as well as water reuse potential were developed in this work.



---

Abstract.....	i
Contents.....	v
List of Tables.....	xi
List of Figures.....	xiii
Abbreviations.....	xviii
1. INTRODUCTION	
1.1. Oleaginous bacteria and bio-oil production .....	2
1.2. Zero waste closed-loop bio-refinery .....	4
2. LITERATURE REVIEW	
2.1. Petroleum refinery configuration.....	6
2.2. Petroleum refinery wastewater (PRWW) treatment.....	12
2.2.1. Primary treatment .....	12
2.2.2. Secondary treatment.....	13
2.2.3. Tertiary treatment.....	13
2.3. Advanced methods for PRWW treatment.....	14
2.3.1. Advanced oxidation.....	14
2.3.2. Electrochemical .....	14
2.3.3. Electro-coagulation.....	15
2.3.4. Other processes.....	16
2.4. Bioreactor systems for PRWW treatment.....	18
2.4.1. Fixed-film bioreactor.....	20
2.4.2. Airlift bioreactor.....	22
2.4.3. Up-flow anaerobic sludge blanket (UASB) bioreactor.....	22
2.4.4. Fluidized bed bioreactor (FBB).....	23

---

2.4.5. Continuous stirred tank bioreactor (CSTR).....	24
2.4.6. Sequencing batch reactor (SBR).....	24
2.5. Advanced membrane bioreactor systems for PRWW treatment.....	26
2.5.1. Integrated membrane bioreactor (MBR).....	26
2.5.2. Submerged membrane bioreactor (SMBR).....	26
2.5.3. Membrane bioreactor (MBR).....	31
2.6. Toxicity assessment.....	33
2.6.1. Cyto-toxicity assays.....	35
2.6.1.1. Minimal essential medium (MEM) elution assay.....	35
2.6.1.2. Colony formation assay (CFA).....	36
2.6.1.3. Hen's egg test-chorioallantoic membrane test (HET-CAM).....	37
2.6.1.4. MTT assay.....	39
2.6.1.5. Brine shrimp lethality assay (BSLA).....	40
2.6.2. Phytotoxicity assay.....	41
2.7. Biomass for bio-oil production.....	41
2.7.1. Lignocellulosic biomass.....	42
2.7.2. Waste biomass.....	42
2.7.3. Oleaginous microorganisms.....	42
2.8. Oleaginous microorganisms.....	43
2.8.1. Composition of oleaginous biomass.....	44
2.8.2. Types of oleaginous microorganisms.....	48
2.8.2.1. Algae.....	51
2.8.2.2. Bacteria.....	52
2.8.2.3. Yeasts.....	54
2.8.2.4. Fungi.....	55

2.9. Bio-oil production technologies.....	56
2.9.1. Thermo-chemical .....	56
2.9.2. Pyrolysis.....	57
2.9.3. Hydrothermal liquefaction (HTL) .....	58
2.9.4. Effect of process parameters on bio-oil yield by HTL.....	63
2.9.4.1. Temperature.....	63
2.9.4.2. Reaction time.....	63
2.9.4.3. Feedstock and biomass/water ratio.....	64
2.9.4.4. Catalysts.....	65
2.10. HTL based bio-refinery.....	66
2.10.1. Types of bio-refinery.....	68
2.11. Aim and objectives.....	69
3. MATERIALS AND METHODS	
3.1. Chemicals and reagents.....	72
3.2. Feasibility of PRWW treatment using <i>R. opacus</i> .....	72
3.2.1. Wastewater collection and characterization.....	72
3.2.2. <i>Rhodococcus opacus</i> and seed culture cultivation.....	73
3.2.3. Batch shake flask experiments.....	74
3.3. Effect of different factors on PRWW treatment .....	75
3.3.1. Effect of different factors on lipid-rich biomass production from refinery wastewater.....	75
3.4. Effect of different COD concentration on biomass growth, lipid production and kinetic modelling.....	76
3.4.1. Kinetics of wastewater COD utilization, biomass growth and lipid production.....	76

3.4.2. Kinetics of COD inhibition on biomass growth .....	80
3.5. Performance evaluation of a continuously stirred tank reactor (CSTR) for PRWW treatment and lipid-rich biomass production under different operation modes....	81
3.6. Performance evaluation of a bubble column reactor (BCR) for PRWW treatment and lipid-rich biomass production .....	86
3.7. Performance evaluation of submerged tubular membrane bioreactor (STMBR) for PRWW treatment and lipid-rich biomass production by <i>R. opacus</i> .....	88
3.8. Toxicity assessment of treated wastewater from two-stage STMBR.....	90
3.8.1. Seed germination assay.....	90
3.8.2. Brine shrimp lethality assay (BLSA).....	91
3.8.3. MTT [3-(4,5-dimethylthiazol-2-yl)-2,5-diphenyltetrazoliumbromide] assay .....	91
3.8.4. Fluorescence activated cell sorting (FACS) analysis.....	92
3.8.4.1. Cell seeding/preparation.....	92
3.9. Characterization and hydrothermal liquefaction (HTL) of <i>R. opacus</i> biomass for bio-oil production.....	93
3.9.1. <i>R. opacus</i> biomass characterization.....	93
3.9.2. HTL experiments.....	93
3.9.3. Optimization of HTL process parameters.....	95
3.9.4. Characterization of bio-oil and HTL by products.....	96
3.9.4.1. HTL product characterization and analysis.....	96
3.9.5. HTL with different catalysts for enhancing bio-oil yield.....	97
3.10. Analytical methods.....	97
4. RESULTS AND DISCUSSION	
4.1. PRWW treatment using <i>R. opacus</i> : Batch shake flask study .....	100

4.1.1. Feasibility study.....	100
4.1.1.1.Characterization of refinery wastewater.....	100
4.1.2. Selection of cultivation condition.....	103
4.1.2.1. One-variable-at-a-time study.....	103
4.1.2.2. Plackett-Burman study.....	106
4.1.3. Kinetics of COD utilization, biomass growth and lipid accumulation.....	109
4.1.3.1. COD utilization.....	110
4.1.3.2. Specific COD utilization rate.....	112
4.1.3.3. Biomass growth .....	114
4.1.3.4. Kinetics of COD inhibition on <i>R. opacus</i> biomass growth .....	116
4.1.3.5. Lipid production.....	118
4.2. Performance evaluation of CSTR for PRWW treatment and lipid-rich biomass production.....	121
4.2.1. Batch, fed-batch and sequential batch modes of operation.....	121
4.2.2. Continuous mode of operation.....	124
4.2.3. Cell-recycle mode.....	125
4.3. Performance evaluation of a bubble column reactor (BCR) for PRWW treatment and lipid-rich biomass production .....	128
4.4. Performance evaluation of a submerged tubular membrane bioreactor (STMBR) for PRWW treatment and lipid-rich biomass production.....	132
4.4.1. Biomass growth, COD removal, lipid concentration and membrane flux in STMBR.....	132
4.4.1.1. Characterization of the cake layer formed on the membrane .....	137
4.5. Toxicity analysis of PRWW in different reactors for re-use and recycle application	

.....	140
4.5.1. Seed germination assay .....	140
4.5.2. Brine shrimp lethality assay (BLSA).....	142
4.5.3. MTT [3-(4,5- dimethylthiazol-2-yl)-2,5-diphenyl tetrazoliumbromide] assay..	143
4.5.4. Propidium iodide flow cytometric assay (PI FACS).....	144
4.6. Bio-oil production by hydrothermal liquefaction (HTL) of <i>R. opacus</i> biomass and its characterization .....	145
4.6.1. <i>R. opacus</i> biomass characterization .....	145
4.6.2. HTL of <i>R. opacus</i> biomass and optimization of process parameters involved .....	148
4.6.3. Bio-oil characterization and fuel properties .....	152
4.6.4. Characterization of HTL by-products.....	158
4.6.5. HTL with different catalysts for enhancing bio-oil yield.....	162
4.6.5.1. Homogenous catalysts.....	162
4.6.5.2. Heterogenous catalysts.....	166
5. SUMMARY AND CONCLUSIONS.....	169
Scope for Future work.....	175
Bibliography.....	176
APPENDIX	
LIST OF PUBLICATIONS	

## List of Tables

S. No.	Description	Page No.
<b>Table 2.1</b>	Different bioreactors for treating petroleum refinery wastewater	18
<b>Table 2.2</b>	Different membrane bioreactor configuration studies for treating PRWW	29
<b>Table 2.3</b>	Various assay methods and regulatory approvals in toxicity studies	34
<b>Table 2.4</b>	Comparison of different types of microorganisms for bio-oil production	43
<b>Table 2.5</b>	Various classes of lipids found in oleaginous microorganisms (Adopted from Dong et al., 2016)	46
<b>Table 2.6</b>	Lipid content of oleaginous microorganisms reported in the literature	48
<b>Table 2.7</b>	Various feedstock and operation conditions used for hydrothermal liquefaction for bio-oil production	59
<b>Table 3.1</b>	Plackett-Burman experimental design matrix for studying the effect of different variables affecting biomass growth, COD removal and lipid production	76
<b>Table 4.1</b>	Composition of raw refinery wastewater	100
<b>Table 4.2</b>	Plackett-Burman experimental design matrix for studying the effect of different variables affecting biomass growth, COD removal and lipid production by <i>R.opacus</i>	107
<b>Table 4.3</b>	ANOVA of (a) COD removal and (b) biomass growth in the Plackett Burman study	109
<b>Table 4.4</b>	Estimated values of bio-kinetic model parameters of COD utilization for lipid-rich biomass production by <i>R. opacus</i>	111
<b>Table 4.5</b>	Estimated values of bio-kinetic model parameters on specific COD utilization rate by <i>R. opacus</i>	113
<b>Table 4.6</b>	Estimated values of bio-kinetic model parameters on <i>R. opacus</i> biomass growth at different COD concentrations	115
<b>Table 4.7</b>	Estimated values of bio-kinetic parameters of substrate inhibition of <i>R. opacus</i> biomass specific growth rate	117
<b>Table 4.8</b>	Estimated values of biokinetic parameters on lipid production by <i>R. opacus</i> using modified Gompertz Model	119
<b>Table 4.9</b>	FTIR bands and the corresponding functional groups of compounds present	139

---

	on the cake layer	
<b>Table 4.10</b>	Characterization of the <i>R. opacus</i> biomass	146
<b>Table 4.11</b>	Experimental design matrix showing coded and un-coded values of independent variables in each experimental run along with their responses in the optimization study	149
<b>Table 4.12</b>	Analysis of Variance (ANOVA) of bio-oil yield by HTL of <i>R. opacus</i> biomass	150
<b>Table 4.13</b>	Functional groups identified from FTIR spectra of the bio-oil produced by HTL of <i>R. opacus</i> biomass	154
<b>Table 4.14</b>	<sup>1</sup> H NMR spectra analysis results of bio-oil according to chemical shift range	154
<b>Table 4.15</b>	Hydrocarbons present in bio-oil obtained by HTL of <i>R. opacus</i>	155
<b>Table 4.16</b>	Estimated property values of the transesterified bio-oil obtained by HTL of <i>R. opacus</i> biomass and comparison with that of the International Standards	157
<b>Table 4.17</b>	Hydrocarbons identified in aqueous phase by product obtained by HTL of <i>R. opacus</i>	159
<b>Table 4.18</b>	Characterization results of solid residue obtained by HTL of <i>R. opacus</i> biomass	161

---

List of Figures

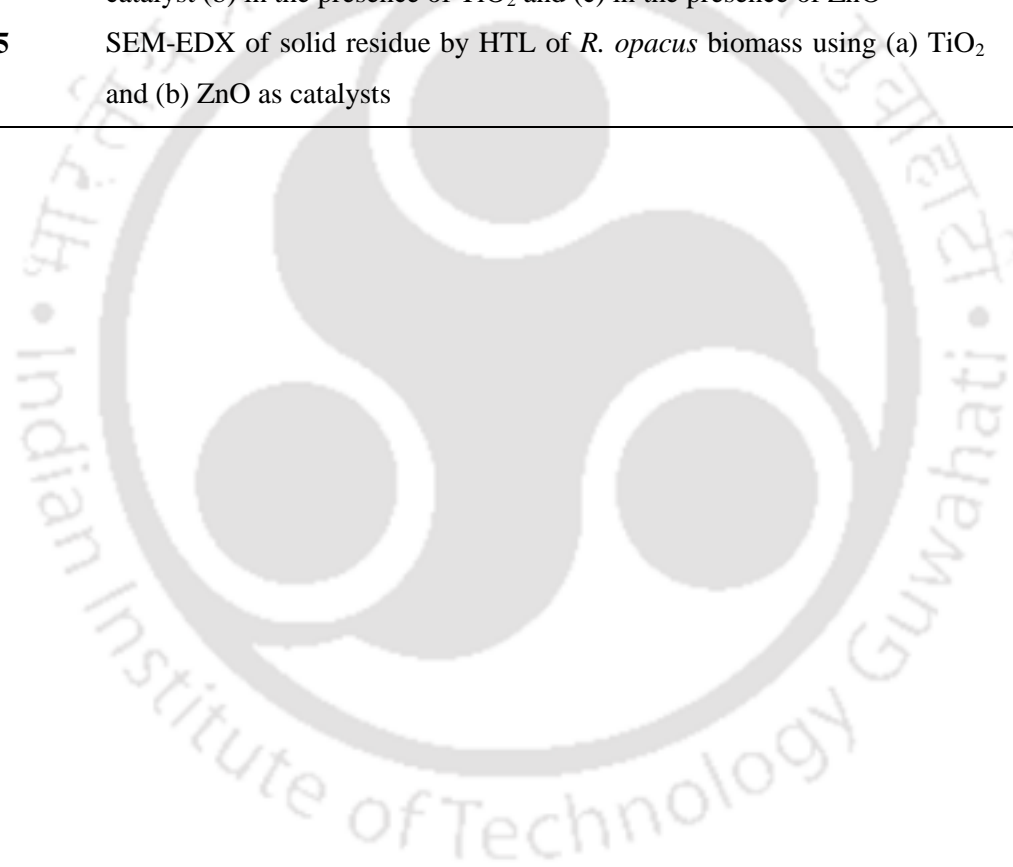
S. No.	Description	Page No.
<b>Fig. 1.1</b>	Zero waste discharge sustainable strategy for wastewater treatment and bio-oil production using oleaginous microorganisms	5
<b>Fig. 2.1</b>	Typical petroleum refinery process	7
<b>Fig. 2.2</b>	(a) Schematic showing general pathway involved in aerobic degradation of hydrocarbons by microorganisms (b) enzymatic reactions involved in biodegradation of hydrocarbons	10
<b>Fig. 2.3</b>	Different physicochemical and biological processes reported for petroleum refinery wastewater treatment	11
<b>Fig. 2.4</b>	Schematic of different bioreactor configurations used for PRWW (a) fixed-bed bioreactor, (b) airlift bioreactor, (c) up-flow anaerobic sludge blanket bioreactor, (d) continuous membrane bioreactor, and (e) sequential batch bioreactor (SBR)	20
<b>Fig. 2.5</b>	Schematic showing (a) membrane bioreactor and (b) submerged membrane bioreactor	28
<b>Fig. 2.6</b>	Overview of MTT assay	40
<b>Fig. 2.7</b>	TEM images of high-lipid <i>Scenedesmus</i> biomass (Adapted from Lai et al., 2016)	44
<b>Fig. 2.8</b>	Pathway followed by <i>Rhodococci</i> for TAGs (Adapted from Amara et al., 2016)	45
<b>Fig. 2.9</b>	Different thermo-chemical routes for biomass conversion to bio-crude oil and upgradation/ purification	57
<b>Fig. 2.10</b>	Bio-refinery approach using oleaginous microorganisms for production of bio-crude oil and other valuable products	69
<b>Fig. 3.1</b>	(a)Schematic and (b) Image of experimental set up showing reactor carried out with the CSTR mode for treatment of refinery wastewater	83
<b>Fig. 3.2</b>	Schematic showing cell recycle approach using tubular ceramic membrane	84
<b>Fig. 3.3</b>	Experimental set-up showing cell recycle using tubular ceramic membrane	85
<b>Fig. 3.4</b>	Schematic representation of tubular ceramic membrane fabrication	86
<b>Fig. 3.5</b>	(a) Schematic and (b) Image of the experimental set up showing the BCR used in the study	87
<b>Fig. 3.6</b>	(a) Schematic and (b) image showing experimental setup with two-stage STMBR system for PRW treatment	90

<b>Fig. 3.7</b>	Schematic showing the steps followed for bio-oil production from <i>R. opacus</i> biomass by HTL and products separation	94
<b>Fig. 4.1</b>	(a) Presumptive tests results for determining the Most Probable Number (MPN) (b) Confirmatory tests for evaluation of MPN results	101
<b>Fig. 4.2</b>	Effect of different inoculum size on <i>R. opacus</i> biomass growth on PRWW and MSM at different ratios (a) 5% (v/v) and (b) 10% (v/v) inoculum size	103
<b>Fig. 4.3</b>	Time profile of (a) <i>R. opacus</i> biomass growth, (b) COD removal, and (c) lipid accumulation by <i>R. opacus</i> (inoculum size:10% (v/v))	104
<b>Fig. 4.4</b>	(a) FESEM image of <i>R. opacus</i> and (b) TEM image showing lipid globules accumulated inside the bacterium	105
<b>Fig. 4.5</b>	Effect of different process parameters on <i>R. opacus</i> biomass growth using PRWW (a) C/N ratio, (b) nitrogen source	105
<b>Fig. 4.6</b>	Time profile of <i>R. opacus</i> biomass growth in the Plackett-Burman screening study	108
<b>Fig. 4.7</b>	Pareto chart showing the effect of individual variables in the (a) COD removal and (b) biomass growth in the Plackett-Burman study	109
<b>Fig. 4.8</b>	COD removal (%) by <i>R. opacus</i> at different initial COD concentrations	110
<b>Fig. 4.9</b>	Experimental and predicted values of COD utilization due to (a) first order, (b) logarithmic and (c) logistic kinetic models	112
<b>Fig. 4.10</b>	Experimental and predicted values of specific COD utilization rate at different initial COD concentrations	114
<b>Fig. 4.11</b>	Experimental and predicted <i>R. opacus</i> biomass growth at different initial COD concentrations using (a) modified Gompertz and (b) Logistic models	116
<b>Fig. 4.12</b>	Experimental and model predicted <i>R. opacus</i> biomass specific growth rate at different initial COD concentrations	117
<b>Fig. 4.13</b>	Experimental and model predicted (a) lipid production and (b) cumulative lipid production by <i>R. opacus</i> at different initial COD concentrations	120
<b>Fig. 4.14</b>	Biomass production, lipid accumulation and COD removal by <i>R. opacus</i> in the bioreactor operated under (a) batch, (b) fed-batch, and (c) sequential batch modes	122
<b>Fig. 4.15</b>	Biomass production, lipid accumulation and COD removal by <i>R. opacus</i> during the continuous experiments with the CSTR at different HRTs: (a) 8	125

	h (b) 16 h and (c) 24 h	
<b>Fig. 4.16</b>	Biomass production, lipid accumulation and COD removal by <i>R. opacus</i> in the CSTR operated under continuous mode with cell recycle experiment at 16 h HRT	126
<b>Fig. 4.17</b>	FESEM images of <i>R. opacus</i> biomass collected from (a) recycle stream and (b) effluent stream of the bioreactor operated in continuous with cell recycle mode	127
<b>Fig. 4.18</b>	GC-MS analysis results showing hydrocarbon profile of the wastewater at (a) 0 h and (b) 168 h of treatment using the continuous with cell recycle reactor system (CSTR)	128
<b>Fig. 4.19</b>	Visual comparison of raw PRWW, treated water and permeate water	128
<b>Fig. 4.20</b>	COD removal, biomass concentration and lipid accumulation by <i>R. opacus</i> in the BCR operated under (a) batch and (b) continuous modes	131
<b>Fig. 4.21</b>	Time profile of biomass concentration ( $\text{g L}^{-1}$ ), COD removal efficiency (%) and lipid concentration ( $\text{g L}^{-1}$ ) during different phases of STMBR operation. (Phase divisions in the figure show the membrane washing carried out during the single-stage STMBR operation)	133
<b>Fig. 4.22</b>	Variation in membrane flux during different phases of single-stage STMBR operation. (Phase divisions in the figure show the membrane washing carried out during the single-stage STMBR operation)	134
<b>Fig. 4.23</b>	Schematic showing factors influencing the flux declining mechanism during different phases of single-stage STMBR operation	134
<b>Fig. 4.24</b>	Biomass concentration ( $\text{g L}^{-1}$ ), COD removal efficiency (%) and lipid concentration ( $\text{g L}^{-1}$ ) in the two-stage STMBR system (a) R1 and (b) R2 (Phase divisions in the figure show the membrane washing carried out during the two-stage STMBRs operation)	136
<b>Fig. 4.25</b>	FESEM images of (a) virgin and (b) fouled membrane	137
<b>Fig. 4.26</b>	M images of (a) virgin and (b) fouled membrane	138
<b>Fig. 4.27</b>	FESEM images of <i>R. opacus</i> biomass from the two-stage STMBR (a) before and (b) at the end of continuous operation	138
<b>Fig. 4.28</b>	FT-IR spectrum of cake layer formed on the membrane surface	139

<b>Fig. 4.29</b>	Plates showing reduced CFU count in different dilutions following treatment of PRW using two-stage STMBR system	140
<b>Fig. 4.30</b>	Permeate water obtained following treatment of refinery wastewater in a two-stage STMBR system	140
<b>Fig. 4.31</b>	Germinated <i>Cicerarietinum</i> L seeds incubated with (a) distilled water (b) tap water (c) raw refinery wastewater (untreated) and (d) permeate (treated water) obtained following cell recycle and (e) permeate (treated water) obtained following two-stage STMBR for their eco-toxicity analysis	142
<b>Fig. 4.32</b>	Image showing experimental set-up used for growing brine shrimps in synthetic saline water	142
<b>Fig. 4.33</b>	Results of MTT assay for evaluation of cell viability in treated wastewater samples following treatment	143
<b>Fig. 4.34</b>	(a) Raw data obtained using FACS caliber for different samples (b) Evaluation of apoptotic effect of the different wastewater following treatment by using PI FACS	144
<b>Fig. 4.35</b>	TGA profile of <i>R. opacus</i> biomass grown using refinery wastewater as the substrate	147
<b>Fig. 4.36</b>	3-D Response surface and 2-D contour plots showing the interaction effect between HTL parameters on bio-oil yield: (a) reaction time and temperature (b) biomass-water ratio and temperature and (c) biomass-water ratio and time	152
<b>Fig. 4.37</b>	(a) FTIR (b) <sup>1</sup> H NMR (c) GC-MS spectra of bio-oil fraction from HTL of <i>R. opacus</i> biomass	153
<b>Fig. 4.38</b>	Schematic showing (a) the steps involved in HTL and (b) main steps involved in lipid biosynthesis by <i>R. opacus</i> from PRWW and its conversion to bio-oil by HTL (GPAT, glycerol-3-phosphate acyl transferase; AGPAT, acylglycerol-3-phosphate acyl transferase; PAP, phosphatidic acid phosphatase; DGAT, diacylglycerol acyl transferase)	158
<b>Fig. 4.39</b>	(a) IC, (b) FTIR and (c) GC-MS spectra of aqueous phase derived from hydrothermal liquefaction (HTL) of <i>R. opacus</i> biomass.	160
<b>Fig. 4.40</b>	(a) FESEM-EDX, (b) TGA, (c) XRD and (d) FTIR spectra of solid residue derived from hydrothermal liquefaction (HTL) of bacterial biomass	162

<b>Fig. 4.41</b>	(a)FT-IR spectra of bio-oil produced by HTL of <i>R. opacus</i> biomass using Na <sub>2</sub> CO <sub>3</sub> and H <sub>2</sub> SO <sub>4</sub> , (b)FT-IR spectra of aqueous phase produced by HTL of <i>R. opacus</i> biomass using Na <sub>2</sub> CO <sub>3</sub> , and H <sub>2</sub> SO <sub>4</sub> as catalysts	163
<b>Fig. 4.42</b>	(a) FT-IR spectra and (b) SEM-EDX of solid residue produced by HTL of <i>R. opacus</i> biomass using Na <sub>2</sub> CO <sub>3</sub> and H <sub>2</sub> SO <sub>4</sub> as catalysts	165
<b>Fig. 4.43</b>	(a) FT-IR spectra of bio-oil produced by HTL of <i>R. opacus</i> biomass using TiO <sub>2</sub> and ZnO, (b) FT-IR spectra of aqueous phase produced by HTL of <i>R. opacus</i> biomass using TiO <sub>2</sub> and ZnO as catalysts	167
<b>Fig. 4.44</b>	XRD profile of solid residue by HTL of <i>R. opacus</i> biomass (a) without catalyst (b) in the presence of TiO <sub>2</sub> and (c) in the presence of ZnO	167
<b>Fig. 4.45</b>	SEM-EDX of solid residue by HTL of <i>R. opacus</i> biomass using (a) TiO <sub>2</sub> and (b) ZnO as catalysts	168



**Abbreviations**

**AAS:** Atomic absorption spectroscopy

**AFM:** Atomic force microscopy

**ANOVA:** Analysis of variance

**AP:** Aqueous phase

**APHA:** American Public Health Association

**ASTM:** American Society for Testing and Materials

**B/W:** Biomass to water ratio

**BCR:** Bubble column reactor

**BET:** Brunauer–Emmett–Teller

**BLSA:** Brine shrimp lethality assay

**BOY:** Bio-Oil Yield

**C/N ratio:** Carbon/Nitrogen ratio

**CDW:** Cell Dry Weight

**CFU:** Colony Forming Unit

**CHNS:** Carbon Hydrogen Nitrogen Sulphur

**CN:** Cetane number

**COD:** Chemical Oxygen Demand

**CP:** Cloud Point

**CSTR:** Continuous Stirred Tank Reactor

**DCM:** Dichloromethane

**DMEM:** Dulbecco's Modified Eagles Medium

**DMSO:** Dimethyl sulfoxide

**DO:** Dissolved oxygen

**EDX:** Energy Dispersive Spectroscopy

**EN:** European nations

**EPS:** Exo-polysaccharides

**FAME:** Fatty Acid Methyl Ester

**FBS:** Fetal Bovine Serum

**FC:** Fixed Carbon content

**FESEM-EDX:** Field Emission Scanning Electron Microscopy

**FTIR:** Fouriertransform Infrared Spectrometry

**g:** Gravitational acceleration

**GC-MS:** Gas Chromatography-Mass Spectroscopy

**GI%:** Germination Index

**HHV:** High heating value

**HRT:** Hydraulic retention time

**HTL:** Hydrothermal Liquefaction

**LB:** Luria Bertani

**MC:** Moisture Content

**MSM:** Mineral Salt Medium

**MTCC:** Microbial Type Cell Culture

**MTT:** 3-(4,5- dimethylthiazol-2-yl)-2,5-diphenylte- trazoliumbromide

**NB:** Nutrient Broth

**NMR:** Nuclear magnetic resonance

**OD:** Optical density

**PAH:** Polycyclic aromatic hydrocarbon

**PBS:** Phosphate buffer solution

**PRWW:** Petroleum refinery wastewater

**RSM:** Response Surface Methodology

**SMBR:** Submerged membrane bioreactor

**SRY:** Solid residue yield

**STMBR:** Submerged tubular membrane bioreactor

**TEM:** Transmission Electron Microscopy

**TGA:** Thermo-gravimetric analysis

**VM:** Volatile matter

**WSPY:** Water soluble product yield


**XRD:** X-ray diffractometer

**ZP:** Zeta Potential




---

---



**CHAPTER-1**

INTRODUCTION



---

---

## 1. Introduction

The global demand for petroleum and petrochemical products is significantly increasing every year. Petroleum refineries occupy a significant position among the industrial sectors due to fuels and other high-value products (Pajoumshariati et al., 2017). However, refineries use huge amounts of water for various unit operations and thus produce wastewater containing complex toxic hydrocarbons that are known to cause adverse effects on human health. Other than hydrocarbon, it also contains a mixture of oil and petroleum fractions such as diesel oil, gasoline, kerosene etc (Jamaly et al., 2015). Hence, safe disposal of refinery wastewater is of major environmental concern.

Existing methods to treat petroleum refinery wastewater include photo-degradation, Fenton and photo-Fenton process, coagulation (Demirci et al., 1997; El-Naas et al., 2009), adsorption, chemical oxidation, electrochemical flocculation methods (Diya'Uddeen et al., 2011), as well as UV treatment and ozonation. However, such processes require a large amount of oxidants for the complete degradation of organics present in the wastewater. Electro-coagulation and flocculation, on the other hand, require electrodes, which are quite difficult for maintaining high efficiency of the process. Moreover, coagulation is used to only pretreat such wastewater, requiring further treatment steps (El-Naas et al., 2009; Santo et al., 2012). Compared with these physicochemical treatment methods, which suffer from one drawback or the other, biological treatment of such industrial effluents is gaining importance owing to its low cost of operation and maintenance, eco-friendly and industrial-scale application potential. However, secondary sludge production due to excessive biomass growth may be a problem with biological treatment methods (Ishak et al., 2012). Moreover, inhibition due to toxic compounds present in wastewater may prolong sludge settling time, delay time required for start-up, or resist in the formation of scum-foam, etc.

In order to overcome the disadvantages of biological treatment processes, proper design of bioreactor and its configuration is a significant focus area of research in the field (Jou and Huang, 2003).

### 1.1. Oleaginous bacteria and bio-oil production

Alternative energy can be any energy source that can be substituted for fossil fuels, intended to minimize the environmental threats caused by the usage of fossil fuels. Marine energy, geothermal energy, solar energy are all alternative forms. One of the principal sources of renewable energy is bio-oil, which can be produced from renewable biomass of microorganisms capable of accumulating triacyl-glycerol (TAGs). Biomass of oleaginous microorganisms has gained massive importance in this regard, which can accumulate 20% or more of lipids (TAGs).

TAG synthesis and accumulation have been reported in *Actinomycetes*, including those belonging to the genera *Mycobacterium*, *Streptomyces*, *Actinobacter*, *Nocardia*, and *Rhodococcus*. Bacteria, yeast, and fungi produce TAGs with the same fatty acid composition as that of vegetable oils. The accumulated lipids in these microorganisms can be extracted for various beneficial purposes by following specific techniques. In hydrothermal liquefaction (HTL) technique, the biomass is thermally degraded at elevated temperature and pressure conditions for bio-oil production from biomass.

HTL is more advantageous than pyrolysis due to its ability to use wet biomass directly and without any pre-treatment, which greatly reduces the process costs and facilitates ease of operation (Hu et al., 2019). Hydrothermal liquefaction is usually carried out under high temperature and pressure to keep water in its supercritical state.

Bio-oil is viscous hydrophobic organic liquids, dark brown in color with a distinctive smoky odour. It consists of several organic compounds, mainly acids, aldehydes, alcohols, esters, ketones, and phenols (Arun et al., 2018; Sharifzadeh et al., 2019). Although bio-oil is a high-density fuel, it

has some undesired properties, such as high viscosity, high water content, high oxygen content (low heating value), and high ash content along with high corrosiveness. This limits its direct use as a fuel. However, different up-gradation techniques, including hydro-treating, hydro-cracking, esterification, and steam reforming, can significantly improve the properties of bio-oil for successful application as engine fuel (Baldwin, 2019). The quality and yield of bio-oil from biomass greatly depend on the biomass type, water content, catalyst used, temperature and pressure conditions, and reaction time. There are various advantages of bio-oil production from biomass employing thermo-chemical conversion technologies as it involves simple operation, reduced costs, and non-selective processes. Bio-oil is CO<sub>2</sub> and greenhouse gas (GHG) neutral and, hence, considered as a clean fuel (Chen et al., 2014). In addition, it burns with emitting less harmful gases like sulfur oxide (SO<sub>x</sub>) (Xu et al., 2018).

Extensive research has been done on bio-oil production from lignocellulosic biomass such as wood residue, plant material, and grass as well as waste biomass such as municipal solid waste, waste sludge, and animal manure (Haarlemmer et al., 2016; Cao et al., 2016; Pedersen et al., 2015). However, other than algal biomass, very few literature reports are available on oleaginous microbial biomass for bio-oil production (Kang and Yu 2015). Oleaginous microorganisms are primarily used for biodiesel production, where lipid extracted from the biomass is trans-esterified to produce biodiesel (Qadeer et al., 2017). Direct conversion of oleaginous microbial biomass to bio-oil significantly improves the biomass utilization and product yield. Also, the properties of bio-oil are more similar to hydrocarbon fuel than biodiesel. Thus, bio-oils from oleaginous microorganisms can be a promising renewable energy source that can be used as an alternative fuel (Isa and Ganda, 2018).

## 1.2. Zero waste closed-loop bio-refinery

A biorefinery is a sustainable technology for the generation of bioenergy products from different types of biomass feedstocks upon incorporating certain conversion technologies. It is a holistic approach developed in the past half of the decade, considering increasing attention to a circular economy and focusing on its socio-economic aspects. Biorefinery, therefore, acts as a strategic technology for achieving a circular-based economy (Ubando et al., 2020).

Biomass, in this regard, is the main key point for establishing a successful biorefinery system. However, its utilization as a valuable carbon source is challenging owing to its variation in its composition based on seasons, geographical availability, and lower calorific value (Basu, 2018). For maximizing the use of biomass feedstock, including waste, an integrated biorefinery system is favorably considered. A biorefinery system, however, incorporates various infrastructure facilities for efficiently producing biofuel and other bio-based bioenergy products in a sustainable manner. This concept has been designed to utilize various biomass, such as lignocelluloses, algae, and other wastes. For instance, the microalgal biorefinery approach exploits all upstream and downstream processes for the production of value-added products from microalgal biomass (Venkata Mohan et al., 2016). However, limited literature is available focussing on bacteria as an oleaginous microorganism based biorefinery for the production of biofuels.

The use of cheaply available wastewater as a substrate for cultivating oleaginous microorganism for bio-oil production reduces the overall process costs. It also overcomes environmental hazards due to wastewater discharge. This study described simultaneous treatment and utilization of refinery wastewater by oleaginous hydrocarbonoclastic bacterium *R. opacus* in batch and continuous systems for bio-oil production. In addition to bio-oil as the main product, HTL of *R. opacus* biomass yields by-products such as aqueous phase rich in nutrients such as chloride, sulfate, phosphate and biochar as the solid residue for reuse. This research demonstrates a closed-loop

sustainable zero waste strategy for refinery wastewater treatment with provisions for resource recovery.

Considering the environmental impact due to the discharge of large volumes of wastewater, several wastewater treatment methods, including biological methods, are employed to treat industrial, municipal, and domestic wastewater prior to discharge. In case of biological treatment methods, microorganisms utilize the chemical oxygen demand (COD) present in the wastewater as the substrate for their own metabolism and growth. In addition to biomass, some useful products can be generated from the wastewater treatment scheme, thereby providing incentives to the industry to employ such technologies. Thus, bio-oil production by hydrothermal treatment of oleaginous microorganisms grown using wastewater as the substrate can become an alternative zero waste strategy for industrial wastewater disposal (Figure 1.1).

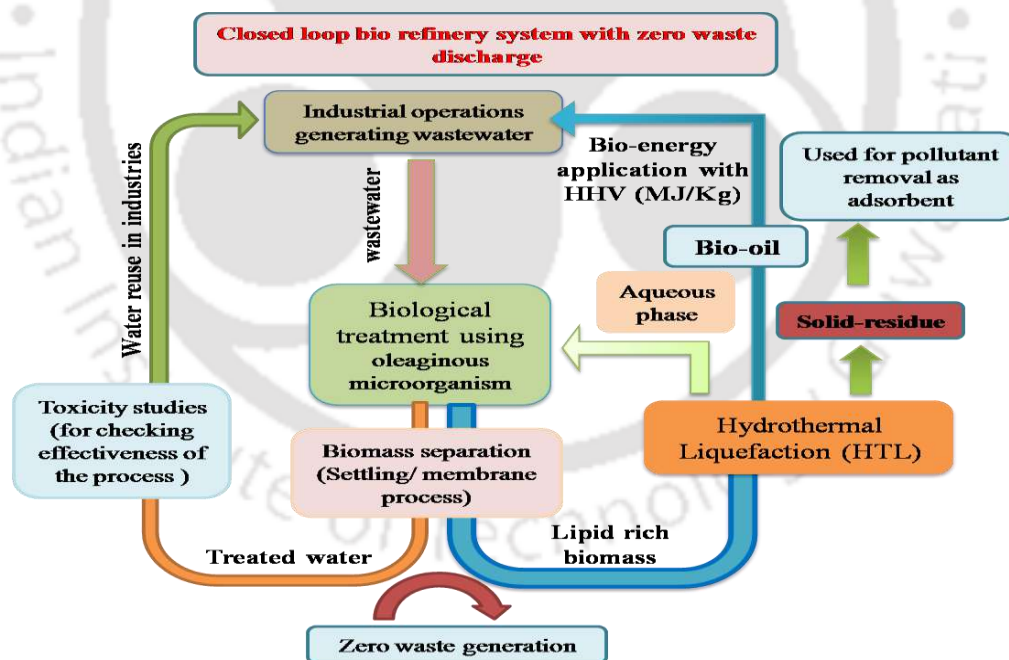


**Figure 1.1** Zero waste discharge sustainable strategy for wastewater treatment and bio-oil production using oleaginous microorganisms



## CHAPTER-2

### LITERATURE REVIEW

## 2.1. Petroleum refinery configuration

The present-day modern economy is majorly based on petroleum products and petrochemical industry growth. The petroleum refining process is completely based on chemical engineering principles consisting of various unit operations designed to produce certain specific products. Processing of petroleum crude is followed by product generation in each chemical unit operation. Liquefied petroleum gas (LPG), gasoline or petrol, kerosene, jet fuel, diesel oil and fuel oils are the main products that are produced by the refining of raw petroleum crude. A typical refining process includes unit operations such as crude oil distillation, vacuum distillation, naphtha hydrotreater, catalytic reforming, alkylation, isomerization, distillate hydrotreater, fluid catalytic cracking (FCC), hydrocracker, and stream reforming (Fig. 2.1) (Favenec, 2001). In literature, a refinery is classified as having four different units (Wake 2005), whereas some other source categorizes a refinery into a main hydro-skimming unit comprising of three sub-units, namely crude distillation unit, a desulphurizing unit, and a reforming unit. A crude distillation unit is dedicated to the fractionation of crude oil into different components. The second and the desulphurizing unit is responsible for the reduction of sulfur component, mainly in naphtha and kerosene fractions. The third and the last unit generates reformate and includes complex catalytic cracking processes. Each of these units, regardless of its configuration, generates waste and, therefore, significantly contributes to the generation of overall effluent in the refinery. It is reported that the volume of effluent generated in a refinery is almost 0.4-1.6 times the crude oil processed (Coelho et al., 2006).

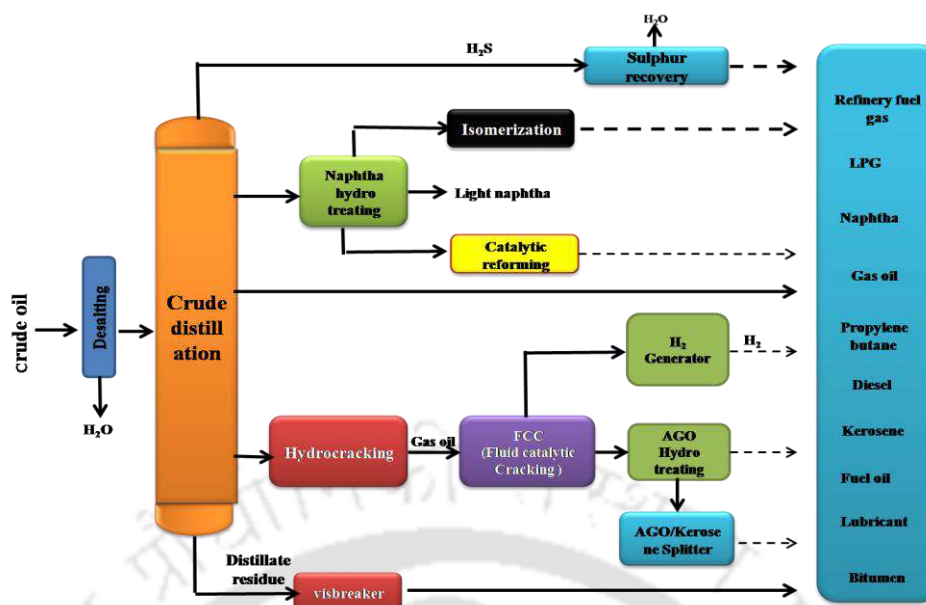


Fig. 2.1 Typical petroleum refinery process

Petroleum wastewater contains a large number of hydrocarbons, which are organic compounds (Al Zarooni and Elshorbagy, 2006; Benyahia et al., 2006; Paul et al., 2019). Biochemical oxygen demand (BOD), as compared with chemical oxygen demand (COD) of refinery wastewater, is significantly less due to the presence of recalcitrant organic compounds. The discharge limits for BOD and COD in wastewater are fixed at  $17 \text{ mg L}^{-1}$  and  $120 \text{ mg L}^{-1}$ , respectively (CPCB, 1996). Total petroleum hydrocarbon (TPH) present in the wastewater as determined by the presence of soluble and insoluble hydrocarbons is due to the presence of phenolic compounds, and the discharge limit of TPH is reported to be  $2.4 \text{ mg L}^{-1}$  (Ocasio, 2012). Polyaromatic hydrocarbons (PAHs), e.g., naphthalene present in refinery wastewater, are highly carcinogenic. Also, the limit for total Kjeldahl nitrogen (TKN) in the form of  $\text{N}\cdot\text{NH}_4$ ,  $\text{NH}_4^+$ ,  $\text{NH}_3$ , and  $\text{H}_2\text{S}$  in refinery wastewater, generated due to the hydrocracker and hydro skimmer operation units, is fixed in the range of  $10\text{-}100 \text{ mg L}^{-1}$ . Besides, sulfate compounds are in a high amount in the wastewater due to its use in crude oil processing. Polychlorinated biphenyls (PCB), if present more than  $0.5 \text{ ppb}$  ( $0.0005 \text{ mg L}^{-1}$ ) present in the wastewater, can cause liver and kidney failure, miscarriages, and cancer (Al Zarooni and

Elshorbagy, 2006). It is thus implicative that the treatment of petroleum refinery wastewater (PRWW) is essential to avoid environmental hazards.

Toxic organics present in PRWW are listed under top priority organic pollutants, and their persistent nature gives rise to severe health hazards (Goswami et al., 2018).

Petroleum hydrocarbons, also termed as recalcitrant compounds, are classified as major pollutants. Petroleum hydrocarbons can be divided into four classes: the saturates, the aromatics, the asphaltenes (phenols, fatty acids, ketones, esters, and porphyrins), and the resins (pyridines, quinolines, carbazoles, sulfoxides, and amides). Petroleum mainly consists of paraffin, poly aromatic hydrocarbons (PAHs) resins and asphaltenes (Varjani, 2014). Saturates are hydrocarbons without unsaturated (double/triple) bond, representing highest percentage of crude oil constituents, whereas asphaltenes constitute non-hydrocarbon polar compounds. Contamination of groundwater with petroleum hydrocarbon can occur mainly due to spillages and leakages from steamers, underground tanks. Due to their inherent bio-magnification property, a petroleum hydrocarbon causes extensive damage to the ecosystem (Chandra et al., 2013). Also, due to the presence of some hemotoxic, teratogenic and carcinogenic compounds like BTEX and PAH they are considered as recalcitrant and highly toxic.

PAHs in crude oil can induce malignant tumors that mostly affect epithelial tissues present in the skin owing to their affinity for nucleophilic centre of macromolecules like DNA, RNA and proteins (Perez-Cadahia et al., 2007; Desforjes et al., 2016). Toxicity due to petroleum hydrocarbons include disturbances in metabolic reactions, suffocation and hormonal imbalance, acute necrosis, mortality and developmental abnormalities (Varjani, 2014; Van Meter et al., 2006; Alonso-Alvarez et al., 2007; Desforjes et al., 2016).

Bioremediation is one of the important methods for effective degradation of these compounds. Bioremediation employs hydrocarbonoclastic microorganisms that are capable of degrading hydrocarbons. Hydrocarbonoclastic bacteria are ubiquitous in the environment and can be isolated for hydrocarbon degradation. Biodegradation is eco-friendly and employs catalytic activity of various enzymes present in microorganisms capable of hydrocarbon degradation. Among the different classes of hydrocarbons, linear alkanes are more susceptible to microbial attack followed by branched alkanes, small aromatics and cyclic (Das et al., 2011). Resistance of some compounds to microbial degradation depends on the molecular weight as well as number of rings. Fig. 2.2 (a) shows schematic of general pathway involved in aerobic degradation of hydrocarbons by microorganisms and Fig. 2.2 (b) shows enzymatic reactions involved in biodegradation of hydrocarbons.

As shown in the figure, hydrocarbon degradation involves incorporation of oxygen as the key enzymatic reaction, mostly catalyzed by oxygenases and peroxidases, followed by sequential degradation which forms intermediates of central metabolism, such as tricarboxylic acid (TCA) cycle. More details on the enzymes involved and different intermediates formed during hydrocarbon degradation can be found in Maeng et al. 1996; McDonald et al., 2006; Das et al., 2010.

Various microorganisms can degrade recalcitrant hydrocarbons because of the presence of various enzymes which plays an important role in the microbial degradation of oil, chlorinated hydrocarbons, fuel additives, and many other compounds. Depending on the chain length, enzyme systems are required to introduce oxygen in the substrate to initiate biodegradation. Bacteria, yeasts and fungi consist of a super family of ubiquitous Heme-thiolate monooxygenases. The capability of several yeast species to use n-alkanes and other aliphatic hydrocarbons as a sole source of carbon and energy is mediated by the existence of multiple microsomal Cytochrome P450 forms. These cytochrome P450 enzymes had been

isolated from yeast species such as *Candida maltosa*, *Candida tropicalis*, and *Candida apicola* (Scheuer et al., 1998). *Pseudomonas*, *Burkholderia*, *Rhodococcus* and *Mycobacterium* are reported to have AlkB related Alkane Hydroxylases responsible for degradation of hydrocarbons (Jan et al. 2003) while *Acinetobacter* sp. has dioxygenases (Maeng et al., 1996).

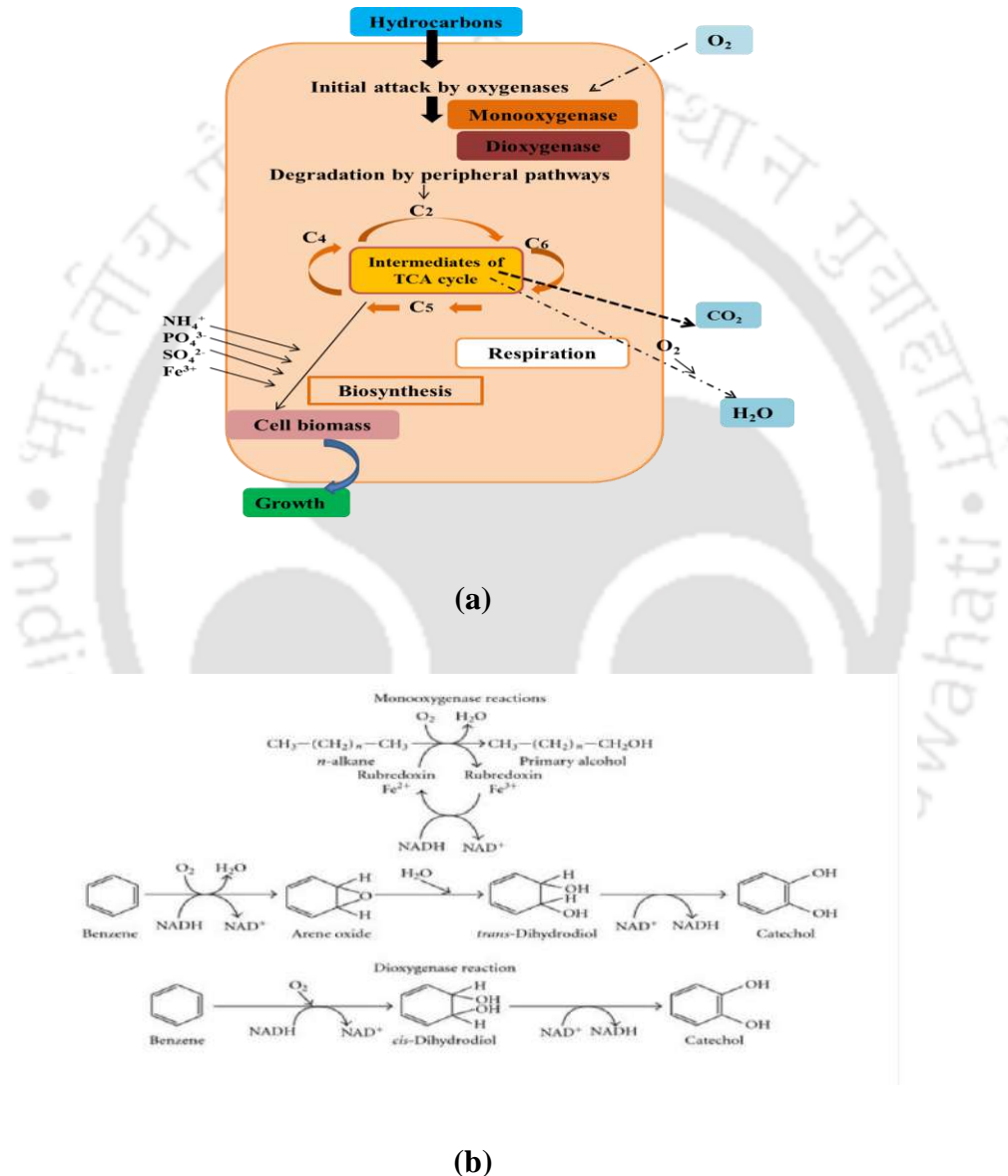


**Fig. 2.2** (a) Schematic showing general pathway involved in aerobic degradation of hydrocarbons by microorganisms (b) enzymatic reactions involved in biodegradation of hydrocarbons

Undoubtedly, the marine ecosystem is adversely affected by contamination due to the organics present in PRWW as also water bodies contaminated with PRWW experience reduced algal activity (El Naas et al., 2009). Moreover, the discharge of such high organic matter into the water bodies reduces the minimum amount of dissolved oxygen (DO) required ( $2 \text{ mg L}^{-1}$ ) for supporting various aquatic life forms through the consumption of oxygen by bacteria responsible for oxidizing the organics present in the PRWW (Attiogbe et al., 2007). Phenolics and other nitrogen or sulfur-containing compounds also pose a severe threat due to their toxic effects on organisms (Yang et al., 2008). Besides, oil and grease, which constitute the PRWW, tend to aggregate and block the pipelines, thereby creating unwanted anaerobic conditions. Fig. 2.3 presents an overview of the various processes used to treat refinery wastewater.

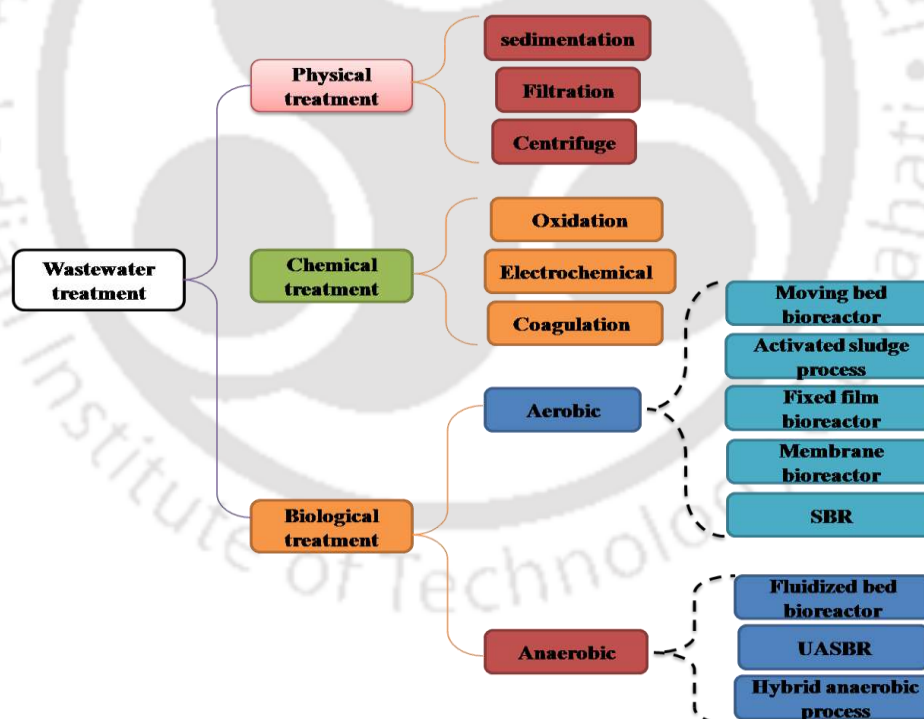


**Fig. 2.3** Different physicochemical and biological processes reported for petroleum refinery wastewater treatment

## 2.2. Petroleum refinery wastewater (PRWW) treatment

Treatment of PRWW is mainly divided into primary, secondary, and tertiary treatment. Primary treatment includes physical and chemical treatment methods such as photo-degradation, Fenton and photo-Fenton process, coagulation, adsorption, chemical oxidation, flocculation, and electrochemical methods. In secondary treatment, only biological treatment is followed, and tertiary treatments include adsorption and filtration/ decontamination or further precipitation prior to discharge into water bodies.

### 2.2.1. Primary treatment

Primary treatment methods are physical and chemical methods for separation of oil and water, and there are mainly Fenton and Photo-Fenton process, coagulation, adsorption, chemical oxidation, flocculation, electrochemical and chemical precipitation. Adsorption is generally followed in industries owing to its excellent advantages for recycling the treated stream (El-Naas et al., 2010). The Photo-Fenton process is considered as an alternative to the conventional treatment method, as it can be used to achieve 75% COD removal even at the initial stages of primary treatment (Tony et al., 2012). Separation of oil and suspended solids by physio-chemical methods such as coagulation and flocculation are highly desired due to their high removal efficiency (Santo et al., 2012). Organic and inorganic pollutants are generally removed from the PRWW by electrochemical treatment methods. An electrochemical method requires a high amount of electricity and therefore increases the operating cost (Yan et al., 2011). Chemical precipitation is followed to remove compounds present in PRWW by adding chemicals in the form of coagulants. It is reported that even sulfide can be precipitated by adding coagulants such as  $[\text{Ca}(\text{OH})_2]$  and  $[\text{CaCO}_3]$  in wastewater in the presence of metals (Altaş and Büyükgüngör, 2008).

### 2.2.2. Secondary treatment

Physical and chemical methods ensure the removal of small particles and suspended pollutants in PRWW during the primary treatment. In secondary treatment, biological methods can ensure treated water within discharge limits (Vendramel et al., 2015). Biological methods can be classified based on the aerobic or anaerobic condition for converting the soluble form of organic compounds into simple compounds as CO<sub>2</sub> and water (Visvanathan et al., 2000). To date, the most common biological treatment method used in the industries is the activated sludge process (ASP) in which bioreactor plays a major role. As reported by Ebrahimi et al. (2016), optimization of the biological treatment process for PRWW by activated sludge process is essential and is generally carried out under external aeration supply of 3.7 mg L<sup>-1</sup> and 46 % of sludge yield from the process. Many studies have been reported on bioreactor working conditions for achieving high treatment efficiency and low sludge production in ASP. However, the recent focus is on the use of a membrane in the bioreactor, which serves to retain the sludge or microorganisms and improve the removal efficiency (Paul et al., 2019).

### 2.2.3. Tertiary treatment

Tertiary treatment of wastewater is the final stage of treatment before its discharge or reuse as for e.g. coolant. Tertiary treatment methods include electro-dialysis, reverse osmosis and ion exchange, which ensure the removal of dissolved salt and organic compounds present (Jafarinejad and Jiang, 2019). Interestingly, tertiary treatment of PRWW involves a combination of adsorption and ion exchange processes. A recent study compared ion exchange with adsorption, which revealed 55% lower adsorptive efficiency than that of the activated carbon process. Moreover, removal of organics ranged from 57 to 94% by the ion-exchange method was also reported, which ranges up to 12 to 79% of resins for organic compound removal from the natural sources (de Abreu Domingos and da Fonseca, 2018).

## 2.3. Advanced methods for PRWW treatment

### 2.3.1. Advanced oxidation

In an oxidation process, organic matter present is converted into its simpler compounds of CO<sub>2</sub> and H<sub>2</sub>O (Cañizares et al., 2007). Advanced oxidation process (AOP), conductive diamond electro-oxidation (CDEO), oxidation, and Fenton oxidation are some examples under this category. In a novel catalytic wet air oxidation (CWAO) technology, conditions such as the temperature of 150 °C and 0.8 MPa oxygen applied pressure are followed. Under these conditions, 5000 mg L<sup>-1</sup> of COD and 220 mg L<sup>-1</sup> of BOD of PRWW was oxidized and converted to a simple organic compound. BOD<sub>5</sub>/COD ratio was initially 0.0, which increased to 0.47 within 30 minutes of treatment (Sun et al., 2008). Fenton reaction is a well-known method to treat wastewater using a low concentration of iron, (<1 mM). Fenton system uses ferrous irons in the range of 1- 10mM to achieve maximum treatment efficiency, and the oxidation process is mainly influenced by temperature and pressure. However, this process requires and the use of a costly oxidizing agent, which are used as catalysts, further adding to its cost (Luck, 1996).

### 2.3.2. Electrochemical

Electrochemical treatment is another type of oxidation method, and it is usually carried out by applying electricity to oxidize non-degradable compounds into simple organic compounds. The main advantage of this method is that it is environmental-friendly delivering high efficiency of treatment along with ease of operation (Feng et al., 2003). Electrochemical process developed for treating wastewater offers high efficiency depending upon the type of electrodes used (Tröster et al., 2002). For instance, boron-doped diamond electrodes increased the treatment efficiency of wastewater (García-García et al., 2015). The use of IrO<sub>2</sub>-Pt coated electrode is reported to improve the treatment efficiency of whey wastewater by this method; with a maximum COD removal obtained was 53.2 % (Markou et al., 2017). Electrochemical

process is reported for heavy oil refinery wastewater treatment by using a three-dimensional electrode reactor under operating conditions of 75% granular activated carbon, 30mA/cm<sup>2</sup> current density, 100 minutes treatment time. The experimental setup consisted of a three-dimensional electrode reactor with granular activated carbon and porous ceramsite. This method helped to achieve removal efficiency of COD, total organic carbon (TOC), and toxicity with the values 45.5%, 43.3%, and 67.2%, respectively (Wei et al., 2010). Another study reported treatment of refinery wastewater by electrochemical oxidation treatment process using boron-doped anode and ruthenium mixed oxide (Ru-MMO) electrode, which resulted in 99.53% and 75.78% removal of phenol and COD respectively, at 5 mA/cm<sup>2</sup> of current density (Yavuz et al., 2010). However, requirement of a large amount of electricity is a drawback of this method (Feng et al., 2003).

### 2.3.3. Electro-coagulation

Electro-coagulation method is one of the most widely used physiochemical method for wastewater treatment following electrolysis for the removal of the dissolved organic compounds, metals, solid particles, and micro-pollutants. The benefits of using this electrochemical method for treating wastewater include compatibility, versatility, energy efficiency, safety, automation, and low-cost (Feng et al., 2003). Electro-coagulation methods have been reported for treating different types of wastewater using various electrode materials. Dairy wastewater treatment by an integrated system consisting of electro-coagulation, Fenton and ozone process was achieved with 30% COD removal (Torres-Sánchez et al., 2014); textile wastewater treatment by electro-coagulation with chemical coagulation by adding poly aluminum chloride (PAC) resulted in 80% COD removal (Inan et al., 2004); poultry slaughterhouse wastewater treatment was achieved by this method using aluminum electrode (Kobyta et al., 2006). Similarly, olive oil mill wastewater was treated with aluminum and iron electrode (Can et al., 2006). Also, a novel approach of electro-coagulation with solar cells as

the power source has been reported to treat industrial wastewater (García-García et al., 2015). Abdelwahab et al. (2009) reported the removal of phenol from PRWW by electro-coagulation with the aluminum oriented cathode and aluminum screen anode. Some of the parameters that influenced this process include pH, time, current density and electrolyte concentration. 97% of phenol removal was achieved within 2 h of consuming 6.4-23.6 ma/cm<sup>2</sup> of current. Interestingly, increasing the number of aluminum screen anode enhances the removal of phenol. The major drawback of this method includes high energy consumption (Kabdaşlı et al., 2012). Electro-coagulation was carried out by using aluminum, stainless steel and iron electrodes for PRWW treatment, and the effect of parameters such as temperature, pH, electrolysis time, current density, electrode arrangement was investigated for the removal of sulfide and COD in the wastewater. High removal of sulfide and COD (93% and 63%, respectively) were attained at an optimum temperature of 25°C and pH of 8 (El-Naas et al., 2009). The electro-coagulation method was used for the removal of sulfide and other caustic pollutants from PRWW by single and double units under the optimum conditions of 30 minutes treatment time, 9 pH, 21.2mA/cm<sup>2</sup> current density, and 72,450 mg L<sup>-1</sup> organic compounds. The study reported removal efficiency of sulfide and COD using a single EC unit in the process. Using two EC units in parallel, maximum removal efficiency of more than 95% of sulfide and COD was achieved (Ben Hariz et al., 2013). The electro coagulation method is advantageous as it can treat colloidal pollutants, heavy metals, emulsions, suspensions present in the wastewater (Ben Hariz et al., 2013).

#### 2.3.4. Other processes

Other than the afore-mentioned techniques for PRWW treatment, some advanced methods have been reported in the literature. PRWW treatment using a catalytic vacuum distillation process is reported in which the effect of different catalysts such as FeCl<sub>3</sub>, Kaolin, H<sub>2</sub>SO<sub>4</sub>, and NaOH was studied for promoting the reaction rate. Among these catalysts, NaOH

was found to be highly effective, which yielded a maximum COD removal of 99% at 35-45° C evaporation temperature (Yan et al., 2010),

In another study, nano-scale, zero-valent iron particles in combination with ultrasound treatment, has been reported for PRWW treatment. Nano-particles are advanced materials with a size in the range of 1 – 100 nm, and a large interfacial surface area. The parameters which mainly influenced COD removal in the process were NIZI dosage and initial pH. A maximum COD removal was achieved at an initial pH of 5 and an NIZI dosage of 0.15 g L<sup>-1</sup> (Rasheed et al., 2011).

Microbial Fuel Cells (MFCs) are another advanced treatment technology reported for PRWW treatment. MFC is a bioelectrical device consisting of microorganisms that convert organics present in the wastewater to electrical energy. The benefits of MFCs are its high treatment efficiency and eco-friendly nature, which helps to reduce pollution. In addition, its ability to generate power from the wastewater treatment process makes it more interesting. A single chamber MFC with electrochemically active anodic bio-film was used for electrogenesis and bio-electrochemical treatment of PRWW (Mohanakrishna et al., 2018), The voltage and maximum current density supplied to operate the MFC were 500 mV and 132 MW/m<sup>2</sup>, respectively. Substrate removal efficiency of 48%, 37%, 32%, 27% were obtained for different applied voltages. Maximum efficiency of 89% at 500 mV was achieved, which is comparatively higher than the control system (59%).

Photo catalytic reactors consist of suspended catalysts and offer very good contact between the photo catalyst and wastewater impurities, thereby improving the treatment efficiency in the reactor. The main advantages of photo catalytic reactors are simple configuration and the high contact surface, whereas low efficiency of incident light and separation of photo-catalyst from the reactor are some of its drawbacks. Saïen and Nejati, (2007) reported the performance of a photo-catalytic reactor with 100 mg L<sup>-1</sup> TiO<sub>2</sub> added as a catalyst and UV intensity 100W. The reactor operated with influent pH 3 and temperature 318K

resulted in more than 90% removal of pollutants from PRWW within 4h irradiation and 73% removal at 90min irradiation time.

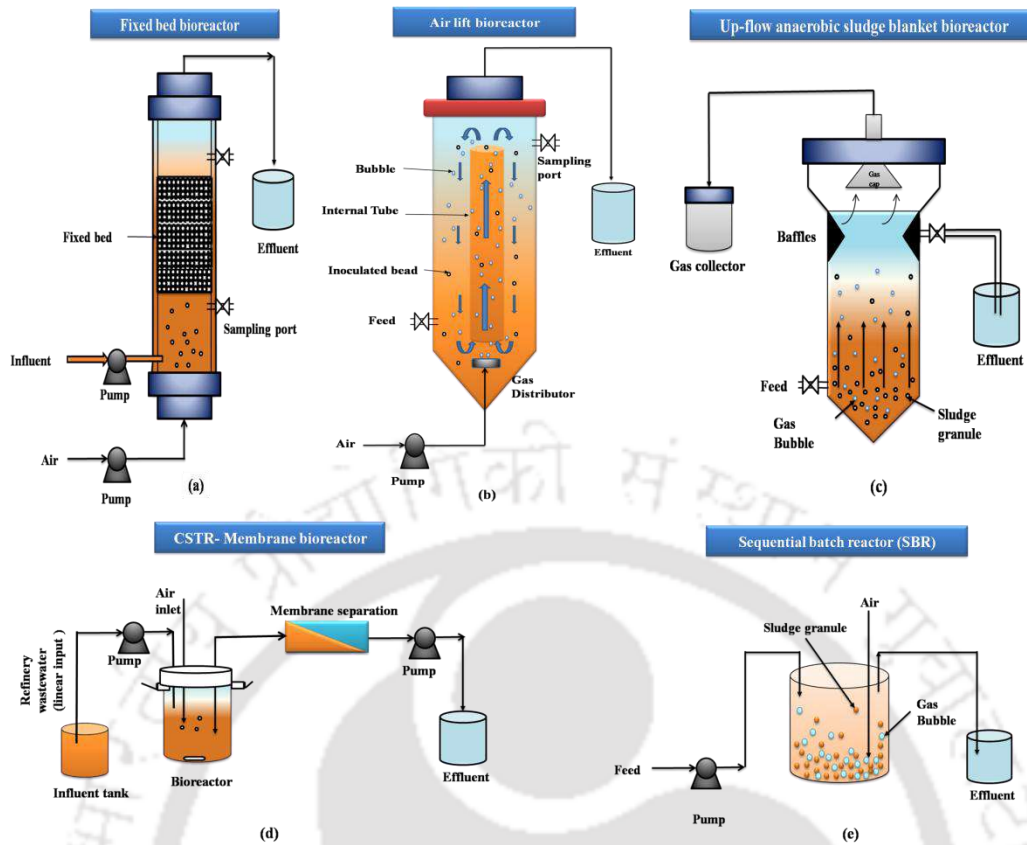
#### 2.4. Bioreactor systems for PRWW treatment

Table 2.1 presents different types of bioreactors configurations used for the treatment of refinery wastewater. Fig. 2.4 illustrates the schematic of different reactor configurations used for treating PRWW.

**Table 2.1** Different bioreactors for treating petroleum refinery wastewater

S. No	Reactor	Treating process	Removal efficiency	Reference
1.	Fixed film bioreactor	Polypropylene beads were used to attain growth of activated sludge	85-90%	Jou and Huang, 2003
2.	Airlift loop bioreactor (ALBR)	Three phase of gas-liquid-solid treatment by activated sludge process	-	Xianling et al., 2005
3.	Up-flow anaerobic sludge blanket bioreactor (UASB)	Digested sludge (anaerobic treatment process)	76.3%	Rastegar et al., 2011
4.	Fluidized bed bioreactor (solid-liquid-gas)	Activated sludge with low density particle	90%	Sokół, 2003
5.	Electro-coagulation, (SBBR) bed bioreactor	Sequence bed bioreactor (SBBR)	97%	El-Naas et al., 2014
6.	Moving bed bioreactor (MBBR)	Activated sludge biomass	62%	Johnson et al., 2000
7.	Hybrid Fenton-	Activated sludge biomass	76.5 %	Diya'uddeen et

	sequencing batch reactor			al., 2015
8.	Sequential batch reactor	Activated sludge biomass	57.8-77.1%	Mizzouri et al., 2013
9.	Moving bed biofilm reactor (MBBR)	Moving bed bio-film reactor, ozonation unit, BAC connected in series	69-89%	Schneider et al., 2011
10.	Anaerobic-aerobic moving-bed biofilm reactor (MBBR)	Ceramsite	85%	Lu, M et al., 2013
11.	Up-flow anaerobic sludge bed (UASB) reactor	Activated sludge biomass	70%	Wang et al., 2016
12.	Aerobic submerged fixed-bed reactor (SFBR)	Convectional biological method of bio-film process	91%	Vendramel et al., 2015
13.	Sequential batch reactor (SBR)	Activated sludge with bio-surfactants	81-97%	Alexandre et al., 2016
14.	Sequential batch reactor (SBR)	Activated sludge biomass	95.3±0.5%	Lee et al., 2004



**Fig. 2.4** Schematic of different bioreactor configurations used for PRWW (a) fixed-bed bioreactor, (b) airlift bioreactor, (c) up-flow anaerobic sludge blanket bioreactor, (d) continuous membrane bioreactor, and (e) sequential batch bioreactor (SBR).

### 2.4.1. Fixed- film bioreactor

A fixed-film bioreactor consists of biomass support material packed inside, and bio-film formation takes place on the surface and within the porous structure of the support material. A fixed film bioreactor offers certain advantages such as simple construction and no external mixing (Acharya et al., 2008). Polyurethane foam slabs with polypropylene are usually used as packing material in the reactor for a high surface area to volume ratio ( $210 \text{ ft}^2/\text{ft}^3$ ). A pilot-scale fixed-film bioreactor operated at pH of 6.5 -7.5, temperature  $15^\circ\text{C}$ - $39^\circ\text{C}$ , and HRT of 8h resulted in 85% COD removal and 100% phenol removal from PRWW (Jou and Huang, 2003). Johnson et al. (2000) studied PRWW treatment using a Moving Bed Biofilm Reactor (MBBR) with activated sludge for enhancing the treatment efficiency. This

study contributed to the scale-up of the process for treating 4514kg/day to 10,454kg/day of ammonia-nitrogen containing wastewater with a maximum COD and BOD removal of 86.5 % and 90%, respectively. MBBR integrated with ozonation helps in enhanced COD reduction and improvement of biodegradability of organics present in PRWW; a biological activated carbon (BAC) column was further used for removing the residual organic matter present in the wastewater. The MBBR operated at an HRT of 12 h could achieve 89 % of COD removal along with a reduction in N-NH<sub>4</sub> concentration below the discharge level of 0.20 mg L<sup>-1</sup>. The BAC column served as an alternative to GAC columns for achieving a very low COD content of 2-4 mg L<sup>-1</sup> in the treated water (Schneider et al., 2011). In a recent study, an anaerobic reactor with a working volume 2L and filled with 50% (v/v) of a bio-carrier was used to achieve 85% removal of both COD and ammonium at 72 and 36 h of HRT respectively (Lu et al., 2013). Although this type of bioreactor has been widely studied for PRWW treatment, its implementation at an industrial scale is challenging in terms of recycling or retention of cells, which increases the initial process cost of the system.

Another configuration is a packed bed reactor, which is a type of tubular reactor with immobilized microorganisms to treat wastewater. High conversion rate, easy and low cost of construction, excellent contact between pollutants and microorganisms, low operation and maintenance costs, etc. are some of its advantages for wastewater treatment. In the literature, Banerjee and Ghoshal, (2017) reported PRWW treatment using two packed bed reactors with immobilized *Bacillus. cereus* onto in the polyurethane foam (PUF) and inside calcium-alginate beads. The removal of COD, TOC, phenolics, total phosphate-phosphorus, and ammonium-nitrogen were analyzed using the bioreactors. Initial values of COD(9200 mg L<sup>-1</sup>), TOC (4548 mg L<sup>-1</sup>), phenolics (3561 mg L<sup>-1</sup>), PO<sub>4</sub><sup>3-</sup>-P 121.1 mg L<sup>-1</sup>, and NH<sub>4</sub><sup>+</sup>-N (121.09 mg L<sup>-1</sup>) were reduced to 70 mg L<sup>-1</sup>, 184.97 mg L<sup>-1</sup>, 8 mg L<sup>-1</sup>, 67.3 mg L<sup>-1</sup>, and 61.3 mg L<sup>-1</sup> by using the bioreactor with the calcium alginate immobilized biomass.

### 2.4.2. Airlift bioreactor

An airlift bioreactor consists of a gas-liquid or gas-liquid-solid pneumatic contacting device and is characterized by a defined cyclic pattern of fluid circulation through channels presented in the bioreactor. The advantages of airlift bioreactors are its flexibility in operation and high efficiency of treatment even at high organic loading (Jianping et al., 2003). Airlift bioreactors have been reported for treating different types wastewater such as nitrate containing wastewater (Loh and Liu, 2001), lubricants containing wastewater (Jianping et al., 2003), high strength phenolic wastewater (Guo et al., 2005), synthetic wastewater containing high amount of nitrogen (Khondee et al., 2012). In a study by Xianling et al., (2005), pilot-scale airlift loop bioreactor operated at optimum parameters of pH of 7.0-8.0, airflow rate of  $3.3 \text{ min}^{-3} \text{ air (m}^3 \text{ liquid h)}^{-1}$  and HRT of 6.5 for treating PRWW resulted in more than 80% COD removal along with a very minimal amount of sludge waste generated which was only one-third of the sludge generated in conventional activated sludge process. However, disadvantages of airlift bioreactors include the requirement of oxygen/air supply for good contact between solids and liquid inside the reactor. Moreover, immobilized microbial cells experience shear damage, which is a major drawback of this reactor configuration (Loh and Liu, 2001).

### 2.4.3. Up-flow anaerobic sludge blanket (UASB) bioreactor

Up-flow anaerobic sludge blanket bioreactor consists of a single tank with an inflow of wastewater at the bottom of the reactor, and the liquid flows through the reactor in the upward direction. In this reactor, mixing takes place due to rising bubbles and without the aid of external mixing system. UASB reactor for wastewater treatment has several advantages as it does not require external mixing and has very low energy requirements (Parawira et al., 2006). UASB reactor has been used for treating different wastewaters such as slaughterhouse effluent (Torkian et al., 2003), high starch containing wastewater (Lu et al., 2015), wastewater from unbleached pulp plant (Buzzini et al., 2006), brewery wastewater, (Chen and Dong, 2005),

potato waste leachate wastewater (Parawira et al., 2006) and municipal wastewater (Nair and Ahammed, 2014). UASB reactor for PRWW treatment is influenced by HRT and inlet COD; high COD removal (81%) has been reported to be achieved within 48h HRT and 500 mg L<sup>-1</sup> influent COD. Additionally, simultaneous biogas production rate of 559 ml h<sup>-1</sup> was achieved with an increase in HRT to 40h (Rastegar et al., 2011). This type of reactor has been investigated for PRWW treatment with different seed sludge concentration of 17.23 g L<sup>-1</sup> MLSS, and 8.74 g L<sup>-1</sup> MLVSS in a total volume of 4.45L; a three-phase separator volume of 0.27 L was used to separate gas and sludge formed inside the bioreactor. Effect of shock loading on the bioreactor performance was conducted at different influent flow rate of 1.81L/d, 2.72 L/d, 3.63L/d, 4.54 L/d at corresponding HRTs of 45h, 30h, 22h, and 18h, respectively. The reactor achieved 70-72% COD removal within 75- 285 days of operation (Wang et al., 2016). However, in UASBR, low pathogen removal, scum formation on surface, which requires frequent removal and less flexibility in operating conditions are main drawbacks.

#### 2.4.4. Fluidized bed bioreactor (FBB)

In a fluidized bed bioreactor, wastewater passes through a solid granular material at a high velocity, which establishes excellent contact between microorganisms and pollutants. Granular material fluidized in the reactor consists of immobilized sludge or microorganisms for biological treatment purpose. The major advantages of fluidized bed bioreactors are uniform particle mixing, uniform temperature gradients, ability to operate the reactor in a continuous state, low HRT, and also high biomass retention (Patel et al., 2006). Fluidized bed bioreactor has been studied to treat different wastewater such as textile wastewater (Şen and Demirer, 2003), acidic wastewater (Kaksonen et al., 2003), diesel fuel contaminated wastewater (Lohi et al., 2008), nitrogen containing wastewater (Jianping et al., 2003), municipal wastewater (Patel et al., 2006). PRWW treatment using FBB is reported using a low density (910 kg/m<sup>3</sup>) polypropylene material with enhanced bio-film formation. At an optimum ratio of bed volume

to bioreactor volume ( $V_b/V_R$ ) of 0.55 and air velocity of  $0.029 \text{ m s}^{-1}$ , 90% of COD removal was achieved using the bioreactor (Sokół, 2003). A novel approach to treat PRWW is reported by electro-coagulation using a fixed bed electrochemical reactor. Although certain constraints such as electrochemical properties and connection issues were encountered in the study, phenolic compound removal of 100% from refinery wastewater (El-Ashtoukhy et al., 2013) was achieved. Countercurrent flow of gas and liquid in the reactor overcomes the disadvantages with the co-current flow of the two-phases in other conventional reactors (Patel et al., 2006).

In another study, PRWW was treated by using moving bed bioreactor with sludge immobilized moving particles inside the bioreactor. Experiments with the moving bed bioreactor were carried out in series mode and the parameters were optimized by employing response surface methodology. 97% removal efficiency of the pollutants was achieved under the operating conditions of 23 h HRT,  $164.78 \text{ mg L}^{-1}$  total hydrocarbon content, and 45% media filling ratio (Qaderi et al., 2018).

#### 2.4.5. Continuous stirred tank bioreactor (CSTR)

Oil refinery wastewater has been reported to be treated by using CSTR in the presence of bio-surfactants to reduce coalescence and disintegrate flakes. Using this reactor system, influent COD of  $3000 \text{ mg L}^{-1}$ , volumetric organic load (VOL) of  $1.2 \text{ kg COD/ m}^3 \text{ d}$ , HRT of 5.5 h, and a total working period of 266 days were followed to achieve COD removal in the range 81-97%. The major drawback of this reactor configuration is the requirement of external mixing. Moreover, this bioreactor systems is more prone to contaminations than other types of bioreactors (Alexandre et al., 2016).

#### 2.4.6. Sequencing batch reactor (SBR)

In a sequencing batch reactor, wastewater is first treated in a batch system with the help of activated sludge and following which the treated water is discharged, like in any

conventional biological treatment process. The SBR is highly efficient in treating wastewater, flexible in operation conditions, low electric power consumption and space (City and Governorate, 2017)

SBR has been reported for treating different wastewaters, such as phenol containing wastewater (Chan and Lim, 2007), ammonium rich wastewater (Li et al., 2011), complex chemical wastewater (Mohan et al., 2005), dairy wastewater (Schwarzenbeck et al., 2005) and soybean processing wastewater (Su and Yu, 2005). In a recent study, SBR was combined with the Fenton oxidation method, which increased the treatment efficiency of PRWW. In this study (Diya'uddeen et al., 2015), the Fenton reactor consisted of a 0.22 mm iron filter, and  $H_2O_2$  was fed at 170 rpm constant stirring for oxidation. The wastewater was subjected to sequencing batch mode of operation for a treatment timing of 10h per cycle to attain maximum biodegradability in the range 0.14-0.37 along with overall COD and TOC removal of 76.5 % and 45%, respectively. Similarly, in another study, SBR was combined with electro coagulation and adsorption column for enhancing PRWW treatment efficiency. Electro coagulation method achieved 90% COD removal and biological treatment using the SBR with immobilized cells of *Pseudonymous putida* on polyvinyl alcohol (PVA). The treated water from SBR was passed through date pits activated carbon (DC-AC) containing adsorption column to further reduce the residual COD (El-Naas et al., 2014). In another study, SBR was connected in series for treating of oil refinery wastewater with 4000 mg L<sup>-1</sup> of COD along with oil and grease (O&G). The feed rates of 1<sup>st</sup> and 2<sup>nd</sup> stage SBR were 5.0-7.5 mg/COD/mg MLVSS/d and 1.5-1.8 mg COD/mg MLVSS/d respectively, STR of reactors was 24 d to attain COD removal of SBR 47±2.4 % and 95.3±0.5%. Overall removal of COD with the two-stage reactor was 97±16 mg L<sup>-1</sup> (Lee et al., 2004). Despite the high treatment efficiency with the SBR, some of its drawbacks include low pathogen removal and high maintenance cost (City and Governorate, 2017).

## 2.5. Advanced membrane bioreactor systems for PRWW treatment

### 2.5.1. Integrated membrane bioreactor (MBR)

A cross-flow- membrane bioreactor consists of a membrane in cross-flow direction to the interior of the bioreactor. The major advantages of this system include low membrane fouling due to the cross-flow operation, ability to work with high MLSS and under high flux, excellent permeate quality and prolonged membrane life. CF-MBR was reported for the treatment of PRWW under optimum HRT of 21h to achieve a maximum of 94% COD removal efficiency with an MLSS loading of  $3000 \text{ mg L}^{-1}$ . The membrane surface was cleaned by backwashing with an acidic detergent to avoid fouling. PRWW also contains highly recalcitrant surfactant and lubricating oil, which can be treated by using CF-MBR under optimum operating conditions of DO- $3 \text{ mg L}^{-1}$ , HRT-13.3 h, and the temperature  $30^\circ\text{C}$  (Fuchs, 2000). More than 99% removal of surfactant and 98% removal of lubricant along with 93-98% removal of COD were achieved in the study. The main drawback of the cross-flow membrane separation process is maintaining constant pressure, which reduces the treatment efficiency of the system by membrane fouling.

### 2.5.2. Submerged membrane bioreactor (SMBR)

In this membrane bioreactor configuration, the membrane is directly submerged inside the bioreactor, and biomass separation takes place by applying suction pressure inside the membrane. SMBR is relatively economical in treatment, which helps in achieving high biomass recovery in a continuous process. This type of configuration has been reported for the treatment of oil refinery wastewater with maximum COD removal of 67% and a very high biomass recovery of 64% by the membrane filtration process (Viero et al., 2008). Membrane fouling phenomenon is, however, the most predominant drawback of this bioreactor, which is contributed by microbial products such as polyetherimide (PS) and proteins (PT) (Yuliwati et al., 2012). The major parameters that need to be optimized for operating this bioreactor include

air bubble flow-rate (ABFR), hydraulic retention time (HRT), mixed liquor suspended solids (MLSS) concentration and pH. In a study by Yuliwati et al. (2012), at optimum values of 2.25 ml min<sup>-1</sup>, 276.93 min, 4.50 g L<sup>-1</sup>, and 6.5, respectively of the afore-mentioned parameters, maximum COD removal efficiency of 90.28% was allowed. In another study, membrane ON/OFF condition as an alternative method was followed for reducing membrane fouling and enhance the biomass separation efficiency with constant flux (Zhidong et al., 2009). The optimum conditions followed in this study were influent flow rate of 42 L/h and pH: 6.2 - 7.0. The membrane filtration was carried out with 13 min on and 2 min off, and the removal of COD, total phosphorus (TP), total suspended solids (TSS), suspended solids (SS), and phenol, BOD<sub>5</sub>, NH<sub>3</sub>-N, oil, and turbidity were 92%, 93.7%, 75.3%, 94.6%, 98.5%, 97.9%, 93.8%, and 99.9% respectively. Integrated submerged membrane bioreactor under, anaerobic/aerobic conditions, has been studied for achieving a very high removal of COD, BOD, nitrogen, and phosphorus (Zhidong, 2010). In another study, an Integrated Submerged Membrane Bioreactor Anaerobic/Aerobic (ISMBR-A/O) system with an airflow rate of 42L/hr, and 13min on/4min off mode yielded an overall removal of COD and BOD of 91% and 90%, respectively. Denitrification and nitrification processes were carried out using the anaerobic and aerobic tank systems. The main drawback of the cross-flow membrane separation process is maintaining constant pressure. Fig. 2.5 shows a schematic of the submerged membrane-based separation process studied for wastewater treatment.

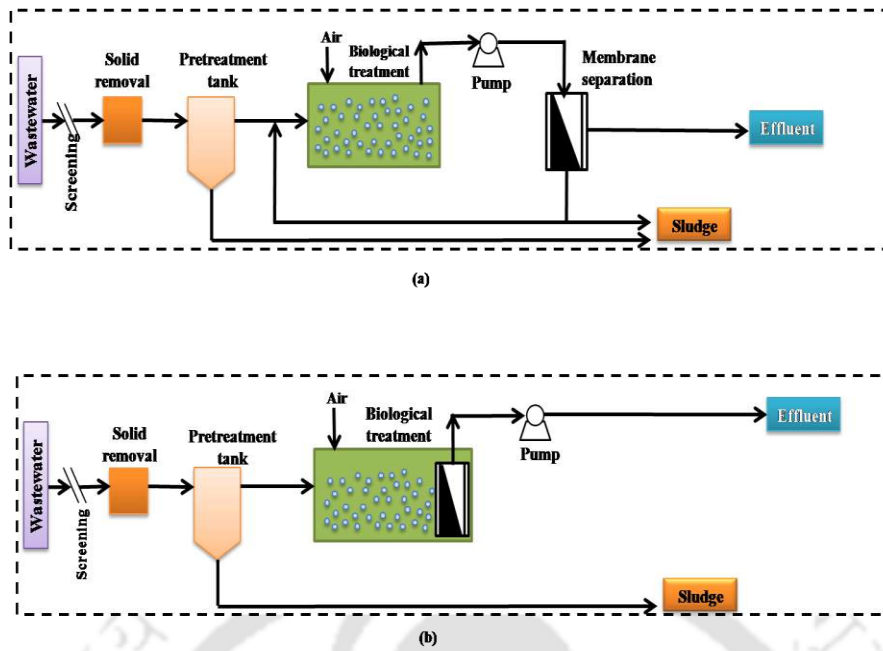


**Fig. 2.5** Schematic showing (a) membrane bioreactor and (b) submerged membrane bioreactor

Membrane sequencing batch reactors have been used to treat synthetic petroleum refinery wastewater at different HRT of 8, 16, 24 h, which yielded nearly similar removal efficiency of hydrocarbon pollutants present in the wastewater. Relationship between HRT and MLSS concentration was studied, and the results showed a significant decrease in MLSS with an increase in the HRT. The membrane fouling rate was directly proportional to the sludge particle size, apparent viscosity and soluble microbial products (SMP) concentration (Shariati et al., 2011)

**Table 2.2** Different membrane bioreactor configuration studies for treating PRWW

S.NO	Membrane bioreactor configuration	COD removal (%)	Type of membrane	Membrane composition	Pore size of membrane ( $\mu\text{m}$ )	Surface area of membrane ( $\text{m}^2$ )	Reference
1.	Submerged membrane bioreactor (A/O SBR)	90	Flat sheet membrane module	Polyvinylidene fluoride (PVDF)	0.08	0.45	Zhidong et al., 2009
2.	Submerged membrane sequencing batch reactor	80	Flat sheet membrane module	Chlorinated polyethylene	0.4	0.11	Pajoumshariat i et al., 2017
3.	Submerged membrane bioreactor	89.4	Hollow fiber modules	Polyvinylidene fluoride	0.040	0.9	Alkmim et al., 2016
4.	Submerged membrane bioreactor	90	Flat sheet membrane of three	Chlorinated polyethylene	0.4	0.3	Llop et al., 2009
5.	Submerged membrane bioreactor	93	Flat sheet membrane	Chlorinated polyethylene	0.4	0.3	Wiszniowski et al., 2011
6.	Membrane bioreactor (MBR)	69-86	Hollow fiber membrane module	Polyvinylidene fluoride	0.04	21.7	Di Fabio et al., 2013
7.	CSTR-membrane bioreactor	99	Tubular ceramic membrane	Low-cost inorganic precursors	0.339	-	Paul et al., 2019
8.	Ultra-filtration method by using membrane		Hollow fiber membrane module	Modified PVDF membrane were lithium chloride	0.01493-0.0282	0.1142	Yuliwati and Ismail, 2011

				monohydrate (LiCl·H <sub>2</sub> O) and titanium dioxide (TiO <sub>2</sub> ) nanoparticles			
9.	Hollow fiber membrane bioreactor	82	Hollow- fiber membrane	Polypropylene	0.1-0.2	0.39	Razavi and Miri, 2015
10.	Submerged membrane bioreactor (MBRs)	90.8	Hollow- fiber membrane	Polyvinylidene fluoride	0.3405	1.84	Yuliwati et al., 2012
11.	Membrane bioreactor (MBR)	97.5	Hollow- fiber membrane	Teflon membrane	0.45	0.012	Pendashteh, A. R et al, 2012
12.	Membrane bioreactor (MBR)	94-96	Tubular cross flow membrane	Polyvinylidene fluoride	-	0.23	Fuchs, 2000
13.	Submerged membrane bioreactor (MBRs)	67	Hollow- fiber membrane	Polyetherimide	0.3	-	Viero et al., 2008
14.	Cross-flow membrane bioreactor (CF- MBR)	82-97	Hollow tubular	Alumina ceramic	0.2	0.022	Rahman and Al-Malack, 2006
15.	Submerged membrane bioreactors (MBRs)	90	Flat sheet membranes	Poly- vinylidene fluoride	0.1	0.02	Yu et al., 2018
16.	Integrated submerged membrane bioreactor (ISMBR-A/O)	91	Flat sheet membrane	Polyvinylidene fluoride	0.08	0.45	Zhidong, 2010

### 2.5.3. Membrane bioreactor (MBR)

A membrane bioreactor combines biological treatment and membrane separation for removing organics and suspended solids in the treated water. Membrane bioreactors have been reported to treat several types of wastewater, such as municipal wastewater (Mohammed et al., 2008), hyper saline oily wastewater (Pendashteh et al., 2011), high strength wastewater (Fu et al., 2009), explosives process wastewater (Zoh and Stenstrom, 2002). Table 2.2 presents different types of membrane bioreactors studied for the treatment of PRWW. Membrane bioreactor with activated sludge has been proved effective for hydrocarbon removal from PRWW. Hyper saline oily synthetic wastewater was treated by using MBR with combined SBR, which could handle high organic loading conditions. The main operating parameters were determined to be DO, temperature, pH, and HRT. The removal efficiency of COD, TOC, oily, and grease was 97.5%, 97.2%, and 98.9%, respectively (Pendashteh et al., 2012). In another study, PRWW was treated using an MBR system with a hollow fiber membrane by initially seeding the reactor with activated sludge in fed batch mode. Airflow rate of 70 L/min, reactor temperature of 20°C, HRT of 25-36h, and mixed liquor suspended solids (MLSS) concentration of 3-6.6 g L<sup>-1</sup> were maintained in this study. Under these optimum conditions, the removal of COD, BOD<sub>5</sub>, TSS, VSS and turbidity were 82%, 89%, 98%, 99% and 98%, respectively (Razavi and Miri, 2015).

In another study, by (Yuliwati and Ismail, 2011), membrane separation efficiency was enhanced following addition of additives such as lithium chloride monohydrate (LiCl·H<sub>2</sub>O) and titanium dioxide (TiO<sub>2</sub>) nano-particles in different (*wt %*) ratios of 19 *wt%* of PVDF and 1.95 *wt%* of TiO<sub>2</sub>. It was observed that 18.3% of flux got reduced in case of membrane without any added additives. In another study, sequencing batch reactor with membrane separation was used for treating PRWW with 510.3-3234 mg L<sup>-1</sup> of activated sludge. The MSBR was operated at a fixed SRT, HRT, total cycle time and volume exchange ratio of 8h, 4h, 0.5 respectively

and temperature of 27°C for achieving COD and TOC removal of 92.6% and 93.6% respectively. The foulants in the cake layer were removed by adding 1% (v/v) sodium hypochlorite (NaClO) followed by 1% (w/v) oxalic acid during backwashing of the membrane. The cake layer formed in the membrane was analyzed and identified as foulants containing functional groups such as carbonate, nitrates, and sulphate esters, aldehyde and acids that were hydrolysis products of hydrocarbons present in the wastewater (Pajoumshariati et al., 2017).

In another study using a membrane bioreactor, filtration was employed by adding cationic polyelectrolyte which enhanced the sludge filterability and reduced the membrane fouling (Alkmim et al., 2016). Different dosage of cationic polyelectrolyte with operating conditions of 8 h HRT, 45 days sludge retention time, of 16 L/m<sup>2</sup>/h<sup>1</sup> permeate flow, 15 seconds backwash and 25 L h<sup>-1</sup> flow, 3.6 L h<sup>-1</sup> biological tank flow and of 3.0 L h<sup>-1</sup> membrane tank, pH 7 for 220 days yielded 89.4% of COD removal. Llop et al. (2009) reported membrane bioreactor for treating PRWW under the operating conditions of pH 9, HRT 12.5 and 5h, DO 1-2 mg L<sup>-1</sup> and filtration time for 9 min with 1 min of rest to avoid membrane fouling. Removal of COD and TOC at these optimum conditions were 92% and 83%, respectively. The pollutant present in the wastewater were identified as hydrocarbons, alkyl benzenes, phenols, acidic acids, and esters by using sequential solid phase extraction (SSPE) and gas chromatography-mass spectrometry (GC-MS) analyses. Synthetic refinery wastewater was reported to be treated using a seed culture of activated sludge in a plug flow membrane bioreactor (PF-MBR) at working conditions of temperature 22±4 °C, DO maintained at 1-4 mg L<sup>-1</sup>, solid retention time of 75±14 d and HRT of 25±3 h. Following acclimatization of the sludge to treat the wastewater, enhanced removal of COD, TOC, and BOD were obtained with the values 93%, 96% and 100% respectively along with simultaneous removal of ammonia by oxidation to nitrate (99%) (Wiszniewski et al., 2011). Membrane bioreactor is considered as a novel approach where researchers can work under transient conditions of external carbon source for

the anoxic reactor, low anoxic compartment volume for aerobic reactor, alternation in configuration of adding acetic acid in aerobic reactor and increase in the influent load. Influent COD ( $\text{mg L}^{-1}$ ) of refinery wastewater feed was varied from  $108.0 \pm 19.7$ ,  $74.1 \pm 31.5$ ,  $195.8 \pm 22.1$ ,  $101.7 \pm 28.1$ ,  $222.7 \pm 27.1$  respectively. The overall removal of COD and organic nitrogen were 69-86% and 29-60%, respectively (Di Fabio et al., 2013). The effect of solids retention time (SRT) on treatment of synthetic oil refinery wastewater was studied using three submerged membrane bioreactors (MBRs) connected in series at MLSS concentrations of 4000, 7000, 10000  $\text{mg L}^{-1}$ , respectively and SRTs of 10, 30, 60, respectively (Yu et al., 2018). The overall removal of COD of the MBR system was 90% and the removal of toluene, anthracene was 99%. However, the major drawback in the case of membrane is its fouling due to chemicals and solid particles which hinders the efficiency of the treatment process.

## 2.6. Toxicity assessment

*In-vitro* toxicology studies include a series of methods followed by various pharmaceutical industries as well as regulatory bodies for evaluation of toxicity, safety, and risk involved with any product/environmental sample. These tests are performed based on all events occurring *in vitro*, including cellular and molecular correlated with all physiological changes occurring in a body (*in vivo*). Hence, a selection of suitable *in vitro* assay provides a better understanding of an overall detailed outcome along with specific events occurring *in vivo*. The main principles of *in vitro* toxicology assays ensure bridging the gap between animal-based toxicity screening assays and new cell/tissue-based *in vitro* testing, which includes 3Rs (Reduction, Refinement, and Replacement) (Srivastava, 2018). The very first R focuses on the reduction of animal practices to a few by applying statistical designs. In contrast, the second R refinement focuses on reducing pain to the animals used for testing. However, the third R replacement emphasizes the use of techniques based on cell lines and tissues, thus reducing the use of animal testing.

Most of the regulatory authorities are committed to specific guidelines following *in vitro* testing methods for toxicity assessment. There is a rising concern based on ethical practices on animal-related experimental protocols. Thus, the adoption of the 3Rs principle for toxicity assessment is essential, focusing more on reducing animal testing and encouraging more *in vitro* based test assays. Cell culture tests are being evaluated for further validation in the United States (U.S.) and European Union (E.U.) (Barile and Cardona 1998). Good Cell Culture Practices (GCCP) share regulatory guidelines focusing on proper protocol for cell culture testing in a laboratory, which includes six main principles as detailed by Srivastava (2018). The first performed biocompatible assay prior to *in vivo* testing is cyto-toxicity assay. These tests follow GCCP guidelines and reduce the non-essential testing on animals for toxicity analysis. However, various assay methods and regulatory approvals in toxicity studies are mentioned in Table 2.3.

**Table 2.3** Various assay methods and regulatory approvals in toxicity studies

Serial No.	Toxicity	Assay methods	Regulatory approvals & standards	References
1.	Cyto-toxicity	Agar diffusion, MTT, CFU, NRU, MEM elution, Direct contact test	ISO 10993-5 FDA., 2016 MHLW., 2012	Goud, 2017; Srivastava et al., 2018
2.	Genotoxicity	FISH, Metaphase analysis, Ames assay	ISO 10993-3 ISO 10993-33 OECD guidelines	Goud, 2017; Srivastava et al., 2018; Ames et al., 1975;
3.	Systemic toxicity	Material-mediated pyrogen test, Bacterial endotoxin (limulus amoebocyte lysate) test	ISO 10993-11	Goud, 2017; Srivastava et al., 2018

				Goud, 2017; Srivastava et al., 2018;
4.	Immuno-toxicity	MTT, Human whole-blood cytokine release assay	ISO 10993-20 (TS)	Lankveld et al., 2010
5.	Drug toxicity	DAPI, PI assay, Caspase 3/7 assays	FDA, NDA, IND FDA OECD TG-418 OECD TG-419 OECD TG-424	Li et al., 2005; Srivastava et al., 2018;
6.	Neurotoxicity	MTT, LDH assay, Trypan-blue exclusion	OECD TG-426 OECD- 414 OECD- 415	Srivastava et al., 2018; Harry et al., 1998 Goud, 2017;Srivastava et al., 2018;
7.	Embryo-toxicity	FACS-EST method, Embryonic stem cell test	OECD- 416 OECD- 421	Seiler et al., 2011

[MTT- 3-(4,5-dimethylthiazol-2-yl)-2,5-diphenyl tetrazolium bromide, CFU- Colony Forming Unit, NRU- Neutral Red Uptake, MEM- Minimal Essential Medium, FISH- Fluorescence *In situ* Hybridization, DAPI- 4,6-diamidino-2-phenylindole, PI-Propidium Iodide, LDH- Lactate Dehydrogenase, FACS-EST- Fluorescent Activated Cell Sorter – Embryonic Stem Cell Test, OECD- Organization for Economic Cooperation and Development, OECD (TG)- Organization for Economic Cooperation and Development (Test guidelines), FDA- Food and Drug Administration, NDA- New Drug Application. IND-Investigational New Drug, ISO- International Organization for Standardization, MHLW- Ministry of Health, Labour and Welfare].

### 2.6.1. Cyto-toxicity assays

#### 2.6.1.1. Minimal essential medium (MEM) elution assay

Minimal essential medium (MEM) Elution assay is one of the critical tests designed for assessment of toxicity of extract/elute from a device on L929 cells in tissue culture media. Following incubation, percentage of cells lysed or deformed, confirms the reactivity grade to be normal, moderate or severe. This test is sensitive for biomedical devices intended for use with limited tissue contacts, such as ocular devices or lens care solutions (Lehmann and Richardson, 2010, Liu et al., 2018). Another assay commonly used *in vitro* cyto-toxicity assay,

and it is designed to check the presence of any toxic material eluted from a test sample in the presence of confluent L929 cell cultures. Similarly one of the most characteristic feature of viable cells in toxicity determination is their indefinite proliferation (Puck and Marcus, 1956; Rafehi et al., 2011). Viable cells contain integrity synthesizing proteins and DNA to form a colony (50 cells), which can be visualized through the naked eye (Puck and Marcus, 1956; Rafehi et al., 2011). The colony-forming assay effectively measures cells' ability to proliferate within a sample, and it is one of the most commonly used tests for hematopoietic stem and progenitor cells (HSPCs). The cell's ability to differentiate is analyzed by observation of the colonies (consisting of more differentiated cells), which are produced by first progenitor cells.

#### **2.6.1.2. Colony Formation Assay (CFA)**

One of the most characteristic feature of viable cells in toxicity determination is their indefinite proliferation (Puck and Marcus, 1956; Rafehi et al., 2011). Viable cells contain integrity synthesizing proteins and DNA to form a colony (50 cells), which can be visualized through naked eye (Puck and Marcus, 1956; Rafehi et al., 2011). The colony-forming assay effectively measures cell's ability to proliferate within a sample, and it is one of the most commonly used tests for hematopoietic stem and progenitor cells (HSPCs). The cell's ability to differentiate is analyzed by observation of the colonies (consisting of more differentiated cells), which are produced by first progenitor cells.

In this assay, log-phase cells are carefully cultured in a six-well plate where only a few live cells are added (50 cells/well) to avoid overgrowth and overlapping colonies with high cell densities, which are otherwise difficult to count. After incubating the plate containing the cells for 6-9 days, the cells are fixed with methanol and stained with Giemsa stain solution. The test sample is considered potentially cytotoxic, if plating efficiency with highest concentration of the sample is less than 70% of the negative control group.

This assay is universally accepted as a standard method for testing cell viability and proliferation (Franken et al., 2006; Munshi et al., 2005; Rafehi et al., 2011; Sinclair, 1964; Sinclair and Morton, 1963). Moreover, this assay can be used with suitable modification to analyze other specific cellular processes like apoptosis (Gavrieli et al., 1992; Katz et al., 2008; Vermes et al., 1995) and senescence (Muir et al., 1990, Bassaneze et al., 2008; Debacq-Chainiaux et al., 2009), which can be time consuming as these processes are evaluated independent of colony counting. However, in this method cells can undergo physical/mechanical damage due to their direct contact with test materials. Moreover, size of the colony formed by this method is not specified in ISO and other standards (ISO 10993-5, 2009; MHLW, 2012).

### 2.6.1.3. Hen's Egg test-Chorioallantoic Membrane Test (HET-CAM)

Chicken embryo has been used as a simple model with different advantages for testing embryo-toxicity (Luepke, 1985). Due to increase in number of chemicals being produced by industries that affect the environment, rapid and reliable methods are required for evaluating the toxicity of these compounds. The Hen's Egg Test, or Hühner-Embryonen-Test (HET) is one such rapid, cost-effective and sensitive test that provides information on teratogenicity, embryotoxicity/embryoletality, systemic toxicity, including immunopathology and metabolic pathways and immune-pathological effects of chemical substances. Chick embryo chorioallantoic membrane (CAM) is an alternative model for distinctive toxicological testing. Besides, this model serves between *in vivo* and *in vitro* testing systems, and hence there are no conflicts of ethics and legal standards for using this method. Although this method cannot completely replace animal testing and toxicity testing trials on mammals, it can reduce the number of comprehensive investigations performed on animals, thus overall reducing the pain and suffering caused to animals during animal testing protocols.

In addition to toxicity assessment of environmental samples, this method is useful to predict the toxicity of lab chemicals and their possible irritation to the human eye. In this testing, the test sample is directly applied to the CAM of chicken eggs on the 9<sup>th</sup> day of embryogenesis. For exposing the chorioallantoic membrane, following 9 days of incubation, the eggshell is scratched on the 10<sup>th</sup> day and pared off by applying 0.9% NaCl at 37 °C. Test samples are then applied to the membrane. The allantois present in chick embryo functions to maintain its viability, thus facilitating the embryonic respiration, excretion and storage. It increases in size and surrounds the embryo with the chorion to form CAM. A positive control used in this method is 0.1 N NaOH and 1% sodium dodecyl sulfate, whereas negative control is 0.9% NaCl. Potential irritation index is calculated using the following equation (Spielmann et al 1996).

$$\text{Irritancy potential} = \frac{(301-H) \times 5}{300} + \frac{(301-V) \times 7}{300} + \frac{(301-C) \times 9}{300} \quad (\text{Eq. 2.1})$$

Where, H is the time in seconds at which haemorrhage appears, V is the time in seconds at which vasoconstriction occurs first and C is the time in seconds at which coagulation of protein or blood is first noted. Hence, toxicity of the sample can be determined by the acute irritating effects. The endpoints of lysis, haemorrhage and coagulation are assessed during an observation period of 5 min after the application of a test sample at the CAM.

For each sample, 6 eggs are taken and based on the calculated score, samples are classified as non-irritant (0.0-0.9), slightly irritant (1.0-4.9), moderately irritant (5.0-8.9) or strongly irritant (9.0-21.0). Detailed protocol followed in this method is reported by Barile and Cardona (1998). This test is useful for evaluating ocular corrosion and other severe effects as defined by U.S., the E.U. (2001) and by the U.N. GHS of Classification and Labelling of Chemicals (UN,

2003). HET-CAM test is suggested as a suitable alternative to the Draize rabbit eye test for ocular toxicity assessment (ICCVAM, NIH Publication No. 06-4511, 2006).

#### 2.6.1.4. MTT assay

MTT assay is a quantitative colorimetric cytotoxicity assay based on the reduction of a yellow dye, 3-(4,5-dimethylthiazol-2-yl)-2,5-diphenyl tetrazolium bromide, by the mitochondrial enzyme succinate dehydrogenase. It is high throughput, rapid assessment of cell viability, metabolism and function (Berridge et al., 2005). The main principle of this assay is based on the ability of mitochondrial dehydrogenase present at cytochrome b and c sites of a living cell that can cleave the tetrazole ring present in MTT, thus reducing the water-soluble MTT to purple crystalline formazan. These insoluble crystals are soluble in DMSO (dimethyl sulfoxide). Hence, the number of live cells present can be directly correlated with the amount of formazan present.

This assay is widely used by researchers for toxicity assessment of anti-cancer drugs, antibodies, environmental contaminants, extractable materials from biomedical devices, etc. Besides, this method has been used for confirmation of toxic components present in industrial wastewater (Yang et al., 2015). The main advantages of this assay include fast screening of many samples, all together in a 96 well plate. It gives the quantitative viability of cells, which is an added advantage of this method. However, this assay cannot give any information about the underlying cell death phenomenon or mechanism of cell death, i.e., induced cell death or apoptosis, thus it detects cell death at the later stages only. In this method, the cell lines ( $1 \times 10^4$  cells per well) are seeded in 96 well plates and treated with test articles, and incubated for 24, 48 and 72 h in a humidified incubator at 37°C. Following incubation, the cells are stained with MTT and incubated for another 2 h (Fig. 2.6). The insoluble purple formazan formed is then dissolved in DMSO and its absorbance is measured at 570 nm. The results are compared with that of control for toxicity evaluation. Hence, cytotoxicity of the test material is calculated

based on the insoluble formazan crystals formed, which is largely dependent on the MTT concentration, availability of metabolically active cells and incubation time (Riss et al., 2004; Van de Loosdrecht et al., 1994). An overview of this assay is shown in Fig. 2.6. In addition to the disadvantages with the afore-mentioned tests, this tetrazolium dye-based assay has certain other limitations. The cell growth and metabolism might be hindered when the growth is inhibited due to excessive cell adhesion (Green 2012, Riss et al., 2004). Moreover, certain reducing agents that affect the mitochondrial function and MTT formazan formation can interfere with the results (Bruggisser et al., 2002).

#### 2.6.1.5. Brine shrimp lethality assay (BSLA)

Brine shrimp lethality assay (BSLA) is another one such assay for toxicity assessment of the treated water. Brine shrimps (*Artemia salina*) nauplii are easy to hatch in a hatching tank with simulated seawater (2.5% saline) under constant illumination and aeration for 24 h, as reported in the literature (Meyer et al., 1982; Ahmed et al., 2016). Hence, the main advantage of this assay is it can be performed in laboratory any time.

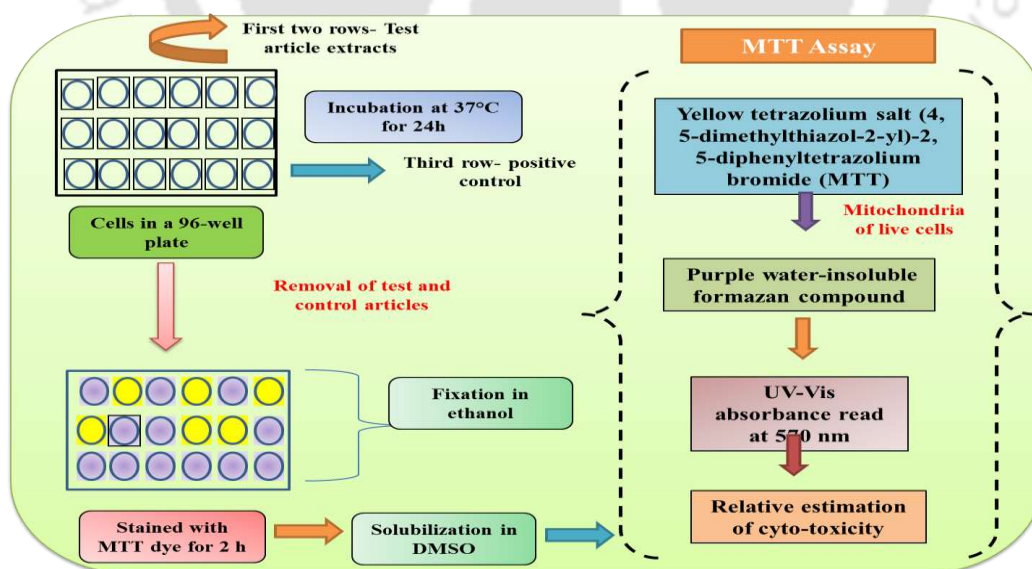


Fig. 2.6 Overview of MTT assay

### 2.6.2. Phytotoxicity assay

Phytotoxicity/eco-toxicity analysis is another most important method to analyze toxicity of any sample for avoiding environmental risk (Tiquia et al., 1996). Estimation/calculation of seed germination index (GI) is an important parameter for phytotoxicity analysis. It is one of the most reliable tests carried out in research labs because of its simplicity and easy analysis of the results. This assay is widely used to test toxic substances and some other physical and chemical properties of compost (Zucconi et al., 1985). Removal of phytotoxic compounds following the wastewater treatment process increases the GI % when compared with a control (untreated raw wastewater).

The Germination index (GI) combines measure of relative seed germination (G%) and relative root elongation (L%) upon treatment with a test sample (Tiquia et al., 1996). It has been noted that a GI value of 80% indicated the disappearance of phytotoxins in composts (Zucconi et al., 1981; Tiquia et al., 1996). However, a GI% of 50 infers a phytotoxin free sample (Zucconi et al., 1981). For a better assessment of the wastewater treatment efficiency following various different treatment process in a reactor, ecotoxicity of the sample can be used for seed germination, and the results can be compared with control for interpretation of the data using chickpea (*Cicer arietinum* L.) seeds.

### 2.7. Biomass for bio-oil production

The distribution of macromolecules varies among different types of biomass, such as herbaceous, lingo-cellulosic, waste biomass and oleaginous biomass. Amongst the different biomass types, oleaginous biomass consists of carbohydrates (cellulose, starch, and sugars), proteins and lipids. Additionally, the elemental composition in terms as amount of carbon (C), nitrogen (N), hydrogen (H), sulphur (S) and oxygen (O) in the cell structure of the biomass is important as the elements C and H contribute to the overall heating value of the bio-oil (de Caprariis et al., 2017).

### 2.7.1. Lignocellulosic biomass

Ligno-cellulosic biomass is abundant in nature with a lot of potential as primary feedstock for producing a wide range of products including bio-crude oil. The major constituents of a woody/lignocellulosic biomass are hemicelluloses (15-47%), cellulose (20-50%) and lignin (8-35%), which make it highly complex with a rigid crystalline matrix (Shen et al., 2017). Ligno-cellulosic biomass thus has promising applications towards bio-crude production, but certain drawbacks still limit its commercial application (Xue et al., 2016). The rigid structure of the lingo-cellulosic biomass is challenging and requires pretreatment for bio-crude oil production, which further increases the production costs.

### 2.7.2. Waste biomass

Different types of residual biomass and waste generated from municipal and industrial sectors, which can be used as a feedstock for bio-crude oil production, received huge interest for years. Diverse types of waste biomass can be replaced as feedstock for bio-crude oil production, viz. swine manure (He et al., 2000; Xiu et al., 2010; Vardon et al., 2011), cattle manure (Ocfemia et al., 2006; Yin et al., 2010), sewage sludge (Goudriaan et al., 2000; Zhai et al., 2014; Fonts et al., 2012; Malins et al., 2015), garbage waste and cattle manure (Minowa et al., 1995; Wang et al., 2011). Solid wastes and swine manures were tested as feedstock, but the produced bio-crude oil showed unfavorable properties as a biofuel and hence required additional fractionation units (Skaggs et al., 2018).

### 2.7.3. Oleaginous microorganisms

Several studies suggest that almost any kind of waste can be processed for obtaining bio-crude oil. However, it involves the collection, transportation and efficient pretreatment, which substantially increase the overall production costs. Therefore, considering the drawbacks associated with the use of lingo-cellulosic and waste biomass, microorganisms,

particularly oleaginous microorganisms, have gained importance for bio-crude oil production.

Table 2.4 compares the different types of microorganisms reported for bio-oil production.

**Table 2.4** Comparison of different types of microorganisms for bio-oil production

Microorganism	Advantages	Disadvantages
Micro/Macro algae	<ul style="list-style-type: none"> <li>Fatty acid composition similar to that of common vegetable oils</li> <li>Under certain condition, lipid content could be as high as 85% of the dry weight</li> <li>Short-time growth cycle</li> </ul>	<ul style="list-style-type: none"> <li>Most algal lipids have a lower fuel value than diesel fuel</li> <li>Currently, the cost of cultivation is higher compared to common crop oils</li> </ul>
Bacteria	<ul style="list-style-type: none"> <li>Fast growth rate</li> </ul>	<ul style="list-style-type: none"> <li>Most of the bacteria do not yield lipids but complicated lipoids</li> </ul>
Yeast	<ul style="list-style-type: none"> <li>Relatively abundant</li> <li>High oil content in some species</li> <li>Short-time growth cycle</li> </ul>	<ul style="list-style-type: none"> <li>Filtration and cultivation of yeasts and mildews with high-content oils are required</li> <li>The processing of oils extracted from oleaginous yeast is complex and existing technology is insufficient</li> </ul>
Fungi	<ul style="list-style-type: none"> <li>Growth under different cultivation conditions is possible</li> </ul>	<ul style="list-style-type: none"> <li>The cost of fungus cultivation is currently high compared to that of oil yielding common crops</li> </ul>

## 2.8. Oleaginous microorganisms

Oleaginous microorganisms are primarily defined as microbes that possess the ability to convert carbon substrates into tri-acylglycerides (TAGs) and accumulate it intracellularly. The accumulated lipid content can be as high as 87% of the dry weight of the microbial biomass (Shruthi et al., 2014). Fig. 2.7 shows TEM images of *Scenedesmus* species having accumulated lipid globules. The oil accumulates in the biomass cell structure mainly in the form of polar lipids, triacylglycerides, free fatty acids, sterols, pigments and hydrocarbons. TAGs accumulated in most eukaryotic organisms are generally non-polar, water-insoluble fatty acid triesters of glycerol (Alvarez and Steinbuchel, 2002). These microbial lipids (single cell

oils) are potential sources for biodiesel production. Conversion of the whole oleaginous microorganisms for bio-crude production is less explored.

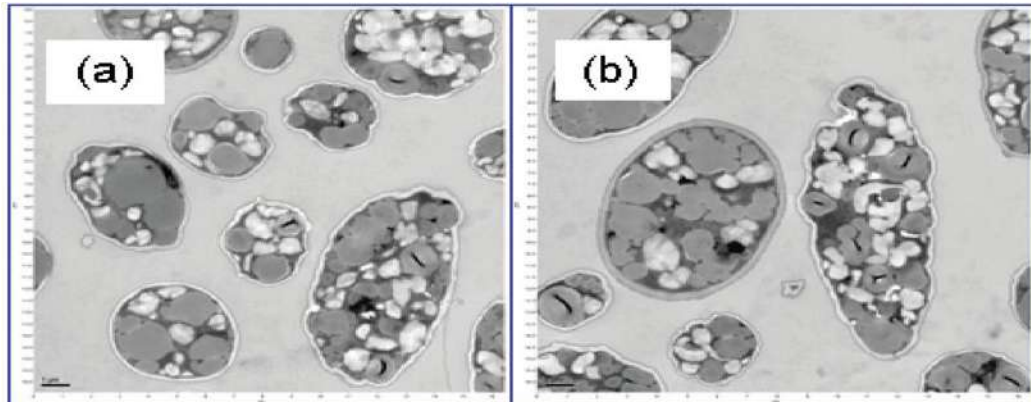


Fig. 2.7 TEM images of high-lipid *Scenedesmus* biomass (Adapted from Lai et al., 2016)

In case of HTL, conversion of lipids, carbohydrates and proteins present in the biomass follow the order: lipids>proteins>carbohydrates (Biller and Ross, 2011). Lipid conversion to bio-oil by HTL has been recently described in Paul et al. (2020).

### 2.8.1. Composition of oleaginous biomass

An oleaginous microbe primarily comprises of lipids, glycerol, protein/amino acids and other carbohydrates, among which the total lipid and protein content accounts for approximately 50% by wet basis (Paul et al., 2019). Lipids are an effective form of energy with a high energy value of about 39 kJ/g. Lipids are non-polar compounds and water-insoluble at normal conditions. Degradation of lipids produces glycerol, which can be fragmented to acetaldehydes, propionaldehydes, allyl alcohol, formaldehyde, ethanol, CO, CO<sub>2</sub> and H<sub>2</sub> (Dong et al., 2016). Almost all quantity of lipids can be converted to bio-crude oil by a high temperature (250- 350 °C) treatment without any intermediate formation (Li et al., 2014).

The composition of lipid produced by different bacteria varies from other lipid produced. A typical pathway for TAG (Triacylglycerol) production in microorganism is shown in Fig. 2.8 (Amara et al., 2016). Kennedy pathway is known to be involved in TAG

biosynthesis by *Rhodococci*. In this pathway, glycerol-3-phosphate, which is synthesized from the glycolysis intermediate dihydroxyacetonephosphate, acts as the starting compound for lipid synthesis and undergoes sequential acylation with different enzymes encoded by responsible genes present in the bacteria to finally produce lipids.

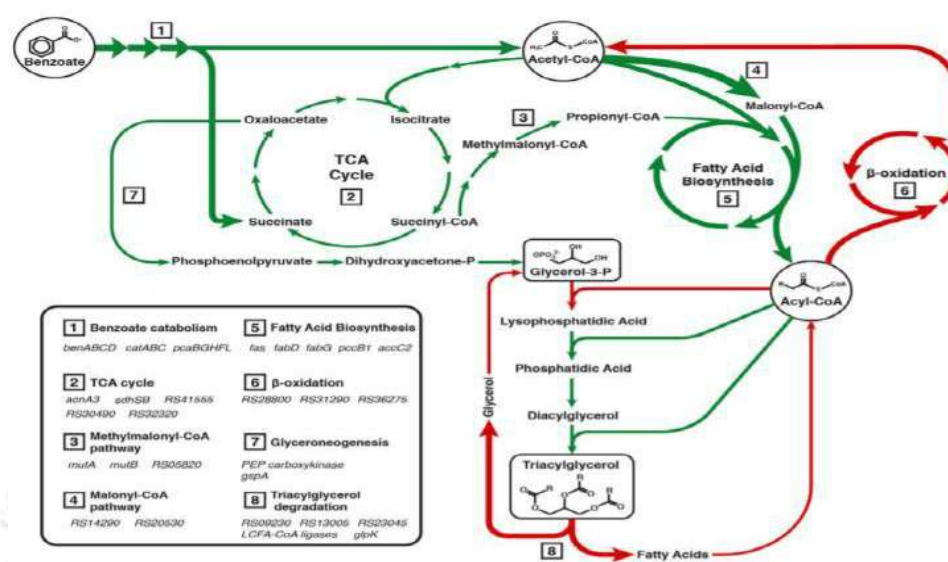


**Fig. 2.8** Pathway followed by *Rhodococci* for TAGs (Adapted from Amara et al., 2016)

Lipid composition in microorganisms vary according to their metabolism, but it can be easily manipulated by altering certain culture conditions viz. temperature, nutrients, growth stage at harvest, pH, etc. During nitrogen limiting conditions, the rate of lipid accumulation increases (Meng et al., 2009). Oleaginous microalgae such as *Chlorella* sp., *Nannochloropsis* sp., and *Scenedesmus* sp., yeast strains belonging to *Rhodospiridium* sp., *Rhodotorula* sp., and *Lipomyces* sp., as well as *Cryptococci* bacteria, such as *Arthrobacter* sp., *Rhodococcus opacus* and *Acinetobacter calcoaceticus* are reported to produce lipids (Dong et al., 2016). These oleaginous microorganisms possess a great variety of lipid classes viz. acylglycerides, phospholipids, glycolipids, lipoprotein, free fatty acids and sterols which differ mainly on their polarity, solubility and viscosity. Cytoplasm of the microorganisms consists of lipid bodies, which mainly include TAGs and sterol esters

surrounded by a phospholipid monolayer as a storehouse of energy. Polar lipids such as phospholipids, glycolipids, lipoproteins, sulfolipids, and acylglycerides are present in microorganisms, whereas autotrophic microalgae depending on growth conditions, consist of glycolipids and phospholipids as 17–90% of the total lipids (Yao et al., 2012). TAGs and FFAs present in oleaginous microorganisms are preferred as favorable precursors for bio-fuel production.

In particular, polar lipids present in microbial biomass consisting of acyl chains are considered as direct precursors for potential bio-fuel production with a remarkably high yield. However, phytol chains in chlorophyll as well as hydrocarbon backbones in sterols, can also be converted into biofuels by catalytic upgrading processes (Dong et al., 2016). A wide range of lipid classes is found in microbes such as acylglycerides, phospholipids, glycolipids, lipoprotein, free fatty acids, sterols, pigments and hydrocarbons (Table 2.5)

**Table 2.5** Various classes of lipids found in oleaginous microorganisms (Adopted from Dong et al., 2016)

Microorganisms	Neutral lipids (%)		Free fatty acids (%)	Polar lipids (%)		Reference
	Acylglyceride	Sterol ester		Phospholipid	Glycolipid	
<i>Nitzschia laevis</i>	79.2	-	-	11.6	8.1	Chen et al., 2007
<i>Pavlova lutheri</i>	56.5	5	0.6	9.7	18.9	Meireles et al., 2003
<i>Chlorella sorokiniana</i>	78.9	2.7	11.2	7.1	-	Zheng et al., 2013
<i>Dunaliella viridis</i>	0.5–21.5	4.1–7.5	6.2–13.7	31.8–38.2	-	Gordillo et al., 1998

	<i>Scenedesmus sp.</i>	81.3– 82.3	-	-	6.1–6.7	10.9–12.6	Ren et al., 2014
	<i>Gymnodinium sp</i>	7.5– 28.8	1.3–3.0	0.7–1.3	66.4–84.7	-	Mansour et al.,2003
	<i>Schizochytrium limacinum</i>	69	-	12.6	14	-	Chen et al., 2012
	<i>Nannochloropsis sp.</i>	41.4	-	9.3	37	-	Wang et al., 2017
<b>Yeast</b>	<i>Candida 107</i>	66.0– 92.0	-	-	2.0–25.0	5.0–21.0	Ratledge and Botham, 1977
	<i>Rhodospiridium toruloides</i>	81–87.7	-	-	4.0–6.6	8.3–12.4	Wu et al., 2010
<b>Fungus</b>	<i>Cunninghamella Echinulata</i>	44.5– 87.9	-	-	1.7–7.7	3.6–14.8	Fakas et al., 2007

Microbial lipid composition varies depending on the metabolic pathways followed by these organisms, which can be manipulated by adopting a suitable operating strategy or by genetic engineering in order to improve the lipid content of the biomass. One such strategy is nitrogen limitation in the growth medium, which increases the lipid content of the microbial biomass. As nitrogen limitation is known to favor lipid accumulation in oleaginous microorganisms, C/N ratio of a substrate plays an important role in bio-oil production from oleaginous microorganisms (Meng et al., 2009).

In addition, high protein content in the microbial biomass produces amino acids and carboxylic acids during hydrolysis, the decomposition of amino acids can be done in two ways: through deamination or decarboxylation (Scott et al., 2007). Protein consists of several chains of peptides and can be converted to a nitrogen-limited bio-oil (Du et al., 2012). Another category of important compounds of oleaginous microbes is carbohydrates, which show an

unusual composition and yield of bio-crude oil (Colin et al., 2011). Carbohydrates may be converted to propionic acid, benzene, and 4-hydroxyphenethyl alcohol at high temperature (above 350 °C). Moreover, glucose can decompose into ethanol, methanol, lactic acid, acrylic acid and furfural which, however, affect the bio-crude oil yield. Another abundant compound, particularly in phototrophic oleaginous microorganisms, is the pigment chlorophyll which generally decomposes into phytol which is then converted to phytane (Jinkerson et al., 2011).

### 2.8.2. Types of oleaginous microorganisms

A wide range of microorganisms including the genera of algae, yeast, fungi and bacteria are capable of accumulating significant amounts of oil inside their cells. Table 2.6 presents different oleaginous microorganisms reported in the literature for lipid accumulation. Important factors influencing the choice of organisms for lipid extraction are the amount of oil produced, quality of the oil produced and utilization of cheap and alternative substrates (e.g. wastewater) for their cultivation (Duong et al., 2012). Microorganisms are more advantageous compared to other biomass feed stocks for bio-crude oil production due to their rapid growth rates, strong ability to survive in a variety of environments, high lipid content and high bio-oil yield (Thevenieau and Nicaud, 2013).

**Table 2.6** Lipid content of oleaginous microorganisms reported in the literature

Oleaginous microorganisms	Lipid content (% dry weight)	Reference
<b>Algae</b>		
<i>Botryococcus braunii</i>	<75	Metzger and Largeau, 2005
<i>Cylindrotheca sp.</i>	<37	Guschina and Harwood, 2006
<i>Nitzschia sp.</i>	<47	Abou-Shanab et al., 2011
<i>Schizochytrium sp.</i>	<77	Sawangkeaw et al., 2013

<i>Chlorella sp.</i>	<32	Hsieh and Wu, 2009
<i>Chlorella zofingiensis</i>	<52	Sawangkeaw et al., 2013
<i>Cryptocodinium cohnii</i>	23	Couto et al., 2010
<i>Chaetoceros muelleri</i>	<68	Araujo et al., 2011
<i>Nannochloropsis oculata</i>	23	Sawangkeaw et al., 2013
<i>Chlorella protothecoides</i>	<64	Gao et al., 2010
<i>Chaetoceros gracilis</i>	<60	Araujo et al., 2011
<i>Chlorella vulgaris</i>	<42	Feng et al., 2011
<i>Chlorella ellipsoidea</i>	32	Abou-Shanab et al., 2011
<i>Dunaliella sp.</i>	<30	Araujo et al., 2011
<i>Haematococcus pluvialis</i>	<34	Damiani et al., 2010
<i>Neochloris oleoabundans</i>	<40	Li et al., 2008
<i>Neochloris oleoabundans</i>	<56	Gouveia et al., 2009
<i>Pseudochlorococcum sp.</i>	<52	Li et al., 2011
<i>Scenedesmus obliquus</i>	<58	Abou-Shanab et al., 2011
<i>Tetraselmis chui</i>	<23	Araujo et al., 2011
<i>Tetraselmis sp.</i>	<33	Huerlimann et al., 2010
<i>Tetraselmis tetrathele</i>	<30	Araujo et al., 2011
<i>Skeletonema sp.</i>	20	Rodolfi et al., 2009
<i>Thalassiosira pseudonana</i>	31	Rodolfi et al., 2009
<i>Phaeodactylum tricornutum</i>	19	Rodolfi et al., 2009
<i>Isochrysis sp.</i>	<34	Huerlimann et al., 2010
<i>Isochrysis zhangjiajiensis</i>	<40	Feng et al., 2011
<i>Nannochloropsis oculata</i>	<41	Chiu et al., 2009

<i>Nannochloropsis sp.</i>	37	Huerlimann et al., 2010
<i>Pavlova salina</i>	30	Rodolfi et al., 2009
<i>Rhodomonas sp.</i>	20	Huerlimann et al., 2010
<i>Thalassiosira weissflogii</i>	14	Araujo et al., 2011

---

**Bacteria**

<i>Arthrobacter sp.</i>	>40	Kalscheuer et al., 2004
<i>Acinetobacter calcoaceticus</i>	<38	Kalscheuer and Steinbuchel, 2003
<i>Rhodococcus opacus</i>	>50	Miller, 2012; Gouda et al., 2008
<i>Bacillus alcalophilus</i>	<24	Miller, 2012; Gouda et al., 2008
<i>Escherichia coli</i>	<21	Kalscheuer et al., 2006
<i>Acinetobacter baylyi</i>	13	Santala, et al., 2011
<i>Alcanivorax borkumensis</i>	>23	Kalscheuer et al., 2006
<i>Gordonia sp.</i>	57	Gouda et al., 2008
<i>Mycobacterium tuberculosis</i>	12	Bacon et al., 2007
<i>Nocardia globerula</i>	>50	Alvarez et al., 2001
<i>Streptomyces coelicolor</i>	83	Arabolaza et al., 2010

---

**Yeast**

<i>Candida curvata</i>	58	Evans and Ratledge, 1983
<i>Cryptococcus curvatus</i>	65	Hassan and Blanc, 1996
<i>Lipomyces starkeyi</i>	64	Zhao et al., 2008
<i>Rhodosporidium toruloides</i>	66	Li et al., 2007
<i>Rhodotorula glutinis</i>	72	Xue et al., 2008
<i>Yarrowia lipolytica</i>	36	Papanikolaou and Aggelis, 2002

<i>Rhizopus arrhizus</i>	57	Wu et al., 2011
<i>Trichosporon fermentans</i>	62	Zhu et al., 2008
<b>Fungi/Molds</b>		
<i>Aspergillus oryzae</i>	<57	Thevenieau and Nicaud, 2013
<i>Mortierella isabellina</i>	86	Papanikolaou et al., 2004
<i>Humicola lanuginosa</i>	75	Thevenieau and Nicaud, 2013
<i>Mortierella alpine</i>	66	Takeno et al., 2005
<i>Mucor circinelloides</i>	25	Thevenieau and Nicaud, 2013
<i>Pthium ultimum</i>	48	Thevenieau and Nicaud, 2013
<i>Aspergillus terreus</i>	23	Thevenieau and Nicaud, 2013
<i>Pellicularia praticola</i>	28	Thevenieau and Nicaud, 2013
<i>Claviceps purpurea</i>	23	Thevenieau and Nicaud, 2013
<i>Mucor mucedo</i>	62	Certik et al., 1997
<i>Cunninghamella echinulata</i>	<58	Fakas et al., 2009

### 2.8.2.1. Algae

Algae are one of the most promising alternative energy sources, and these are often referred to as cell factories driven by sunlight which can convert carbon dioxide to bio-fuels such as bioethanol, biodiesel and biohydrogen (Jazrawi et al., 2015, Togarcheti et al., 2017). Several studies have reported that micro- algal biomass contains around 80% of triglyceride with a fatty acid profile rich in C<sub>16</sub> and C<sub>18</sub> and a substantial amount of amino acids (e.g. leucine, isoleucine and valine). The lipid content of any algal cells varies from 1% to 70%, but it can attain up to 90% of its dry weight under certain cultivation conditions (Dong et al., 2015). Praveen kumar et al. (2012) reported *Stigeoclonium sp.* had maximum oil productivity

of 525.1 kg/m<sup>3</sup>/yr under heterotrophic conditions using a two-phase culturing system designed to increase biomass production along with lipid content.

Oleaginous microalgae can be classified into the following three categories: (1) photoautotrophic microalgae using CO<sub>2</sub> as the carbon source and sunlight as the energy source, (2) heterotrophic microalgae using organic substrates as the carbon source and (3) mixotrophic microalgae that can use both CO<sub>2</sub> and organic carbon as the substrates. Among these microalgae, heterotrophic and mixotrophic microalgae accumulate lipids by growing on cheap organic substrates such as wastewater (Perez-Garcia and Bashan, 2015, Vo et al., 2020). The commonly used microalgae reported for bio-oil production are *Botryococcus braunii* (Watanabe et al., 2014), *Chlorella* sp. MP-1 (Phukan et al., 2011), *Dunaliella tertiolecta* (Shuping et al., 2010), *Enteromorpha prolifera* (Zhou et al., 2010), *Nannochloropsis salina* (Sudasinghe et al., 2014), *Scenedesmus* sp. (Kim et al., 2015) and *Spirulina platensis* (Jena et al., 2011).

#### 2.8.2.2. Bacteria

Compared with bacteria, algae need a larger cultivation area and a prolonged culture period, whereas bacteria grow at a much faster rate under dark conditions in bioreactors. In general, the average oil accumulated by bacteria is 20-40% of its cell dry weight (Brooks et al., 2009). However, bacteria such as *Acinetobacter calcoaceticus* and *Arthrobacter* sp. can accumulate lipid up to more than 40% of their cell dry weight (Thevenieau and Nicaud, 2013). Sriwongchai et al. (2012) reported that the lipid content in *Gordonia* sp. and *Rhodococcus* sp. could be as high as 80% of their cell biomass, which is comparable with the lipid value accumulated by algae. *Pseudomonas* species are also known to produce biomass with high lipid content (Pinkart and White 1998).

Some of the bacteria, particularly those belonging to *Actinomycetes* group such as *Mycobacterium*, *Nocardia* and *Streptomyces* sp., are capable of accumulating high lipid

content by utilizing simple carbon sources (Shruthi et al., 2014). Bacterial growth depends on macro and micronutrients provided in the growth medium. Many species belonging to *Rhodococcus* such as *Rhodococcus ruber*, *Rhodococcus erythropolis*, *Rhodococcus opacus*, and *Rhodococcus fascians* have been studied for biosynthesis of triacylglycerides (TAGs) and their application in energy production (Cortes and de Carvalho, 2015). The capability of these bacteria to grow on complex waste substrates such as wastewater from different industries is commercially attractive (Paul et al., 2019). Hence, this class of bacteria is often reported in the literature as a feedstock for the biodiesel industry. Microbial oils differ in composition and properties depending on the organism and substrate used (Albuquerque et al., 2011). In order to improve lipid production, different strategies such as media optimization, genetic strain improvement, metabolic engineering and improvement in cultivation techniques can be followed. For example, Zhang et al. (2012) reported a more than 80% increase in fatty acid esters produced by *E. coli* by a change in cultivation method and optimization of the growth medium.

Over the past 25 years, *Rhodococcus* has gained immense importance for biodegradation of hydrocarbons (Finnerty 1992). *Rhodococci* can be found in variety of sources including soils, rocks, guts of insects, groundwater, marine sediments, animal dung, and from healthy / diseased animals and plants (Good fellow 1989; Ivshina et al., 1994). The genus *Rhodococcus* is best known for degrading a wide range of chemicals thus making it an ideal microorganism for application in environmental and industrial sectors. Certain *Rhodococcus* sp. can also produce surfactants, polymers, flocculants as well as various pigments. Various genes responsible for biodegradation of various compounds, present in *Rhodococcus* species, can be transferred to other microorganisms by genetic manipulation and cloning techniques.

*Rhodococci* are non-sporulating aerobic bacteria and classified into mycolate-containing nocardioform actinomycetes. The cell wall of *Rhodococcus* contains mycolic acids, similar to that of microorganisms belonging to the genera *Mycobacterium*, *Nocardia* and *Corynebacterium*. The long aliphatic chains of mycolic acids in the cell envelope facilitate the uptake of hydrophobic substrates, which further support the production of surfactants. The fatty acid composition of the membrane lipids can be changed by adding various substrates thus altering the fluidity of the cell envelope.

Production of biodiesel (alternative source of fuel) from lipid rich biomass of *Rhodococcus sp.* is well-reported (Goswami et al., 2017). Lipid production along with industrial wastewater treatment by *R. opacus* is also well-reported (Gupta et al., 2018). Owing to the presence of diverse catabolic enzymes in *R. opacus*, it is capable of degrading various recalcitrant compounds present in industry wastewater and accurate lipids inside. Simultaneous treatment of wastewater from industries such as dairy and biomass gasification and lipid-rich biomass production is well-reported in the literature (Kumar et al., 2015; Goswami et al., 2017). However, its potential to treat PRWW and produce bio-oil has not been explored, so far, which is not only attractive from the standpoint of wastewater treatment and reuse of the treated water, but also for energy recovery in the form of bio-oil.

### 2.8.2.3. Yeasts

The best known oleaginous yeasts are *Lipomyce sp.* (Angerbaucer et al., 2008), *Cryptococcus* (Chi et al., 2011), *Trichosporom* (Huang et al., 2013), *Rhodospiridium* (Xu et al., 2012), *Rhodotorula* (Zhao et al., 2010), *Yarrowia* and *Rhizpous* (Chatzifragkou et al., 2011). Similar to bacteria, oleaginous yeasts can accumulate, on average 40% of the lipid content on dry weight basis, but this can be as high as 70% under certain limiting nutrient conditions. Carbon substrates such as xylose, glucose, starch hydrolysate, glycerol, municipal and industrial organic wastes can be used as the substrate for oleaginous yeast cultivation.

However, depending on the species and substrate used, the lipid content and fatty acid profiles can be different. Papanikolaou and Aggelis (2011) reported that *Cryptococcus albidus*, *Lipomyces lipofer*, *Rhodospiridium toruloides*, *Lipomyces Starkeyi*, *Trichorporon pullulans* and *Yarrowia lipolytica* have been well studied for lipid accumulation and energy production. Sugars or other substrates such as glycerol and molasses under certain culture conditions not only favor lipid accumulation in yeasts, but also govern the fatty acid composition of the lipids produced.

#### 2.8.2.4. Fungi

Moulds are known as efficient oleaginous microorganisms (Donot et al., 2014). They can accumulate TAGs primarily rich in polysaturated fatty acids and limited content of palmitic (16:0), linoleic (18:2), oleic (18:1) and palmitoleic (16:1) acids. The filamentous fungus, *Mortierella isabellina* NRRL 1757 strain accumulated 46.1 g L<sup>-1</sup> of TAGs (Gao et al., 2013, Sankaran et al., 2010). In addition, *Asperfillus terreus*, *Clariceps purpurea*, *Mortierella isabellina* and *Mortierella alpine* also produce uncommon lipids such as arachidonic acid, gamma linolenic acid, docosahexaenoic acid and eicosapentaenoic acid. Different strategies can be followed to enhance the lipid accumulation, as demonstrated by Dyal and Narine (2005), for high lipid accumulation in *Mucorrouxii* by the use of potassium nitrate as a nitrogen source. Sawangkeaw and Ngamprasertsith (2013) reported a very high accumulation of oil (18.0 g L<sup>-1</sup>) by *Mortierella isabellina* when cultivated under nitrogen limited conditions and high glucose containing growth medium.

The growth of oleaginous bacteria, algae and fungi on wastewater is well reported in the literature. Goswami et al. (2019) reported biodegradation of organics by *Rhodococcus opacus* grown on different industrial wastewaters: pulp and paper, biomass gasification and dairy with a COD removal efficiency of 46.1%, 68.9%, and 56.8%, respectively, and biodiesel production from the residual biomass.

## 2.9. Bio-oil production technologies

### 2.9.1. Thermo-chemical

Thermo-chemical conversion (TCC) is most commonly used for the conversion of biomass to bio-crude oil. Based on the type of biomass and process conditions used, the oil yield on biomass and its properties may vary. The criteria for selecting an efficient methodology rely on the purity of the desired end-product, process costs and environmental safety (Nigam and Singh, 2011).

Thermo-chemical conversion (TCC) is applicable to almost any kind of biomass feedstock for bio-crude oil production. TCC treatment consists of pretreatment, thermal processing, purification and upgrading, as depicted in Fig. 2.9. Purification of the end product is carried out to enhance its stability. There are two major types of TCC processes for the production of bio-crude oil from different types of biomass feedstock: pyrolysis and hydrothermal liquefaction (HTL). Diverse products can be produced using the TCC process is, for example, hydrothermal carbonization is usually carried out for the production of solid biochar, liquefaction for the production of bio-crude oil, gasification and pyrolysis for the production of syngas, biochar and bio-oil. These processes produce an aqueous phase containing organics and inorganics, such as  $\text{NH}_4^+$ ,  $\text{PO}_4^{3-}$  and metallic ions such as  $\text{K}^+$ ,  $\text{Na}^+$ , and  $\text{Mg}^{2+}$ . Different thermo-chemical routes for biomass conversion to bio-crude oil and upgradation/ purification is mentioned in Fig. 2.7.

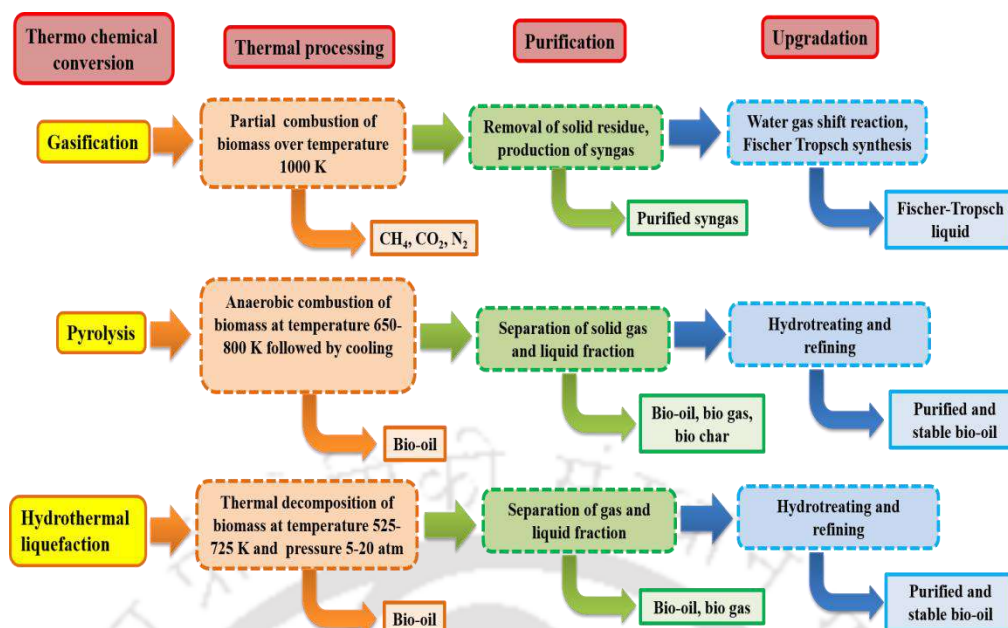


**Fig. 2.9** Different thermo-chemical routes for biomass conversion to bio-crude oil and upgradation/ purification.

### 2.9.2. Pyrolysis

Pyrolysis is an anaerobic biomass decomposition process that occurs at a temperature in the range of 350-550°C for the production of liquid bio-oil, gases and solid products. It can be used to produce bio-oils or biogases from lignocellulosic biomass (Jahirul et al., 2012). Recently, this technique has also been used for the conversion of microalgal biomass due to requirements of fixed temperature treatment and high quality bio-oil yield (Voloshin et al., 2016). Miao and Wu (2004) reported fast pyrolysis for microalgae conversion to bio-oil production using a fluidized bed reactor. Demirbas (2006) investigated the production of bio-oil by pyrolysis using different microalgal species namely *C. protothecoides*, *Microcystis aeruginosa* and *C. protothecoides* with observed bio-oil yields of 18%, 24% and 58%, respectively. A major drawback of pyrolysis is the requirement of a high temperature for the conversion process. Moreover, this process is not suitable for biomass containing moisture, necessitating extra energy for drying of the wet biomass.

Depending on the process conditions, pyrolysis can be classified as fast pyrolysis, flash pyrolysis, slow pyrolysis, and catalytic pyrolysis (Goyal et al., 2008). Bio-oil thus obtained from slow and flash pyrolysis is less stable and less miscible compared to conventional fuels. Therefore, catalytic or fast pyrolysis is the best for high-quality bio-crude oil production (Bridgwater, 2012). The oil obtained by catalytic pyrolysis of biomass also does not require costly up-gradation techniques, such as condensation and re-evaporation. Among the different pyrolysis types, fast pyrolysis is highly suitable for producing bio-crude oil in the absence of air even in the temperature range of 400-550°C and at atmospheric pressure conditions. Moreover, it gives a high oil and gas yield of 70% on biomass.

### 2.9.3. Hydrothermal liquefaction (HTL)

Table 2.7 presents the different parameters used for hydrothermal liquefaction of various types of biomass. Gollakota et al. (2018) studied different types of biomass, including *Nannochloropsis gaditana*, swine manure and *Spirulina* treated with different TCC technologies for bio-oil production and reported HTL to be the best in terms of bio-oil yield on biomass and bio-oil quality. The major advantage of HTL is that wet biomass without any drying can be directly used to produce liquid bio-crude oil. Other than saving energy, the use of wet biomass improves the ease of operation due to the easily formed slurries of biomass with water (Elliott et al., 2015). Moreover, wet biomass feedstock contains hydrogen in the form of water, which can additionally promote hydrogenolysis (Jazrawi et al., 2013; Boens et al., 2016). Various feedstock and operation conditions used for hydrothermal liquefaction for bio-oil production are mentioned in Table 2.7.

**Table 2.7** Various feedstock and operation conditions used for hydrothermal liquefaction for bio-oil production

Feedstock	Experimental conditions	Bio-oil yield (wt%)	Reference
Algal biomass ( <i>Laminaria saccharina</i> )	Temperature: 350°C Pressure: 16.5 bar Reactor: muffle furnace	79 (dry and ash free)	Bach et al., 2014
Macro algae ( <i>Laminaria digitata</i> , <i>Laminarias accharina</i> , <i>Laminaria hyperborean</i> and <i>Alaria esculenta</i> )	Temperature: 350°C Pressure: Reactor: Batch	9.8 and 17.8	Anatasakis and Ross, 2015
Cyanophyta ( <i>Microcystis</i> , Basketball algae, <i>Oscillatoria sp.</i> , <i>Nostoc sp.</i> )	Temperature: 370°C Pressure: 1.5 psi Reactor: Batch	39.54	Guo et al., 2015
Residual bacterial biomass (Dairy manure)	Temperature: 250°C Pressure: NA Reactor: Pressure reactor	28	Wei et al., 2015
Bacterial biomass ( <i>Cupriavidus necator</i> )	Temperature: 300°C Pressure: 0.1 MPa Reactor: Stainless steel thermal reactor	45	Shimin Kang and Jian Yu, 2015
Cyanophyta biomass ( <i>Microcystis</i> , Basketball algae, <i>Oscillatoria sp.</i> , <i>Nostoc sp.</i> )	Temperature: 350°C Pressure: NA Reactor: Batch	29.24	Song et al., 2017
Mixed-algal culture (Wastewater treatment system)	Temperature: 300°C Pressure: 0.69 MPa Reactor: Batch	35.7	Chen et al., 2014
Fresh water alga ( <i>Arthrospira platensis</i> and marine microalga <i>Tetraselmis sp.</i> )	Temperature: 200-350°C Pressure: 180 bar Reactor: Batch	76-77 (post blending)	Lavanya et al., 2016
Algal biomass ( <i>Nannochloropsis gaditana</i> and <i>Chlorella sp.</i> )	Temperature: 300°C Pressure: 200 psi Reactor: Batch	47.5 and 32.5	Reddy et al., 2016
<i>Nannochloropsis oceanica</i>	Temperature: 240-300°C	60	Caporgno et al., 2016

	Pressure: NA		
	Reactor: Batch		
<i>Nannochloropsis</i> sp.	Temperature: 320-400°C	42.5	Xu and Savage, 2017
	Pressure: 16.5 MPa		
	Reactor: Batch		
<i>Chlorella vulgaris</i>	Temperature: 350°C	47	Biller et al., 2012
	Pressure: -		
	Reactor: Batch		
<i>Spirulina</i> sp. and <i>Tetraselmis</i> sp.	Temperature: 300- 350°C	42 and 58	Eboibi et al., 2014
	Pressure: 30 bar		
	Reactor: Batch		
<i>Nannochloropsis</i> sp.	Temperature: 100- 400°C	46	Hietala et al., 2016
	Pressure: 400 bar		
	Reactor: Batch		
<i>Nannochloropsis</i> , <i>Pavlova</i> , <i>Isochrysis</i>	Temperature: 250-300°C	48.67 (non- catalytic)	Shakya et al., 2015
	Pressure: 35 Psi	and	
	Reactor: Batch	47.05 (catalytic)	
<i>Scenedesmus</i> sp.	Temperature: 250, 300, 350°C	36	Wądrzyk et al., 2018
	Pressure: 50-100 bar		
	Reactor: Continuous		
<i>Scenedesmus obliquus</i> (UTEX2630) , <i>Scenedesmus almerensis</i> (CCAP 276/24), and <i>Chlorella</i> <i>vulgaris</i> (SAG 211- 11b), <i>Phaeodactylumtricornutum</i> (C CAP1055/1), <i>Tetraselmis suecica</i> (C CAP 66/4), <i>Nannochloropsi</i> <i>sgaditana</i> (Lubián CCMP 527), <i>Porphyridium purpureum</i> (SA G 113.79), <i>Dunaliella</i> <i>tertiolecta</i> (SAG 13.86)	Temperature: 250-375°C	17.6 to 44.8 (250 °C) and 45.6 to 58.1 (375 °C)	Barreiro et al., 2013
	Pressure: -		
	Reactor: Batch		

Hydrothermal liquefaction uses the property of subcritical water, i.e. water at high temperature and pressure, to break the bonds, thus releasing the monomers. Water acts hence as both solvent and reactant in the liquefaction process (Zhou et al., 2010). During the biomass conversion, two main degradation mechanisms occur: i) depolymerisation of biomass, ii) degradation of monomers followed by recombination of components being fragmented (Chen et al., 2014, Selvaratnam et al., 2016), i.e., the complex macromolecules present in the biomass feedstock first dissociate into water-soluble compounds by hydrolysis which further degrade to form oligomers. Compared with other thermo-chemical processes for biomass conversion, HTL is a more preferred technique as there is no requirement of biomass pretreatment such as drying and the reaction is carried out at a relatively low temperature. Moreover, it is reported that bio-oil obtained from the HTL process contains less O content than fast pyrolysis, thereby resulting in favorable HHV of the product (Guo et al., 2015). Besides, the HTL process converts not only lipids but also proteins and carbohydrates present in the biomass to bio-oil, which is the key advantage of this process (Biller and Ross 2011).

Yang et al. (2015) reported that this complex conversion process occurs at a lower temperature for protein-based monomers than for lipids and carbohydrates. Hence, the temperature is an important factor that governs the quality of the bio-oil produced. High-temperature results in the production of more complex bio-oil consisting of cyclic and heterocyclic compounds (Yu et al., 2011).

The quality of the bio-oil yield is also determined by various other factors such as feedstock composition, reaction time and catalyst type (Boens et al., 2016, Barreiro et al., 2013). Song et al. (2017) recently studied bio-oil production by HTL of waste *Cyanophyta* biomass and the influence of different process variables, viz. time, temperature and algae/water ratio on the bio-oil yield. Feedstock composition and concentration also influence the bio-oil

yield (Valdez et al., 2014). Chen et al. (2014) observed that a high ash content (>30wt %) in the feedstock reduces the bio-oil yield and results in high amounts of the aqueous phase.

Bio-oil, hence produced by different thermo-chemical processes can be further upgraded for enhancing the fuel properties and for its better usage (Xiu and Shahbazi., 2012). Various techniques, such as solvent addition, emulsification, esterification, hydrocracking/hydrotreating and supercritical fluids (SCFs) have been applied for bio-oil up-gradation. (Shakya et al., 2018; Leng et al., 2018). Bio-oil being relatively GHG free (produces less greenhouse gases) and renewable liquid fuel, can be used as an alternative for fuel or diesel in many applications. Other than for its use as a combustion and transportation fuel for boilers, engines and furnaces, it has many other uses such as the production of chemicals, e.g., agri-chemicals, fertilizers, acids and adhesives (Fini et al., 2012).

In the HTL process, in addition to bio-oil as the main product, nutrient-rich aqueous media is obtained, which can be reused for biomass culture for maximizing and multiplying the bio-energy production per unit biomass (Biller et al., 2012). Ross et al. (2010) reported that the aqueous phase obtained following HTL of microalgae contained  $\text{PO}_4^{3-}$ ,  $\text{NH}_4^+$  and some minerals (Ross et al., 2010). By the reuse of nutrient-rich aqueous phase from the HTL process, an increase in bio-oil yield from 29.4 wt% to 38.9 wt% without change in composition has been reported for bio-oil production from *C. vulgaris* (Hu, Gong et al., 2019).

Another byproduct of HTL is carbon-rich solid residue or biochar, which also contains traces of organics/inorganics, essential nutrients (N, P, K), and it can be used to enhance the nutrient and water retention capacity of soil. It also can be used as an adsorbent for the removal of metals, dyes and other pollutants from wastewater (Hu, Gong et al., 2019). The yield of the solid residue is, however, dependent on the ash content of the original feedstock used for HTL.

## 2.9.4. Effect of process parameters on bio-oil yield by HTL

### 2.9.4.1. Temperature

Temperature is by far the most crucial parameter for thermo-chemical processes like HTL (Hu, Qi et al., 2019). The re-polymerization of the monomers and hydrolysis of the polymers are determined by the temperature used for HTL. Temperature in the range of 230–350°C is usually reported as optimum for bio-oil production. A very high temperature is, nevertheless, not suggested for HTL as it causes secondary decomposition, often leading to gaseous products or recombination of material (char), which eventually reduces the bio-oil yield from biomass. Akalin et al. (2012) reported the synergistic effect of temperature on bio-oil yield by HTL of cornelian cherry stone. In general, an increase in temperature from 260 to 340 °C increases the process efficiency (Akhtar and Amin, 2011; Yang et al., 2018). Shuping et al. (2010) performed HTL treatment on *Dunaliella tertiolecta* and observed 360°C to be the optimum temperature for bio-oil production. However, physical as well as chemical parameters of bio-oil vary according to the temperature used. Reddy et al. (2016) reported a change in the chemical composition of bio-oil obtained from HTL of *Nannochloropsis* sp. in the 180–330°C temperature range. The study found that at a temperature above 250 °C, fatty acids were obtained due to 90% decomposition of the total lipids present in the biomass.

### 2.9.4.2. Reaction time

Similar to temperature, reaction time influences the qualitative and quantitative nature of bio-oil. Almost all studies in the literature suggest that a short reaction time is highly effective for bio-oil production using HTL (Sasaki et al., 2003). Boocock and Sherman (2009) reported that a prolonged treatment time suppressed or even inhibited further bio-oil production. A small increase in the bio-oil yield was observed with an increase in reaction time (Yan et al., 1999). Eboibi et al. (2014) performed hydrothermal liquefaction on *Tetraselmis* sp. at 310–370 °C. Experiments were carried out at 310 °C for 5 min and yielded ~40 wt% of bio-

crude oil, and a further increase in the reaction time even up to 60 min resulted in only a slight increase in the oil yield up to 43 wt%. Duan et al. (2013) studied the influential effect of the reaction time (5–120 min) on the bio-oil production from the biomass (*C. pyrenoidosa*) by HTL at 350 °C. The authors concluded that the bio-oil yield increased slightly from 56.8 wt% in 5 minutes to 65.1 wt% at 70 min and did not increase any further when the reaction time was increased up to 120 min.

#### 2.9.4.3. Feedstock and biomass/water ratio

The composition of feedstock greatly influences the quality and overall yield of the bio-oil by HTL: biomass with high concentrations of cellulose, hemicelluloses and lignin, i.e., lingo-cellulosic biomass, gives a high bio-oil yield, which is comparable with that using oleaginous biomass that contains carbohydrate, protein and lipids. Very few studies have reported bio-oil production from bacterial biomass by HTL in comparison with that on algal biomass (Paul et al., 2019). Biller and Ross (2011) studied HTL at 350 °C of three strains of microalgae with different biochemical composition for 60 min reaction time. The contribution towards bio-oil yield was more than that due to the protein and carbohydrate fraction present in the biomass. Barreiro et al. (2015) studied the effect of microalgae cell structure on the bio-oil production by HTL and observed that microalgae with resilient and thick cell wall yield a high amount of bio-oil at 250 °C. However, at a temperature of 375 °C the effect of the structure of cell wall on the bio-oil yield was minimal. Bio-oil by HTL of sonicated *Spirulina platensis* biomass gave a maximum yield of bio-oil around 50% at 340 °C, suggesting that ultrasonication mediated cell disruption enhances the bio-oil yield by HTL (Zhang et al., 2018).

Another important feedstock component affecting the yield of bio-oil by HTL is the biomass ash content. Interestingly, microalgae with high ash content have a direct negative impact on the yield of bio-oil, which could be due to hindrance caused by the ash content

during the conversion of organics into bio-crude oil. High ash content also corresponds to a reduced availability of organics for thermo-chemical conversion to obtain a high bio-oil yield (Hu, Gong et al., 2019).

In addition to feedstock composition, the water content or biomass to water ratio plays a crucial role in the HTL process. According to Wang et al. (2008), a high solvent to water ratio results in a low amount of solid residues in the final product and decreases the gas yield. Contrary to these findings, Bookcock and Sherman (2009) observed that at a low biomass/solvent ratio, the amount of liquid oils decreases, and the highest yield obtained was 45%. Vardon et al. (2012) reported that HTL is more favorable than pyrolysis in terms of energy requirement for converting wet biomass with 80% moisture content to bio-oil. Anastasakis and Ross (2011) studied bio-crude production using brown macro-algae *Laminaria saccharina* by HTL. The optimum conditions were 1:10 biomass: water ratio, 350 °C temperature and 15 min residence time.

#### 2.9.4.4. Catalysts

The bio-oil yield by HTL can be improved by the addition of catalysts such as sodium carbonate ( $\text{Na}_2\text{CO}_3$ ), potassium hydroxide (KOH), acetic acid ( $\text{CH}_3\text{COOH}$ ), formic acid ( $\text{HCOOH}$ ), nickel oxide (NiO), calcium phosphate ( $\text{Ca}_3(\text{PO}_4)_2$ ), sulfuric acid ( $\text{H}_2\text{SO}_4$ ) and zeolite (Shakya et al., 2015). Among these catalysts, one of the most commonly used homogenous catalysts for the liquefaction process is  $\text{Na}_2\text{CO}_3$ . Zou et al. (2009) reported an increase in the bio-oil yield due to the use of  $\text{H}_2\text{SO}_4$  as a catalyst, which reduced the nitrogen content in the biomass. Ross et al. (2010) studied the effect of acid ( $\text{CH}_3\text{COOH}$  and  $\text{HCOOH}$ ) and base catalysts ( $\text{Na}_2\text{CO}_3$  and KOH) on the HTL process for bio-oil production from *C. vulgaris*. The bio-oil yield using acid catalysts was more than that of using base catalysts. Moreover, the bio-oil showed superior flow properties with acid catalysts in the HTL process. Other than these acid/base homogenous catalysts, heterogeneous catalysts are also reported for

liquefaction of biomass. As compared with homogenous catalysts, heterogeneous catalysts are recyclable and can be used under severe reaction conditions (Galadima and Muraza, 2018). Biller et al. (2011) used specific heterogeneous catalysts like Pt/Al<sub>2</sub>O<sub>3</sub>, Ni/Al<sub>2</sub>O<sub>3</sub>, or Co/Mo/Al<sub>2</sub>O<sub>3</sub> for liquefaction of *C. vulgaris* and *N. occulta*, which improved the bio-oil yield. However, the exact mechanism of action of such heterogeneous catalysts in HTL of biomass is not well-known. Nevertheless, Duan and Savage (2011) used heterogeneous catalysts with Pt/C and H<sub>2</sub> for enhancing the bio-oil yield, which showed a heating value of 43 MJ Kg<sup>-1</sup> and a substantial amount of hydrocarbon molecules, including mostly aromatic compound and alkanes.

### 2.10. HTL based bio-refinery

Bio-refineries are increasingly becoming essential parts of our growing economy, which involves various processes for obtaining biofuel and other value-added products and chemicals via different biomass conversion technologies (Garcia-Nunez et al., 2016). The bio-refinery approach is sustainable and helps in reducing the carbon footprint and greenhouse gas emissions (Chew et al., 2017, Merzari et al., 2019). Fig. 2.10 presents an overview of the bio-refinery approach for the production of bio-crude oil and other valuable products from oleaginous microorganisms by the HTL process. A bio-crude oil-based bio-refinery can provide a variety of substances, particularly fuels for heating, cooking and transportation, lubricants for mechanical devices as well as chemicals and materials for industries. Besides, gaseous fuels such as propylene, valuable byproducts such as bio-char (carbon-rich, one of the byproducts of HTL), N<sub>2</sub> rich fertilizer were produced by HTL treatment of microbial biomass.

In addition to bio-oil, certain algal strains such as *Chlamydomonas* and *Dunaliella* capable of producing high-value pigments and phycobiliproteins, have been genetically modified for the production of cellulases and hemicellulases, thus integrating enzyme production within an algal bio-refinery system (Subhadra, and Grinson-George, 2011).

Gouveia et al. (2014) reported different routes for the production of value-added products from algae. For example, under high salinity and light stressed condition, *Chlorella protothecoides* acts as an excellent source of lipids and carotenoids (Campenni et al., 2013). Wagner et al. (2016) produced a high-value gaseous product, propylene, along with bio-oil by HTL of polyhydroxybutyrate (PHB) producing cyanobacterial strains.

Wei et al. (2015) investigated bio-oil production from HTL of bacterial biomass following the extraction of polyhydroxyalkanoates (PHA). The authors reported a maximum of 15 % (w/w) bio-oil production, HTL based 52% solid residue and 20% water-soluble fraction by HTL treatment of the residual biomass at 250 °C. In another study by the same research group, pyrolysis of the residual biomass after PHA extraction yielded 28% bio-oil and 46% biochar at 500 °C (Wei et al., 2015).

Fungi produce industrially important products, including enzymes, organic acids, antibiotics, chitin and pigments. However, integrating HTL with other processes for value-added chemicals produced by fungi is thus far not reported in the literature. Kamat et al. (2013) reported single cell oil production together with xylitol and xylanase from sugarcane bagasse as the substrate using two fungi (*Williopsis saturnus* and *Aspergillus terreus*) isolated from tropical mangrove soil. The authors found 0.19 g of single cell oil per g of biomass and a very high biomass concentration (9.8 g L<sup>-1</sup>) using the *Aspergillus terreus* strain. The single cell oil was successfully converted to biodiesel by transesterification.

The main challenges with bio-crude oil production from biomass are the high energy requirement and the cost involved for product separation, conversion and upgrading. Moreover, commercialization of a HTL based bio-refinery is not yet realized due to high process costs and problems associated with net energy consumption, feedstock availability, feedstock pretreatment and processing.

### 2.10.1. Types of bio-refinery

There are different types of bio-refinery based on process use (Ubando et al., 2020). However, the main utility of the bio-refining concept is the production of energy products and other high-value materials, simultaneously minimizing waste and enhancing its utilization. Bio-refining can be made more sustainable by the use of highly renewable feedstock for yielding novel high-value products. Lignocellulosic biomass can be used to produce bio-fuels and other value-added products, but competition for land cultivation with food crops is seen to be a major drawback of using it as the feedstock (De Bhowmick et al., 2018).

On the other hand, photosynthetic algae strains for the production of fuel-based compounds, high-value pigments and phycobiliproteins can be grown in fabricated photobioreactors and their land requirement is less (Ubando et al., 2016). Microalgal bio-refinery thus enhances sustainable production of microalgal based products (Chew et al., 2017; Barreiro et al., 2014). Also, certain strains of *Chlamydomonas* and *Dunaliella* have been genetically modified for enhanced production of cellulases and hemicellulases, thus integrating enzyme production with an algal bio-refinery system (Subhadra and Grinson-George, 2011). Another study reported *Chlorella protothecoides* as a source of lipids and carotenoids, grown under high salinity and excess light conditions (Campenni et al., 2013). However, the main bottleneck of algal bio-refinery system are low biomass productivity and high energy requirement for efficient biomass separation.

Waste bio-refinery is aimed at the production of fuels, power, heat and value-added chemicals from waste resources, also thereby overcoming waste disposal problems (Venkata Mohan, 2014). Different types of wastes can contribute to this bio-refinery, which includes food waste, lignocellulosic waste, paper waste, municipal solid waste and manure (Ubando et al., 2020). Bio-refinery thus plays a significant role in addressing the concept of a circular economy. Different bio-refinery models are recently detailed by Ubando et al. (2020) along

with their conversion platforms and sustainability assessment, which included life cycle (LCA) and techno-economic analysis (TEA).

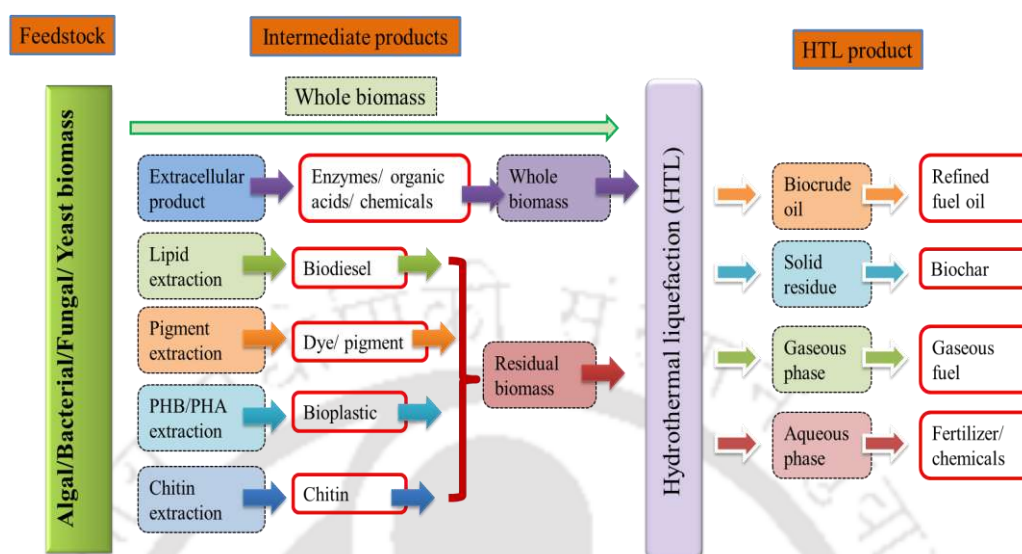


**Fig. 2.10** Bio-refinery approach using oleaginous microorganisms for production of bio-crude oil and other valuable products

Based on the afore-mentioned literature, this study focused on PRWW treatment and lipid-rich biomass production by *R. opacus* for subsequent conversion to bio-oil by hydrothermal liquefaction. Thus a sustainable zero waste strategy for PRWW treatment with provisions for resource recovery is demonstrated through this study.

### 2.11. Aim and Objectives

This present work is aimed at the removal/degradation of toxic recalcitrant compounds present in refinery wastewater by using *Rhodococcus opacus* and bio-oil production by hydrothermal liquefaction (HTL) of lipid-rich bacterial biomass. To achieve this aim, the following investigations were carried out:

1. Characterization of wastewater from a petroleum refinery and optimization of culture conditions for treatment using *R. opacus* in batch system.

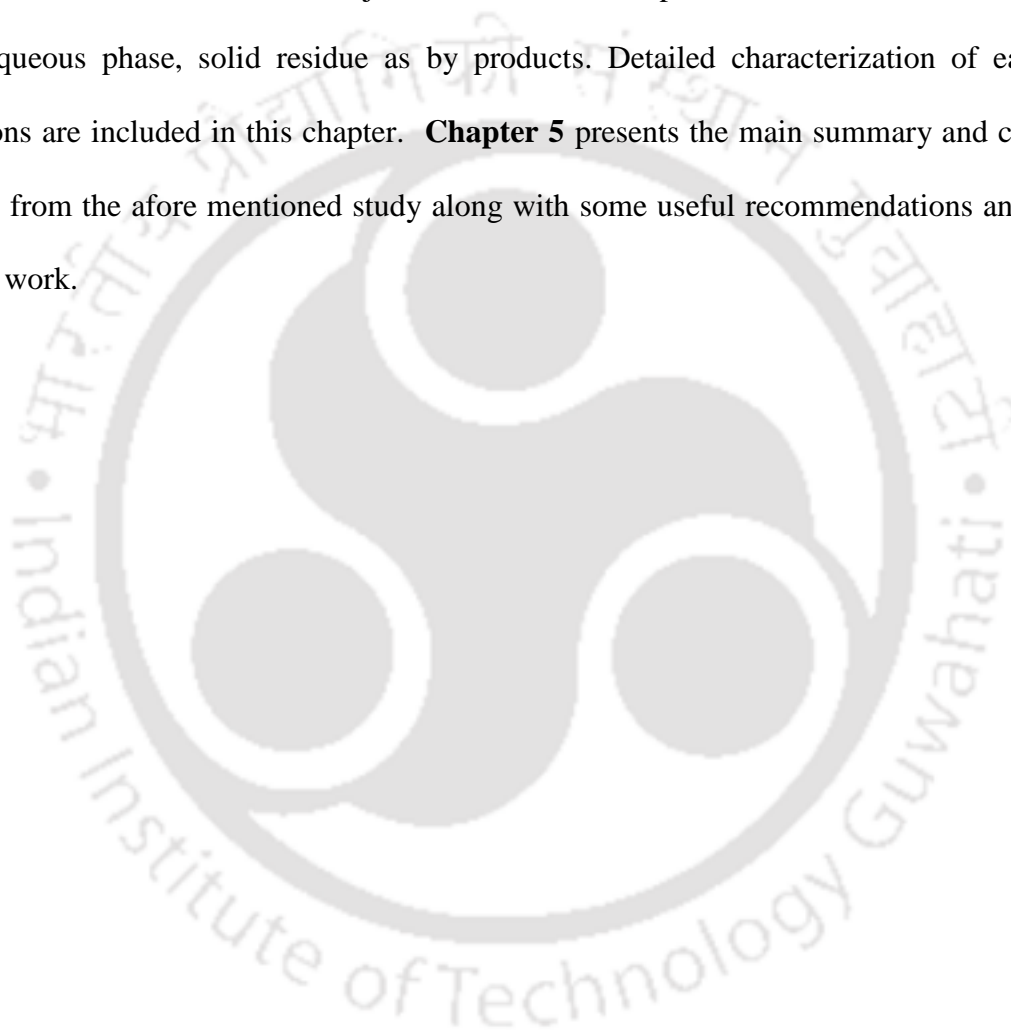
2. Effect of COD concentration in petroleum refinery wastewater (PRWW) on biomass growth and lipid production by *R. opacus* and kinetic modeling
3. Performance evaluation of a simple continuous stirred tank reactor (CSTR) for PRWW treatment and lipid-rich biomass production by *R. opacus* under different operation modes.
4. Performance evaluation of a bubble column reactor (BCR) for PRWW treatment and lipid-rich biomass production by *R. opacus* under continuous operation mode.
5. Performance evaluation of a two-stage submerged tubular membrane bioreactor (STMBR) for PRWW treatment and lipid-rich biomass production by *R. opacus* under continuous operation.
6. Bio-oil production by hydrothermal liquefaction (HTL) of lipid-rich *R. opacus* biomass and characterization of bio-oil and other by-products (aqueous phase and soli residue) obtained.

### 2.11.1. Presentation and lay out of the thesis

The present thesis covers five chapters with appropriate sections and subsections and also contains references and visible research output. A brief description of these chapters are mentioned as follows:

**Chapter 1** details introduction to the present work. The potential of *Rhodococcus opacus* for treatment of refinery wastewater along with scope of bio oil production, thus establishing a zero waste bio-refinery strategy is discussed. **Chapter 2** includes detailed discussion and reported literatures based on this present work. **Chapter 3** details the methodology followed for screening of different parameters for COD removal from PRWW by *R. opacus* biomass in batch shake flasks. Furthermore, it details the PRWW treatment using different bioreactor systems and analytical methods followed to assess the treatment efficiency. Methods followed

for bio-oil production by *R. opacus* and optimization of factors involved are mentioned in detail in this chapter. **Chapter 4** mainly presents and discusses the results obtained in this research work. The results of optimization of parameters affecting refinery wastewater treatment followed by kinetic modeling in batch system are initially discussed. It further describes the refinery wastewater treatment efficiency of different lab scale bioreactors. The residual *R. opacus* biomass obtained was subjected to HTL, which produced bio-oil as the main product and aqueous phase, solid residue as by products. Detailed characterization of each of the fractions are included in this chapter. **Chapter 5** presents the main summary and conclusions drawn from the afore mentioned study along with some useful recommendations and scope of future work.



---

---



# CHAPTER-3



## MATERIALS AND METHODS

---

---

### 3. Material and methods

This section describes different techniques and methods followed in the present research.

#### 3.1. Chemicals and reagents

All chemicals and reagents used in this study were of analytical grade and supplied by Hi-Media Pvt. Ltd, India, SRL Chemicals Pvt. Ltd., India, Merck India Ltd. Membrane filtered water (reverse osmosis (RO)) was used for carrying out all experiments in the study (Sartorius, Arium 61316RO & 611UF, Germany).

#### 3.2. Feasibility of PRWW treatment using *R. opacus*

##### 3.2.1. Wastewater collection and characterization

Raw refinery wastewater was collected from a petroleum refinery plant located at Bongaigaon, Assam, India, and was stored at 4°C until required for further use. Characteristics of the raw wastewater are as follows: pH 10.5, light brown color, petrol like odor, 3.5 mS/cm conductivity, 5.19 mg L<sup>-1</sup> dissolved oxygen, 1253 mg L<sup>-1</sup> total dissolved solids (TDS), 558 mg L<sup>-1</sup> total suspended solids (TSS), 4500 mg L<sup>-1</sup> chemical oxygen demand (COD), 0.1 mg L<sup>-1</sup> sulphate content, 8.34 mg L<sup>-1</sup> ammonia content and 0.582 mg L<sup>-1</sup> total heavy metal content. Additionally, the wastewater contained a high amount of toxic aliphatic and aromatic hydrocarbons.

As the refinery wastewater contained mostly recalcitrant organics with negligible concentration of nutrients such as nitrogen and phosphorous, no efforts were made to measure these micronutrients in the wastewater. However, in order to facilitate the growth of *R. opacus* using refinery wastewater as the sole organic substrate, the wastewater was supplemented with a required amount of mineral salt medium (MSM). The composition of the MSM media is mentioned in the next section.

Most Probable Number (MPN) Test is yet another test most commonly performed for water quality testing for detection of the presence of bacteria. It mainly focuses on a group of bacteria known as fecal coliforms and confirms its presence in any water sample. The presence of such microorganisms in water samples is considered harmful and not fit for consumption or usage purpose. It is mainly based on the utilization of lactose present in the growth media by the fecal coliforms present in it. Lactose fermentation in the media is confirmed by a change in the color of the media and the production of gas. This test mainly consists of presumptive, confirmatory and complete tests. The presumptive test helps to analyze the basic idea about the presence of bacteria in the sample. For the presumptive test, the sample is incubated in three different volume (0.5 ml, 5ml and 10ml) in the presence of lactose broth in two different concentration (1X and 2X), 5 tubes each, and incubated at 37 °C for 24 h (Guidelines for drinking water quality, WHO). The lactose broth contains pH indicators, mainly bromocresol purple or bromothymol blue. Following incubation, if any of the incubated tubes (15 tubes) per sample, shows change in color, a confirmatory test is performed for further confirmation regarding the presence of fecal coliform in the water sample. For confirmation, the sample from the positive tubes was streaked on EMB and Mac-Conkey agar plates and incubated for 24-48 h for proper growth of bacterial colonies.

### 3.2.2. *Rhodococcus opacus* and seed culture cultivation

The oleaginous gram-positive bacterium *Rhodococcus opacus* PD630 was obtained from Microbial Type Culture Collection (MTCC), Chandigarh, India. For maintenance, the strain was grown on 1.8% (w/v) Nutrient Broth (NB) agar slants and was stored at 4°C. The pure strain was regularly sub-cultured in every four weeks by growing at 30°C for 48 h. The seed culture of *R. opacus* was cultivated in a 250 ml Erlenmeyer flask containing 50 ml of Luria Bertani (LB) broth. A full loop of the bacteria was inoculated into sterile medium followed by incubation at 30 °C and

120 rpm until the absorbance of the culture reached to 0.99, as measured at 660 nm using a UV-Vis Spectrophotometer (Agilent Technologies, Singapore). For wastewater treatment and lipid-rich biomass production by *R. opacus*, the wastewater was supplemented with Mineral Salt Medium (MSM) in the ratio 1:4 (v/v). The MSM contained the following ingredients (g L<sup>-1</sup>): MgSO<sub>4</sub>·7H<sub>2</sub>O, 0.409; CaCl<sub>2</sub>·2H<sub>2</sub>O, 0.0265; KH<sub>2</sub>PO<sub>4</sub>, 1; Na<sub>2</sub>HPO<sub>4</sub>·12H<sub>2</sub>O, 6; FeCl<sub>3</sub>·6H<sub>2</sub>O, 0.0833 and 1% of trace metal solution, i.e., 50µL of each of the trace elements (g L<sup>-1</sup>): FeCl<sub>3</sub>, 1.7; CaCl<sub>2</sub>, 0.6; ZnSO<sub>4</sub>, 0.2; CuSO<sub>4</sub>·7H<sub>2</sub>O, 0.2; MnSO<sub>4</sub>, 0.2; CoCl<sub>2</sub>, 0.8; H<sub>3</sub>BO<sub>3</sub>, 0.1 and Na<sub>2</sub>MoO<sub>4</sub>·2H<sub>2</sub>O, 0.3. Composition of the *R. opacus* biomass was determined as follows: 45.52% of carbon, 7.23% of hydrogen, 12.76% of nitrogen, 2.181% of sulphur, 28 mg L<sup>-1</sup> of carbohydrates, 0.7 mg L<sup>-1</sup> of proteins and 52% (CDW) of lipids.

### 3.2.3. Batch shake flask experiments

Biomass growth due to *R. opacus* using the petroleum refinery wastewater (PRWW) was first studied under batch mode using 250 ml flasks of 100 ml working volume each and by adding the wastewater as the sole carbon source. For evaluating COD removal from wastewater using *R. opacus*, six different Erlenmeyer flasks with MSM and the refinery wastewater in different ratios were employed. Flask 1 used in this batch study contained only PRWW; Flasks 2, 3, 4, 5 and 6 contained MSM and refinery wastewater in different individual proportions of 1:1, 1:2, 1:3, 1:4 and 1:5. After inoculation with 10% (v/v) of *R. opacus* culture, flasks were kept in a shaking incubator at 30°C and 120 rpm for 144 h. Initial pH of the solution was adjusted to 7, and during the experiments, samples were taken at required intervals of time for the analysis of biomass, lipid and COD as described later in section 3.10.

For optimum growth and COD removal by *R. opacus*, shake flask experiments were carried out under batch condition using 250 ml Erlenmeyer flasks with 100 ml working volume

each and containing refinery wastewater supplemented with MSM in the ratio MSM: WW – 1:4. Following inoculation with a 10% (v/v) of *R. opacus* seed culture, the flasks were incubated at 30° C, 120 rpm for 120 h. For evaluating the effect of different parameters, levels of each parameter was varied one-at-a-time and levels of other parameters were kept constant. Samples were taken during the experiments at regular interval of time and analyzed for evaluation of biomass growth and COD removal efficiency.

For evaluating the effect of carbon-nitrogen (C/N) ratio, Flask 1 contained only refinery wastewater, Flasks 2, 3, 4 and 5 contained wastewater supplemented with minimal salt media with different C/N ratio viz. 25:1, 35:1, 45:1 and 55:1 respectively. For optimum pH evaluation on *R. opacus* biomass growth and COD removal from refinery wastewater, initial solution pH of Flask 1 containing raw refinery wastewater, Flasks 2, 3, 4, 5, 6, 7 and 8 containing wastewater supplemented with MSM were adjusted to with different initial pH adjusted viz. 3,4,5,6,7,8 and 9 respectively. For studying the effect of different nitrogen sources, Flask 1 contained only raw refinery wastewater and Flasks 2, 3, 4 and 5 contained  $\text{NH}_4\text{Cl}$ ,  $(\text{NH}_4)_2\text{SO}_4$ , urea and  $\text{NH}_4\text{H}_2\text{PO}_4$  respectively.

### 3.3. Effect of different factors on PRWW treatment

#### 3.3.1. Effect of different factors on lipid-rich biomass production from refinery wastewater

Plackett-Burman experimental design consisting of a set of 12 experimental runs was used to determine the relative significance of the different parameters on *R. opacus* biomass growth, COD removal and lipid production by *R. opacus*. The factors in this study included three media constituents viz.  $\text{NH}_4\text{Cl}$ ,  $\text{KH}_2\text{PO}_4$ , and  $\text{Na}_2\text{HPO}_4$  and three physicochemical variables i.e., pH, agitation and temperature. All the batch experimental runs were thus statistically designed and the studies were performed in duplicate using 250 ml Erlenmeyer flasks with 100 ml working volume.

Table 3.1 presents the combination of each factor and their levels along with the responses obtained in each of the experimental runs.

**Table 3.1** Plackett-Burman experimental design matrix for studying the effect of different variables affecting biomass growth, COD removal and lipid production

Exp Run no.	Variables and their levels						Responses		
	NH <sub>4</sub> Cl (g L <sup>-1</sup> )	KH <sub>2</sub> PO <sub>4</sub> (g L <sup>-1</sup> )	Na <sub>2</sub> HPO <sub>4</sub> (g L <sup>-1</sup> )	pH	Agitati on (rpm)	Temp (C)	Absorbance (660 nm)	COD removal %	Lipid (%CD W)
1	0.5	0.5	3	6	100	25	0.988	73	22
2	1.5	1.5	9	6	200	35	0.576	54	19
3	1.5	0.5	3	6	200	35	0.613	44	33
4	0.5	0.5	9	8	200	25	0.886	38	27
5	1.5	1.5	3	8	100	25	0.576	36	37
6	0.5	1.5	9	8	100	35	0.286	35	27
7	0.5	0.5	3	8	200	35	0.872	61	36
8	1.5	0.5	9	8	100	35	0.233	59	34
9	0.5	1.5	3	6	100	35	0.287	78	36
10	0.5	1.5	9	6	200	25	0.755	53	36
11	1.5	1.5	3	8	200	25	0.381	39	33
12	1.5	0.5	9	6	100	25	0.899	54	39

### 3.4. Effect of different COD concentration on biomass growth, lipid production and kinetic modelling

#### 3.4.1. Kinetics of wastewater COD utilization, biomass growth and lipid production

For evaluating the kinetics of wastewater COD utilization, biomass growth and lipid accumulation by *R. opacus*, batch experiments were carried out using Erlenmeyer flasks with

different initial COD concentration in the range 2.5-4.5 g L<sup>-1</sup> and 100 ml working volume each. For obtaining different initial COD concentrations in the study, the raw wastewater was suitably diluted with MSM and adjusted to pH 7. Following inoculation with *R. opacus* seed culture (10% (v/v)), the flasks were incubated at 30 °C temperature and 120 rpm agitation speed. Samples were routinely taken during the experiments at a regular time interval and analyzed for biomass growth, residual COD and lipid contents. Biomass dry weight, expressed as cell dry weight (CDW, g L<sup>-1</sup>), was measured at every 12 h time interval, and the biomass specific growth rate ( $\mu$ ) was calculated as per the following Equation 3.1.

$$\mu = \frac{1}{X} \frac{dX}{dt} \quad (\text{Eq. 3.1})$$

where  $\mu$  is the biomass specific growth rate (h<sup>-1</sup>),  $X$  is the biomass concentration (g L<sup>-1</sup>) corresponding to the time  $t$  (h).

The bio-kinetics of COD utilization by *R. opacus* was analyzed by fitting the experimental data to first order, logarithmic and logistic kinetic models (Equations 3.2-3.4) (Saravanan et al., 2011).

First order 
$$S = S_0 e^{(-Kt)} \quad (\text{Eq. 3.2})$$

Logarithmic 
$$S = S_0 + X_0 [1 - e^{(\mu_{max} t)}] \quad (\text{Eq. 3.3})$$

Logistic 
$$S = \frac{S_0 + X_0}{1 + \frac{X_0}{S_0} \left[ e^{\left( \frac{\mu_{max}}{K_S} \right) (S_0 + X_0) t} \right]} \quad (\text{Eq. 3.4})$$

Where  $S$  and  $S_0$  are the instantaneous and initial COD concentrations (g L<sup>-1</sup>), respectively.  $X_0$  is the initial biomass concentration (g L<sup>-1</sup>),  $K$  is the first-order rate constant (h<sup>-1</sup>),  $\mu_{max}$  is the maximum biomass specific growth rate (h<sup>-1</sup>), and  $K_S$  is the half-saturation coefficient (g L<sup>-1</sup>).

The effect of initial COD concentration on specific utilization rate ( $q$ ,  $h^{-1}$ ) by the bacterium was calculated by using the following Equation 3.5, and the experimental data fitted to modified bio-kinetic models reported in the literature (Equations 3.5-3.12) (Mitra et al., 2017).

$$q = -\frac{1}{X} \frac{dS}{dt} \quad (\text{Eq. 3.5})$$

Monod  $q = \frac{q_{max} S}{K_S + S} \quad (\text{Eq. 3.6})$

Haldane  $q = \frac{q_{max} S}{K_S + S + \frac{S^2}{K_i}} \quad (\text{Eq. 3.7})$

Han-Levenspiel  $q = \frac{q_{max} S \left[1 - \frac{S}{S_m}\right]^n}{K_S + S \left[1 - \frac{S}{S_m}\right]^m} \quad (\text{Eq. 3.8})$

Edward  $q = \frac{q_{max} S}{K_S + S + \left(\frac{S^2}{K_i}\right) \left(1 + \frac{S}{K_S}\right)} \quad (\text{Eq. 3.9})$

Moser  $q = \frac{q_{max} S^n}{K_S + S^n} \quad (\text{Eq. 3.10})$

Yano and Koga  $q = \frac{q_{max} S}{K_S + S + \left(\frac{S^2}{K_1}\right)^n} \quad (\text{Eq. 3.11})$

Luong  $q = \frac{q_{max} S}{K_S + S} \left[1 - \frac{S}{S_m}\right]^n \quad (\text{Eq. 3.12})$

where  $q$  is the specific COD utilization rate ( $h^{-1}$ ),  $q_{max}$  is the maximum specific COD utilization rate ( $h^{-1}$ ),  $S$  is the COD concentration ( $g L^{-1}$ ),  $S_m$  is the COD concentration above which net growth ceases ( $g L^{-1}$ ),  $K_S$  is the half-saturation constant ( $g L^{-1}$ ),  $K_i$  is the inhibition constant ( $g L^{-1}$ ),  $K_1$  is a positive constant and  $n$  and  $m$  are empirical constants.

In addition to the above, the following two bio-kinetic models (Equations 3.13-3.14) were further applied to simulate the biomass growth (Mu et al., 2007).

$$\text{Gompertz} \quad X - X_0 = X_{max} e^{\left[ -e^{\left[ \left( \frac{r_{xmax} \times 2.71828}{X_{max}} \right) (\lambda - t) + 1 \right]} \right]} \quad (\text{Eq. 3.13})$$

$$\text{Logistic} \quad X - X_0 = \frac{X_{max}}{\left[ 1 + e^{\left[ \left( \frac{4r_{xmax}}{X_{max}} \right) (\lambda - t) + 2 \right]} \right]} \quad (\text{Eq. 3.14})$$

Where  $X_{max}$  is the maximum biomass concentration ( $\text{g L}^{-1}$ ),  $r_{xmax}$  is the maximum rate of biomass growth ( $\text{g L}^{-1} \text{h}^{-1}$ ) and  $\lambda$  is the time for lag phase (h).

For describing lipid production by *R. opacus* biomass, the following modified form of Gompertz model equation was fitted to the experimental data:

$$P = P_{max} e^{\left[ -e^{\left[ \left( \frac{r_{pmax} \times 2.71828}{P_{max}} \right) (\lambda - t) + 1 \right]} \right]} \quad (\text{Eq. 3.15})$$

Where  $P$  is cumulative lipid production ( $\text{g L}^{-1}$ ),  $P_{max}$  is maximum lipid production ( $\text{g L}^{-1}$ ), and  $r_{pmax}$  is the maximum rate of lipid production ( $\text{g L}^{-1} \text{h}^{-1}$ ). The bio-kinetic model parameters were estimated by minimizing the sum of squared errors (SSE) between the experimental and model predictable values by using the 'Solver' function tool in Excel 2016. Additionally, lipid yield was calculated from lipid and COD concentration, whereas specific lipid production rates was calculated from  $\mu$  and biomass concentration.

## 3.4.2. Kinetics of COD inhibition on biomass growth

Monod model can be used to study the effect of substrate on the specific growth rate of microorganisms. However, at a high substrate concentration, this kinetic model is unsatisfactory due to substrate inhibition on the biomass growth. Hence, the following substrate inhibition models were applied in this study to describe the effect of COD present in the wastewater on *R. opacus* specific growth rate (Equation 3.16-3.24) (Saravanan et al., 2011; Agarry et al., 2010; Mitra et al., 2017).

$$\text{Andrews} \quad \mu = \frac{\mu_{max} S}{K_S + S + \frac{S^2}{K_i}} \quad (\text{Eq. 3.16})$$

$$\text{Aiba} \quad \mu = \frac{\mu_{max} S}{K_S + S} e^{\left(\frac{-S}{K_i}\right)} \quad (\text{Eq. 3.17})$$

$$\text{Han and Levenspiel} \quad \mu = \frac{\mu_{max} S \left[1 - \frac{S}{S_m}\right]^n}{K_S + S \left[1 - \frac{S}{S_m}\right]^m} \quad (\text{Eq. 3.18})$$

$$\text{Luong} \quad \mu = \frac{\mu_{max} S}{K_S + S} \left[1 - \frac{S}{S_m}\right]^m \quad (\text{Eq. 3.19})$$

$$\text{Tiessier} \quad \mu = \mu_{max} \left[ e^{\left(\frac{-S}{K_i}\right)} - e^{\left(\frac{-S}{K_S}\right)} \right] \quad (\text{Eq. 3.20})$$

$$\text{Edward} \quad \mu = \frac{\mu_{max} S}{K_S + S + \left(\frac{S^2}{K_i}\right) \left(1 + \frac{S}{K_S}\right)} \quad (\text{Eq. 3.21})$$

$$\text{Webb} \quad \mu = \frac{\mu_{max} S \left(1 + \left(\frac{S}{K_i}\right)\right)}{K_S + S + \left(\frac{S^2}{K_1}\right)^n} \quad (\text{Eq. 3.22})$$

$$\text{Tseng and Wayman} \quad \mu = \left( \mu_{max} \left( \frac{S}{K_S + S} \right) \right) - (K_i (S - S_m)) \quad (\text{Eq. 3.23})$$

Yano and Koga

$$\mu = \frac{\mu_{max} S}{K_s + S + \left(\frac{S^2}{K_i}\right)^n} \quad (\text{Eq. 3.24})$$

where  $\mu$  is the biomass specific growth rate ( $\text{h}^{-1}$ ),  $\mu_{max}$  is the maximum biomass specific growth rate ( $\text{h}^{-1}$ ),  $S$  is the COD concentration ( $\text{g L}^{-1}$ ),  $S_m$  is the maximum COD inhibition constant above which cells cease to grow ( $\text{g L}^{-1}$ ),  $K_s$  is the half-saturation constant ( $\text{g L}^{-1}$ ),  $K_i$  is the inhibitory COD concentration ( $\text{g L}^{-1}$ ), and  $K_i$ ,  $n$ , and  $m$  are constants.

### 3.5. Performance evaluation of a continuously stirred tank reactor (CSTR) for PRWW treatment and lipid-rich biomass production under different operation modes

Simultaneous biodegradation of toxic hydrocarbons present in the refinery wastewater and lipid production by *R. opacus* was investigated using an indigenous lab-scale bioreactor (2.5 L total volume) under different operating modes, viz, batch, fed-batch, sequential batch (SBR), continuous and continuous with cell recycle using a low cost tubular ceramic membrane. Based on the results of the batch study, the wastewater was supplemented with MSM for supporting the bacteria for COD utilization, biomass growth and lipid accumulation. All the experiments were carried out with 1.5 L of working volume under the controlled conditions of pH 7, temperature 30 °C and agitation of 250 rpm. The influent pH was adjusted by addition of 1M NaOH or 0.5 M  $\text{H}_2\text{SO}_4$  as needed. The dissolved oxygen (DO) concentration in the reactor was controlled at above 2 mg  $\text{L}^{-1}$  by continuous stirring at 250 rpm and aeration at 1 L/min. Initially, the reactor was operated under batch mode for 5 days using 10% (v/v) of *R. opacus* as the inoculum and the refinery wastewater was supplemented with MSM in the ratio of 4:1 (v/v). Based on the batch results, the reactor was operated under fed batch mode, and for which the feed was started after 24h of initial batch operation and maintained for 18 h. The SBR operation was carried out for one cycle at a HRT of 18 h following inoculation. Under continuous operating mode, different HRTs of 8, 16 and 24 h were evaluated for its effect on the reactor performance.

During the experiments, samples were taken at every 6 h interval and analyzed for biomass concentration ( $\text{g L}^{-1}$ ), COD removal (%) and lipid concentration ( $\text{g L}^{-1}$ ). All the analyses were carried out in triplicate and the results were obtained within  $\pm 4\%$  standard deviation.

For fed-batch mode of operation with the bioreactor, the feed rate (F) was calculated using the following Equation 3.25:

$$F = \frac{X_0 V_0 e^{\mu t}}{Y_{X/S} S_0} \quad (\text{Eq. 3.25})$$

where F,  $X_0$ ,  $V_0$ ,  $S_0$ ,  $\mu$  and  $Y_{X/S}$  denote feed rate ( $\text{L h}^{-1}$ ) of the wastewater, bacterial biomass concentration ( $\text{g L}^{-1}$ ) at the end of the batch operation, wastewater volume (L) in the bioreactor at the end of the batch, initial wastewater COD ( $\text{g L}^{-1}$ ), biomass specific growth rate ( $\text{h}^{-1}$ ) and biomass yield, respectively. The  $\mu$  (specific growth rate) was estimated from the results of the previously conducted batch experiment and the biomass yield was calculated using the following Equation 3.26:

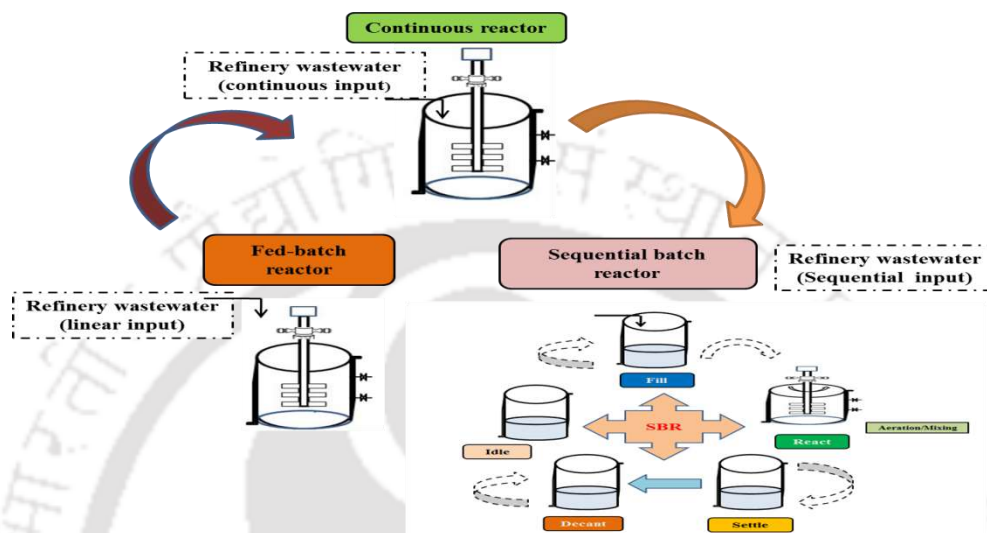
$$Y_{X/S} = \frac{X_m - X_0}{S_0 - S_m} \quad (\text{Eq. 3.26})$$

Where  $X_m$ ,  $X_0$ ,  $S_m$  and  $S_0$  represent maximum biomass concentration ( $\text{g L}^{-1}$ ) at time (t), initial cell concentration ( $\text{g L}^{-1}$ ) at initial time ( $t = 0$ ), total substrate concentration ( $\text{g L}^{-1}$ ) at time (t) and total substrate concentration ( $\text{g L}^{-1}$ ) at initial time ( $t = 0$ ), respectively.

Cell recycle ratio in the continuous with cell recycle experiments was calculated according to the following Equation 3.27:

$$X_1 = \frac{Y_{X/S} (S_m - S_0)}{(1 + \alpha - \alpha C)} \quad (\text{Eq. 3.27})$$

where  $\alpha$ ,  $C$ ,  $X_1$ ,  $S_0$  and  $S$  denote recycle ratio, concentration factor in the cell recycle stream, initial and final substrate concentrations ( $\text{g L}^{-1}$ ) respectively. The schematic showing different reactor modes operated for treating PRWW is presented in Fig. 3.1 and Fig. 3.2.



(a)



(b)

**Fig. 3.1** (a) Schematic and (b) Image of experimental set up showing reactor carried out with the CSTR mode for treatment of refinery wastewater

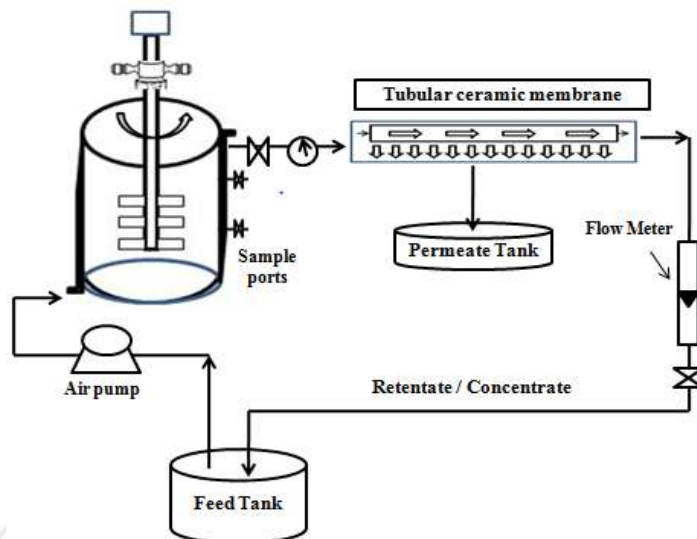


**Fig. 3.2** Schematic showing cell recycle approach using tubular ceramic membrane

The membrane was found to have a mean pore size of  $0.339 \mu\text{m}$  and was characterized as needed for corrosion resistance and flexural strength. Also, permeate flux value of the membrane was  $3.40 \times 10^{-5} \text{ m}^3/\text{m}^2\text{s}$  under a pressure of 68 kPa by employing a cross flow filtration system (Kumar et al., 2015). For biomass separation in this study, the microfiltration module was packed into stainless steel pellicon holder fixed with diaphragm, pressure gauges at the inlet and outlet ports (Fig. 3.3). A peristaltic pump was used to supply the driving force required for achieving the trans-membrane flux. For cell-recycle following membrane separation using the tubular membrane set up, effluent from the bioreactor was fed to the membrane system and retentate containing the cell fed directly to the bioreactor. The working volume of the reactor was maintained constant by supplying the retentate i.e. cell suspension from the microfiltration module into the bioreactor with HRT of 16h. After each cycle of the membrane operation, the membrane was washed with Milli Q water to avoid reduction in the membrane flux and clog formation.

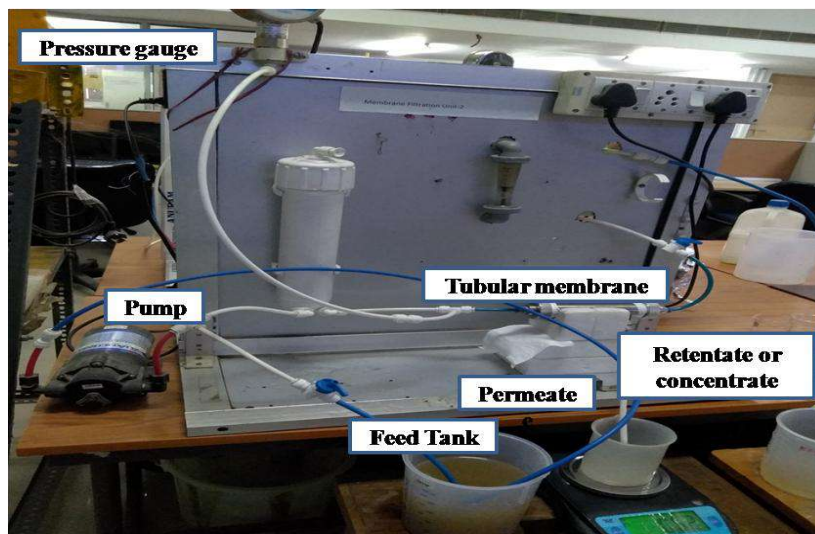


**Fig. 3.3** Experimental set-up showing cell recycle using tubular ceramic membrane

For biomass separation and recycle following wastewater treatment and lipid accumulation by the bacteria, the bioreactor was connected to an indigenously prepared tubular ceramic membrane. An extrusion process was adopted to form a tubular-shaped ceramic membrane. The table top hand extruder (M/s VB Ceramic Consultants, Chennai, India) made of stainless steel was used for obtaining tubular ceramic tubes consisting of a feed chamber, extruder screw shafts, cone, and die assemblies. The dough was prepared from a mixture of Ball clay—18 wt%, Feldspar —6 wt%, Kaolin—15 wt%, Pyrophyllite-15 wt%, Quartz—28 wt%, and Calcium carbonate—18 wt%. The membrane preparation steps are shown in Fig. 3.4.

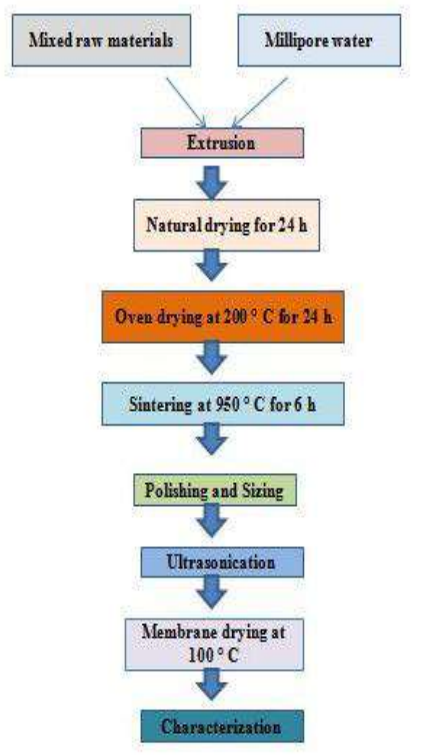


**Fig. 3.4** Schematic representation of tubular ceramic membrane fabrication

In order to determine the hydrocarbon degradation profile following continuous with cell recycle experiments with the bioreactor, samples were taken at regular time interval and analyzed by GC-MS (Perkin Elmer Clarus 600).

### **3.6. Performance evaluation of a bubble column reactor (BCR) for PRWW treatment and lipid-rich biomass production**

For lipid-rich biomass production from refinery wastewater under continuous operation mode a bubble column reactor (BCR) with total volume of 2 L and working volume of 1.8 L was fabricated out of Perspex material. The reactor height and diameter were 45 and 8 cm, respectively. The reactor bottom consisted of a stainless steel made nozzle for air inlet along with another port for introducing wastewater into the reactor by means of a peristaltic pump. The

reactor was operated in top flow mode and samples were drawn from the reactor outlet. Fig. 3.5 illustrates a schematic of the bubble column bioreactor used in the study.

Initially, the bioreactor was operated under batch mode of operation by adding where wastewater along with MSM (1:4 ratio) and (10% v/v) of *R. opacus* seed culture as the inoculum followed by continuous aeration. The reactor was then operated at different hydraulic retention time (HRT) ranging from 24 to 8 h under continuous operation mode to study the effect of HRT on the reactor performance. No effort was made to control the temperature and pH inside the bioreactor. The influent pH was adjusted to 7.0 and the ambient temperature of the reactor during the continuous operation was  $27 \pm 2^\circ\text{C}$ . Sample analysis was carried out in triplicate and results were presented as mean  $\pm$  standard deviation.

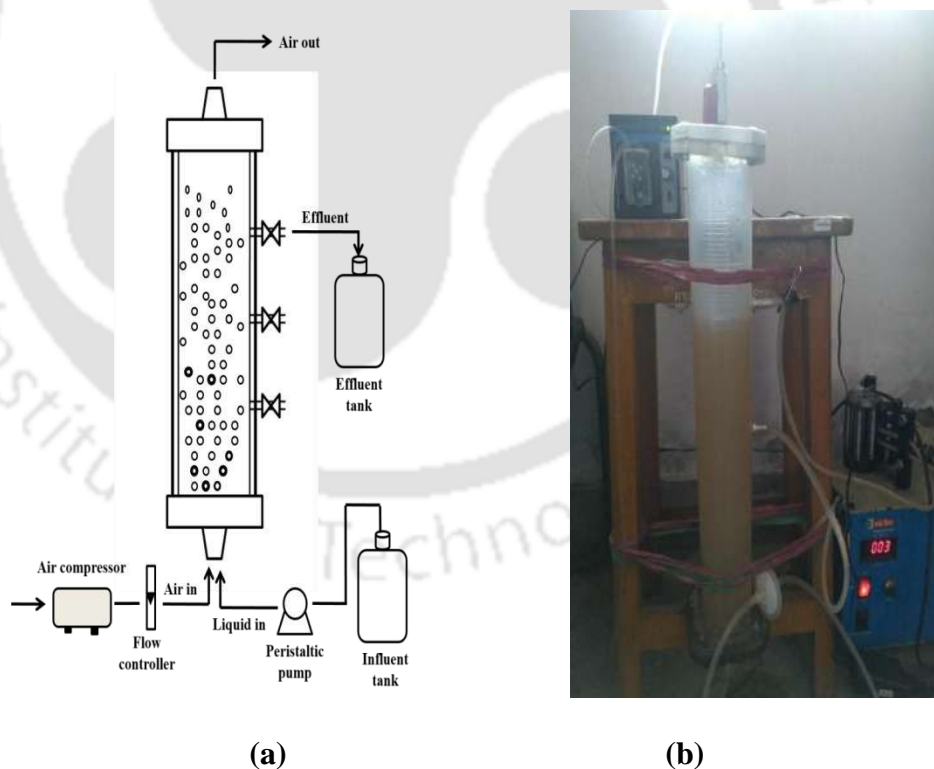


**Fig. 3.5** (a) Schematic and (b) Image of the experimental set up showing the BCR used in the study

### 3.7. Performance evaluation of submerged tubular membrane bioreactor (STMBR) for PRWW treatment and lipid-rich biomass production by *R. opacus*.

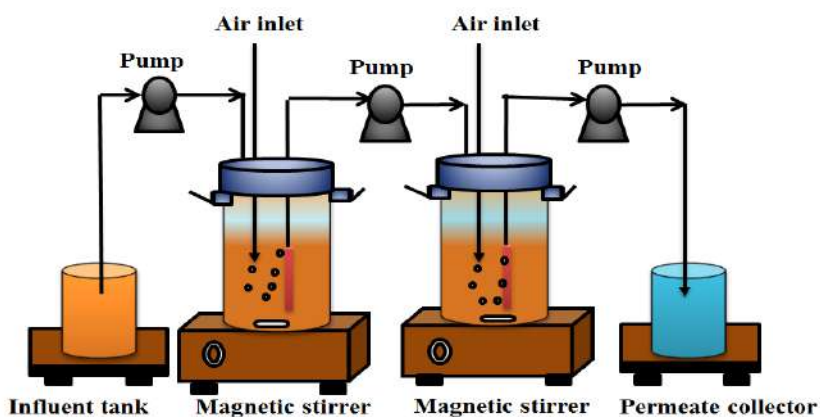
Wastewater treatment by *R. opacus* was initially examined using a single-stage submerged tubular membrane bioreactor (STMBR). Fig. 3.4 (a) shows a schematic and the image of the STMBR used in this study. The set up consisted of a feed tank, a peristaltic pump for feeding the wastewater into the STMBR, a submerged tubular ceramic membrane module (average pore size 0.3  $\mu\text{m}$ ) and an outflow booster pump for withdrawing the permeate (treated water) through the membrane. The refinery wastewater with an initial COD of 3500  $\text{mg L}^{-1}$  (diluted with MSM in the ratio 4:1) was fed into the reactor by means of a variable speed peristaltic pump. The STMBR with a working volume of 1.5 L was operated at 30 °C and agitation speed of 250 rpm; the pH of the wastewater was adjusted to 7 with either 1M NaOH or 0.5 M  $\text{H}_2\text{SO}_4$  solutions.

Prior to the bioreactor operation, the *R. opacus* seed culture was acclimatized with PRW for 5 days. The tubular ceramic membrane used in this study was prepared from locally available raw materials, as detailed earlier in section 3.5. Compressed air at 2  $\text{L min}^{-1}$  was supplied to the membrane module for oxygen supply and proper mixing in the reactor as well as to reduce membrane fouling. The single-stage STMBR was operated at a constant pressure of 207 kPa and continuous mode for a total period of 18 days. After an initial startup of the STMBR under batch mode, the bioreactor was operated under continuous mode in five phases with each phase lasting for about 78 h. At the end of each phase, membrane backwashing was carried out to ensure a constant permeate flux, thereby maintaining 16 h HRT throughout the experiments. The permeate flux analysis was carried out at the beginning of each phase, i.e. immediately after the backwashing of membranes in the single-stage STMBR. In addition to the backwashing of membranes, the surface of the membrane was cleaned at the end of each phase by manually

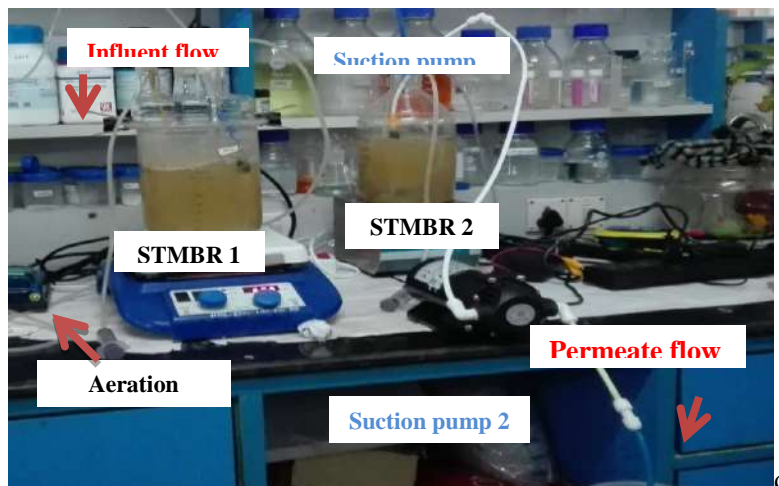
removing the cake layer formed on the surface with the help of tap water in order to restore the membrane flux and avoid blockage of membrane pores.

Following experiments with the single-stage STMBR, a two-stage STMBR system was evaluated under the same operating conditions as before (Fig. 3.4 (b)). However, the two-stage operation was divided into three phases and each phase lasted for about 24 h. Membrane washing was carried out at the end of each phase to restore regain the original permeate flux as mentioned earlier. Thus, the total operation time with the two-stage STMBR system was greatly reduced as the system could remove the wastewater COD completely from the inlet stream, obviating any further treatment step.

Samples were withdrawn from the STMBR at regular intervals of time for the analyses of COD removal (%), biomass growth ( $\text{g L}^{-1}$ ) and lipid concentration ( $\text{g L}^{-1}$ ). Sample analysis were carried out in triplicate and results were reported as average with a standard deviation of  $\pm 4\%$ .



(a)



(b)

**Fig. 3.6** (a) Schematic and (b) image showing experimental setup with two-stage STMBR system for PRW treatment.

### 3.8. Toxicity assessment of treated wastewater from two-stage STMBR

#### 3.8.1. Seed germination assay

The permeate obtained following wastewater treatment using the two-stage STMBR was analyzed for the presence of phyto-toxins by performing seed germination assay. Using chickpea (*Cicer arietinum* L.) seeds (AmalBadshah Khattak et al., 2007). The assay was performed with distilled water (control), tap water, raw (untreated) PRW and treated water and the results were compared. Required amount of chickpea seeds were taken into petriplates and soaked in 20ml of the water samples; the petriplates were incubated at room temperature in the dark for 24 h. After removing the excess water, the seeds were rinsed and wrapped in an absorbent cloth for maintaining a moist environment at 28 °C. Following incubation, the number of seeds germinated in each case along with root length was calculated for determining seed germination index (GI %) using the following Equation 3.28.

$$\text{Germination index (GI)\%} = \frac{\text{Seed germination of sample (\%)} \times \text{Root length of treatment (\%)}}{\text{Seed germination of control (\%)} \times \text{Root length of control (\%)}} \times 100 \quad (\text{Eq. 3.28})$$

3.28)

### 3.8.2. Brine shrimp lethality assay (BSLA)

Brine shrimp lethality assay (BSLA) for toxicity assessment of the treated water was performed as described in Meyer et al. (1982) with some minor modifications. Brine shrimps (*Artemia salina*) nauplii were hatched in a glass tank with simulated seawater (2.5% saline) under constant illumination and aeration for 24 h. After the eggs were hatched, 30 nauplii in each sample vials were transferred to different test samples: tap water, distilled water, raw PRW, and treated water; three replicates for each sample were taken. Positive control for this assay consisted of 30 nauplii in seawater only, and negative control consisted of 30 nauplii in Dimethyl sulfoxide (DMSO). After 24 h of incubation and constant light supply, the percentage death of nauplii per each test sample was calculated as per Equation 3.29 (Meyer et al., 1982). The hatched larvae after incubation were considered dead if they failed to show any external movement during observation (Ahmed et al., 2016).

$$\% \text{ Death} = \frac{\text{Test} - \text{control}}{100 - \text{control}} \times 100 \quad (\text{Eq. 3.29})$$

### 3.8.3. MTT [3-(4,5- dimethylthiazol-2-yl)-2,5-diphenylte- trazoliumbromide] assay

In this assay, viability of HacaT cells is checked with 3-(4,5- dimethylthiazol-2-yl)-2,5-diphenylte- trazoliumbromide (MTT) dye by measuring the conversion of this dye into dark blue formazan precipitation which is attributed to the succinate dehydrogenase enzyme present in intact mitochondria of the live cells. HacaT cells were seeded into 96 well plates consisting of  $1 \times 10^4$  cells per well with Dulbecco's Modified Eagles Medium (10% FBS) followed by incubation for 24 h. After attaining proper confluency, the cells were exposed to the treated water for 72 h. PRW was used as the negative control and distilled water acted as the positive control for this assay. Following treatment with the sample, the media was replaced with fresh culture media containing MTT at a concentration of  $5 \text{ (mg ml}^{-1}\text{)}$  and the plates were incubated at  $37^\circ\text{C}$  for 2 h.

After this time period, the media was again removed and the obtained formazan crystals were dissolved in DMSO (of equal volume as the media added). Optical density (OD) was measured at 570 nm using a microplate reader (Spectramax M2 series, Molecular Devices, USA). Relative cell viability was determined by calculating the percentage viability.

### 3.8.4. Fluorescence activated cell sorting (FACS) analysis

#### 3.8.4.1. Cell seeding/preparation

Plate containing HEK cells was taken and the media was discarded from the plate for cell washing using PBS. The cells were treated with 200  $\mu$ L trypsin and incubated at CO<sub>2</sub> incubator for 3-5 minutes. 2 ml of fresh media was added to the plate and the cells were then gently collected by centrifugation at 12000 rpm for 6 minutes at 4°C. Following centrifugation, the supernatant was discarded and the obtained pellet mixed with 1 ml fresh media. 50  $\mu$ L of the cells were then treated with 50  $\mu$ L trypsin blue in the ratio 1:1. The cell count was checked prior to further treatment prior to seeding of 1 ml of cell solution (containing 50000 cells per ml) in 6 well plate along with the addition of 1 ml fresh media. This plate was incubated in a CO<sub>2</sub> incubator for 24 h and treated with different treated wastewater samples except the control well.

The cells from the respective wells in the plates were then collected and centrifuged at 4000 rpm for 20 min at 4 °C. The cell pellet obtained was then mixed gently with 1 ml PBS (1x PBS) and centrifuged again at 4000 rpm for 10 min at 4 °C. The cell washing was carried out twice. The collected pellet was then added with 495  $\mu$ L of 1xPBS and mixed gently and kept in ice. To the cell mixture in a polystyrene tube, 5  $\mu$ L of PI (propidium iodide) dye was added to each tube and incubated in ice for 7-10 min prior to the FACS analysis (FACS Caliber TM, BD Biosciences, USA).

### 3.9. Characterization and hydrothermal liquefaction (HTL) of *R. opacus* biomass for bio-oil production

#### 3.9.1. *R. opacus* biomass characterization

For a detailed characterization of the *R. opacus* biomass produced from PRW, the biomass was first washed with Milli Q water and lyophilized. The lyophilized *R. opacus* biomass was analyzed for its ash content, volatile matter (VM), moisture content (MC) and fixed carbon content (FC) according to ASTM standards E870-82 (Wei et al., 2015). Elemental composition of the biomass was analyzed by CHNS analyzer (EuroEA3000 Elemental Analyser, Euro Vector, Italy); oxygen content and high heating value (HHV) were calculated by using the following empirical Equation (Equation 3.30 and 3.31):

$$O(\text{wt}\%) = 100 - (C + H + N) \quad (\text{Eq. 3.30})$$

$$\text{HHV}_{\text{Boie}} (\text{MJkg}^{-1}) = 0.3516 C + 1.16225 H - 0.1109 O + 0.0628 N \quad (\text{Eq. 3.31})$$

For determining biochemical composition of the biomass, total lipids, carbohydrate and protein contents were analyzed (Song et al., 2017). All these analyses were done in triplicates and average values were obtained.

#### 3.9.2. HTL experiments

HTL of the lipid rich *R. opacus* biomass following wastewater treatment was carried out using a 50 ml stainless steel vessel of 30 ml working volume and at 250 °C temperature for a reaction time of 2 h. The biomass (3-4 g) was added with 15 ml of deionized water and mixed well for 5 minutes before transferring into the HTL vessel. After the reaction time, the entire vessel was placed in an ice-water bath to quench the reaction and liquid phases were collected following solvent extraction with dichloromethane for further analysis. During collection, the vessel was washed with chloroform and mixed well. The oil and aqueous phases were separated and

dichloromethane was evaporated eventually. The bio-oil thus obtained was further weighed and characterized for its properties. The other liquid phase containing mostly water soluble products was dried in an oven at 105 °C and its final weight was determined. The experiments were repeated thrice and the average bio-oil yield obtained along with standard deviation was reported.

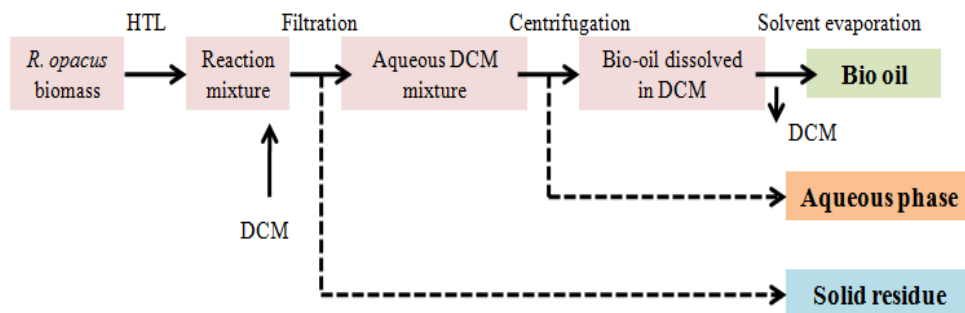


**Fig. 3.7** Schematic showing the steps followed for bio-oil production from *R. opacus* biomass by HTL and products separation.

After cooling down the contents inside, samples taken from the reactor were extracted using dichloromethane for further analysis. The solvent extract was then added with de-ionized water followed by centrifugation of the mixture to obtain solvent phase containing bio-oil and water soluble by-products. The solid residues obtained during the solvent extraction step were also recovered, heated at 105 °C and analyzed for its contents. The experiment was repeated thrice to ensure reproducibility; average bio-oil yield and standard deviations were reported. Schematic of the experimental procedure followed for carrying out the HTL process in this study is shown in Fig. 3.7.

The yield of Bio-oil (BOY) and other by products *viz.* Solid Residue (SRY) and Water Soluble Product (WSPY) were calculated as % ( $w/w$ ) of initial biomass loaded in the HTL reactor.

The yield of these different products were determined as per the following Equation (3.32-3.34):

$$\text{BOY (wt\%)} = \frac{\text{Mass of bio-oil}}{\text{Mass of } R.\textit{opacus} \text{ biomass}} \times 100 \quad (\text{Eq. 3.32})$$

$$\text{SRY (wt\%)} = \frac{\text{Mass of solid residue}}{\text{Mass of } R.\textit{opacus} \text{ biomass}} \times 100 \quad (\text{Eq. 3.33})$$

$$\text{WSPY (wt\%)} = \frac{\text{Mass of water soluble products}}{\text{Mass of } R.\textit{opacus} \text{ biomass}} \times 100 \quad (\text{Eq. 3.34})$$

Furthermore, the biomass conversion was determined on dry weight basis according to the following Equation (3.35) as follows,

$$\text{Conversion (wt\%)} = 1 - \frac{\text{Mass of solid residue}}{\text{Mass of } R.\textit{opacus} \text{ biomass}} \times 100 \quad (\text{Eq. 3.35})$$

### 3.9.3. Optimization of HTL process parameters

In order to optimize HTL process conditions for achieving a maximum bio-oil yield from *R. opacus* biomass, HTL experiments were carried out as per the statistical experimental design technique response surface methodology (RSM). Values of the HTL process parameters *viz* temperature (°C), reaction time (min) and biomass to water ratio (B/W) investigated in this optimization study were in the range 180-250, 50 -200 and 0.10 -0.40, respectively.

Relationship between the output variable (bio-oil yield) and the independent parameters in RSM is generally expressed by the following second order polynomial equation given below (Equation 3.36).

$$Y = \beta_0 + \sum_{i=1}^k \beta_i X_i + \sum_{i=1}^k \beta_{ii} X_i^2 + \sum_{i=1}^k \sum_{j=1}^k \beta_{ij} X_i X_j \quad (\text{Eq. 3.36})$$

Where,  $Y$  is the predicted response (i.e. bio-oil yield, %),  $\beta_0$ ,  $\beta_i$ ,  $\beta_{ii}$  and  $\beta_{ij}$  are the intercept, coefficient of linear, quadratic and interaction effects, respectively.  $X_i$  and  $X_j$  are the independent variables (temperature, reaction time and biomass-water ratio) in coded levels and  $k$  is the number of independent variables ( $k=3$ ).

Regression and statistical analysis of the regression coefficients were performed using Design-Expert Software (Version 7.1.5, State-Ease, USA). Response surfaces and contour plots were generated to examine the overall effect of the test variables on percentage yield of bio-oil.

### 3.9.4. Characterization of bio-oil and HTL by products

#### 3.9.4.1. HTL product characterization and analysis

Aqueous phase obtained as a byproduct of HTL and containing water soluble product was analyzed gravimetrically (Barreiro et al., 2013), and the functional groups of compounds present in the organic liquid fraction were determined by using FTIR system (Perkin Elmer, USA). Elemental composition analysis of the bio-oil was determined by elemental analyzer (EuroEA3000 Elemental Analyser, Euro Vector, Italy) for evaluating its properties as a bio-fuel. Oxygen content in the bio-oil was calculated, whereas its HHV was estimated using the Dulong formula (Song et al., 2017) as given by Equation (3.37)

$$HHV_{Dulong} (MJkg^{-1}) = 0.338 C + 1.428(H - 0.125O) + 0.095 S \quad (3.37)$$

The solid residue was characterized by field emission scanning electron microscopy with energy dispersive x-ray spectroscopy (FESEM-EDX) (Zeiss, Sigma, Germany), elemental analyzer (EuroEA3000, Euro Vector, Italy), X-ray powder diffraction (XRD) in the range of 5-80° (Rigaku, Micromax-007HF), Thermo-gravimetric analysis (TGA) (Mettler Toledo TGA/SDTA 851® (Schwerzenbach, Switzerland) and FTIR. The zeta-potential (ZP) value was obtained using a particle size analyzer (DelsaTM Nano, Beckman Coulter). Brunauer–Emmett–Teller (BET) analysis of the solid residue for determining was carried out using Autosorb-IQ MP instrument (Quantachrome, USA). For FESEM analysis, the sample was kept on a stub with a carbon tape and double coated with thin layer of gold before analysis. For thermal property analysis, sample

(10g) of the solid residue was kept in platinum crucibles, heated in the range of 25-500 °C under N<sub>2</sub> atmosphere at 10 °C min<sup>-1</sup> rate.

GC-MS analysis was carried out to characterize both the bio-oil and aqueous phase. A GC-MS equipment (Clarus 680 GC & Clarus 600C MS, PerkinElmer, USA; Library Software: Turbomass NIST 2008) with having column of dimensions (60 m × 250µm) and initial oven temperature of 50 °C was used. The temperature was raised to 300°C at a heating rate of 10 °C. The sample injection temperature was kept at 280°C and detector temperature was set at 300 °C. For this analysis, samples were injected after dissolving in required volume of methanol and with a split of ratio 10:1 using He as the carrier gas. Results were obtained within the range of 40-600 Da.

Fatty Acid Methyl Ester (FAME) analysis of transesterified bio-oil product was carried out using a gas chromatograph and FAME mix obtained from Sigma, Aldrich, (USA) as the standard. Data obtained was matched with that available in the MS library for compound identification.

### 3.9.5. HTL with different catalysts for enhancing bio-oil yield

Lipid rich *R. opacus* biomass was converted to bio-oil by HTL by further adding some catalyst. For homogenous catalysts such as sodium carbonate and sulphuric acid required amount of catalyst were added in the reactor for each experiment individually viz. Na<sub>2</sub>CO<sub>3</sub> (5% wt) (Shakya et al., 2015); ZnO (3% wt) (Arun et al., 2018); TiO<sub>2</sub> (10:1 ratio) (Kumar et al., 2018); H<sub>2</sub>SO<sub>4</sub> (2.4%) (Zou et al., 2009) and followed the same steps as mentioned above for HTL.

### 3.10. Analytical methods

*R. opacus* culture growth was determined by analyzing optical density (OD<sub>660</sub>) of the culture, and for which absorbance (optical density) of the bacterial culture was measured at 660

nm in a UV-Vis spectrophotometer (Agilent Technologies, Cary-100 series). Biomass determination was also verified based on its cell dry weight (CDW) by lyophilization of the biomass obtained after centrifugation and the cell pellet was then washed with sterile saline (0.8% w/v NaCl solution) for further analysis.

Total content of lipid contained in the biomass was determined by Folch method, which involved initial harvesting of the biomass culture and centrifuging it at 10,000×g followed by addition of a mixture of methanol and chloroform (1:2 ratio) for biomass homogenization. The homogenized biomass was later centrifuged to collect the solvent phase containing chloroform and lipid. The bacterial lipids obtained were evaporated and finally, after extraction, the lipids obtained were quantified by weighing (gravimetric analysis).

For routine COD analysis of the PRWW, samples were centrifuged at 10,000×g for 10 minutes for separation of any suspended solids and the supernatant was suitably diluted prior to COD analysis as per the Standard Methods (APHA, 1998).

To examine any effect on the surface morphology of the *R. opacus* biomass after the cell recycle operation, Field Emission Scanning Electron Microscopy (FESEM) of the biomass was performed. For sample analysis, 1 ml of a sample was taken before and after completion of the continuous cell-recycle experiment and was centrifuged at 10000× g for 10 minutes followed by washing with sterile water (MilliQ). Following centrifugation, the pellet obtained was suitably diluted and mixed properly with MilliQ water and placed in the specimen stub and coated with gold for analysis under FESEM (Zeiss, Sigma, Germany).

For BOD analysis required amount of samples were taken in airtight BOD bottles of specified size with diluted and seeded samples and incubated at the specified temperature for 5

days. The initial and final DO is measured and BOD is measured by the difference in the DO values (APHA, 1998).





# CHAPTER-4

## RESULTS AND DISCUSSION

## 4. Results and Discussion

The key highlight of the present study as outlined in the objectives was treatment of raw refinery wastewater using *R. opacus* biomass and bio-oil production from the residual bacterial biomass. This chapter describes the results of initial batch shake flask study carried out to optimize the parameters for the refinery wastewater treatment, performance of various indigenously made lab-scale reactors and production of bio-oil from the lipid-rich *R. opacus* biomass by hydrothermal liquefaction (HTL). Analysis results of HTL product and by-products and bio-oil up-gradation by using catalysts are presented.

### 4.1. PRWW treatment using *R. opacus*: Batch shake flask study

#### 4.1.1. Feasibility study

##### 4.1.1.1. Characterization of refinery wastewater

Raw petroleum refinery (wastewater) PRWW obtained from a petroleum-based refinery located nearby Guwahati, Assam, and was characterized for its pH, colour, total solids, chemical oxygen demand (COD), total dissolved solids, total Kjeldahl nitrogen (TKN). Table 4.1 presents detailed characterization of the refinery wastewater.

**Table 4.1** Composition of raw refinery wastewater

Parameters	Value
pH	7.42
Odor	Petrol like
Conductivity	2527 $\mu$ S/cm
Color	Light brown
Dissolved oxygen	5.19 mg/L
Total Dissolved Solid (TDS)	1253 mg/L
Total Suspended solids (TSS)	558 mg/L
Chemical Oxygen Demand (COD)	4575 mg/L
Biological Oxygen Demand (BOD)	722.18 mg/L
Sulphate	0.1 mg/L
Ammonia	8.34 mg/L
Nitrate	-

Heavy metals	
Lead (Pb)	0.12 mg/L
Nickel (Ni)	0.407 mg/L
Copper (Cu)	0.02 mg/L
Zinc (Zn)	0.135 mg/L
Most Probable Number (MPN)	7/100 ml

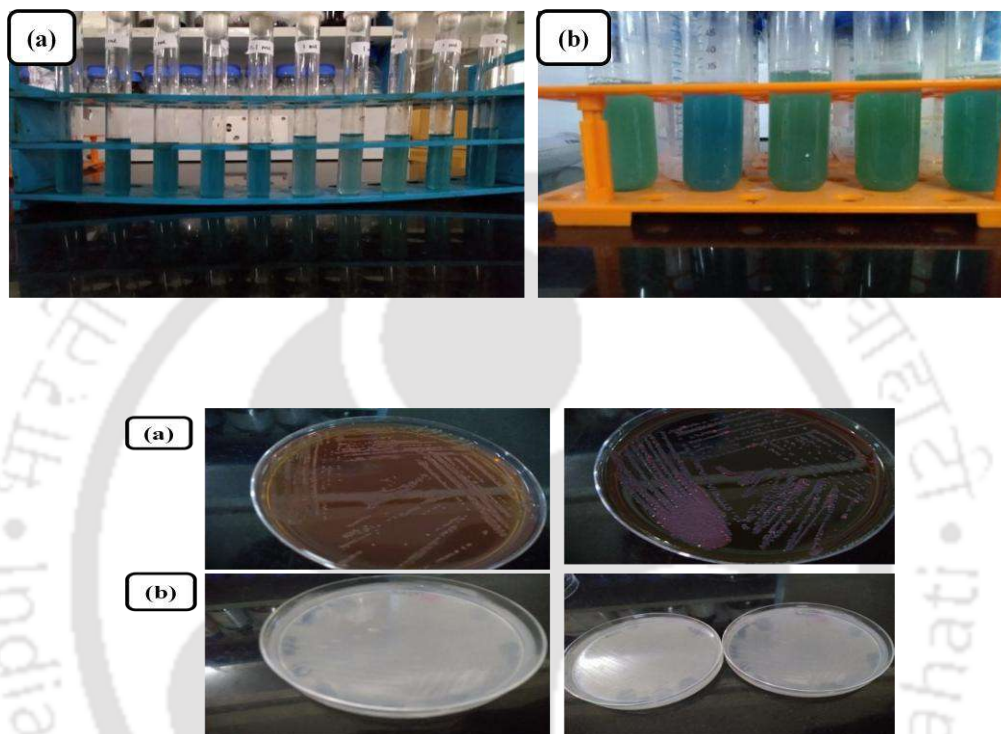


**Fig. 4.1** (a) Presumptive tests results for determining the Most Probable Number (MPN)  
 (b) Confirmatory tests for evaluation of MPN results

For microbial characterization of the PRWW, most probable number (MPN) of the bacterium present was determined. The wastewater was incubated along with lactose broth at 37 °C for 24h. Fig. 4.2 shows the results of the MPN determination in the study. Presumptive test results for determining the MPN, as shown in Fig. 4.1 (a), revealed colour change in 1-2 tubes as per the dilution followed.

For further confirmation of the presence of fecal coliform in the wastewater, the samples from the positive tubes were streaked in two differential and selective media plates, Eiosin

Methylene Blue (EMB) and Mac-Conkey. Both EMB and Mac-Conkey are selective as well as differential media, which enable the growth of Gram negative bacteria e.g. *Shigella*, *Salmonella*, *E. coli*. However, if the colonies are white/non colored in EMB agar, it is termed as non-lactose fermenting. This media consist of eosin and methylene blue dye, which inhibits most of the Gram-positive bacteria and allows Gram- negative bacteria to grow (Wanger et al., 2017). Gram-negative bacteria fermenting lactose produce acid, which turns colonies to dark purple or metallic sheen color, which helps in easy identification. However, rapid fermentation of lactose and production of strong acids changes the pH, showing green metallic sheen colour. MacConkey agar also allows the growth of both lactose fermenting as well as non-fermenting bacteria. Bile salts present in this media specifically inhibits species of gram-positive bacteria to grow. Lactose fermenting bacteria shows pink color colonies surrounded by acid precipitated bile salts, while the non-lactose fermenting bacteria shows colorless colonies (Wanger et al., 2017). In this media, neutral red is used as the pH indicator. However, EMB uses methylene blue as the pH indicator. In this study, MacConkey agar plates showed colourless colonies, which confirmed the presence of non-lactose fermenting bacteria, whereas EMB agar plates showed light pink color colonies confirming their inability to ferment lactose.

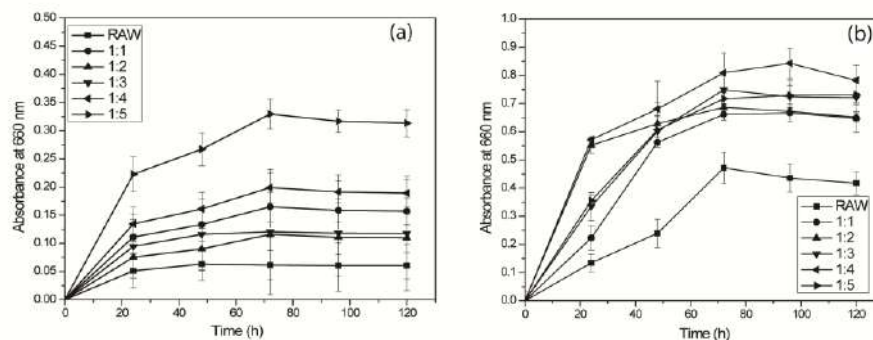
The BOD of the refinery wastewater was found to be  $722.18 \text{ mg L}^{-1}$ . Biological Oxygen Demand (BOD) is measured to evaluate the amount of oxygen required to decompose/oxidize and remove waste organic matter in the sample (APHA, 1998). Chemical Oxygen demand is another such routine tests done in Wastewater Treatments Plants (WTPs). Both BOD and COD analyses measure the amount of organic matter present in the wastewater; however, BOD is more specific than COD, which only measures everything that can be oxidized chemically in the sample (Kumar et al., 2010). The ratio  $\text{BOD}_5/\text{COD}$  is a characteristic of any wastewater: a ratio less than 0.5

generally indicates the presence of highly recalcitrant organics in a wastewater. Hence, for any wastewater treatment process, analysis of BOD and COD is of utmost importance.

#### 4.1.2. Selection of cultivation conditions

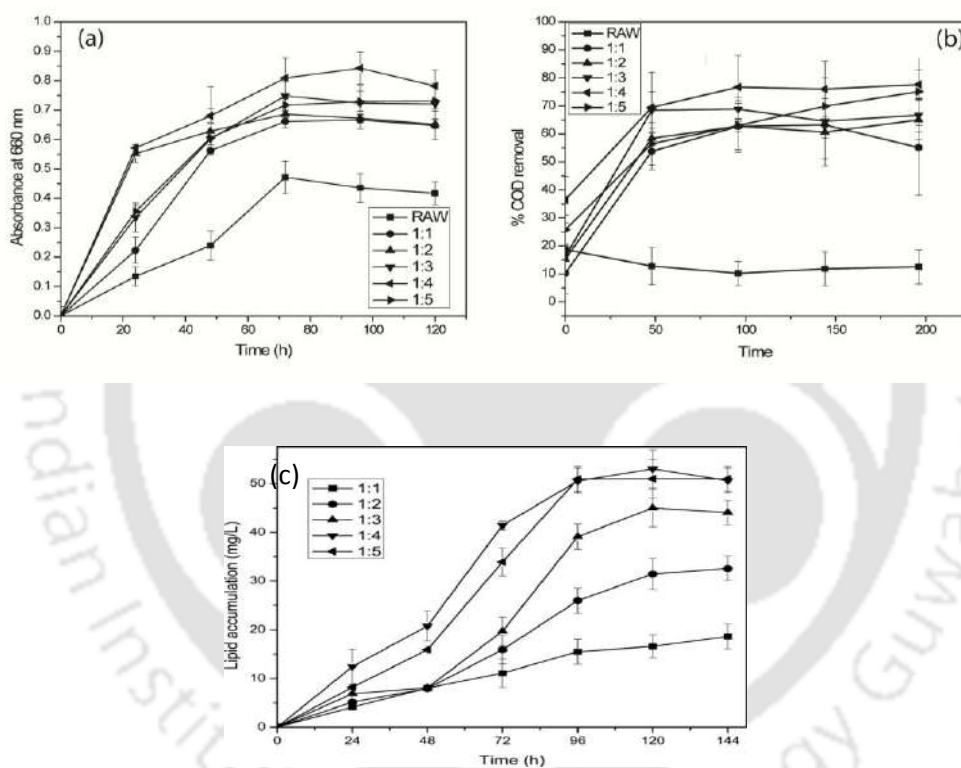
##### 4.1.2.1. One-variable-at-a time study

Fig. 4.2 depicts effect of inoculum size 5% (v/v) and 10% (v/v) on *R. opacus* biomass growth on PRWW and MSM at different ratios. The PRWW in the study has a BOD/COD ratio of 0.15 which suggest the wastewater contains highly recalcitrant organics, such as asphaltenes, polyaromatics and heavy oils (El-Naas et al. 2014). A petroleum refining process consist of various refining processes such as vacuum ditillation unit, fluid catalytic cracking unit, hydrorefining, hydrocracking etc thus generating wide varieties of point-source wastewater (Ye et al., 2020). The electric desalting wastewater (EDW) contributes 40-70% of the pollutant content in WWTP and its characteristics is completely dependent on the properties of the crude oil (Liu et al., 2013; El-Naas et al., 2014; Ye et al., 2020). Heavy oils have higher density and contain more resins (polar molecules with heteroatoms O, N and S) as well as asphaltenes (polyaromatic core and high molecular weight) in comparison to light oils (Speight, 1991; Varfolomeev et al., 2016) contributing more COD.



**Fig. 4.2** Effect of different inoculum size on *R. opacus* biomass growth on PRWW and MSM at different ratios (a) 5% (v/v) and (b) 10% (v/v) inoculum size

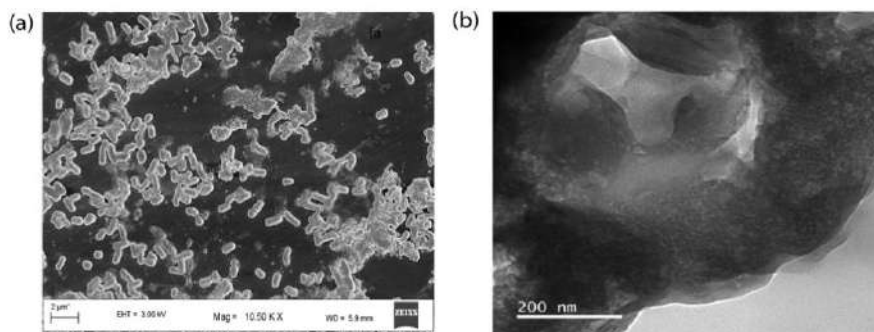
Fig. 4.3 depicts the *R. opacus* biomass growth and COD removal by *R. opacus* at different ratios of PRWW and MSM, which clearly reveals that at MSM:PRWW ratio of 1:4, maximum *R. opacus* biomass growth along with a very high COD removal are obtained. About  $70 \pm 5\%$  of COD was removed under this condition, along with a high lipid accumulation of 0.54 (w/w). Hence, a 1:4 ratio of MSM: PRWW was chosen, for evaluating the effect of other different cultivation parameters.



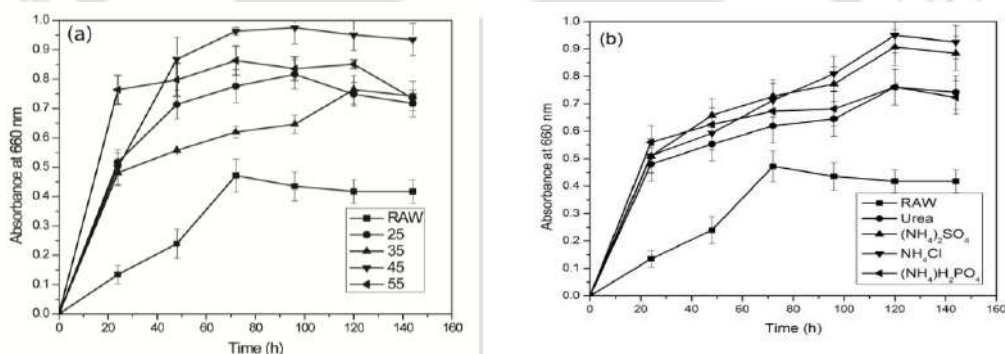
**Fig. 4.3** Time profile of (a) *R. opacus* biomass growth, (b) COD removal, and (c) lipid accumulation by *R. opacus* (inoculum size:10% (v/v))

Fig. 4.4 depicts (a) FESEM image of *R. opacus* and (b) TEM image showing lipid globules accumulated inside the bacterium. Fig. 4.5 depicts *R. opacus* biomass growth on refinery wastewater under different conditions of (a) C/N ratio, (b) pH, (c) nitrogen source. At pH 7, 10% (v/v) inoculum size and 45:1 C/N ratios, highest biomass growth was attained. Among the

different nitrogen sources,  $\text{NH}_4\text{Cl}$  showed maximum biomass growth compared to  $\text{NH}_4\text{H}_2\text{PO}_4$  and urea. With  $(\text{NH}_4)_2\text{SO}_4$ , biomass growth was almost similar as that with  $\text{NH}_4\text{Cl}$ .



**Fig. 4.4** (a) FESEM image of *R. opacus* and (b) TEM image showing lipid globules accumulated inside the bacterium.



**Fig. 4.5** Effect of different process parameters on *R. opacus* biomass growth using PRWW (a) C/N ratio, (b) nitrogen source

Batch studies were conducted for optimizing the inoculum size and wastewater:MSM ratio for proper supplementation of the growth media and efficient COD removal from PRWW. The results obtained from the optimization study considering one variable at a time were selected for carrying out further experiments for further screening of variables and their levels.

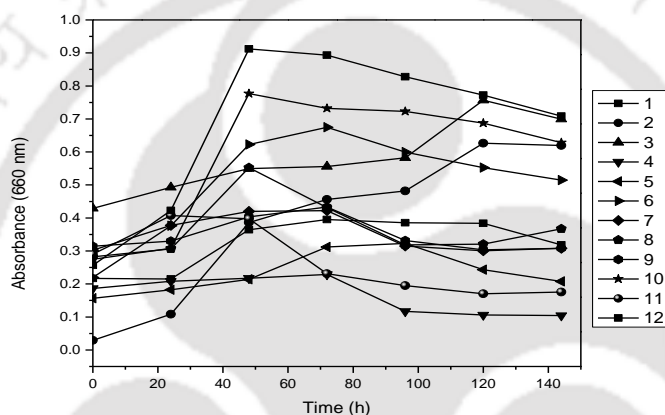
#### 4.1.2.2. Plackett-Burman study

In order to validate the effect of agitation, temperature, pH and nitrogen source on *R. opacus* biomass growth, COD removal and lipid production in this study, Plackett-Burman experimental design was employed. The results presented in Table 4.2 indicate variation in COD removal (%), biomass concentration ( $\text{g L}^{-1}$ ) and lipid accumulation ( $\text{g L}^{-1}$ ) in the batch experiments carried out by varying the levels of the six variables in this study. The COD removal efficiency is maximum in experimental run 9 with the factors set at their respective low levels. Maximum biomass concentration is observed in the case of experimental run 1, whereas maximum lipid accumulation is obtained in experimental run 12, which was followed closely in experimental runs 5, 9, and 10. The variations in the results in the different experimental runs can be attributed to the different roles played by the factors on biomass growth, lipid accumulation and COD utilization by the bacterium. For example, nitrogen limitation or physical stress enhances lipid accumulation in *R. opacus* (Kumar et al., 2015). However, physicochemical factors (pH, temperature, and agitation), as well as media constituents, play a combined role for efficient biomass growth and substrate utilization. Furthermore, the substrate used in this, i.e., refinery wastewater, is known to contain several toxic compounds that inhibit biomass activity (Iqbal et al., 2016). Thus due to the presence of recalcitrant toxic compounds present in the refinery wastewater, microbial biomass attains optimal growth after a prolonged treatment time as compared to simple substrates such as glucose (Kumar et al., 2015).

**Table 4.2** Plackett-Burman experimental design matrix for studying the effect of different variables affecting biomass growth, COD removal and lipid production by *R. opacus*

Exp. Run no.	Variables and their levels						Responses		
	NH <sub>4</sub> Cl (g/L)	KH <sub>2</sub> PO <sub>4</sub> (g/L)	Na <sub>2</sub> HPO <sub>4</sub> (g/L)	pH	Agitation (rpm)	Temp (°C)	Absorbance (660 nm)	COD removal %	Lipid (%C DW)
1	0.5	0.5	3	6	100	25	0.988	73	22
2	1.5	1.5	9	6	200	35	0.576	54	19
3	1.5	0.5	3	6	200	35	0.613	44	33
4	0.5	0.5	9	8	200	25	0.886	38	27
5	1.5	1.5	3	8	100	25	0.576	36	37
6	0.5	1.5	9	8	100	35	0.286	35	27
7	0.5	0.5	3	8	200	35	0.872	61	36
8	1.5	0.5	9	8	100	35	0.233	59	34
9	0.5	1.5	3	6	100	35	0.287	78	36
10	0.5	1.5	9	6	200	25	0.755	53	36
11	1.5	1.5	3	8	200	25	0.381	39	33
12	1.5	0.5	9	6	100	25	0.899	54	39

Analysis of variance (ANOVA) of the individual responses revealed that  $\text{KH}_2\text{PO}_4$  (F-value 5.60 and p-value 0.064) and temperature (F value=5.83 and p-value 0.060) played a major role towards utilizing refinery wastewater as the substrate by the bacterium (Table 4.3 a, Fig. 4.7 a). The other parameters did not show any significant effect in case of biomass growth as well as COD removal by *R. opacus* (Table 4.3b), (Fig. 4.6). These results suggest the bacterium is robust in treating the PRWW.

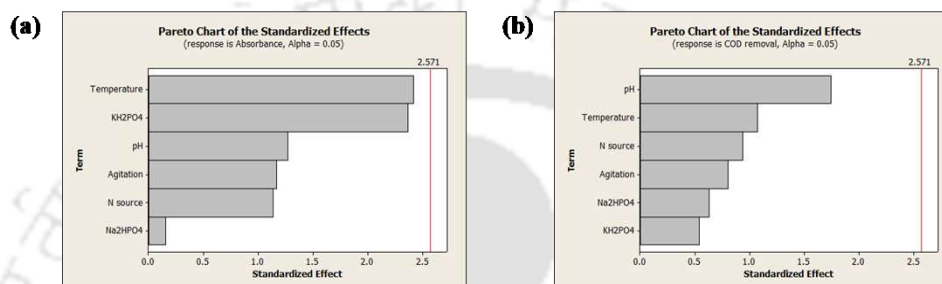


**Fig. 4.6** Time profile of *R. opacus* biomass growth in the Plackett-Burman screening study.

In such statistical analysis, a large F value and low p value of a particular model parameter indicates its very high significance on a given response. In this study, the parameter temperature showed low p value with high F value which shows it can be a governing parameter for COD removal from PRWW by *R. opacus*. Other parameters did not show any significant response. Since, Plackett-Burman experimental design showed no significant effect due to variation in the levels of these parameters, it revealed that *R. opacus* is robust for such environmental applications.

**Table 4.3** ANOVA of (a) COD removal and (b) biomass growth in the PlackettBurman study

(a) Source	F	P	(b) Source	F	P
Main effects	2.62	0.155	Main effects	1.07	0.482
N source	1.29	0.307	N source	0.88	0.391
KH <sub>2</sub> PO <sub>4</sub>	5.60	0.064	KH <sub>2</sub> PO <sub>4</sub>	0.29	0.615
Na <sub>2</sub> HPO <sub>4</sub>	0.02	0.885	Na <sub>2</sub> HPO <sub>4</sub>	0.39	0.559
pH	1.61	0.260	pH	3.04	0.142
Agitation	1.36	0.297	Agitation	0.65	0.458
Temperature	5.83	0.060	Temperature	1.15	0.332

**Fig. 4.7** Pareto chart showing the effect of individual variables in the (a) COD removal and (b) biomass growth in the Plackett-Burman study

#### 4.1.3. Kinetics of COD utilization, biomass growth and lipid accumulation

Fig. 4.8 presents the time profile of COD utilization (%) by *R. opacus* at different initial concentrations, which shows that complete COD removal (100%) is achieved for an initial concentration of 2.5 g L<sup>-1</sup>. However, a moderate COD removal efficiency of 80-85% is observed at a concentration in the range of 3 - 4.5 g L<sup>-1</sup>. Furthermore, no initial lag phase in COD removal is observed at all the initial concentrations; 60% of the COD was utilized within 50 h of incubation time. Also, a maximum COD utilization is observed within 96 h of incubation time for a very low initial COD concentration. Recalcitrant organics in such wastewater are generally present as hydrocarbons (Ye et al. 2020). These results indicate that the hydrocarbons present in PRWW, measured as COD were well-utilized by *R. opacus*, revealing its hydrocarbonoclastic nature.

Refinery wastewater mainly consists of aliphatic and aromatic hydrocarbons like naphthalene, phenanthrene, and fluoranthene. These organics present in such industrial wastewater

are metabolized by *R. opacus* via both ortho as well as meta cleavage pathways, as recently reported by Goswami et al. (2018). However, detailed kinetics of COD utilization by the bacterium for its lipid-rich biomass growth is largely unknown. Hence, different bio-kinetic models were applied to describe the COD utilization, *R. opacus* biomass growth, product (lipid) formation by *R. opacus*.

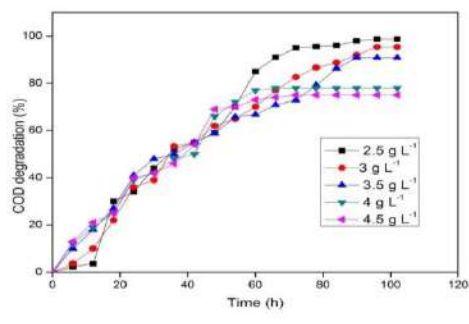


**Fig. 4.8** COD removal (%) by *R. opacus* at different initial COD concentrations.

#### 4.1.3.1. COD utilization

Fig. 4.9 compares the experimental values of COD utilization by *R. opacus* with the values predicted using the three bio-kinetic models (first-order, logarithmic, and logistic). Although no initial lag phase in COD utilization is observed at all the initial COD concentrations, COD removal reached a saturation value more quickly at a high initial concentration than at a low initial COD concentration. The COD utilization rate in the study varied from 0.05 to 0.101 mg L<sup>-1</sup> h<sup>-1</sup>. Estimated values of bio-kinetic parameters from the three models are presented in Table 4. 4. Amongst the three models evaluated, the logistic model best fitted the experimental data with a coefficient of determination ( $R^2$ ) value greater than 0.95 for all the initial COD concentrations tested in the study. In the literature, Sinharoy et al. (2019) reported similar values of the biokinetic parameters estimated using the logistic model for carbon monoxide utilization by anaerobic

biomass for biohydrogen production. Both the logistic and Gompertz models accurately described the data on bio-hydrogen production using a soluble substrate. Considering that the logistic model is derived based on microbial growth associated phenomenon, it can be concluded that the COD removal and utilization resulted in *R. opacus* biomass growth. The values of bio-kinetic parameters estimated using the logistic model further reveal that *R. opacus* is highly efficient in utilizing recalcitrant organics present in the refinery wastewater, even at a high initial COD concentration, for its growth and metabolism.

**Table 4.4** Estimated values of bio-kinetic model parameters of COD utilization for lipid-rich biomass production by *R. opacus*

Model parameters	Initial COD concentration (g L <sup>-1</sup> )				
	2.5	3	3.5	4	4.5
<b>First order</b>					
S <sub>0</sub> (g L <sup>-1</sup> )	2.874	3.311	3.594	4.021	4.400
K (h <sup>-1</sup> )	0.027	0.023	0.020	0.019	0.018
R <sup>2</sup>	0.836	0.905	0.935	0.993	0.992
<b>Logarithmic</b>					
S <sub>0</sub> (g L <sup>-1</sup> )	2.338	2.778	3.0519	3.356	3.6940
X <sub>0</sub> (g L <sup>-1</sup> )	82.521	102.920	103.653	126.956	118.033
μ <sub>max</sub> (h <sup>-1</sup> )	0.0003	0.0002	0.0002	0.0002	0.0002
R <sup>2</sup>	0.805	0.903	0.931	0.847	0.822
<b>Logistic</b>					
S <sub>0</sub> (g L <sup>-1</sup> )	2.533	3.071	3.464	4.0231	4.395
X <sub>0</sub> (g L <sup>-1</sup> )	0.474	1.487	4.986	6.654	5.539
μ <sub>max</sub> (h <sup>-1</sup> )	0.077	0.088	0.100	0.081	0.0499
K <sub>S</sub> (mg L <sup>-1</sup> )	4.094	10.565	31.460	27.18	14.48
R <sup>2</sup>	0.948	0.981	0.960	0.999	0.999

S<sub>0</sub>, initial COD concentration (g L<sup>-1</sup>); X<sub>0</sub> is the initial biomass concentration (g L<sup>-1</sup>), K, first-order rate constant (h<sup>-1</sup>); μ<sub>max</sub>, maximum biomass specific growth rate (h<sup>-1</sup>); K<sub>S</sub>, half-saturation coefficient (g L<sup>-1</sup>).

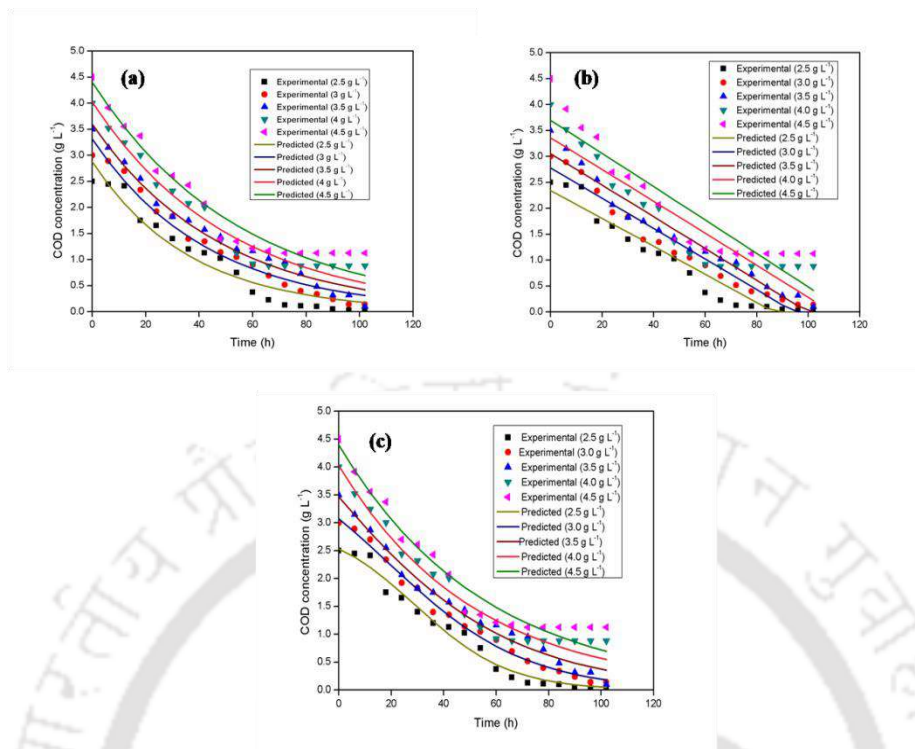


**Fig. 4.9** Experimental and predicted values of COD utilization due to (a) first order, (b) logarithmic and (c) logistic kinetic models.

#### 4.1.3.2. Specific COD utilization rate

Fig. 4.10 shows the effect of initial COD concentration on its specific utilization rate by the bacterium. It can be observed that the specific substrate utilization rate decreased with an increase in the COD concentration, indicating substrate inhibition, similar to *R. opacus* biomass growth rate inhibition at a high COD substrate concentration. Several kinetic models have been previously reported to predict substrate utilization rate and substrate inhibition on the growth rate of microorganisms (Sinharoy et al., 2019). These models include Haldane, Monod, Edward, Moser, Han-Levenspiel, Yano-Koga, and Luong models. Hence, in order to elucidate the inhibition on *R. opacus* growth due to a high COD concentration, the experimental data were fitted to all these kinetic models reported in the literature. Table 4.5 presents the values of bio-kinetic constants estimated using the various specific substrate utilization rate models.

**Table 4.5** Estimated values of biokinetic model parameters on specific COD utilization rate by *R. opacus*

Model/parameters	$q_{max}$ ( $h^{-1}$ )	$K_s$ ( $g L^{-1}$ )	$K_i$ ( $g L^{-1}$ )	$S_m$ ( $g L^{-1}$ )	$n$	$m$	$K_1$	$R^2$
Luong	0.117	2.856	-	9.095	0.557	-	-	0.991
Han-Levenspiel	0.021	-0.687	-	4.5	1	1	-	0.795
Yano-Koga	0.124	3.002	-	-	0.925	-	1.01	0.996
Moser	0.0891	2.453	-	-	-0.103	-	-	0.557
Monod	0.020	-0.725	-	-	-	-	-	0.998
Haldane	0.087	2.104	2.038	-	-	-	-	0.999
Edward	0.104	4.049	-	3.693	-	-	-	0.998

$q_{max}$ , maximum specific COD utilization rate ( $h^{-1}$ );  $K_s$ , half-saturation constant ( $g L^{-1}$ );  $K_i$ , inhibition constant ( $g L^{-1}$ );  $S_m$ , COD concentration above which net growth ceases ( $g L^{-1}$ );  $K_1$ , positive constant;  $n$  and  $m$  are empirical constants.

Among the different models evaluated in this study, the Haldane model fitted the experimental data with a very high  $R^2$  value of 0.999, and the values obtained for half-saturation and the inhibition constants from the model were estimated as  $2.104 g L^{-1}$  and  $2.038 g L^{-1}$ , respectively. The value of maximum specific COD utilization rate estimated using this model was  $0.087 h^{-1}$ , which is three times higher than the experimental value of  $0.029 h^{-1}$ . Thus, the estimated values of the kinetic model parameters distinctively show the effectiveness of *R. opacus* in utilizing refinery wastewater, even at a high initial COD concentration. A similar kinetic study on trichloroethylene biodegradation using *R. opacus* was performed by Baskaran et al. (2020), which demonstrated an excellent ability of the bacterium to degrade such toxic compounds.

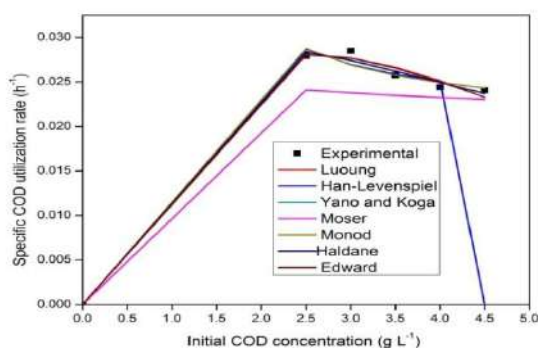


**Fig. 4.10** Experimental and predicted values of specific COD utilization rate at different initial COD concentrations.

#### 4.1.3.3. Biomass growth

Fig. 4.11 shows the influence of different initial COD concentration on *R. opacus* biomass growth, which reveals an efficient and quick growth of the bacterium owing to its well-known capability to metabolize highly toxic recalcitrant compounds. In this study, a maximum *R. opacus* biomass growth is obtained within 80 h for all the initial COD concentrations. However, the maximum biomass concentration obtained is  $1.433 \text{ g L}^{-1}$  within 72 h for a COD concentration of  $3.5 \text{ g L}^{-1}$ . At a COD concentration of more than  $3.5 \text{ g L}^{-1}$  the *R. opacus* biomass growth was reduced probably due to the inhibitory effect of recalcitrant organics present in the wastewater. Raw refinery wastewater contains a wide range of aromatic and aliphatic compounds that are not easily degraded by microorganisms due to their complex molecular structure (Saien et al., 2012).

For estimating the bio-kinetic parameters involved in *R. opacus* biomass growth, the experimental data in this study were fitted to Logistic and modified Gompertz models as detailed in Sinharoy et al. (2019). The model-predicted values, along with the experimental values, are presented as Fig. 4.11, and the estimated values of biomass growth kinetic parameters obtained using the two models are given in Table 4.6. From Table 4.6, the modified Gompertz model fitted

the experimental data more precisely than the Logistic model with an  $R^2$  value of 0.996. The *R. opacus* biomass growth increased with an increase in the initial COD concentration from 2.5 to 3.5  $\text{g L}^{-1}$ , and above which, the biomass concentration decreased. The estimated values of the bio-kinetic parameters  $X_{\max}$  and  $r_{x\max}$  from the model were 1.431  $\text{g L}^{-1}$  and 0.026  $\text{g L}^{-1} \text{h}^{-1}$ , respectively. At a high COD concentration, the decrease in biomass growth could be attributed to its inhibitory effect on the bacterium, which was further verified by analyzing the kinetics of lipid production and specific biomass growth rate by the bacterium at different initial COD concentrations.

**Table 4.6** Estimated values of bio-kinetic model parameters on *R. opacus* biomass growth at different COD concentrations

Model and parameters	Initial COD concentration ( $\text{g L}^{-1}$ )				
	2.5	3	3.5	4	4.5
<b>Modified Gompertz</b>					
$X_{\max}(\text{g L}^{-1})$	0.960	1.26	1.431	1.201	0.821
$r_{x\max}(\text{g L}^{-1} \text{h}^{-1})$	0.029	0.022	0.026	0.019	0.041
$\lambda(\text{h})$	5.721	2.54	7.519	2.114	8.641
$R^2$	0.901	0.985	0.996	0.927	0.971
<b>Logistic</b>					
$X_{\max}(\text{g L}^{-1})$	0.941	1.240	1.379	1.163	0.816
$r_{x\max}(\text{g L}^{-1} \text{h}^{-1})$	0.023	0.020	0.027	0.019	0.041
$\lambda(\text{h})$	6.621	2.4	10.789	3.915	9.533
$R^2$	0.845	0.936	0.997	0.916	0.941

$X_{\max}$ , maximum biomass concentration ( $\text{g L}^{-1}$ );  $r_{x\max}$ , maximum rate of biomass growth ( $\text{g L}^{-1} \text{h}^{-1}$ ).

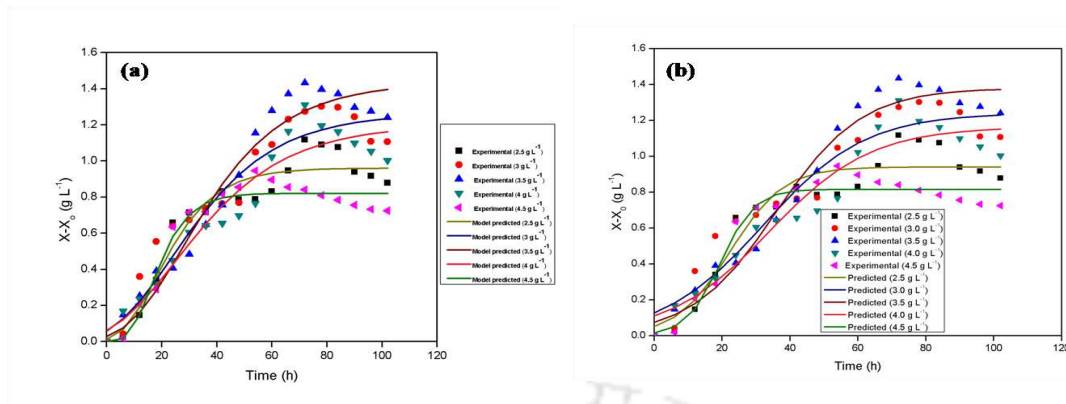


**Fig. 4.11** Experimental and predicted *R. opacus* biomass growth at different initial COD concentrations using (a) modified Gompertz and (b) Logistic models.

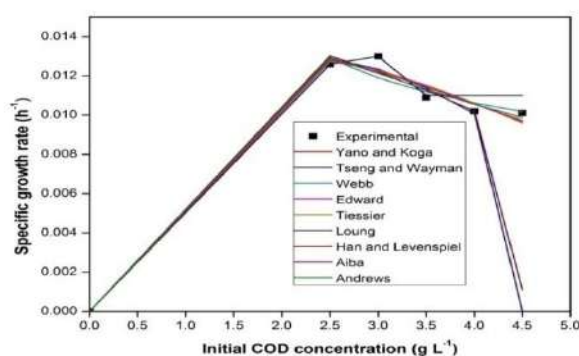
#### 4.1.3.4. Kinetics of COD inhibition on *R. opacus* biomass growth

In order to confirm the results of inhibition of *R. opacus* biomass growth at a high initial COD concentration, the data on specific biomass growth of the bacterium at different initial COD concentrations was fitted to substrate inhibition models reported in the literature. Although the Monod model is known to successfully describe the effect of COD concentration (substrate) on specific growth rates of microorganisms, it fails to address biomass inhibition at a high substrate concentration. Hence, Yano and Koga, Tseng and Wayman, Webb, Edward, Tessier, Luong, Han and Levenspiel, Aiba, and Andrews models were applied in this study to estimate the biokinetic parameters involved. Fig. 4.12 compares the obtained experimental and model-predicted *R. opacus* biomass specific growth rate values for different initial COD concentrations. Table 4.7 presents the estimated bio-kinetic parameters from these models. It is also observed that the biomass specific growth rate increased with an increase in the initial COD concentration up to 3.0  $\text{g L}^{-1}$ , and above which the value decreased.

**Table 4.7** Estimated values of bio-kinetic parameters of substrate inhibition of *R. opacus* biomass specific growth rate

Model and parameter	$\mu_{max}$	$K_s$ (g L <sup>-1</sup> )	$K_i$ (g L <sup>-1</sup> )	$S_m$ (g L <sup>-1</sup> )	n	m	$K_I$	$R^2$
	(h <sup>-1</sup> )							
Yano and Koga	0.038	2.476	-	-	1.24	-	2.97	0.990
Tseng and Wayman	0.002	2.520	2.999	6.61	-	-	-	0.769
Webb	0.3467	-	2.757	-	0.05	-	3.80	0.975
Edward	0.046	3.373	3.479	-	-	-	-	0.991
Tiessier	0.135	2.020	2.617	-	-	-	-	0.745
Luong-inhibition	0.032	2.514	10.354	-	-	0.85	-	0.736
Han and Levenspiel	0.017	2.500	-	6.02	0.44	10.99	-	0.597
Aiba	0.052	2.681	3.699	-	-	-	-	0.990
Andrews	0.037	1.233	1.787	-	-	-	-	0.988

$\mu_{max}$ , maximum biomass specific growth rate (h<sup>-1</sup>);  $K_s$ , half-saturation constant (g L<sup>-1</sup>);  $K_i$ , inhibitory concentration of the substrate (g L<sup>-1</sup>);  $S_m$ , maximum substrate inhibition constant above which cells cease to grow (g L<sup>-1</sup>);  $K_I$ , n, and m are constants

**Fig. 4.12** Experimental and model predicted *R. opacus* biomass specific growth rate at different initial COD concentrations.

Amongst the different substrate inhibition models investigated in this study, the Edward model was found to be the best for describing the inhibitory effect of COD on specific biomass

growth rate of *R. opacus* ( $R^2$  value 0.991). Values of the bio-kinetic parameters, viz.  $\mu_{\max}$ ,  $K_S$ , and  $K_i$ , from the model were estimated to be  $0.046 \text{ h}^{-1}$ ,  $3.373 \text{ g L}^{-1}$ , and  $3.479 \text{ g L}^{-1}$ , respectively, thus revealing that COD at a concentration above  $3.5 \text{ g L}^{-1}$  is inhibitory/toxic to the microorganism growth. It is reported that inhibition of *R. opacus* biomass growth by COD (substrate) at a high initial concentration is due to the recalcitrant organics present in such wastewater. In a study by Saravanan et al. (2011), the values of  $K_S$  ( $121.24 \text{ mg L}^{-1}$ ) and  $K_i$  ( $210.00 \text{ mg L}^{-1}$ ) estimated using the Edward model indicated that *Pseudomonas sp.* could successfully degrade phenol but showed less tolerance towards phenol. Sinharoy et al. (2019) reported an estimated inhibition constant  $K_i$  value of  $6.124 \text{ mmol L}^{-1}$  for utilizing carbon monoxide by anaerobic biomass, which reveals a high tolerance of the biomass towards the gaseous substrate. These results suggest that the level of tolerance by microorganisms largely differs amongst different microbial species as well as depend on chemical structure and toxicity of the substrate used.

#### 4.1.3.5. Lipid production

Fig. 4.13 clearly shows that lipid production by *R. opacus* varied depending upon the initial COD concentration in the wastewater. Maximum lipid accumulation of  $1.30 \text{ g L}^{-1}$  was obtained for an initial COD concentration of  $3.5 \text{ g L}^{-1}$ . These results of lipid accumulation further confirm the inhibitory effect of high COD on *R. opacus* biomass growth, as observed previously. Several batch studies reported the valorization of different wastewaters for lipid production using *R. opacus*. Goswami et al. (2017) reported valorization of biomass gasification wastewater using *R. opacus* and obtained 62.8% (w/w) of lipids and 74% COD removal efficiency by supplementing the wastewater with mineral salt medium (MSM). Similarly, valorization of dairy wastewater is reported to yield 33% (w/w) lipid and 62% COD removal by supplementation with MSM (Kumar et al., 2015).

From Table 4.8, maximum lipid content of 35.6 % (w/w) was achieved for an initial COD concentration of 3.5 g L<sup>-1</sup>, thus revealing an excellent bio-energy potential of *R. opacus* from PRWW. In the literature, oleaginous microorganisms have been reported for lipid accumulation using wastewater from food industry as the substrate (Chiu et al., 2015; Muniraj et al., 2013). Muniraj et al. (2013) evaluated easily degradable potato processing wastewater as the substrate for biodiesel production by an oleaginous filamentous fungus, *Aspergillus oryzae*, and reported a maximum COD removal of 91% along with 3.5 g L<sup>-1</sup> lipid accumulation. The value is slightly high as compared with the results obtained in the present study.

**Table 4.8.** Estimated values of bio-kinetic parameters on lipid production by *R. opacus* using modified Gompertz Model

Model parameters	Initial COD concentration (g L <sup>-1</sup> )				
	2.5	3	3.5	4	4.5
<b>P<sub>max</sub></b> (g L <sup>-1</sup> )	20.21	30.87	31.02	24.34	19.23
<b>r<sub>pmax</sub></b> (g L <sup>-1</sup> h <sup>-1</sup> )	0.119	0.1759	0.2173	0.1682	0.130
<b>λ</b> (h)	42.119	46.064	30.805	34.565	29.246
<b>Lipid yield</b> (%)	27.696	33.013	35.592	24.642	17.144
<b>Specific lipid production rate</b> (h <sup>-1</sup> )	0.0626	0.0738	0.1051	0.085	0.088
<b>R<sup>2</sup></b>	0.9918	0.9976	0.9964	0.999	0.991

*P<sub>max</sub>*, maximum lipid production (g L<sup>-1</sup>); *r<sub>pmax</sub>* is the maximum rate of lipid production (g L<sup>-1</sup> h<sup>-1</sup>).

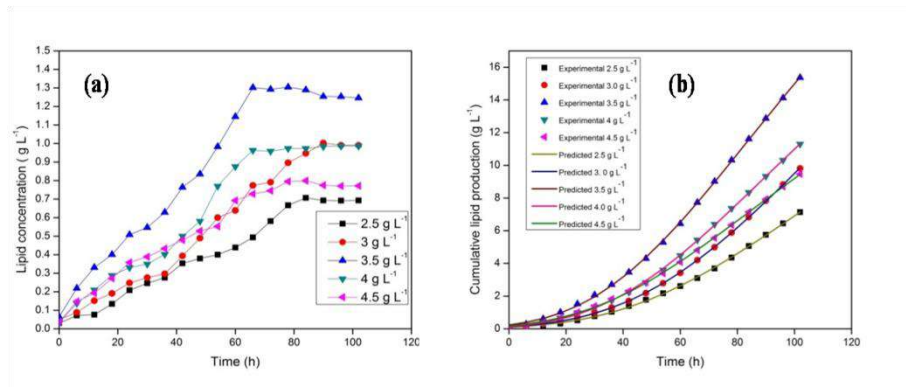


**Fig. 4.13** Experimental and model predicted (a) lipid production and (b) cumulative lipid production by *R. opacus* at different initial COD concentrations.

Analysis of cumulative lipid production by *R. opacus* at different initial COD concentration, shown in Fig. 4.13 (b), indicates that the lipid production by the organism gradually increases with an increase in cultivation time. The data was found to be well-described using the modified Gompertz model with a high  $R^2$  value of 0.99 (Table 4.8). The estimated values of maximum lipid production ( $P_{max}$ ) and lipid production rate ( $r_{Pmax}$ ) from the model were  $31.02 \text{ g L}^{-1}$  and  $0.2173 \text{ g L}^{-1} \text{ h}^{-1}$ , respectively.

Cortes and Carvalho. (2015) examined the effect of different carbon sources on the accumulation of triacylglycerols (TAGs), which is the most predominant lipid required for biodiesel production from *Rhodococcus*. Both *R. opacus* and *R. erythropolis* are reported to accumulate lipids, which can be easily converted to fatty acid methyl esters (FAMES) for bio-fuel production. In the presence of excess carbon source and a distinctively low amount of nitrogen, lipid accumulation is predominant in bacteria during its stationary phase of growth. This is attributed to the fact that during the stationary growth phase, i.e., when nutrient depletion occurs, cell division is hindered, and cells start accumulating lipids inside as storage food. An engineered strain of *R. opacus* strain is also reported to produce  $0.179 \text{ g g}^{-1}$  of TAG per g of glucose and xylose in a fed-batch mode (Fei et al., 2015). Thus the present kinetic study demonstrates the

excellent bio-energy potential of the bacterium in the form of lipid production from refinery wastewater. The kinetic parameters estimated in this study can further be useful to achieve maximum lipid production by *R. opacus* using refinery wastewater as the substrate during scaling up of the process by proper monitoring and control of the parameters.

## 4.2. Performance evaluation of CSTR for PRWW treatment and lipid-rich biomass production

### 4.2.1. Batch, fed-batch and sequential batch modes of operation

COD removal and lipid-rich biomass production by *R. opacus* from the PRWW initially was first carried out using the CSTR operated under batch, fed-batch and sequential batch (SBR) modes. The wastewater was supplemented with MSM (4:1) and inoculated with 10% (v/v) of *R. opacus* seed culture prior to the batch operation. The results of these three modes of operation with the bioreactor are shown in Fig. 4.14. Fig. 4.14 (a), shows the combined profile of biomass growth (OD), lipid accumulation ( $\text{g L}^{-1}$ ) and COD removal (%) in the batch operated bioreactor. The maximum biomass concentration obtained was  $1.5 \text{ g L}^{-1}$  along with a lipid accumulation of  $0.83 \text{ g L}^{-1}$  (55%, w/w). Moreover, a maximum COD removal of 86% was achieved in the batch experiments, confirming that the *R. opacus* could efficiently degrade the toxic hydrocarbons present in refinery wastewater for its metabolism and growth. Thus, 55% (w/w) of lipids were accumulated in the biomass, which indicates its potential for bio-oil production from PRWW. Saisriyoot et al. (2016) studied bio-fuel production by *R. opacus* grown on petroleum wastewater and reported 52% (w/w) of lipid accumulation with wastewater supplemented with molasses as the carbon source. Compared with the value, the lipid accumulation value obtained in the present study is higher, a sole carbon source as a substrate (Alvarez et al., 2000). Better supplementation of the media with required nutrients and proper carbon source in an optimum reaction conditions thus can yield higher lipid productivity.

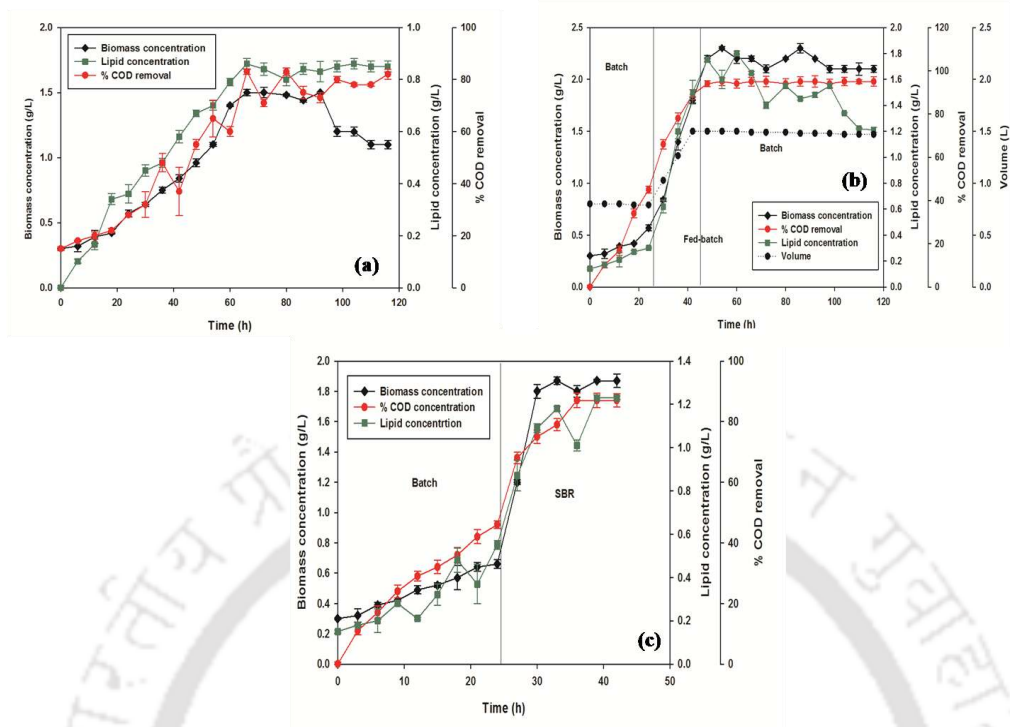


**Fig. 4.14** Biomass production, lipid accumulation and COD removal by *R. opacus* in the bioreactor operated under (a) batch, (b) fed-batch, and (c) sequential batch modes

Based on the results obtained using the batch operated bioreactor, biomass yield of the bacteria ( $Y_{x/s}$ ) was estimated to be 0.62. Feed flow rate required for fed-batch operation was calculated and feeding was initiated at the end of 24 h batch period. From Fig. 4.14b, which shows the results of the fed-batch experiment in a bioreactor, the maximum biomass growth, and lipid accumulation were  $2.3 \text{ g L}^{-1}$  and  $1.8 \text{ g L}^{-1}$ , respectively. Approximately, 78% (w/w) of lipids were accumulated in *R. opacus* biomass under the fed-batch operation mode, which is higher than the value obtained in the batch bioreactor experiments. Moreover, the COD removal efficiency is found to be nearly 95% after 54 h of treatment, which is relatively higher than the removal efficiency obtained in the batch operated reactor. The increased biomass production of the biomass is mainly due to an increase in the volume of the wastewater treated under fed-batch mode than under batch mode. However, a discontinuous trend in lipid production is observed, which could be attributed to lipid utilization as a secondary carbon source by the bacterium (Mahavi 2008).

Disintegration of the lipid-rich *R. opacus* biomass could be another reason for the sudden decrease in the lipid concentration at the end of the fed-batch experiment.

SBR is based on a fill-and-draw batch system, which is conventionally applied for treating wastewater containing a high amount of recalcitrant compounds (Thakur et al., 2014; Rajab et al., 2017). In this study, sequencing batch mode was carried out for a total cycle period of 18 h (HRT) consisting of 2 h of filling, 15 h reaction time, 45 minutes settling and 15 minutes of decanting phase with SRT of 3 days. During the reaction phase, the organic load was maintained at  $3.5 \text{ g L}^{-1}$ . Fig. 4.14c indicate poor performance of the reactor under SBR mode than batch/fed-batch mode. Maximum biomass concentration, lipid production and COD removal efficiency in this SBR study were  $1.87 \text{ g L}^{-1}$ ,  $1.23 \text{ g L}^{-1}$  and 87 %, respectively. Approximately 66% (w/w) of lipids were produced under the SBR mode, which is less than that obtained under the fed-batch mode of operation (Fig. 4.14c). Moreover, biomass settleability was poor which may be due to biomass disintegration. Also, inhibition of microbial activity due to hydrocarbons present in such wastewater may result in poor biomass settling. Thakur et al. (2014) performed aerobic degradation of petroleum wastewater by using activated sludge in a SBR, and observed a maximum 83% of COD removal efficiency at 0.83 d HRT (19 h) with 2 h of filling time; a further increase in the HRT decreased the COD removal efficiency. In the present study, conducted at 18 h HRT and 2h filling time, the COD removal efficiency obtained is 87% which is higher than the literature reported value. These results reveal exceptional efficiency of the bacteria *R. opacus* for wastewater treatment under SBR mode, but not for lipid-rich biomass production.

From the afore-mentioned results of batch, fed-batch and sequential batch modes of operating the CSTR, the lipid accumulation rate decreased at the end of the experiment, which contributes to the fact the bacteria may utilize lipids as a substrate in the absence of a primary

carbon source (Xu et al., 2006; Gupta et al., 2018). Moreover, no significant growth in the biomass was observed after 110 h due to growth inhibition by the remaining (unutilized) COD, which, however, needs to be confirmed further. A similar observation was made by Thakur et al. (2014) where COD removal efficiency decreased or was maintained on increasing the HRT from 19 to 24 h during the treatment of PRWW in SBR mode. Gargouri et al. (2011) operated an aerobic CSTR with petroleum wastewater by using activated sludge for 225 days and reported a maximum of 95% of COD, which is relatively lower than the value obtained in this study (98%).

#### 4.2.2. Continuous mode of operation

For improving the CSTR performance, COD removal and lipid production was studied under continuous operating mode of the bioreactor. The fermenter was initially operated for 24 h under batch mode and then shifted to continuous mode. In this continuous operation mode, the effect of different HRT (8, 16 and 24 h) was investigated, which corresponded to the dilution rates of 0.12, 0.06 and 0.04 h<sup>-1</sup>, respectively. Fig. 4.15 shows the combined profile of biomass growth (OD), lipid production (g L<sup>-1</sup>) and COD removal (%) efficiency at different HRTs with the continuously operated bioreactor. Fig. 4.15 a, b and c shows an increasing trend in the biomass concentration from 1.7 to 2.9 g L<sup>-1</sup> along with an increase in the HRT, and above 16h HRT the biomass concentration slightly decreased to 2.7 g L<sup>-1</sup>. More than 95% of COD was removed under the continuous mode for an optimum HRT of 16 h (dilution rate 0.06 h<sup>-1</sup>). Maximum accumulated lipid content in the biomass of 1.1 g L<sup>-1</sup> (64%, w/w), 2.35 g L<sup>-1</sup> (81%, w/w) and 2.16 g L<sup>-1</sup> (80%, w/w) were obtained at 8, 16 and 24 h HRT, respectively. Thus, 16 h (dilution rate 0.06 h<sup>-1</sup>) HRT proves to be optimum for PRWW treatment, lipid production and biomass growth. However, lipid-rich biomass exhibited poor settling characteristics, as similarly observed in the previous experiments.

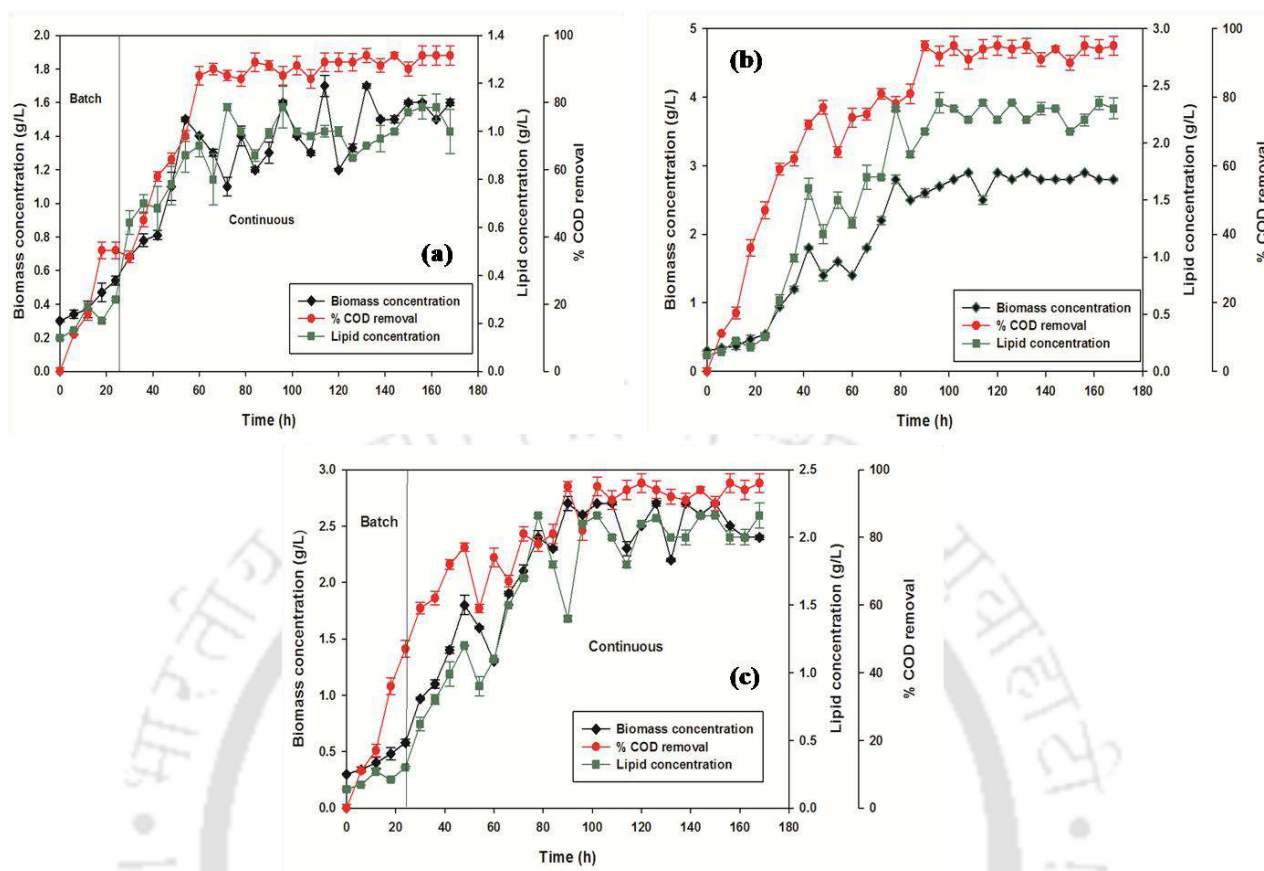


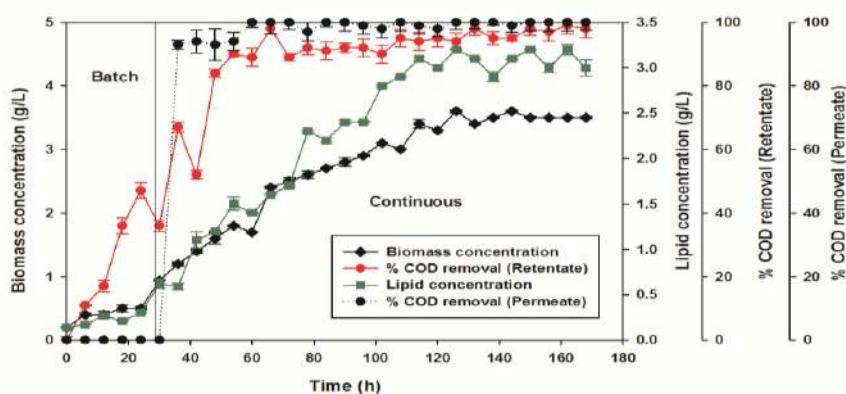
**Fig. 4.15** Biomass production, lipid accumulation and COD removal by *R. opacus* during the continuous experiments with the CSTR at different HRTs: (a) 8 h (b) 16 h and (c) 24 h.

### 4.2.3. Cell-recycle mode

For enhancing the process efficiency of the CSTR, biomass was recycled following continuous treatment of the wastewater at HRT of 16 h, by integrating the bioreactor with a low cost tubular ceramic membrane. Prior to the experiments, the membrane flux was calculated and was found to be  $2.39 \times 10^{-5} \text{ m}^3/\text{m}^2\text{s}$  under a pressure of 68 kPa. Cell-recycling is reported to achieve better performance of such bioreactors. The results obtained in this study are shown in Fig. 4.16, which reveals that maximum biomass concentration and lipid production of  $3.6 \text{ g L}^{-1}$  and  $3.2 \text{ g L}^{-1}$  (89%, w/w), respectively, were obtained. Moreover, complete removal of COD was achieved in the permeate obtained from the membrane system. Membrane bioreactor has been reported for toxicity removal from wastewater due to its potential to be used in low sludge load

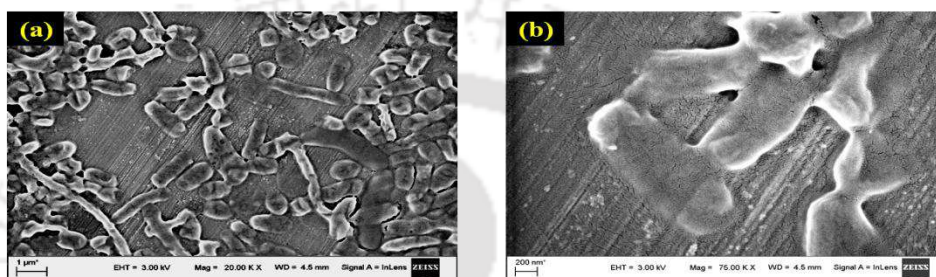
and high sludge age, which supports survival of bacteria present in the sludge, even in the presence of toxic compounds in the wastewater (Ishak et al., 2012); Yaopo et al., 1997). Hence, these results distinctly demonstrate that CSTR under continuous operation mode with cell recycle is best suited for achieving maximum COD removal from wastewater along with high lipid production using *R. opacus*.

Gupta et al. (2018) examined real-time lipid production from dairy wastewater using *R. opacus* and reported the highest lipid accumulation of nearly  $3.4 \text{ g L}^{-1}$  (78% CDW) in continuous cell recycle experiments but without an integrated membrane system. Yaopo et al. (1997) first treated petrochemical wastewater with a membrane bioreactor and obtained a high COD removal efficiency of 78-98%, which is lower than the value obtained in this study. Wiszniowski et al. (2011) evaluated the performance of a plug-flow membrane bioreactor for the treatment of PRWW and observed 93% of COD removal, which is less than that obtained in the present work. Moreover, the lipid production value of 89% (*w/w*) obtained in this study was without any addition of extra carbon source and it is much high as compared to that reported in the literature by Saisriyoot et al. (2016).



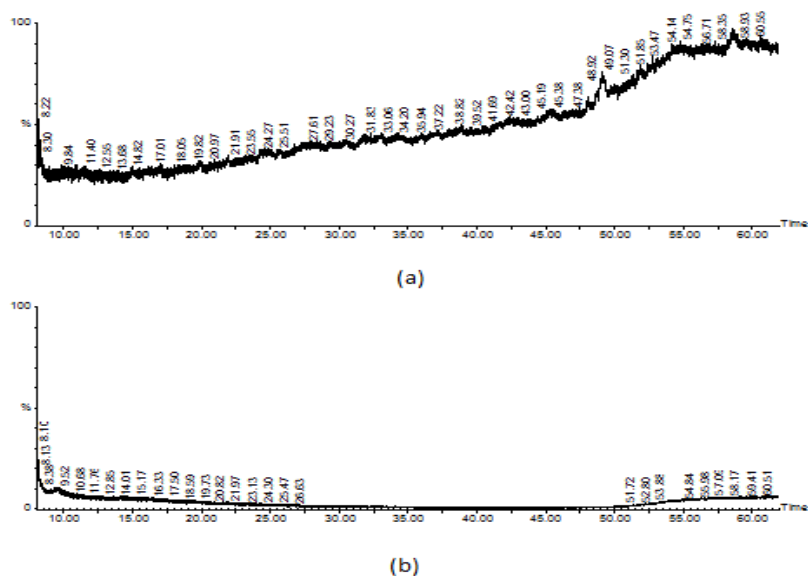
**Fig. 4.16** Biomass production, lipid accumulation and COD removal by *R. opacus* in the CSTR operated under continuous mode with cell recycle experiment at 16 h HRT

Fig. 4.17 (a) and (b) reveals no major change in surface morphology of the *R. opacus* biomass taken from the cell recycle streams and effluent sample port of the integrated membrane bioreactor system; the biomass was intact ( $\sim 2 \mu\text{m}$ ) without any visible damage to it. The Figure also indicates agglomeration of the bacterial biomass following its passage through the membrane for cell recycle; the cells were, however, relatively less disrupted prior to its recycling into the reactor.



**Fig. 4.17** FESEM images of *R. opacus* biomass collected from (a) recycle stream and (b) effluent stream of the bioreactor operated in continuous with cell recycle mode

GC-MS analysis was performed to determine the hydrocarbon profile in the influent and effluent streams of the continuous with cell recycle reactor system. The analysis was conducted using a sample of the untreated wastewater (0 h) and treated wastewater (168h). Fig. 4.18 shows the abundant presence of petroleum hydrocarbon compounds in the influent (0 h) whereas the amount was greatly reduced in the effluent stream (168h), which reveals that the compounds were efficiently degraded by *R. opacus* in the bioreactor and completely eliminated the effluent through the membrane treatment step. These results are found to be in agreement with those reported in the literature by Gargouri et al., (2011). Fig. 4.19 further confirms the efficient treatment of the PRWW by using the CSTR with cell recycle.



**Fig. 4.18** GC-MS analysis results showing hydrocarbon profile of the wastewater at (a) 0 h and (b) 168 h of treatment using the continuous with cell recycle reactor system (CSTR)



**Fig. 4.19** Visual comparison of raw PRWW, treated water and permeate water.

### 4.3. Performance evaluation of a bubble column reactor (BCR) for PRWW treatment and lipid-rich biomass production

Results of COD removal, biomass growth, and lipid accumulation by *R. opacus* in the batch operated BCR are shown in Fig. 4.20a. The COD removal efficiency gradually increased with time and reached its maximum (95%) after 72 h of the initial batch operation, and after this time period, the value almost remained constant. Following a short lag phase of 8h, *R. opacus* biomass growth entered the experimental growth phase and remained in this phase till 36h. The stationary phase lasted for 60h, i.e., until 96h of the batch operation time, and then the bacteria

entered the decline phase. The batch experiment was continued for a period of 112h, and the maximum biomass concentration obtained was  $2.1 \text{ g L}^{-1}$ . The lipid profile matched well with the biomass growth profile as it is a growth-associated product. The maximum lipid accumulation value is found to be  $1.56 \text{ g L}^{-1}$  which is 78% by cell dry weight (CDW).

The results from the batch study are much higher than those obtained previously using the CSTR. COD removal 86% and biomass and lipid concentrations were  $1.5 \text{ g L}^{-1}$  and  $0.83 \text{ g L}^{-1}$ . The better performance of the BCR than that of CSTR is attributed to the improved hydrodynamics, in particular, mixing conditions without damaging or causing shear stress on the bacterial strain. *R. opacus* is well known to degrade recalcitrant compounds in such wastewater and accumulate lipids inside the cell. However, depending upon the waste substrate and bioreactor configuration, lipid accumulation by the bacterium greatly varies. From the results of the batch experiments with the BCR, it is clear that the reactor system is ideal for achieving a maximum lipid accumulation and biomass concentration by *R. opacus* along with efficient utilization of the industrial wastewater as the substrate.

Following batch experiments with the BCR, continuous experiments were carried out to understand the effect of HRT on simultaneous treatment of PRWW treatment and lipid-rich biomass production by *R. opacus*. At 48h HRT, the COD removal efficiency was initially low, and it gradually increased to reach a steady-state value of 97% (Fig. 4.20b). Interestingly, when the HRT was lowered to 24h, the COD removal value quickly dropped to 70%, and later the value increased to a value of 92% on the 40<sup>th</sup> day of continuous bioreactor operation. At 16h HRT, the COD removal efficiency drastically lowered to 56% on 52<sup>nd</sup> day; however, at the later time period, the bioreactor performance improved and, at steady-state, COD removal value of 83% was achieved. In the case of 12h HRT, the COD removal efficiency was nearly 71% after the 85<sup>th</sup> day

of continuous BCR operation. Hence, from these results, 24h is found to be an optimum HRT for efficient utilization of the wastewater by the organism. At 48h HRT, the COD removal efficiency was only 3% higher than at 24hHRT, which is negligible from a treatment perspective.

Similar to the COD removal efficiency values at different HRTs, the biomass concentration varied with a change in the HRT. At 48h HRT, the biomass concentration was  $0.25 \text{ g L}^{-1}$ , which steadily increased to  $2.4 \text{ g L}^{-1}$  on 10<sup>th</sup> day of continuous bioreactor operation and remained almost at steady-state with minor fluctuation until the HRT value was reduced to 24h on the 23<sup>rd</sup> day. A drastic change in the biomass concentration was observed when the HRT was reduced to 24h; however, a steady-state biomass concentration of  $2.34 \text{ g L}^{-1}$  was obtained at this HRT, which is close to the value obtained at 48h HRT. But the value obtained was very low ( $0.95 \text{ g L}^{-1}$ ) at 16 h HRT, and it took a long time to reach a final value of  $1.71 \text{ g L}^{-1}$  at this HRT. The biomass concentration was minimum ( $1.26 \text{ g L}^{-1}$ ) at 12 h HRT. The lipid accumulation profile well-matched with the biomass profile in the bioreactor. The lipid concentration was observed to be 1.33, 1.1, 0.91,  $0.79 \text{ g L}^{-1}$  at 48h, 24h, 16h, and 12h HRT, respectively. The maximum lipid concentration was found to be 58% by cell dry weight (for 48h HRT), which is less when compared with that obtained in the batch operated reactor, which might be due to undesired biomass wash as commonly observed with such continuously operated reactors.

The results of batch studies match well with the COD removal values obtained, which confirms that the HRT significantly affects lipid-rich biomass production from refinery wastewater under continuous operation mode with the BCR. Unlike in a batch system, HRT plays a critical role in continuously operated bioreactor systems for substrate utilization as it determines the contact time between biomass and substrate in the reactor for efficient utilization. Hence, in this study, the COD removal efficiency decreased with a reduction in the HRT due to insufficient

contact between the bacteria and the substrate (Shariati et al., 2011; Thakur et al., 2014). Shariati et al. (2011) found that COD removal using a membrane sequencing batch reactor was better at 24h HRT than at 12h and 16h HRT values, as observed similarly in this study. However, Thakur et al. (2014) reported an optimum HRT value of 0.83d (~20 h) treating PRWW using a sequential batch reactor and obtained maximum COD removal of 77%. A batch operated bubble column reactor (BCR) showed better performance than the batch operated CSTR due to improved hydrodynamics and less shear stress on the bacterial strain.

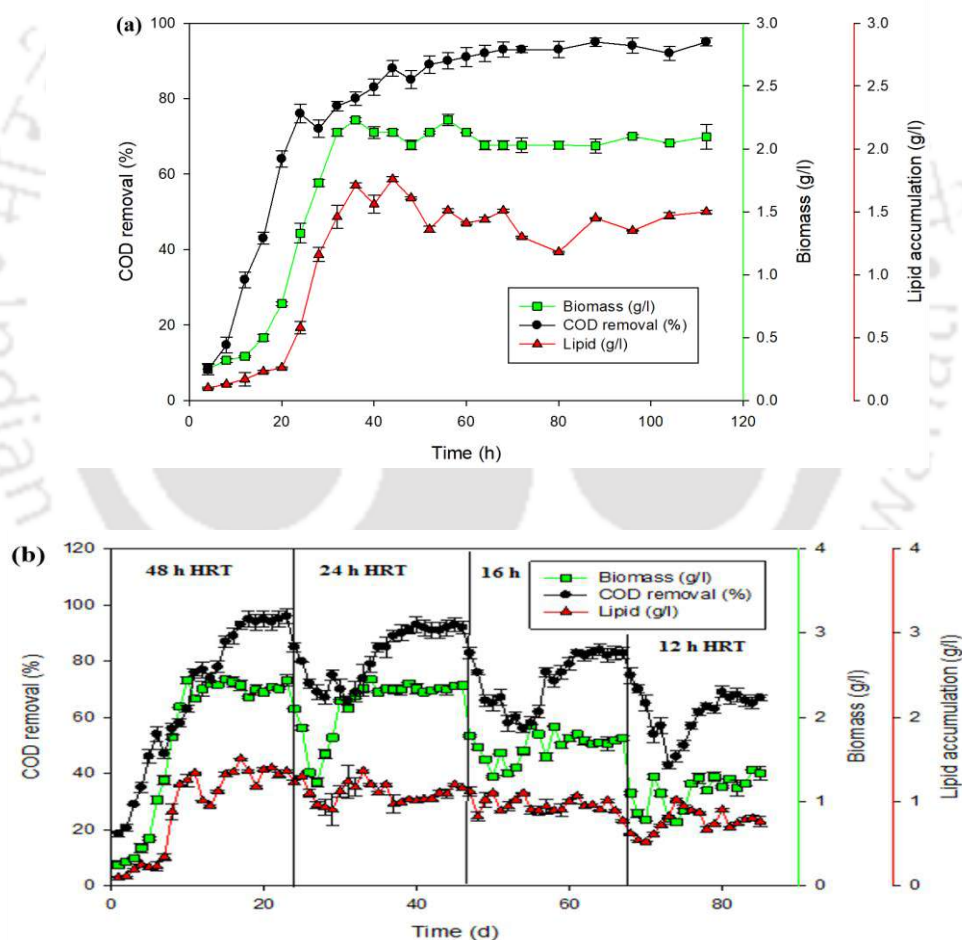


**Fig. 4.20** COD removal, biomass concentration and lipid accumulation by *R. opacus* in the BCR operated under (a) batch and (b) continuous modes.

#### 4.4. Performance evaluation of a submerged tubular membrane bioreactor (STMBR) for PRWW treatment and lipid-rich biomass production

##### 4.4.1. Biomass growth, COD removal, lipid concentration and membrane flux in STMBR

Fig. 4.21 presents the time profile of biomass growth ( $\text{g L}^{-1}$ ), COD removal (%) and lipid concentration ( $\text{g L}^{-1}$ ) attained during the STMBR operation. During the initial stages of the bioreactor operation, high (78%) COD removal efficiency was achieved with no further increase even after 100 h of treatment. Following 24 h of batch operation, the STMBR was operated under continuous mode with a dilution rate of  $0.06 \text{ h}^{-1}$  (16h HRT), which was chosen based on the biomass specific growth rate value ( $0.06 \text{ h}^{-1}$ ) determined previously. The biomass growth and lipid concentration obtained during the initial phase (first 3 days) was  $2.4 \text{ g L}^{-1}$  and  $1.19 \text{ g L}^{-1}$ , respectively. During the 2<sup>nd</sup> phase of the bioreactor operation and after membrane backwashing, the COD removal efficiency significantly increased to 82 %; however, the value gradually decreased with time and reached up to 77% at the end of the second phase. The biomass and lipid concentration values during this phase were  $2.71 \text{ g L}^{-1}$  and  $1.4 \text{ g L}^{-1}$ , respectively. After six days of continuous STMBR operation, i.e., in the third phase, 81% of COD removal efficiency along with  $2.4 \text{ g L}^{-1}$  and  $1.6 \text{ g L}^{-1}$  of biomass concentration and lipid concentration, respectively, were obtained.

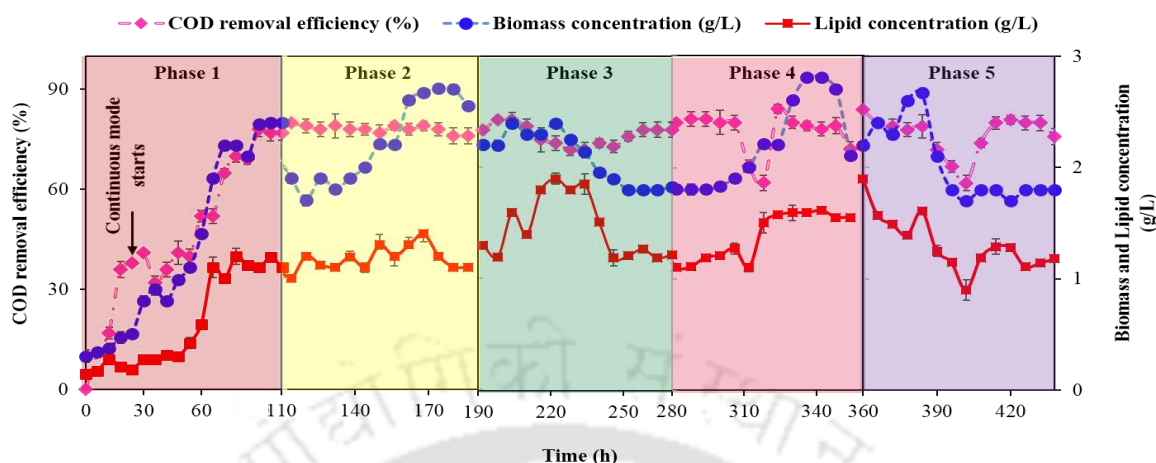
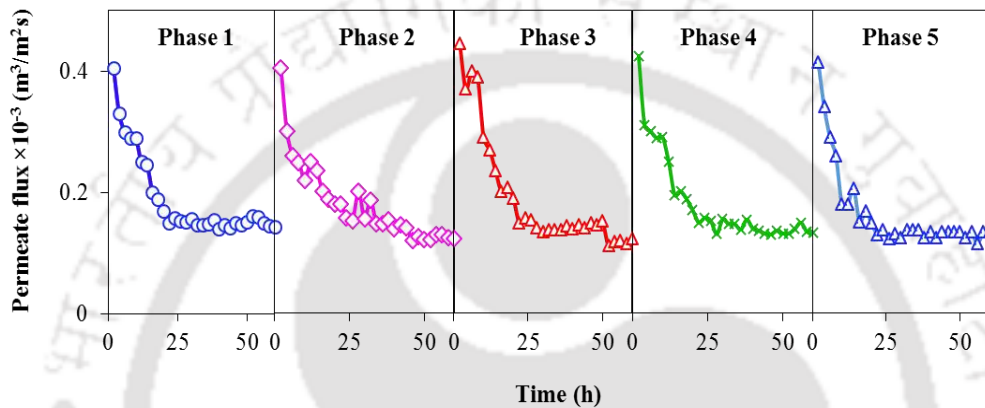


**Fig. 4.21** Time profile of biomass concentration ( $\text{g L}^{-1}$ ), COD removal efficiency (%) and lipid concentration ( $\text{g L}^{-1}$ ) during different phases of STMBR operation. (Phase divisions in the figure show the membrane washing carried out during the single-stage STMBR operation)

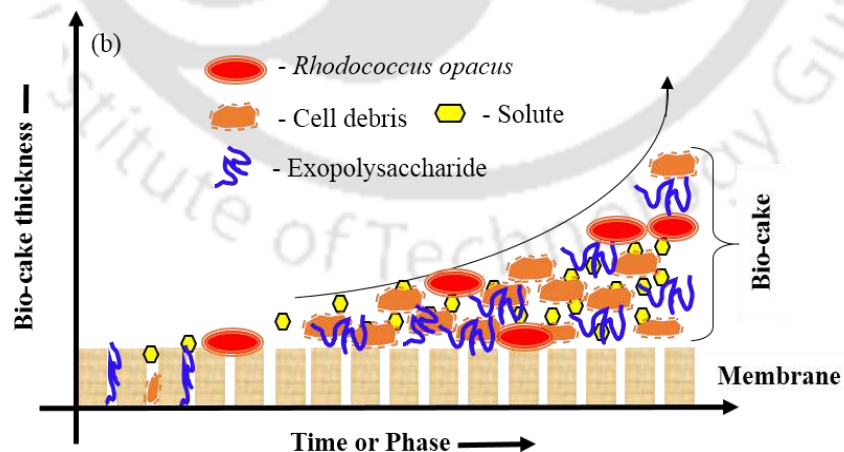
The COD removal values continued to remain high during the 4<sup>th</sup> and 5<sup>th</sup> phases of the membrane bioreactor operation (85% and 84%, respectively). From these results, it is clear that even after the membrane backwashing step performed after every 3 days of continuous operation with the STMBR, complete COD removal could not be achieved.

Fig. 4.22 depicts the variation in membrane permeate flux with time measured at the end of each experimental phase and at an applied pressure of 207 kPa. The decline in the membrane flux is significant during the later stages of the membrane bioreactor operation than during the initial stages. For instance, the average permeate flux with the PRWW (1<sup>st</sup> phase) was  $0.4 \times 10^{-3} \text{ m}^3/\text{m}^2\text{s}$ , which decreased to  $0.12 \times 10^{-3} \text{ m}^3/\text{m}^2\text{s}$  in the 2<sup>nd</sup> phase and finally to  $0.11 \times 10^{-3} \text{ m}^3/\text{m}^2\text{s}$  at the end of 5<sup>th</sup> phase of this study. This drastic reduction in the flux can be attributed to the formation of biomass cake layer, also termed as bio-cake, caused by the deposition and colonization of microorganisms on the membrane surface (Fig. 4.23). Bio-fouling further enhances due to the adsorption of specific solutes and microbial products such as exo-

polysaccharides (EPS) (Hong et al., 2014). Hence, membrane fouling observed in this study is due to the undesired deposition of cell debris and solutes on the membrane surface as well as blockage of pores inside (Yang et al., 2012). The deposition of solutes over the membrane surface is termed external fouling, whereas internal fouling refers to the blocking of pores inside the membrane structure (Brião and Tavares., 2012).



**Fig. 4.22** Variation in membrane flux during different phases of single-stage STMBR operation. (Phase divisions in the figure show the membrane washing carried out during the single-stage STMBR operation)



**Fig. 4.23** Schematic showing factors influencing the flux declining mechanism during different phases of single-stage STMBR operation

In addition to bio-fouling of membranes, an increase in the applied pressure is reported to cause deformation and penetration of oil droplets present in such wastewater, thereby decreasing the membrane flux (Kumar et al., 2016). Abbasi et al.(2012) evaluated the performance of mullite and mullite-alumina based ceramic microfiltration membranes. The authors reported 3 bar (300 kPa) pressure as the optimum condition for the treatment of synthetic oily wastewater. In another study, Fang et al. (2013) reported that 100 kPa is appropriate for microfiltration of oil-water emulsion using a ceramic membrane with a flux rate of  $159 \text{ L m}^{-2} \text{ h}^{-1}$ . Kumar et al. (2016) reported the highest rejection (99.88%) with a flux of  $3.40 \times 10^{-5} \text{ m}^3/\text{m}^2\text{s}$  at 68 kPa for treating oil-in-water emulsion using a ceramic membrane. However, the flux decreased with an increase in the applied pressure due to the formation of cake/gel layer, which effectively trapped oil droplets and restricted their passage through the membrane as also observed in this study carried out at a fixed applied pressure of 207 kPa.

Hence, in order to overcome the limitation of the single-stage STMBR system and to achieve high COD removal efficiency, a two-stage STMBR system involving two STMBRs connected in series with the output of the first STMBR ( $R_1$ ) fed to the second STMBR ( $R_2$ ) was adopted. Fig. 4.24 depicts the time profile of biomass growth ( $\text{g L}^{-1}$ ), COD removal (%) and lipid concentration ( $\text{g L}^{-1}$ ) attained in  $R_1$  and  $R_2$  of the two-stage STMBR system. Both the reactors were operated in continuous mode and at 16 h HRT. After 96 h of continuous operation, 79% COD removal was achieved in  $R_1$ , and 99% COD removal efficiency was achieved in  $R_2$ , thus overcoming the limitations of the previous single-stage STMBR system. Furthermore, unlike the single-stage STMBR, which was operated in 5 phases, the two-stage STMBRs could achieve 100% COD removal efficiency in the first three phases of continuous operation. The values of biomass growth and lipid concentration were also high in the two-stage STMBR system. However, the biomass concentration and lipid concentration in  $R_2$  was obviously lower than that

in  $R_1$  due to the low COD input to  $R_2$  from  $R_1$ . In the literature, maximum biomass and lipid concentration values of  $3.6 \text{ g L}^{-1}$  and  $3.2 \text{ g L}^{-1}$  (89% CDW), respectively, have been reported using an integrated bioreactor-cross-flow membrane system. However, the reactor which was operated under cell-recycle mode, is not favorable for biomass recovery and lipid extraction from the biomass, unlike in the present two-stage STMBR system.

Moreover, under the continuous operated mode with the BCR, 24 h HRT was found to be the optimum HRT which yielded biomass concentration of  $2.34 \text{ g/L}$  and COD removal efficiency of 93%. At 16 h HRT, these values were  $2.9 \text{ g L}^{-1}$  and 95% respectively. Compared with these results, maximum biomass concentration and lipid production of  $3.6 \text{ g L}^{-1}$  and  $3.2 \text{ g L}^{-1}$  (89%, w/w), respectively, along with complete removal of COD were obtained using the CSTR operated under cell recycle mode. Also, the lipid productivities in case of CSTR operated under cell recycle mode (16 h HRT) showed highest lipid productivity as compared to CSTR (16h HRT) and BCR (24 h HRT).

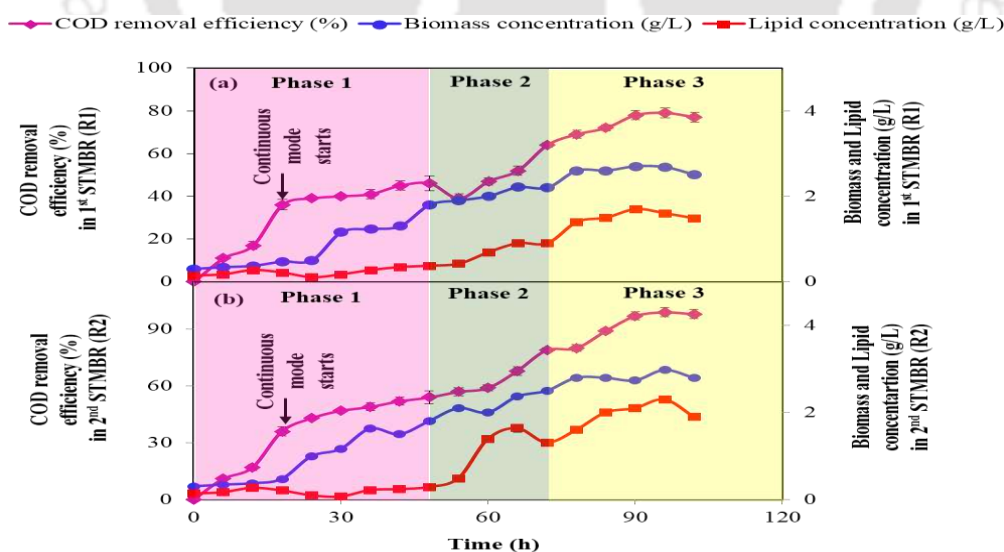


**Fig. 4.24** Biomass concentration ( $\text{g L}^{-1}$ ), COD removal efficiency (%) and lipid concentration

(g L<sup>-1</sup>) in the two-stage STMBR system (a) R1 and (b) R2. (Phase divisions in the figure show the membrane washing carried out during the two-stage STMBRs operation)

#### 4.4.1.1. Characterization of the cake layer formed on the membrane

For characterizing the cake layer formed on the membrane, changes in surface morphology of the tubular ceramic membrane before and at the end of continuous operation of the two-stage STMBR were analyzed by FESEM. Fig. 4.25 compares the FESEM image of the virgin membrane with that of the membrane following PRW treatment, which clearly reveals the deposition of the cake layer, similar to bio-film formation, on the membrane surface. A comparison of AFM images of the virgin and fouled membrane (Fig. 4.26) further confirmed the cake layer formation on the fouled membrane. Root mean square values of roughness calculated from the AFM images for the virgin and fouled membranes were 0.184 nm and 36.7 nm, respectively, which signify that the surface of the fouled membrane is more rough than the virgin membrane (Pajoumshariati et al., 2017). Fig. 4.27 compares the morphology of *R. opacus* biomass sample taken from the two-stage STMBR before and at the end of continuous operation, which indicates intact biomass with no damage to the cells.

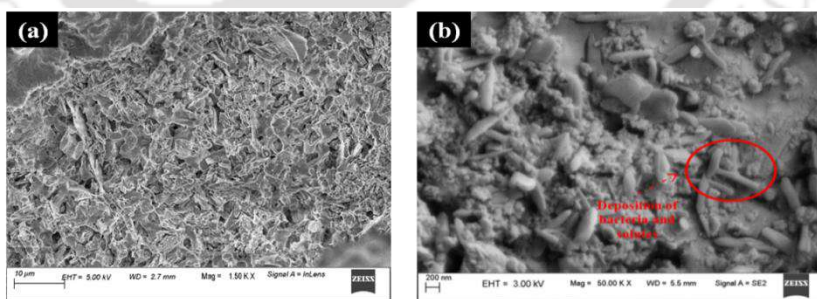


**Fig. 4.25** FESEM images of (a) virgin and (b) fouled membrane

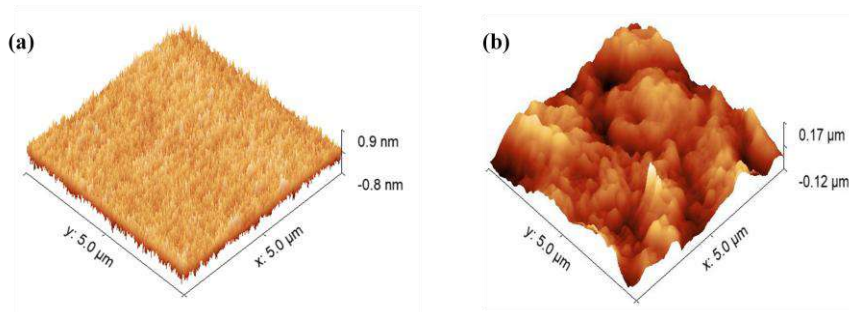


**Fig. 4.26** AFM images of (a) virgin and (b) fouled membrane.

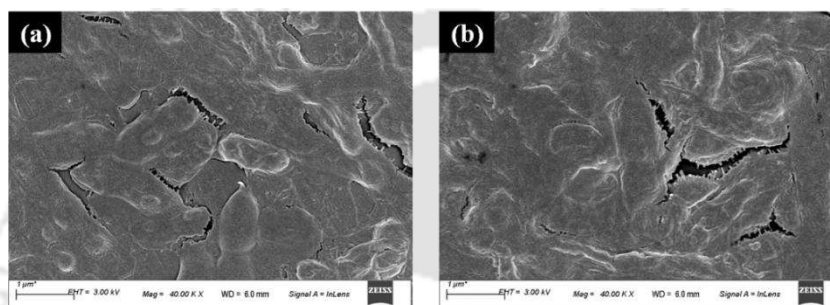


**Fig. 4.27** FESEM images of *R. opacus* biomass from the two-stage STMBR (a) before and (b) at the end of continuous operation.

For a better understanding of the membrane fouling and cake layer formed during the bioreactor operation, a sample of the cake layer was removed from the membrane surface and analyzed by FTIR spectroscopy. The FTIR spectrum shown in Fig. 4.28 reveals different peaks due to distinct and diverse functional groups of various compounds present in the cake layer. Table 4.9 lists the band assignments corresponding to the wave-numbers in the FTIR spectrum. The major bands at 1072, 1386, 1634, and 2928  $\text{cm}^{-1}$  correspond to tertiary alcohols, secondary amines and carboxylates present in the cake layer. Besides, the presence of saturated aliphatic compounds in the cake layer is revealed by the spectrum. A sharp peak at 1634  $\text{cm}^{-1}$  corresponds to the presence of alkenyl (C=C) groups. These findings are in good agreement with those reported by Pajoumshariati et al. (2017). The presence of carbon-rich organics on the cake layer is

attributed to the deposition of biomass and other suspended organics on the membrane surface, thereby contributing to the membrane fouling phenomenon (Melhem et al., 2015).

**Table 4.9** FTIR bands and the corresponding functional groups of compounds present on the cake layer

Wavenumber ( $\text{cm}^{-1}$ )	Functional group
1072	-Tertiary alcohol, C-O stretch -Secondary amine, C-N stretch - Tertiary amine, C-N stretch
1386	- Dialkyl/aryl sulfones - Carboxylate (carboxylic acid salt) - Organic sulfates
1634	- <i>gem</i> -Dimethyl or “iso”- (doublet) - Alkenyl C=C stretch - Amide - Open-chain imino (-C=N-) - olefinic unsaturation (C=C)
2928	- simple C-H stretching vibrations for saturated aliphatic - Methylene C-H asym./sym. stretch
3283	- Hydroxy group, H-bonded OH stretch

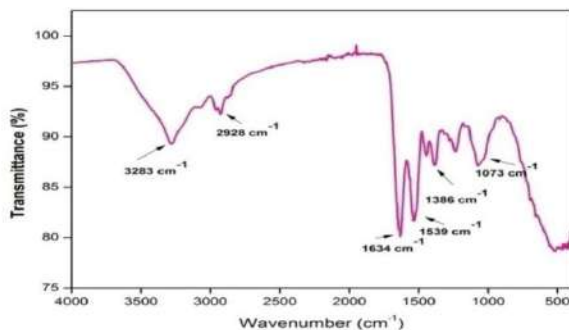


**Fig. 4.28** FT-IR spectrum of cake layer formed on the membrane surface.

As mentioned previously, nearly complete COD removal was achieved using the two-stage STMBR system. Moreover, it was observed that fecal coliforms present in the raw wastewater were drastically reduced (Fig. 4.29). The microbial count was reduced from 310 CFU/100 ml in the influent to 50 CFU/100 ml in the treated water, which is well below the limit set for discharging such wastewater into surface waters (CPCB, 1996). Similar findings were reported by Pajoumshariati et al. (2017) for the treatment of grey wastewater using a submerged membrane bioreactor. However, the initial microbial count in the grey wastewater was higher than that in the PRW used in this study. Fig. 4.30 shows permeate water obtained following treatment of refinery wastewater in a two-stage STMBR system.

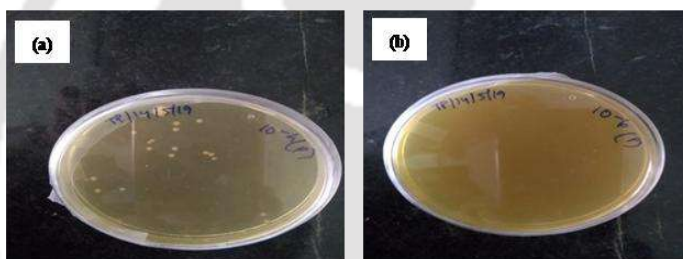


**Fig. 4.29** Plates showing reduced CFU count in different dilutions following treatment of PRW using two-stage STMBR system.



**Fig. 4.30** Permeate water obtained following treatment of refinery wastewater in a two-stage STMBR system.

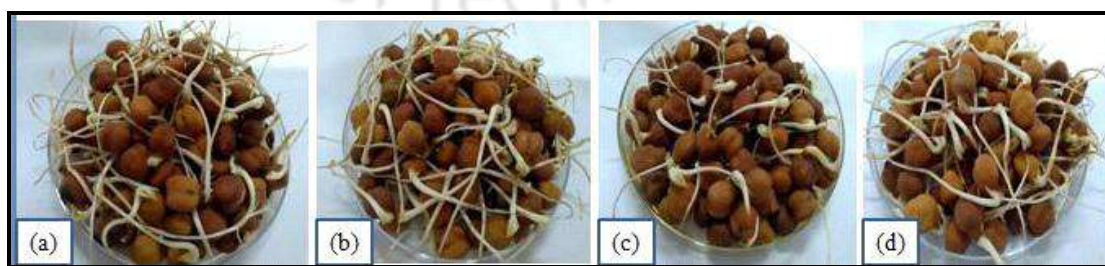
## 4.5. Toxicity analysis of PRWW in different reactors for reuse and recycle application

### 4.5.1. Seed germination assay

Germination Index (GI) of *Cicer arietinum* L. was used in this study to test the toxicity of the untreated (raw) and treated PRWW from the CSTR with cell recycle or STMBR experiment.

The selection of the seed is owing to its high sensitivity towards toxic pollutants (Devipriya et al., 2014) and its potential for protein digestibility following germination. The GI index is a sensitive parameter for evaluating toxicity assessment and is used to monitor changes in phyto-toxicity of the wastewater following its treatment (Zuconni et al., 1981). GI of the tap water as well as that of both the permeate (treated) and untreated PRWW was calculated with respect to distilled water as the control. Fig. 4.31 shows the germinated seeds for GI calculation. A GI of 73.63% with the permeate water obtained following cell-recycle step proves that the treated wastewater is free from any harmful phyto-toxic agents, whereas the untreated (raw) refinery wastewater showed a GI % of 34.63. However, tap water showed a high GI of 91.30 %.

In order to further assess the toxicity of wastewater before and after treatment using the two-stage STMBR system, the seed germination index (GI%) was calculated with distilled water as the control. The treated water from the two-stage STMBR showed a GI value of 82.08 % as compared with a very low GI value of 34.63 % for the raw PRW. A GI value of 50% is considered to be the minimum for a sample to be termed as non-toxic (Tiquia et al., 1996). The GI value of the treated water obtained in this study is also higher than that obtained using the integrated CSTR cross flow membrane system with cell-recycle. The permeate obtained following two-stage STMBR process ensures sequential removal of COD from the PRWW thus contributing to less higher GI resembling less toxicity and higher efficiency of the process.



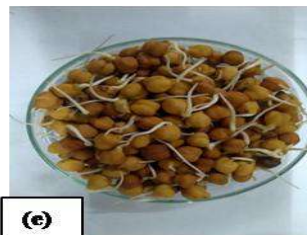


**Fig. 4.31** Germinated *Cicer arietinum* L seeds incubated with (a) distilled water (b) tap water (c) raw refinery wastewater (untreated) and (d) permeate (treated water) obtained following cell recycle and (e) permeate (treated water) obtained following two-stage STMBR for their ecotoxicity analysis

#### 4.5.2. Brine shrimp lethality assay (BLSA)

Toxicity assessment of the treated PRWW from CSTR with cell recycle or two-stage STMBR systems using *Artemia salina* larvae (mature nauplii) showed mortality of only 35% and 39% respectively, as compared with 73% mortality with the raw refinery wastewater. Ahmed et al. (2016) employed this method to examine in this study adopted this test for assessing the toxicity of newly synthesized samples of 1,4,5-trisubstituted 1, 2, 3-triazoles and observed that the degree of lethality of these compounds increases with an increase in their concentration; 100% mortality was observed at 300 mg ml<sup>-1</sup> concentration. Fig. 4.32 shows the experimental set-up used for growing brine shrimps in synthetic saline water.



**Fig. 4.32** Image showing experimental set-up used for growing brine shrimps in synthetic saline water.

#### 4.5.3. MTT [3-(4,5- dimethylthiazol-2-yl)-2,5-diphenylte- trazoliumbromide] assay

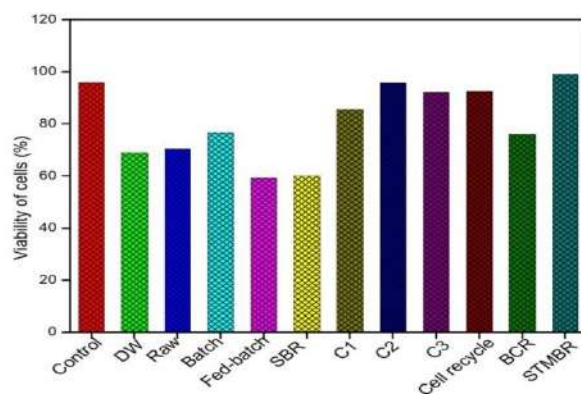


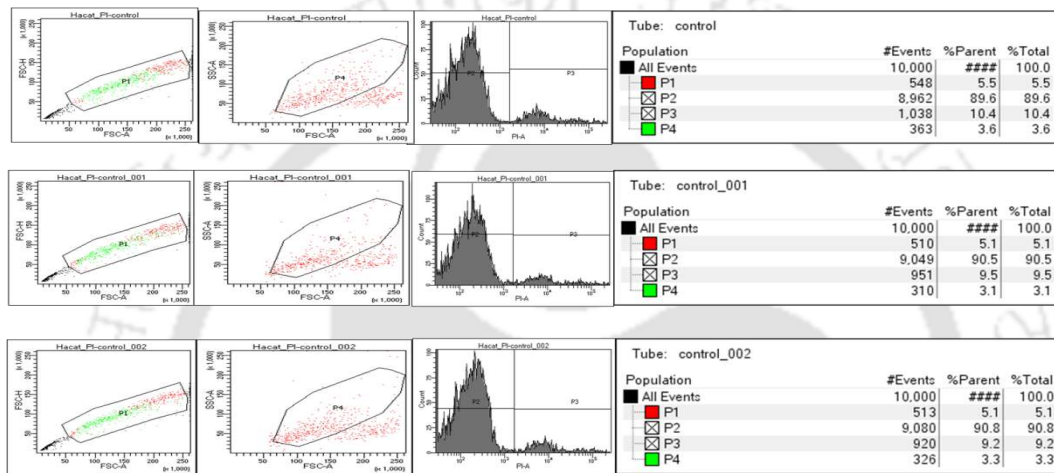
**Fig. 4.33** Results of MTT assay for evaluation of cell viability in treated wastewater samples following treatment

MTT assay is another widely used toxicity assay based on the activity of succinate dehydrogenase enzyme, present in mitochondria of a live cell, which converts MTT into insoluble formazan. Fig. 4.33 shows the viability of HEK cells following treatment with differently treated wastewater samples. It is clear from the Fig. 4.33 that C2 (continuous, 16 HRT), cell recycle and STMBR showed the maximum cell viability.

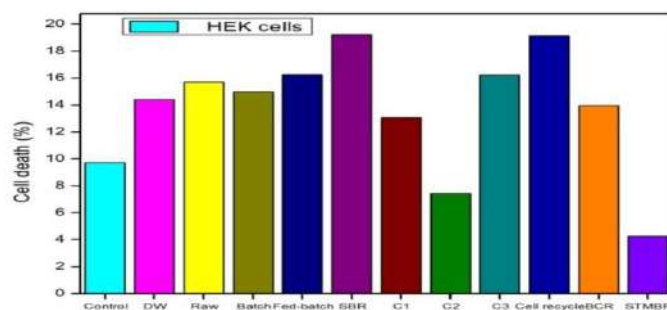
However, the cell viability values are also high with raw PRWW, which may be due to the presence of salts, that are known to promote MTT conversion into insoluble precipitate. Similar findings were reported by Yang et al. (2015) on the toxicity assessment of biologically treated wastewater that contained dissolved organic matter (DOMs). Also, abnormal high MTT signals were reported for HepG2 cells incubated with treated water following secondary treatment of domestic wastewater due to the presence of high glucose content in the sample. Furthermore, in addition to MTT assay, certain other efficient tests such as cytotoxicity assay (*umu*-assay) and plant-based genotoxicity DNA damage tests are recommended to be used for confirming the toxicity of such water samples (Dizer et al., 2002; Feretti et al., 2008). Hence, it could be surmised

that compared with the results of MTT assay, seed germination and brine shrimp assays yielded more reliable results for toxicity assessment of the treated water obtained using CSTR cell-recycle or STMBR system. The results of toxicity assessment of the treated water reveal its potential for reuse application.

#### 4.5.4. Propidium iodide flow cytometric assay (PI FACS)



(a)



(b)

**Fig. 4.34** (a) Raw data obtained using FACS caliber for different samples (b) Evaluation of apoptotic effect of the different wastewater following treatment by using PI FACS

The apoptotic effect of the different treated wastewater was further evaluated by using PI FACS. In this experiment HEK cells were treated with different samples of treated wastewater following treatment for 72 hr following which the apoptosis was determined by flow cytometry. Fig. 4.34(b) shows the HEK cells with different samples resulted in cell death. The dose as well as time dependent study can also be carried out for doing further research in this direction. PI FACS is one of the widely used assay for evaluating apoptotic effect (Bordoloi et al., 2019). This assay was performed to further evaluate and validate the results obtained by performing MTT assay.

In order to correlate the results, it is clear from the obtained data that, C2 (continuous, 16 h HRT) and STMBR showed the least cell death. These results matched well with the cell viability assay performed for this study on different treated wastewater sample as mentioned in section 4.3.3. Apart from PI FACS, other assays are also available for knowing the apoptotic nature of any drug, chemical or any synthesized compound (Bordoloi et al., 2019). These assays helps to evaluate the toxicity potential of the sample.

#### **4.6. Bio-oil production by hydrothermal liquefaction (HTL) of *R. opacus* biomass and its characterization**

##### **4.6.1. *R. opacus* biomass characterization**

Table 4.10 presents the characteristics of the *R. opacus* bacterial biomass grown on refinery wastewater as the substrate. The values of protein, lipid and sugar content of *R. opacus* as well matched with that of other bacterial biomass reported in the literature (Song et al., 2017). After ascertaining these characteristics of *R. opacus* biomass for bio-oil production, the biomass was subjected to the HTL process and the product obtained was analyzed in detail.

**Table 4.10** Characterization of the *R. opacus* biomass

Proximate analysis	Value (wt%)
Ash	1.83
Volatile Matter	91.68
Moisture	2.47
Fixed Carbon	4.02
<b>Ultimate elemental analysis</b>	
C	47.17
H	6.42
N	9.24
S	2.05
O	35.12
HHV (MJ kg <sup>-1</sup> )	20.73
<b>Biochemical composition</b>	
Lipid	39
Carbohydrate	2.8
Protein	62.19

From Table 4.10, ultimate analysis of *R. opacus* biomass revealed C (47.17%), H (6.42%), N (9.24%), S (2.05%) and O (35.12%) present in the biomass contributed to its overall heating value (20.73 MJ kg<sup>-1</sup>). Kang et al,(2015) reported the following values for *C. necator* biomass: C (45.08%), H (6.32%), N (12.85%), O (27.75%) and HHV (20.1MJ kg<sup>-1</sup>), which match well with the values obtained in the present study. However, a slightly high value of oxygen content of biomass is reported to decrease its calorific value and storage stability of the product. However, a slightly high value of oxygen content of biomass is reported to reduce its calorific value and storage stability. HHV of the *R. opacus* biomass (20.73MJ kg<sup>-1</sup>) in this study is higher than that reported by Wei et al. (2015) for products obtained by HTL of biomass following PHA production. The high value of HHV obtained with *R. opacus* is due to its high N content and a high N/C atomic ratio (0.195), which is greater than the value (0.13)

reported by Wei et al., (2015). Other researchers have also reported similar findings on N-rich algal and bacterial biomass for bio-oil production (Chen et al., 2014).

HTL is an effective technique for thermal depolymerisation and decomposition of biomass for bio-oil production. Thermal decomposition profile of *R. opacus* biomass was obtained by thermo gravimetric analysis (TGA), which reveals distinct regions due to change in TG curve; the curve below 300°C is attributed to first stage of thermal decomposition and drying of the sample; and during this stage, the light volatiles and water get evaporated (Fig. 4.35). This is followed by a drastic weight loss corresponding to the pyrolysis temperature range (Stage II) in which weak chemical bonds are destroyed. The third and final stage (up to 500°C) corresponds to 70-80% weight loss, which remains constant. Different thermal decomposition patterns of various feedstocks reported by researchers (Yang et al., 2007, Gasparovic et al., 2010) suggest that DSC-TGA curves can be used to describe the pyrolytic behavior of a feedstock which in turn depends on its composition, such as cellulose, hemicellulose and lignin. Thus, TGA analysis results confirmed maximum thermal degradation and depolymerization of *R. opacus* biomass for potential bio-oil production, which has not been reported so far using any bacterial biomass.

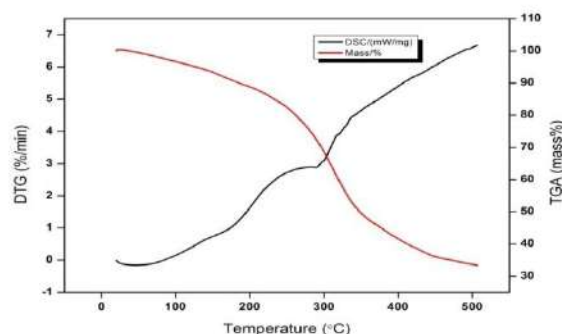


**Fig. 4.35** TGA profile of *R. opacus* biomass grown using refinery wastewater as the substrate

Song et al., (2017) performed proximate analysis of waste *cyanophyta* biomass and reported that the biomass contained 14.62% of ash, 90.87% of VM 9.46% of MC and 7.06% of FC. Compared with these values reported in the literature, the values reported in this study for *R. opacus* indicate very good suitability of the bacterial biomass as a bio-energy feedstock, mainly owing to its low MC and low ash content.

#### 4.6.2. HTL of *R. opacus* biomass and optimization of process parameters involved

Optimizing bio-oil yield from *R. opacus* biomass by HTL, three variables at three different levels were considered. Table 4.11 presents the combination of the levels of the variables used in each experimental run along with the results of bio-oil yield obtained. The obtained bio-oil yield decreased with an increase in temperature and reaction time, whereas a high biomass to water ratio resulted in an enhanced yield of the product. Thus, a very high yield of bio-oil could be achieved at 215 °C temperature, 125 min reaction time and 0.25 biomass to water ratio.

Bio-oil produced in this study is formed due to thermal polymerization of carbohydrates and proteins in the bacterial biomass under high pressure and temperature (Barreiro et al., 2013). Proteins as a major constituent in the biomass are responsible for reactions such as decarboxylation and deamination, which leads to the formation of aldehydes, amines, hydrocarbons and acids (Gollakota et al., 2018). Also, the high content of carbohydrates in the biomass is often reported to reduce bio-oil yield from biomass (Biller et al., 2011). These results reveal that the *R. opacus* biomass obtained by utilizing refinery wastewater is a potential feedstock for value-added bio-energy products via hydrothermal liquefaction.

**Table 4.11** Experimental design matrix showing coded and un-coded values of independent variables in each experimental run along with their responses in the optimization study

Exp	Temp (A)	Reaction time (B)	Biomass-water ratio (C)	Bio-oil yield (%)	
				Observed	Predicted
1	-1	-1	0	8.98	9.65
	180	50	0.25		
2	1	-1	0	11.34	11.61
	250	50	0.25		
3	-1	1	0	17.99	17.71
	180	200	0.25		
4	1	1	0	19.87	19.19
	250	200	0.25		
5	-1	0	-1	19.29	18.97
	180	125	0.10		
6	1	0	-1	20.43	20.51
	250	215	0.10		
7	-1	0	1	17.29	17.20
	180	215	0.40		
8	1	0	1	18.81	19.12
	250	215	0.40		
9	0	-1	-1	11.98	11.62
	215	50	0.10		
10	0	1	-1	20.98	21.57
	215	200	0.10		
11	0	-1	1	12.76	12.17
	215	50	0.40		
12	0	1	1	17.5	17.86
	215	200	0.40		
13	0	0	0	25.42	25.24
	215	125	0.25		
14	0	0	0	25.53	25.24
	215	125	0.25		
15	0	0	0	24.67	25.24
	215	125	0.25		

In order to analyze the effect of temperature, reaction time and biomass-water ratio on bio-oil yield as well as to predict the responses, the following second order polynomial equation was obtained by regression analysis of the experimental data:

$$Y = 25.24 + 0.8625A + 3.91B - 0.79C - 0.12AB + 0.095AC - 1.065BC - 3.7725A^2 - 6.9225B^2 - 2.5125C^2 \quad (\text{Eq. 4.1})$$

Where, Y is the bio-oil yield. A, B, C are temperature ( $^{\circ}\text{C}$ ), reaction time (min) and biomass water ratio (B/W) and AB, AC, BC are the interaction between these variables.

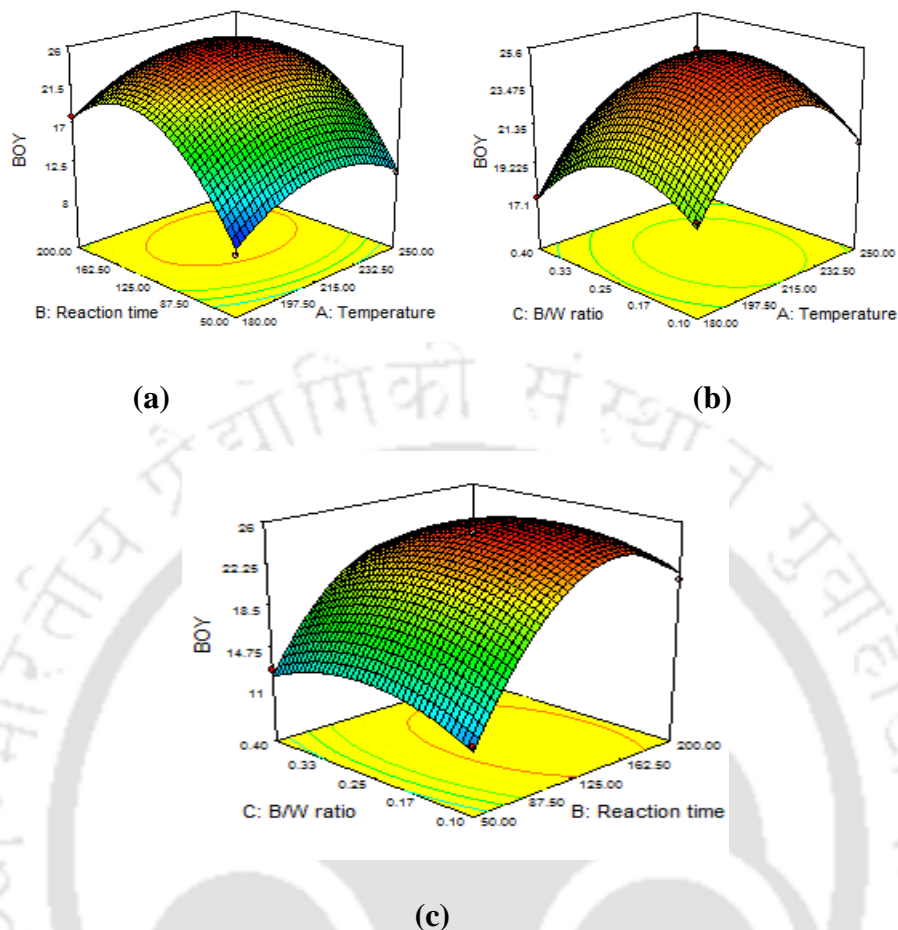
Table 4.12 compares the predicted values of the responses with the observed values in each experimental run. Statistical analysis of the results in the form of analysis of variance (ANOVA) is presented in Table 4.12. A large F value and a low Probability P-value of a particular coefficient in the model indicate its very high significance on a given response. The ANOVA results also suggest that the model is highly accurate in predicting the bio-oil yield with a very high coefficient of determination ( $R^2$ ) value. From the P values shown in Table 4.12, the coefficients of individual as well as squared effects of the three variables were highly significant on the bio-oil yield. Among the coefficients of interaction effects between the variables, only the coefficient of interaction between reaction time and biomass-water ratio was significant.

**Table 4.12** Analysis of Variance (ANOVA) of bio-oil yield by HTL of *R. opacus* biomass

Source	Sum of Squares	Degree of Freedom	Mean Square	F-value	p-value Prob > F
<b>Model</b>	452.79	9	50.31	129.45	< 0.0001
<b>A</b>	5.95	1	5.95	15.31	0.0058
<b>B</b>	122.30	1	122.30	314.70	< 0.0001
<b>C</b>	4.99	1	4.99	12.85	0.0089
<b>AB</b>	0.058	1	0.058	0.15	0.7117

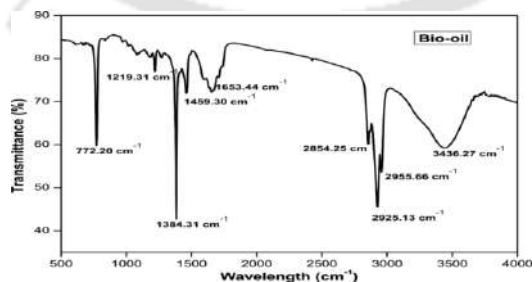
<b>AC</b>	0.036	1	0.036	0.093	0.7694
<b>BC</b>	4.54	1	4.54	11.67	0.0112
<b>A<sup>2</sup></b>	59.92	1	59.92	154.19	< 0.0001
<b>B<sup>2</sup></b>	201.77	1	201.77	519.18	< 0.0001
<b>C<sup>2</sup></b>	26.58	1	26.58	68.39	< 0.0001
<b>Residual</b>	2.72	7	0.39		
<b>Lack of Fit</b>	2.22	3	0.74	5.96	0.0588
<b>Pure Error</b>	0.50	4	0.12		
<b>Cor Total</b>	455.51	16			

Fig.4.36 shows the 3-D response surface and 2-D contour plots between the variables on bio-oil yield, which further confirmed the interaction between biomass-water ratio and reaction time was significant owing to an elliptical nature of the response plot between these two variables; the other two contour plots were circular, indicating very low significance of the interaction between the respective variables (Song et al., 2017). Hence, based on the results obtained, a maximum oil yield of 25% is observed at 215°C, 150 min and 0.25 biomass/water ratio. At higher temperatures, the bio-oil yield gradually reduced, probably due to the formation of products such as aliphatics, aromatics and gaseous products (Brown et al., 2010). Furthermore, under these conditions, the model predicted bio-oil yield value of 25.24% is obtained, which matched well with the experimentally obtained values.



**Fig. 4.36** 3-D Response surface and 2-D contour plots showing the interaction effect between HTL parameters on bio-oil yield: (a) reaction time and temperature (b) biomass-water ratio and temperature and (c) biomass-water ratio and time.

#### 4.6.3. Bio-oil characterization and fuel properties



(a)

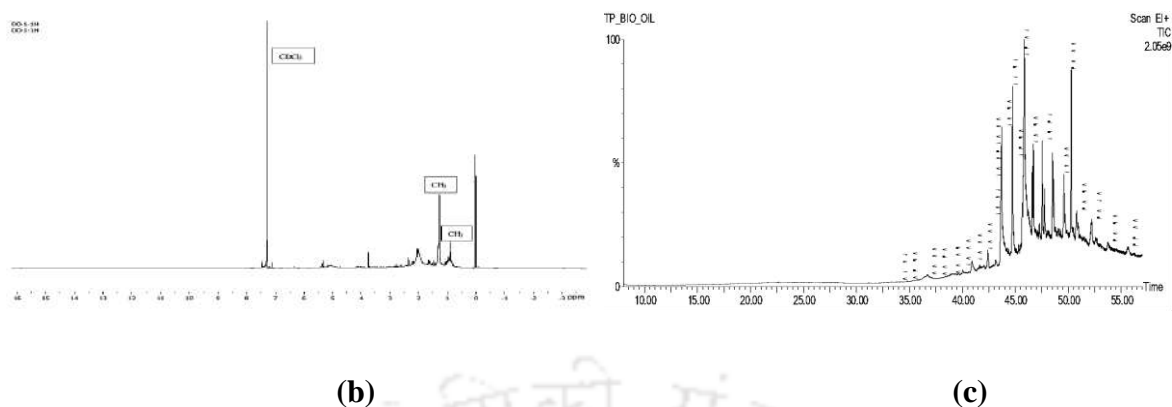


**Fig. 4.37** (a) FTIR (b)  $^1\text{H}$  NMR (c) GC-MS spectra of bio-oil fraction from HTL of *R. opacus* biomass.

FTIR Spectra of the bio-oil obtained is shown in Fig. 4.37 (a) which reveals the O-H vibrations in the range  $3200\text{--}3600\text{ cm}^{-1}$  due to the presence of alcohols and phenols. C-H stretching is seen as sharp peaks at  $2955.66\text{ cm}^{-1}$  and  $2925.13\text{ cm}^{-1}$ . Absorption in the region of  $3000\text{--}2800\text{ cm}^{-1}$  showed the presence of alkanes. Sharp peaks at  $2955.66\text{ cm}^{-1}$ ,  $2925.13\text{ cm}^{-1}$  and  $2854.25\text{ cm}^{-1}$  indicate methyl groups at the terminal position of the bio-oil produced from *R. opacus* biomass. The C=O conjugated double bond at  $1653.44\text{ cm}^{-1}$  indicates the presence of ketones and aldehydes. The peak at  $1384.31\text{ cm}^{-1}$  reveals the presence of primary, secondary and tertiary alcohols, phenols, ethers and ester. The peaks at  $772.20\text{ cm}^{-1}$  infer the presence of mono, polycyclic and other substituted aromatic groups. The peaks showing the presence of oxygenated groups (C=O, O-H, C-O) indicates that the bio-oil is oxygenated and acidic, a property that is typical of any other bio-fuel (Saikia et al., 2015). The functional groups C=C, C-H present in the bio-oil further confirmed its potential as a combustion fuel. Table 4.13 summarizes the various functional groups analyzed in the obtained bio-oil by valorization of *R. opacus* biomass.

**Table 4.13** Functional groups identified from FTIR spectra of the bio-oil produced by HTL of *R. opacus* biomass

Frequency range (cm <sup>-1</sup> )	Functional groups
3436.27 cm <sup>-1</sup>	Alcohol O-H stretch
2955.66 cm <sup>-1</sup>	Alkyl C-H stretch
2925.13 cm <sup>-1</sup>	Aldehyde C-H
2854.25 cm <sup>-1</sup>	C-H stretch
1653.44 cm <sup>-1</sup>	Conjugated double bonds C=O
2459.30 cm <sup>-1</sup>	C=N
1384.31 cm <sup>-1</sup>	CH <sub>3</sub> bend
1219.31 cm <sup>-1</sup>	C-O-C stretch
772.20cm <sup>-1</sup>	C-Br

**Fig. 4.37** (b) shows <sup>1</sup>H NMR spectra of the obtained bio-oil produced in this study; proton content of the bio-oil was thus analyzed through the chemical shifts range mentioned in Table 4.14. A shift in 0.8-2.4 infers the presence of different saturated fatty acids in the bio-oil product (Saikia et al., 2015).

**Table 4.14** <sup>1</sup>H NMR spectra analysis results of bio-oil according to chemical shift range

Chemical shifts (ppm)	Proton assignment
0.4-1.8	Other aliphatic(bonded to aliphatic only) such as alkanes
1.8-3.3	Aliphatic adjacent to aromatic/alkene group
3.3-4.5	Aliphatic adjacent to oxygen/hydroxyl group such as alcohols
4.5-6.5	Phenolic (OH) or methoxy, carbohydrates.
6.5-9	Aromatics

**Table 4.15** Hydrocarbons present in bio-oil obtained by HTL of *R. opacus*

No.	Compound Name	Molecular weight	Formula
1.	n-Hexadecanoic acid	256.42	C <sub>16</sub> H <sub>32</sub> O <sub>2</sub>
2.	Pentadecanoic acid	242.4	C <sub>15</sub> H <sub>30</sub> O <sub>2</sub>
3.	Dodecanoic acid	200.32	C <sub>12</sub> H <sub>24</sub> O <sub>2</sub>
4.	Tridecanoic acid	214.34	C <sub>13</sub> H <sub>26</sub> O <sub>2</sub>
5.	Tetradecanoic acid, 12-methyl-, methyl ester	256.42	C <sub>16</sub> H <sub>32</sub> O <sub>2</sub>
6.	Docosanoic acid, methyl ester	354.61	C <sub>23</sub> H <sub>46</sub> O <sub>2</sub>
7.	Tridecanoic acid, methyl ester	228.37	C <sub>14</sub> H <sub>28</sub> O <sub>2</sub>
8.	15-Hydroxypentadecanoic acid	258.40	C <sub>15</sub> H <sub>30</sub> O <sub>3</sub>
9.	12-Hydroxydodecanoic acid	216.32	C <sub>12</sub> H <sub>24</sub> O <sub>3</sub>
10.	12-Hydroxystearic acid	300.5	C <sub>18</sub> H <sub>36</sub> O <sub>3</sub>
11.	Eicosanoic acid, methyl ester	326.6	C <sub>21</sub> H <sub>42</sub> O <sub>2</sub>
12.	15-Tetracosenoic acid, methyl ester	380.64	C <sub>25</sub> H <sub>48</sub> O <sub>2</sub>
13.	Tridecanedioic acid, dimethyl ester	272.38	C <sub>15</sub> H <sub>28</sub> O <sub>4</sub>
14.	Nonadecane, 2,3-dimethyl-	296.57	C <sub>21</sub> H <sub>44</sub>
15.	Pentadecyl 2-propyl ester	334.6	C <sub>18</sub> H <sub>38</sub> O <sub>3</sub> S
16.	Triacontane, 11,20-didecyl-	703.34	C <sub>50</sub> H <sub>102</sub>
17.	Octadecane, 3-ethyl-5-(2-ethylbutyl)-	366.7	C <sub>26</sub> H <sub>54</sub>
18.	Sulfurous acid, octadecylpentyl ester	404.7	C <sub>23</sub> H <sub>48</sub> O <sub>3</sub> S
19.	Oxalic acid, octadecyl propyl ester	384.6	C <sub>23</sub> H <sub>44</sub> O <sub>4</sub>
20.	1,2-Benzenedicarboxylic acid, diisooctyl ester	390.6	C <sub>24</sub> H <sub>38</sub> O <sub>4</sub>
21.	1,2-Benzenedicarboxylic acid, diisooctyl ester	390.6	C <sub>24</sub> H <sub>38</sub> O <sub>4</sub>
22.	Bis(2-ethylhexyl) phthalate	390.6	C <sub>24</sub> H <sub>38</sub> O <sub>4</sub>
23.	Phthalic acid, 2-ethylhexyl tridecyl ester	460.7	C <sub>29</sub> H <sub>48</sub> O <sub>4</sub>
24.	3',8,8'-Trimethoxy-3-piperidyl-2,2'-binaphthalene-1,1',4, 4'-	487.5	C <sub>28</sub> H <sub>25</sub> O <sub>7</sub> N

tetrone			
25.	Phthalic acid, dodecyl 2-ethylhexyl ester	446.7	C <sub>28</sub> H <sub>46</sub> O <sub>4</sub>
26.	1,2-Benzenedicarboxylic acid, isodecyl octyl ester	418.60	C <sub>26</sub> H <sub>42</sub> O <sub>4</sub>
27.	1,2-Benzenedicarboxylic acid, decyl octyl ester	418.60	C <sub>26</sub> H <sub>42</sub> O <sub>4</sub>
28.	Phthalic acid, dodecyl octyl ester	446.7	C <sub>28</sub> H <sub>46</sub> O <sub>4</sub>

The bio-oil produced in this study was further characterized by GC-MS analysis, and for which oil phase was analyzed (Fig. 4.37 (c)). Most of the peaks were identified by highest similarity match with the available MS library. Chemical compounds identified in the oil phase are presented in Table 4.15, which reveal that the oil phase consisted of a mixture of complex organic compounds, mainly phenols, alcohols, esters, mixed acids, etc.

Properties of obtained bio-oil depend mainly on the composition of feedstock used for HTL. In this study, the bio-oil obtained by valorization of *R. opacus* biomass was analyzed for its fuel properties. Bio-oil as compared with petroleum fuel oil has certain undesired properties, such as high corrosiveness due to its high viscosity, high acidity, high content of water, as well as low chemical stability (Saber et al., 2016). It has a high amount of fatty acids, which causes acidity and corrosiveness. Besides, aldehydes present contribute to unstable fractions in the bio-oil. However, bio-oil can be upgraded by certain chemical reactions to overcome these problems. Hence, owing to a high content of fatty acids present in bio-oil, it was transesterified, as demonstrated in the literature by Xu et al.(2014).

Estimated property values of the transesterified bio-oil in terms of viscosity, flash point, cetane number (CN), pour point (PP), degree of unsaturation (DU), cloud point (CP), calorific value are presented in Table 4.16. These results suggest that the bio-oil properties match well with

those of the European Standards (EN) and American Society for Testing and Materials (ASTM) thus revealing a very good reliability of the transesterified bio-oil for bio-fuel applications (Kim et al., 2019). GC-MS analysis further revealed about 69.54% of the total FAME content is due to methyl stearate (C18:0) and methyl arachidate (C20:0). Similar results were obtained by transesterification of lipids accumulated by *R. opacus* grown in biomass gasification wastewater (Goswami et al., 2017). Nevertheless, bio-fuels with high viscosity show poor flow properties as well as low penetration ability. Also, it is reported that the value of the cloud point of fuel should be low for maintaining its fluidity at low temperatures as obtained in our current study. However, the cetane number was slightly lower as compared to the ASTM and EN standards. Overall, the estimated properties of the bio-oil obtained, followed by hydrothermal liquefaction of *R. opacus* biomass, reveals good potential as an effective bio-fuel.

**Table 4.16** Estimated property values of the trans-esterified bio-oil obtained by HTL of *R. opacus* biomass and comparison with that of the International Standards

Properties	Units	ASTM- D6751 standard	EN 14214	Ex-situ transesterified product
Viscosity	(mm <sup>2</sup> /s)	1.9-6.0	3.5-5.0	4.71
Flash point	(°C)		93	148.65
Cetane number	-	47(minimu m)	51 (minimum)	66.59
Pour point	(°C)	ND	ND	6.26
Calorific Value	MJ/Kg	ND	≤5/≤-20	43.12
Degree of unsaturation	-	ND	ND	21.16
Cloud point	(°C)	ND	ND	15.59

A schematic showing the main steps involved in lipid biosynthesis by *Rhodococci* and its conversion to bio-oil by HTL is depicted in Fig. 4.38.

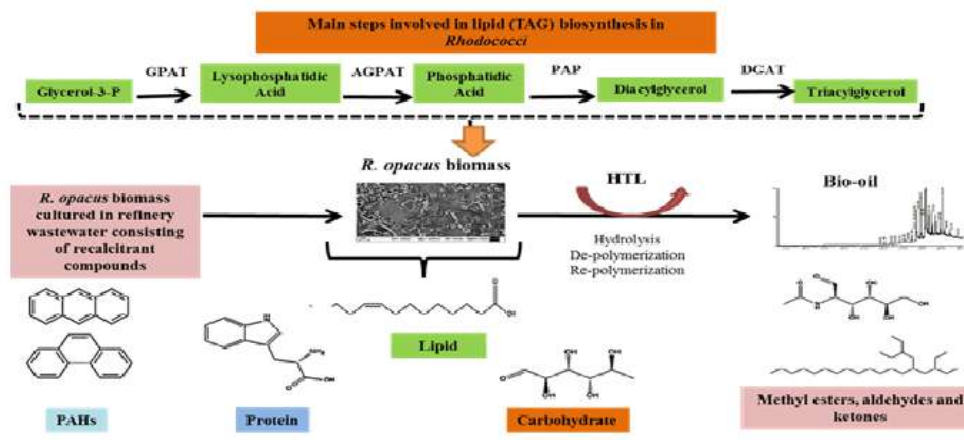


**Fig. 4.38** Schematic showing (a) the steps involved in HTL and (b) main steps involved in lipid biosynthesis by *R. opacus* from PRWW and its conversion to bio-oil by HTL (GPAT, glycerol-3-phosphate acyl transferase; AGPAT, acylglycerol-3-phosphate acyl transferase; PAP, phosphatidic acid phosphatase; DGAT, diacylglycerol acyl transferase)

#### 4.6.4. Characterization of HTL by-products

Characterization results of the aqueous soluble fraction from HTL of the *R. opacus* by IC, FTIR, and GC-MS analyses are present in Fig. 4.39. The IC spectra shown in Fig. 4.39(a) revealed the presence of chloride along with a small amount of sulfate and phosphate. The FTIR analysis revealed that it contains hydroxyl (O-H) and primary amine (N-H) groups with prominent peaks at 3338.7 and 1635.13  $\text{cm}^{-1}$ , respectively (Fig. 4.39b). Some of the amine compounds produced by HTL treatment of the *R. opacus* biomass are water-soluble, and these compounds are detected in the aqueous fraction by FTIR spectra analysis. The GC-MS spectra of the aqueous fraction show the presence of complex hydrocarbons (Fig. 4.39c), but their number and quantities are very less as compared with that in bio-oil (Table 4.17).

**Table 4.17** Hydrocarbons identified in aqueous phase by product obtained by HTL of *R. opacus*

No.	Compound Name	Molecular weight	Formula
1.	cis-5-Dodecenoic acid	198.3	C <sub>12</sub> H <sub>22</sub> O <sub>2</sub>
2.	Pentadec-7-ene, 7-bromomethyl-	303.32	C <sub>16</sub> H <sub>31</sub> Br
3.	4-chloro-3-n-hexyltetrahydropyran	204.73	C <sub>11</sub> H <sub>21</sub> OCl
4.	Cyclohexane, 1,5-diisopropyl-2,3-dimethyl-	196.37	C <sub>14</sub> H <sub>28</sub>
5.	Cyclohexane, 1-(1,5-dimethylhexyl)-4-(4-methylpentyl) cyclohexane	280.53	C <sub>20</sub> H <sub>40</sub>
6.	1,2-15,16-Diepoxylhexadecane	254.41	C <sub>16</sub> H <sub>30</sub> O <sub>2</sub>
7.	2-Dodecen-1-yl(-)succinic anhydride	266.38	C <sub>16</sub> H <sub>26</sub> O <sub>3</sub>
8.	1-Heptadec-1-ynyl-cyclohexanol	334.6	C <sub>23</sub> H <sub>42</sub> O
9.	3-hexen-2-one, 3-cyclohexyl-4-ethyl-	208.34	C <sub>14</sub> H <sub>24</sub> O
10.	4,4-Dimethyl-oct-5-enal	154.25	C <sub>10</sub> H <sub>18</sub> O
11.	2-Isopropyl-1,3-dimethyl- cyclopentane,	140.27	C <sub>10</sub> H <sub>20</sub>
12.	7,11-Hexadecadienal	236.39	C <sub>16</sub> H <sub>28</sub> O

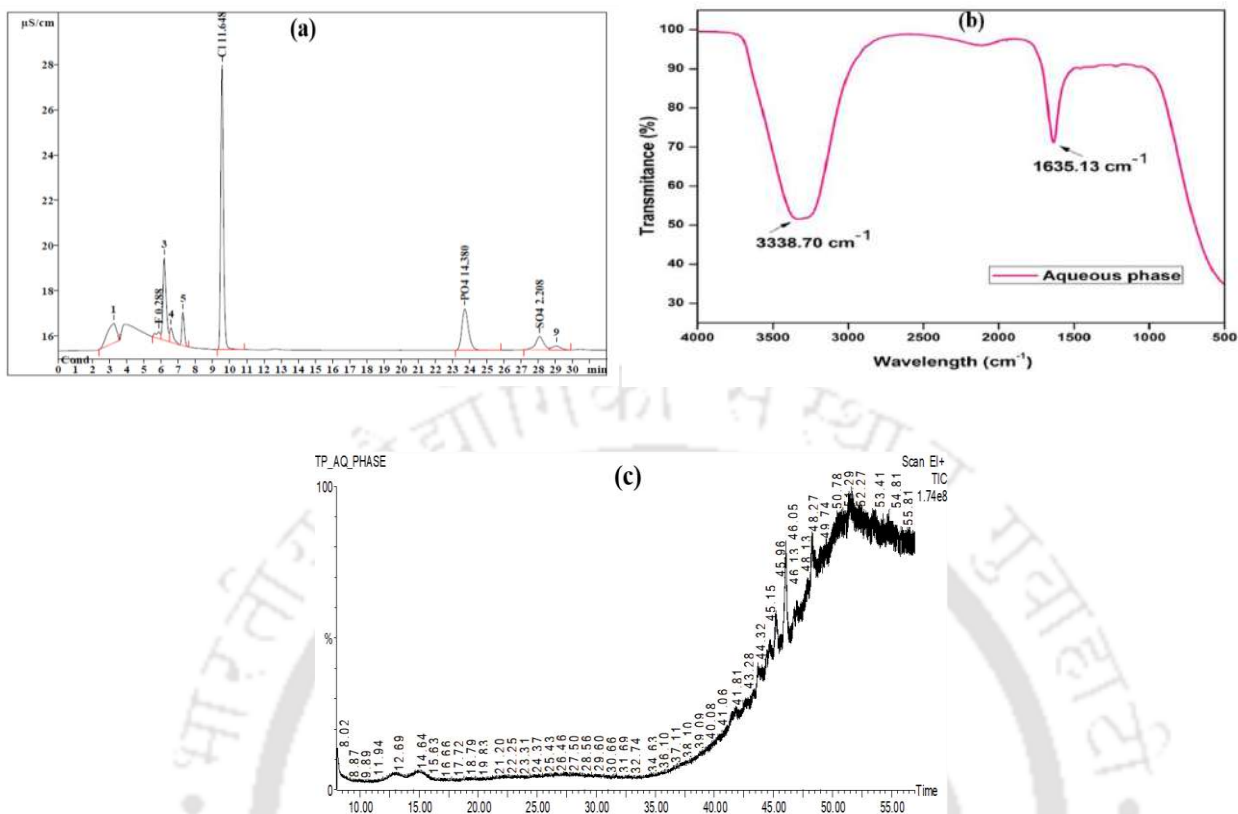


**Fig. 4.39** (a) IC, (b) FTIR and (c) GC-MS spectra of aqueous phase derived from hydrothermal liquefaction (HTL) of *R. opacus* biomass.

The solid residue obtained after HTL treatment of the bacterial biomass was characterized using FESEM-EDX (Fig. 4.40a). These solids recovered from the aqueous phase are primarily bio-char with a very high carbon content (65.1%)(Wei et al., 2015). Detailed characterization results of solid residue obtained following HTL of *R. opacus* biomass are presented in Table 4.18. High ash content of the bio-char is indicated by the presence of high oxygen content. Other elements such as Zn, P, K, Fe, and Mg present in the solid residue are sourced from the wastewater or the MSM. Elemental analysis of the solids further revealed that it contained 41.8% C, 3.9% H, and 5.1% N (Table 4.18). A zeta potential value of  $-38.7$  mV signifies the presence of highly negatively charged species in the bio-char (solid residue). The average particle size of the bio-char was found to be 892.3 nm, with a total surface area of  $16.8 \text{ m}^2 \text{ g}^{-1}$ . Fig. 4.40 b depicts the

thermal characteristics of the solid residue. The weight loss observed in the temperature 100-300°C range is low and is attributed to the loss of moisture in the sample. Major weight loss was observed in the range 300-500°C, due to the exclusion of volatile compounds. Above this temperature, no weight loss is observed until 900°C, and a final weight of 58% of the initial bio-char is obtained.

**Table 4.18** Characterization results of solid residue obtained by HTL of *R. opacus* biomass

Elemental composition	(%)
C (%)	41.771
H (%)	3.947
N (%)	5.129
H/C	0.094
<b>Surface area and porosity</b>	
BET surface area (m <sup>2</sup> g <sup>-1</sup> )	16.864 m <sup>2</sup> /g
Pore volume	6.909e-02 cc/g
Average Pore diameter (nm)	1.63876e+01 nm
<b>General</b>	
Zeta potential (mV)	-38.7 mV
pH	9-10
Average particle size	892.3 nm

Fig. 4.40 (c) shows the XRD profile of the solid residue. The wide peaks at 2  $\Theta$  and 25  $2\Theta$  degree are due to aromatic layers stacking (Liu et al., 2012), whereas the peaks at 33 and 65  $2\Theta$  degree is due to SiO<sub>2</sub> (Ahmad et al., 2019). Other small peaks observed in the figure are due to the presence of CaCO<sub>3</sub>, CaO, MgO, FeO, etc. commonly reported to be present in bio-char derived from biomass (Liu et al., 2012, Ma et al., 2015). FTIR spectra shown in Fig. 4.40 (d) reveal prominent peaks at 551.67, 1453.90, 1532.36, 1626.52, 2924.12, 3276.46 cm<sup>-1</sup>. These peaks

indicate the presence of hydroxyl (O-H), alkanes (-C-H), primary amine (N-H), aliphatic amines (-C-N), aromatic compounds (-C-C-) in the solid residue (Gao et al., 2012; Parsa et al., 2019).

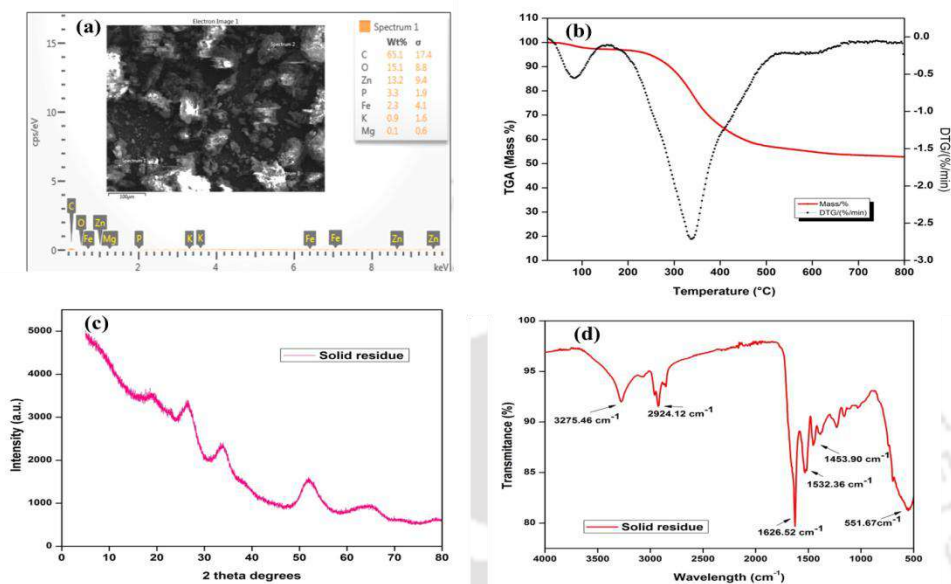


**Fig. 4.40** (a) FESEM-EDX, (b) TGA, (c) XRD and (d) FTIR spectra of solid residue derived from hydrothermal liquefaction (HTL) of bacterial biomass.

This study demonstrated that lipid-rich *R. opacus* biomass obtained using refinery wastewater as the substrate can be converted to bio-oil with excellent potential as a fuel. The HTL process for the production of bio-oil from bacterial biomass is also favored due to the very good properties of the solid residue and aqueous phase as the by-products, which showed excellent reuse potential.

#### 4.6.5. HTL with different catalysts for enhancing bio-oil yield

##### 4.6.5.1. Homogenous catalysts

In order to enhance the bio-oil yield obtained by HTL of *R. opacus* biomass, the effect of adding different catalysts in the process was studied. Various homogenous as well as heterogeneous catalysts, including acids and base catalysts, are reported for bio-oil up-gradation

via HTL. Ross et al. (2010) performed HTL using acid ( $\text{CH}_3\text{COOH}$  and  $\text{HCOOH}$ ) and base catalysts ( $\text{Na}_2\text{CO}_3$  and  $\text{KOH}$ ) for bio-oil production from *C. vulgaris*. In this study, HTL was performed using biomass *R. opacus* and two different catalysts viz.  $\text{Na}_2\text{CO}_3$  and  $\text{H}_2\text{SO}_4$ . Fig. 4.41 (a) and (b) shows FT-IR spectra of bio-oil and aqueous phase obtained by HTL of *R. opacus* biomass in the presence of the catalysts  $\text{Na}_2\text{CO}_3$  and  $\text{H}_2\text{SO}_4$  respectively. The bio-oil yield using acid catalysts was more than that obtained using base catalysts. Moreover, the bio-oil obtained using acid catalyst showed superior flow properties. On the other hand, the base catalyst  $\text{Na}_2\text{CO}_3$  yielded a low bio-oil (23.65 %) as compared with  $\text{H}_2\text{SO}_4$  (24.16%). It is reported that such base catalysts improved the conversion of carbohydrates but it is ineffective for conversion of lipids and proteins to bio-oil by HTL (Shakya et al., 2015).

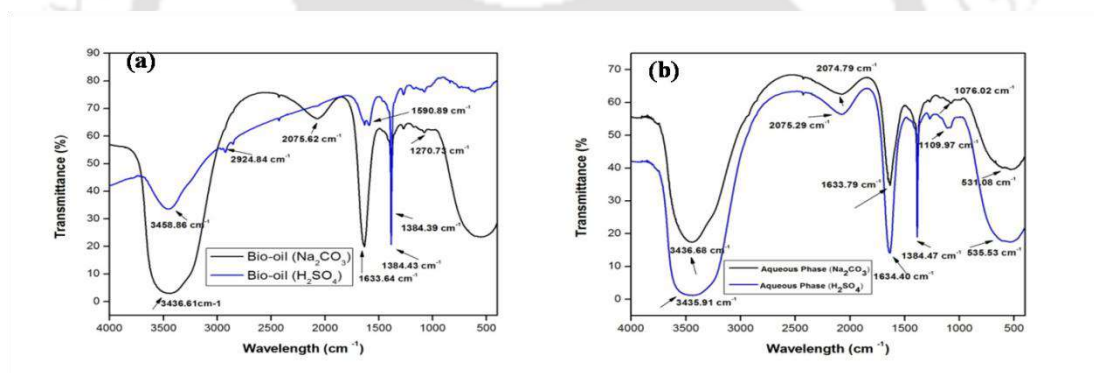
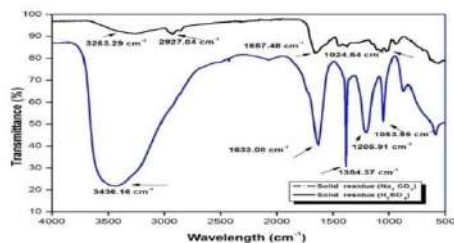


**Fig. 4.41** (a) FT-IR spectra of bio-oil produced by HTL of *R. opacus* biomass using  $\text{Na}_2\text{CO}_3$  and  $\text{H}_2\text{SO}_4$ , (b) FT-IR spectra of aqueous phase produced by HTL of *R. opacus* biomass using  $\text{Na}_2\text{CO}_3$ , and  $\text{H}_2\text{SO}_4$  as catalysts.

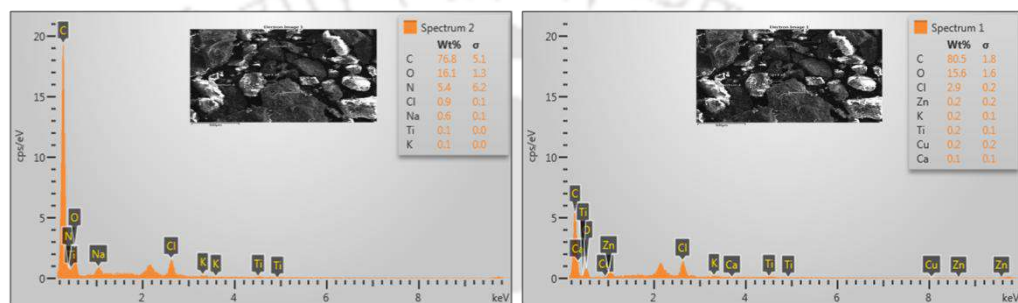
Shakya et al. (2015) reported the effect of temperature and  $\text{Na}_2\text{CO}_3$  catalyst on HTL of algae at three different temperatures of 250, 300 and 350 °C for 60 min. The study showed maximum bio-oil yield of 47.05 wt% in the presence of catalyst at 350 °C from *Pavlova* and without any catalyst (48.67 wt%) from *Nannochloropsis*. It was also reported that  $\text{Na}_2\text{CO}_3$  could increase bio-oil yield from high carbohydrate-rich algae (*Pavlova* and *Isochrysis*) at a higher

temperature. In the case of protein-rich algae (*Nannochloropsis*), the yield was found to be high at a lower temperature of 250 °C. However, the role of alkaline catalyst on HTL of different algal biomass is not clear. Additionally, the use of such alkaline catalysts has been shown to decrease bio-oil yield from sunflower by HTL due to soap formation (reference). Inorganic acids (H<sub>2</sub>SO<sub>4</sub>) also play a critical role in bio-oil production by HTL of microalga (Hu et al., 2017, Zou et al., 2009). Zou et al., (2009) reported that 2.4 % of this acid reduced N content up to 0.96 wt%, resulting in an enhanced bio-oil yield.

FTIR spectra (Fig. 4.41a) of the bio-oil revealed the presence of different functional groups. The O-H stretching indicated by a wide peak at 3436.61 cm<sup>-1</sup> is attributed to alcohols and phenols in the product. The peak at 2075.62 cm<sup>-1</sup> confirmed the presence of a C≡C triple bond of alkynyl stretching. A very sharp peak at 1633.64 cm<sup>-1</sup> is either due to amide C=O stretch or alkenyl C=C stretch, which are typical ketones and aldehydes, confirming the conversion of lipids into fatty acids by HTL reactions. Also, 1384.39 designates C-O bond from the spectra of the bio-oil obtained using Na<sub>2</sub>CO<sub>3</sub> as the catalyst. Almost similar peaks were obtained from FT-IR spectra, which reveal that the composition of the bio-oil is not affected by using a different catalyst; however, relatively sharp peaks were obtained in the case of the base catalyzed process. Also, in the case of aqueous phase obtained by HTL of *R. opacus* biomass in the presence of acid or base catalyst, the spectra were found to be very similar (Fig. 4.41 b). The results of FTIR analysis also revealed the presence of hydroxyl (O-H) and primary amine (N-H) as previously observed in the case of bio-oil obtained without using catalyst for HTL of *R. opacus* biomass.



(a)



(b)

**Fig. 4.42** (a) FT-IR spectra and (b) SEM-EDX of solid residue produced by HTL of *R. opacus* biomass using  $\text{Na}_2\text{CO}_3$  and  $\text{H}_2\text{SO}_4$  as catalysts

The solid residue obtained following HTL of the bacterial biomass in the presence of these two catalysts was characterized using FT-IR and FESEM-EDX (Fig. 4.42). These characterization results of the solid residue confirm that the HTL by-product is bio-char.

Liu et al. (2017) reported that several reactions, including depolymerization, re-polymerization and hydrolysis, were involved in biomass conversion to different compounds by HTL. Besides, it has been reported that HTL produces bio-char as a thermally stable by-product from carbon-rich biomass.

Properties of bio-char vary greatly depending upon biomass used and HTL conditions (Wei et al., 2015). Owing to its high porosity, high surface area and adsorptive capacity, such solid

residue serves as an excellent adsorbent for application in pollutant removal from wastewater streams (Gwenzi et al., 2017). Bio-char has also been extensively used for biogas up-gradation by adsorptive removal of H<sub>2</sub>S from biogas (Sun et al., 2016). Recently, it has been shown to improve biodegradation of polycyclic aromatic hydrocarbon (PAH) by making such highly water-insoluble compounds more bio-available to degrading microorganisms (Goswami et al., 2019). Moreover, high ash content and oxygen content of the bio-char is useful for soil remediation and as a soil amendment to improve soil fertility (Tang et al., 2013).

#### 4.6.5.2. Heterogenous catalysts

Other than acid/base homogenous catalysts, heterogeneous catalysts are reported for liquefaction of biomass. As compared with homogenous catalysts, heterogeneous catalysts are recyclable and can be used even under severe reaction conditions (Galadima et al., 2018). Biller et al. (2011) used certain heterogeneous catalysts like Pt/Al<sub>2</sub>O<sub>3</sub>, Ni/Al<sub>2</sub>O<sub>3</sub>, or Co/Mo/Al<sub>2</sub>O<sub>3</sub> for liquefaction of *Chlorella vulgaris* and *Nannochloropsis occulta*, for improving the bio-oil yield.

Similarly, different catalysts were investigated by Kumar et al., (2019) to HTL of macro-algal blooms; bio-oil yield values of 20.10% with Na<sub>2</sub>CO<sub>3</sub>, 18.74% with TiO<sub>2</sub>, 17.37% with CaO, and 14.6% without a catalyst were reported. In the present study, at optimum conditions of (temperature 215°C, time 125 min and biomass to water ratio 0.25 HTL using TiO<sub>2</sub> and ZnO yielded bio-oil 23.53% and 24.83%, respectively, which are nearly the same as obtained previously without using any catalyst. Fig. 4.43 shows FTIR spectra of the bio-oil obtained using these two catalysts. Interestingly, the values of solid residue obtained following HTL of the bacterial biomass using the two catalysts were higher than the value obtained without any catalyst. The solid residue obtained were further characterized by SEM-EDX and XRD (Fig. 4.44 and 4.45).

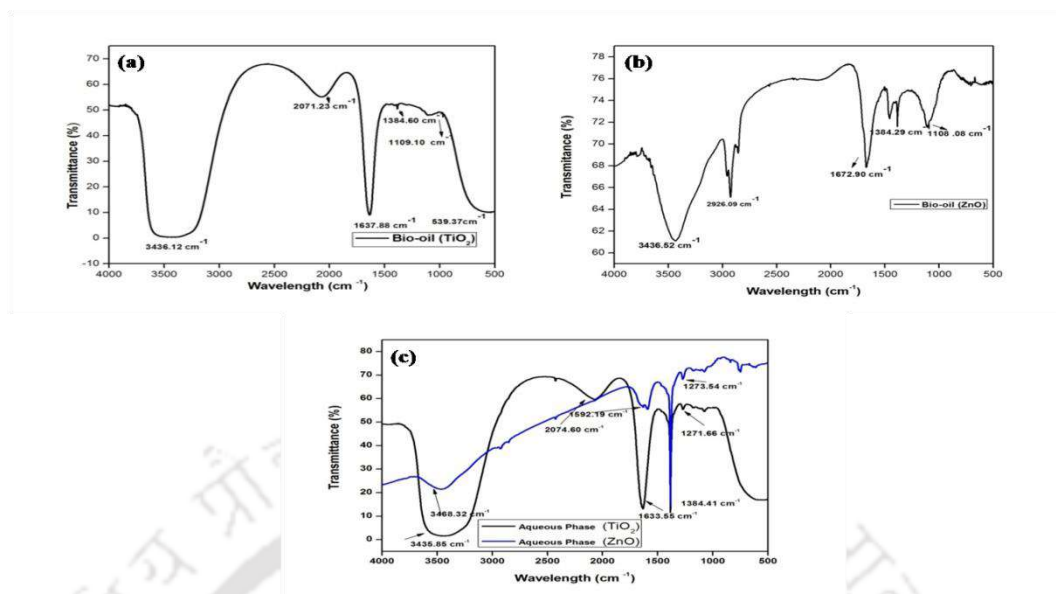


**Fig. 4.43** (a) FT-IR spectra of bio-oil produced by HTL of *R. opacus* biomass using  $\text{TiO}_2$  and  $\text{ZnO}$ , (b) FT-IR spectra of aqueous phase produced by HTL of *R. opacus* biomass using  $\text{TiO}_2$  and  $\text{ZnO}$  as catalysts (c) FT-IR spectra of aqueous phase produced by HTL of *R. opacus* biomass using  $\text{TiO}_2$  and  $\text{ZnO}$

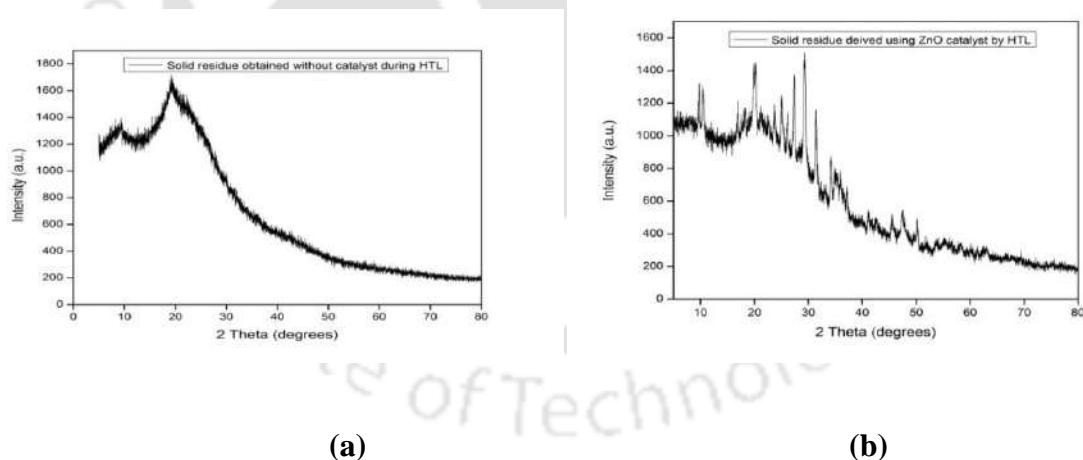


**Fig. 4.44:** XRD profile of solid residue obtained by HTL of *R. opacus* biomass using (a) no catalyst (b)  $\text{TiO}_2$  and (c)  $\text{ZnO}$

Fig. 4.44 a shows XRD profile of solid residue obtained following HTL of *R. opacus* biomass without any catalyst. The wide peaks at 20 2 theta degree are due to the presence of aromatic layers stacking. Similar sharp peaks are found in Fig. 4.44 b and c revealing presence of

aromatic layer stacking. However, both of the graphs (Fig. 4.44 b and c) depict the crystalline nature of the solid-residue obtained. The other peaks observed are attributed to the presence of  $\text{CaCO}_3$ ,  $\text{CaO}$ ,  $\text{MgO}$ ,  $\text{FeO}$ , etc.

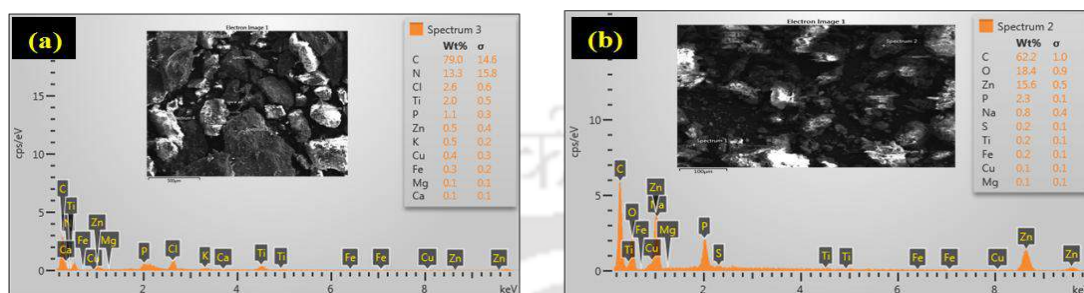



**Fig. 4.45** SEM-EDX of solid residue obtained by HTL of *R. opacus* biomass using (a)  $\text{TiO}_2$  and (b)  $\text{ZnO}$

In order to further improve the properties of bio-oil obtained by HTL of the bacterial biomass, cell disruption followed by cell debris removal and lipid extraction could be evaluated. Moreover, downstream processing of the lipid-rich biomass for enhancing the bio-oil yield needs to be scaled up beyond the commonly used mini reactor and operated under continuous mode. Besides, detailed techno-economic analysis of the HTL method followed for bio-oil production from such oleaginous microorganisms (*R. opacus*) can be carried out and compared with other thermo-chemical methods to establish its large-scale application potential. In addition to the use of different catalysts, other techniques such as solvent addition (Pidtasang et al., 2013), catalytic cracking (Yu et al., 2014), steam reforming (Xu et al., 2010), emulsification (Jiang et al., 2010) etc can be incorporated to enhance the yield and property of the bio-oil.

---

---



**CHAPTER-5**  
SUMMARY AND  
CONCLUSIONS

---

---

## 5. Summary and Conclusions

The present study on refinery wastewater treatment and lipid-rich biomass production using *R. opacus* was aimed at value-addition to the treatment process through resource recovery in the form of bio-oil and other by-products from the bacterial biomass. Following are the main findings in the study.

- Characterization of the petroleum refinery wastewater (PRWW) used in this study revealed the presence of complex long-chain hydrocarbons and phenolics with a total COD of 4575-5000 mg L<sup>-1</sup>. Heavy metals such as nickel (Ni), lead (Pb), copper (Cu), and zinc (Zn) etc were either absent or within the prescribed units.
- *R. opacus* biomass growth and COD removal from the PRWW were first carried under batch condition by supplementing the wastewater with Minimal Salt Media (MSM) in different proportions (1:1, 1:2, 1:3, 1:4 and 1:5). Wastewater supplemented with MSM in the ratio 4:1 showed the best results as it provided both the necessary carbon substrate and micronutrients necessary for its growth and metabolism. The influence of various cultivation parameters viz. C/N ratio, pH, nitrogen source and inoculum size on PRWW treatment and lipid-rich biomass production by *R. opacus* was successfully studied in a batch system. Conditions that favoured maximum COD removal and *R. opacus* biomass growth in the experiments were pH 7, C/N ratio 45:1, 10% inoculum size and ammonium chloride as the nitrogen source.
- In order to validate the effect of agitation, temperature, pH and nitrogen source on *R. opacus* biomass growth, COD removal and lipid production in this study, Plackett-Burman experimental design was employed. However, no significant effect due to variation in the levels of these parameters was observed, thus revealing that *R. opacus* is robust for wastewater treatment and other environmental applications.

- Kinetics of COD utilization, biomass growth and lipid production by *R. opacus* was studied in a batch system. At a high COD concentration, the rate and efficiency of COD utilization was low. Moreover, specific biomass growth rate and specific COD utilization rate decreased at a high initial COD concentration. However, the values of biokinetic parameters on lipid production and biomass growth by *R. opacus*, estimated using different models, revealed a very high tolerance of the bacterium toward toxic recalcitrant organics present in the wastewater. Results obtained from this kinetic study were further used to plan and conduct continuous bioreactor experiments.
- A laboratory-scale continuously stirred tank reactor (CSTR) was operated under different modes of operation for PRWW treatment and lipid-rich biomass production by *R. opacus*. Batch, fed-batch and sequential batch (SBR) modes of operation with the CSTR were first carried out. Among the different operation modes, the fed-batch operated CSTR showed the maximum biomass growth ( $2.3 \text{ g L}^{-1}$ ) and lipid accumulation ( $1.8 \text{ g L}^{-1}$ ) along with 95% COD removal within 54 h of treatment. The effect of different HRT (8, 16, and 24 h) was then examined under continuous operation mode.
- Under the continuous mode of operation, the biomass concentration increased from  $1.7$  to  $2.9 \text{ g L}^{-1}$  along with an increase in the HRT, and beyond which the biomass concentration slightly decreased to  $2.7 \text{ g L}^{-1}$ . More than 95% of COD was removed under the continuous mode at an optimum HRT of 16 h (dilution rate  $0.06 \text{ h}^{-1}$ ). A maximum accumulated lipid content in the biomass of  $1.1 \text{ g L}^{-1}$  (64%, w/w),  $2.35 \text{ g L}^{-1}$  (81%, w/w) and  $2.16 \text{ g L}^{-1}$  (80%, w/w) were obtained at 8, 16, and 24 h HRT, respectively, suggesting that 16 h is the optimum HRT for PRWW treatment, lipid production and biomass growth by *R. opacus*. Thus, CSTR operated under continuous mode with a low HRT proved to be efficient for the treatment of PRWW.

This study further demonstrated the robust nature of the bacterium for simultaneous wastewater treatment and lipid production in bioreactor operated under different modes.

- In order to further improve the performance of the CSTR under continuous operation mode, biomass from the effluent was recycled after separation of the biomass using an indigenously prepared tubular ceramic membrane. The fabricated tubular ceramic membrane was found to have a mean pore size of  $0.339\ \mu\text{m}$  with a flux value of  $2.39 \times 10^{-5}\ \text{m}^3/\text{m}^2\text{s}$  with wastewater under a pressure of 68 kPa. FESEM analysis further confirmed that the membrane surface was smooth and uniform. These properties of the tubular ceramic membrane were found to be highly favourable for the separation of lipid-rich biomass by microfiltration.
- In the CSTR operated under continuous with cell-recycle mode, maximum biomass concentration and lipid production of  $3.6\ \text{g L}^{-1}$  and  $3.2\ \text{g L}^{-1}$  (89%, w/w), respectively, were obtained along with the complete removal of COD from the wastewater. These results suggest that the integrated biodegradation-membrane approach is the best for achieving maximum lipid-rich biomass production and PRWW treatment.
- A batch operated bubble column reactor (BCR) was further evaluated for COD removal, biomass growth, and lipid accumulation by *R. opacus*, which showed better performance than the batch operated CSTR due to improved hydrodynamics and less shear stress on the bacterial strain. However, under continuous operated mode with the BCR, 24 h HRT was found to be optimum for efficient PRWW treatment by the microorganism.
- PRWW treatment was studied using a submerged tubular membrane bioreactor (STMBR) system with indigenous low-cost ceramic membrane, prepared using locally available clay materials. Compared with single-stage STMBR, the two-stage STMBR system proved more efficient in treating the wastewater due to reduced membrane fouling and sequential removal of COD and organics from the wastewater. The foulants from cake layer formed on the

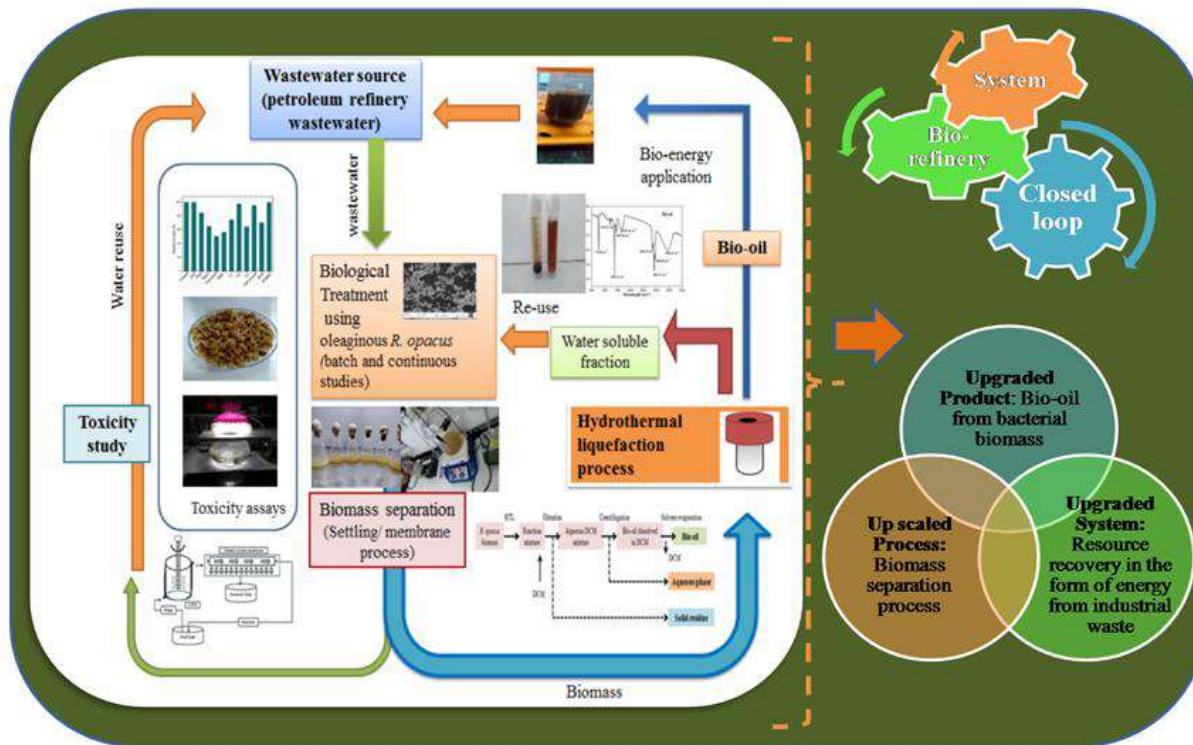
membrane were composed of carbon-rich compounds. Hence, in terms of COD removal and lipid-rich biomass production by *R. opacus*, the STMBR proved more efficient than the continuous BCR as well as the CSTR operated under continuous mode with cell-recycle.

- Toxicity assessment of the treated wastewater using different reactors used in this study established its reuse potential. Compared with MTT assay, seed germination and brine shrimp assays were found to be more suitable for assessing the toxicity of such wastewater. A high germination index (GI) of more than 73.63% of the treated wastewater from CSTR operated under continuous operation mode with cell recycle revealed that it is non-toxic and can be used for reuse purpose. However, a GI value of 82.08% was obtained with the treated wastewater from the two-stage STMBR. Moreover, toxicity assessment of the treated water from the two-stage STMBR using *Artemia salina* larvae (mature nauplii) showed only 39% of mortality as compared with 73% mortality with the raw PRWW. MTT is another widely used toxicity assay based on the activity of succinate dehydrogenase enzyme which however did not yield reliable results on assessing the wastewater toxicity.
- The lipid-rich *R. opacus* biomass obtained by treating PRWW was converted to bio-oil by hydrothermal liquefaction (HTL). Among the different parameters affecting HTL for bio-oil production, the effect due to temperature and retention time were found to be highly significant. The optimum conditions for maximum bio-oil yield (25.53%) were found to be 215 °C, 125 minutes and 0.25 biomass/water ratio; the bio-oil had a high heating value (HHV) of 20.73MJ/Kg, and it also consisted of a very low amount of water-soluble products. Fatty acid methyl esters (FAME) analysis results and other properties of the transesterified bio-oil matched well with the ASTM standard, thus indicating its potential for bio-fuel application.

- GC-MS and NMR analysis of the obtained bio-oil product revealed the presence of a variety of compounds, mainly aldehydes, ketones and fatty acid, whereas the water-soluble products were mainly alcohols and phenolic compounds. FTIR spectra of the bio-oil revealed the presence of C-H bonds due to alkanes as the predominant functional group present in the product.
- HTL not only produces bio-oil as the main product but also generates by-products *viz.* aqueous phase rich in minerals and solid residue. Analysis of the aqueous phase obtained as a by-product concluded its potential for reuse owing to the presence of nutritional compounds which indicated its potential use as a source of micronutrients in growth media for culturing microorganisms. In addition, solid residue obtained as a byproduct of HTL of the *R. opacus* biomass was similar to bio-char with high porosity and surface area.
- The *R. opacus* biomass obtained by treating PRWW was further investigated for bio-oil production by HTL using homogenous and heterogenous catalysts. Acid catalyst yielded bio-oil with desired flow properties, whereas with base catalyst ( $\text{Na}_2\text{CO}_3$ ), mostly carbohydrate content present in the biomass was converted into bio-oil as compared to proteins and lipids.

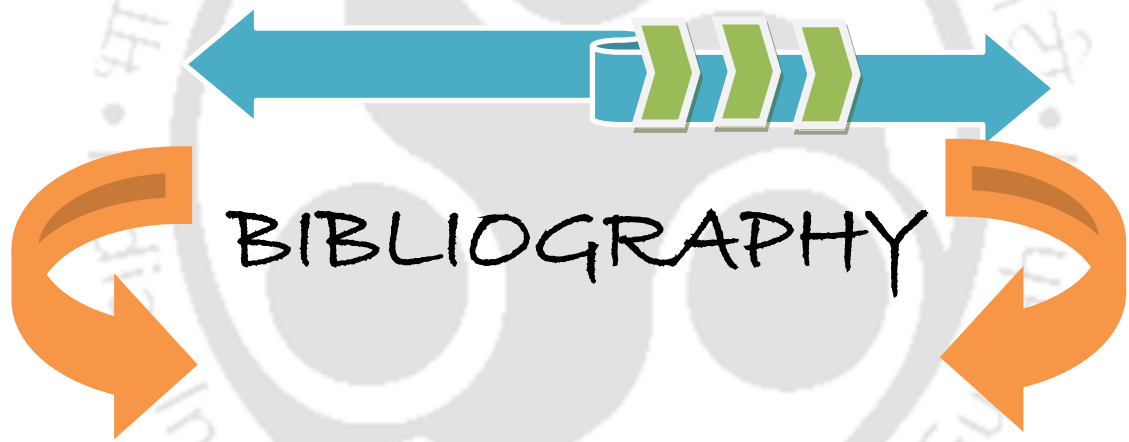
This study demonstrated a closed loop integrated approach for treating wastewater and value addition by using the oleaginous bacterium *R. opacus*. The potential of *R. opacus* to treat refinery wastewater and produce bio-oil is not only attractive from the standpoint of wastewater treatment and reuse of the treated water but also for recovery of potential energy in the form of obtained bio-oil and other by-products. This study further demonstrates a sustainable zero waste strategy for refinery wastewater treatment with provisions for resource recovery.

Summary



**Scope for Future Work**

- ❖ Genetic engineering of *R. opacus* to produce other value added products
- ❖ Detailed techno-economic feasibility and cost benefit analysis of bio-oil production from refinery wastewater
- ❖ Insight into the lipidome of the oleaginous bacteria *R. opacus*
- ❖ Use of solid residue (biochar) as an adsorbent for pollutant removal from wastewater
- ❖ Establishing the potential of *R. opacus* as an industrially relevant strain/renewable feedstock for production of chemicals and other value added products- a biorefinery approach
- ❖ Pilot-scale study of bio-oil production by *R. opacus* using refinery waste water as the substrate



- ❖ Daverey, A., Pakshirajan, K., Sumalatha, S. (2011). Sophorolipids production by *Candida bombicola* using dairy industry wastewater. *Clean Technologies and Environmental Policy*, 13 (3), 481-488.
- ❖ Mahvi, A. H. (2008). Sequencing batch reactor: a promising technology in wastewater treatment.
- ❖ Rajab, A. R., Salim, M. R., Sohaili, J., Anuar, A. N., Lakkaboyana, S. K. (2017). Performance of integrated anaerobic/aerobic sequencing batch reactor treating poultry slaughterhouse wastewater. *Chemical Engineering Journal*, 313, 967-974.
- ❖ Rezvanpour, A., Roostaazad, R., Hesampour, M., Nyström, M., Ghotbi, C. (2009). Effective factors in the treatment of kerosene–water emulsion by using UF membranes. *Journal of Hazardous Materials*, 161(2-3), 1216-1224.
- ❖ Sinharoy, A., Baskaran, D., Pakshirajan, K. (2019). Sustainable biohydrogen production by dark fermentation using carbon monoxide as the sole carbon and energy source. *International Journal of Hydrogen Energy*, 44 (26), 13114-13125.
- ❖ Warhurst, A. M., Fewson, C. A. (1994). Biotransformations catalyzed by the genus *Rhodococcus*. *Critical Reviews in Biotechnology*, 14(1), 29-73.
- ❖ Gollakota, A. R. K., Kishore, N., Gu, S. (2018). A review on hydrothermal liquefaction of biomass. *Renewable and Sustainable Energy Reviews*, 81, 1378-1392.
- ❖ Abou-Shanab, R. A., Hwang, J. H., Cho, Y., Min, B., Jeon, B. H. (2011). Characterization of microalgal species isolated from fresh water bodies as a potential source for biodiesel production. *Applied Energy*, 88 (10), 3300-3306.
- ❖ Akalın, M. K., Tekin, K., Karagöz, S. (2012). Hydrothermal liquefaction of cornelian cherry stones for bio-oil production. *Bioresource Technology*, 110, 682-687.
- ❖ Akhtar, J., Amin, N. A. S. (2011). A review on process conditions for optimum bio-oil yield in hydrothermal liquefaction of biomass. *Renewable and Sustainable Energy Reviews*, 15 (3), 1615-1624.
- ❖ Albuquerque, M. G. E., Martino, V., Pollet, E., Avérous, L., Reis, M. A. M. (2011). Mixed culture polyhydroxyalkanoate (PHA) production from volatile fatty acid (VFA)-rich streams: effect of substrate composition and feeding regime on PHA productivity, composition and properties. *Journal of Biotechnology*, 151(1), 66-76.
- ❖ Alvarez, H. M., Souto, M. F., Viale, A., Pucci, O. H. (2001). Biosynthesis of fatty acids and triacylglycerols by 2, 6, 10, 14-tetramethyl pentadecane-grown cells of *Nocardia globerulea* 432, *FEMS Microbiology Letters*, 200 (2), 195-200.
- ❖ Alvarez, H., Steinbüchel, A. (2002). Triacylglycerols in prokaryotic microorganisms. *Applied Microbiology and Biotechnology*, 60 (4), 367-376.
- ❖ Anastasakis, K., Ross, A. B. (2011). Hydrothermal liquefaction of the brown macro-alga *Laminaria saccharina*: effect of reaction conditions on product distribution and composition. *Bioresource Technology*, 102 (7), 4876-4883.
- ❖ Angerbauer, C., Siebenhofer, M., Mittelbach, M., Guebitz, G. M. (2008). Conversion of sewage sludge into lipids by *Lipomyces starkeyi* for biodiesel production. *Bioresource Technology*, 99 (8), 3051-3056.
- ❖ APHA, Standard Methods for the Examination of Water and Wastewater, twentieth ed., American Public Health Association, Washington, DC, 1998.
- ❖ Appels, L., Dewil, R. (2012). Biomass valorization to energy and value added chemicals: The future of chemical industry.
- ❖ Arabolaza, A., Dangelo, M., Comba, S., Gramajo, H. (2010). FasR, a novel class of transcriptional regulator, governs the activation of fatty acid biosynthesis genes in *Streptomyces coelicolor*, *Molecular Microbiology*, 78 (1), 47-63.
- ❖ Araujo, G. S., Matos, L. J., Goncalves, L. R., Fernandes, F. A., Farias, W. R. (2011). Bioprospecting for oil producing microalgal strains: evaluation of oil and biomass production for ten microalgal strains. *Bioresource Technology*, 102 (8), 5248-5250.

- ❖ Arun, J., Varshini, P., Prithvinath, P. K., Priyadarshini, V., Gopinath, K. P. (2018). Enrichment of bio-oil after hydrothermal liquefaction (HTL) of microalgae *C. vulgaris* grown in wastewater: Bio-char and post HTL wastewater utilization studies. *Bioresource Technology*, 261, 182-187.
- ❖ Caprariis, B., Filippis, P., Petruzzo, A., Scarsella, M. (2017). Hydrothermal liquefaction of biomass: Influence of temperature and biomass composition on the bio-oil production, *Fuel*, 208, 618–625.
- ❖ Gargouri, B., Karray, F., Mhiri, N., Aloui, F., Sayadi, S. (2011). Application of a continuously stirred tank bioreactor (CSTR) for bioremediation of hydrocarbon-rich industrial wastewater effluents. *Journal of Hazardous Materials*, 189 (1-2), 427-434.
- ❖ Nandi, B. K., Moparthi, A., Uppaluri, R., & Purkait, M. K. (2010). Treatment of oily wastewater using low cost ceramic membrane: Comparative assessment of pore blocking and artificial neural network models. *Chemical Engineering Research and Design*, 88(7), 881-892.
- ❖ Metzler-Zebeli, B. U., Khol-Parisini, A., Gruber, L., Zebeli, Q. (2015). Microbial populations and fermentation profiles in rumen liquid and solids of Holstein cows respond differently to dietary barley processing. *Journal of Applied Microbiology*, 119(6), 1502-1514.
- ❖ Bach, Q. V., Sillero, M. V., Tran, K. Q., Skjermo, J. (2014). Fast hydrothermal liquefaction of a Norwegian macro-alga: screening tests. *Algal Research*, 6, 271-276.
- ❖ Bacon, J., Dover, L. G., Hatch, K. A., Zhang, Y., Gomes, J. M., Kendall, S., Marsh, P. D. (2007). Lipid composition and transcriptional response of *Mycobacterium tuberculosis* grown under iron-limitation in continuous culture: identification of a novel wax ester. *Microbiology*, 153, 1435.
- ❖ Baldwin, R. M. (2019). *Upgrading Bio-oil: Catalysis and Refinery*. In *Biorefinery*, Springer, Cham. 111-151.
- ❖ Barla, F. G., Kumar, S. (2019). Tobacco biomass as a source of advanced biofuels. *Biofuels*, 10 (3), 335-346.
- ❖ Barreiro, D. L., Bauer, M., Hornung, U., Posten, C., Kruse, A., Prins, W. (2015). Cultivation of microalgae with recovered nutrients after hydrothermal liquefaction. *Algal research*, 9, 99-106.
- ❖ Barreiro, D. L., Zamalloa, C., Boon, N., Vyverman, W., Ronsse, F., Brilman, W., Prins, W. (2013). Influence of strain-specific parameters on hydrothermal liquefaction of microalgae. *Bioresource Technology*, 146, 463-471.
- ❖ Biller, P., Ross, A. B. (2011). Potential yields and properties of oil from the hydrothermal liquefaction of microalgae with different biochemical content. *Bioresource Technology*, 102, 215-225.
- ❖ Biller, P., Ross, A. B., Skill, S. C., Lea-Langton, A., Balasundaram, B., Hall, C., Llewellyn, C. A. (2012). Nutrient recycling of aqueous phase for microalgae cultivation from the hydrothermal liquefaction process. *Algal Research*, 1 (1), 70-76.
- ❖ Biller, P., Ross, A.B. (2012). Hydrothermal processing of algal biomass for the production of biofuels and chemicals. *Biofuels*, 3 (5), 603-623.
- ❖ Boëns, B., Pilon, G., Bourdeau, N., Adjallé, K., Barnabé, S. (2016). Hydrothermal liquefaction of a wastewater native *Chlorella sp.* bacteria consortium: biocrude production and characterization. *Biofuels*, 7 (6), 611-619.
- ❖ Boocock, D.G.B., Sherman, K.M. (2009). Further aspects of powdered poplar wood liquefaction by aqueous pyrolysis. *Canadian Journal of Chemical Engineering*, 63 (4), 627-33.
- ❖ Bridgwater, A. V. (2012). Review of fast pyrolysis of biomass and product upgrading. *Biomass and Bioenergy*, 38, 68-94.
- ❖ Brooks, K. K., Liang, B., Watts, J. L. (2009). The influence of bacterial diet on fat storage in *C. elegans*. *PloS one*, 4 (10).
- ❖ Leonard, C., Ferrasse, J. H., Boutin, O., Lefevre, S., Viand, A. (2015). Bubble column reactors for high pressures and high temperatures operation. *Chemical Engineering Research and Design*, 100, 391-421.
- ❖ Liu, C., Nanaboina, V., Korshin, G. V., Jiang, W. (2012). Spectroscopic study of degradation products of ciprofloxacin, norfloxacin and lomefloxacin formed in ozonated wastewater. *Water Research*, 46(16), 5235-5246.
- ❖ Stacy, C. J., Melick, C. A., Cairncross, R. A. (2014). Esterification of free fatty acids to fatty acid alkyl esters in a bubble column reactor for use as biodiesel. *Fuel processing technology*, 124, 70-77.

- ❖ Campenni, L., Nobre, B. P., Santos, C. A., Oliveira, A. C., Aires-Barros, M. R., Palavra, A. M. F., Gouveia, L. (2013). Carotenoid and lipid production by the autotrophic microalga *Chlorella protothecoides* under nutritional, salinity, and luminosity stress conditions. *Applied Microbiology and Biotechnology*, 97 (3), 1383-1393.
- ❖ Cao, L., Luo, G., Zhang, S., Chen, J. (2016). Bio-oil production from eight selected green landscaping wastes through hydrothermal liquefaction. *RSC Advances*, 6 (18), 15260-15270.
- ❖ Certik, M., Balteszov, L., Sajbidor, J. (1997). Lipid formation and  $\gamma$ -linolenic acid production by *Mucorales* fungi grown on sunflower oil. *Letters in Applied Microbiology*, 25 (2), 101-105.
- ❖ Chatzifragkou, A., Makri, A., Belka, A., Bellou, S., Mavrou, M., Mastoridou, M., Papanikolaou, S. (2011). Biotechnological conversions of biodiesel derived waste glycerol by yeast and fungal species. *Energy*, 36 (2), 1097-1108.
- ❖ Chen, B. Y., Zhao, B. C., Li, M. F., Liu, Q. Y., Sun, R. C. (2017). Fractionation of rapeseed straw by hydrothermal/dilute acid pretreatment combined with alkali post-treatment for improving its enzymatic hydrolysis. *Bioresource Technology*, 225, 127-133.
- ❖ Chen, G. Q., Jiang, Y., Chen, F. (2008). Variation of lipid class composition in *Nitzschia laevis* as a response to growth temperature change. *Food Chemistry*, 109 (1), 88-94.
- ❖ Chen, L., Liu, T., Zhang, W., Chen, X., Wang, J. (2012). Biodiesel production from algae oil high in free fatty acids by two-step catalytic conversion. *Bioresource Technology*, 111, 208-214.
- ❖ Chen, W. T., Zhang, Y., Zhang, J., Yu, G., Schideman, L. C., Zhang, P., Minarick, M., (2014). Hydrothermal liquefaction of mixed-culture algal biomass from wastewater treatment system into bio-crude oil. *Bioresource Technology*, 152, 130-139.
- ❖ Cheng, S., Dcruz, I., Wang, M., Leitch, M., Xu, C. (2010). Highly efficient liquefaction of woody biomass in hot-compressed alcohol-water co-solvents. *Energy and Fuels*, 24 (9), 4659-4667.
- ❖ Chew, K. W., Yap, J. Y., Show, P. L., Suan, N. H., Juan, J. C., Ling, T. C., Chang, J. S. (2017). Microalgae biorefinery: high value products perspectives. *Bioresource Technology*, 229, 53-62.
- ❖ Chi, Z., Zheng, Y., Ma, J., Chen, S. (2011). Oleaginous yeast *Cryptococcus curvatus* culture with dark fermentation hydrogen production effluent as feedstock for microbial lipid production. *International Journal of Hydrogen Energy*, 36 (16), 9542-9550.
- ❖ Chiu, S. Y., Kao, C. Y., Tsai, M. T., Ong, S. C., Chen, C. H., Lin, C. S. (2009). Lipid accumulation and CO<sub>2</sub> utilization of *Nannochloropsis oculata* in response to CO<sub>2</sub> aeration. *Bioresource Technology*, 100 (2), 833-838.
- ❖ Chopra, J., Mahesh, D., Yerrayya, A., Vinu, R., Kumar, R., Sen, R., (2019). Performance enhancement of hydrothermal liquefaction for strategic and sustainable valorization of de-oiled yeast biomass into green bio-crude. *Journal of Cleaner Production*, 227, 292-301.
- ❖ Coelho, A., Castro, A. V., Dezotti, M., Sant'Anna, G. L., (2006). Treatment of petroleum refinery sourwater by advanced oxidation processes. *Journal of Hazardous Materials*. 137, 178-184.
- ❖ Conti, J., Holtberg, P., Diefenderfer, J., LaRose, A., Turnure, J. T., Westfall, L. (2016). *International Energy Outlook 2016 with Projections to 2040*.
- ❖ Cortes, M.A.L., de Carvalho, C.C. (2015). Effect of carbon sources on lipid accumulation in *Rhodococcus* cells. *Biochemical Engineering Journal*, 94, 100-105.
- ❖ Couto, R. M., Simoes, P. C., Reis, A., Da Silva, T. L., Martins, V. H., Sanchez-Vicente, Y. (2010). Supercritical fluid extraction of lipids from the heterotrophic microalga *Cryptocodium cohni*. *Engineering in Life Sciences*, 10 (2), 158-164.
- ❖ Baskaran, D., Paul, T., Kannan, P., Krithivasan, M., Devanesan, M. G., Rajamanickam, R. (2020). Batch degradation of trichloroethylene using oleaginous *Rhodococcus opacus* in a two-phase partitioning bioreactor and kinetic study. *Bioresource Technology Reports*, 11, 100437.
- ❖ Barreiro, D. L., Gómez, B. R., Hornung, U., Kruse, A., Prins, W. (2015). Hydrothermal liquefaction of microalgae in a continuous stirred-tank reactor. *Energy & Fuels*, 29 (10), 6422-6432.
- ❖ Barreiro, D. L., Prins, W., Ronsse, F., Brilman, W. (2013). Hydrothermal liquefaction (HTL) of microalgae for biofuel production: state of the art review and future prospects. *Biomass and Bioenergy*, 53, 113-127.

- ❖ Vardon, D. R., Sharma, B. K., Blazina, G. V., Rajagopalan, K., Strathmann, T. J. (2012). Thermochemical conversion of raw and defatted algal biomass via hydrothermal liquefaction and slow pyrolysis. *Bioresource Technology*, 109, 178-187.
- ❖ Qi, X., Watanabe, M., Aida, T. M., & Smith, R. L. (2012). Synergistic conversion of glucose into 5-hydroxymethylfurfural in ionic liquid–water mixtures. *Bioresource Technology*, 109, 224-228.
- ❖ Dalrymple, O. K., Halfhide, T., Udom, I., Gilles, B., Wolan, J., Zhang, Q., Ergas, S. (2013). Wastewater use in algae production for generation of renewable resources: a review and preliminary results. *Aquatic Biosystems*, 9 (1) 2.
- ❖ Damiani, M. C., Popovich, C. A., Constenla, D., Leonardi, P. I. (2010). Lipid analysis in *Haematococcus pluvialis* to assess its potential use as a biodiesel feedstock. *Bioresource Technology*, 101 (11), 3801-3807.
- ❖ Bhowmick, G.D., Sarmah, A. K., Sen, R. (2018). Lignocellulosic biorefinery as a model for sustainable development of biofuels and value added products. *Bioresource Technology*, 247, 1144-1154.
- ❖ de Caprariis, B., De Filippis, P., Petrullo, A., Scarsella, M. (2017). Hydrothermal liquefaction of biomass: influence of temperature and biomass composition on the bio-oil production. *Fuel*, 208, 618-625.
- ❖ Demirbaş, A. (2006). Oily products from mosses and algae via pyrolysis. *Energy Sources*, 28, 933-940.
- ❖ Dong, T., Gao, D., Miao, C., Yu, X., Degan, C., Garcia-Pérez, M., Chen, S. (2015). Two-step microalgal biodiesel production using acidic catalyst generated from pyrolysis-derived bio-char. *Energy Conversion and Management*, 105, 1389-1396.
- ❖ Donot, F., Fontana, A., Baccou, J. C., Strub, C., Schorr-Galindo, S. (2014). Single cell oils (SCOs) from oleaginous yeasts and moulds: production and genetics. *Biomass and Bioenergy*, 68, 135-150.
- ❖ Du, Z., Mohr, M., Ma, X., Cheng, Y., Lin, X., Liu, Y., Ruan, R. (2012). Hydrothermal pretreatment of microalgae for production of pyrolytic bio-oil with a low nitrogen content. *Bioresource Technology*, 120, 13-18.
- ❖ Duan, P., Savage, P. E. (2011). Catalytic hydrotreatment of crude algal bio-oil in supercritical water. *Applied Catalysis B: Environmental*, 104 (1-2), 136-143.
- ❖ Duan, P., Xu, Y., Bai, X. (2013). Upgrading of crude duckweed bio-oil in subcritical water. *Energy & Fuels*, 27 (8), 4729-4738.
- ❖ Duong, V. T., Li, Y., Nowak, E., Schenk, P. M. (2012). Microalgae isolation and selection for prospective biodiesel production. *Energies*, 5 (6), 1835-1849.
- ❖ Dyal, S. D., Narine, S. S. (2005). Implications for the use of *Mortierella* fungi in the industrial production of essential fatty acids. *Food Research International*, 38 (4), 445-467.
- ❖ Eboibi, B. E. O., Lewis, D. M., Ashman, P. J., Chinnasamy, S. (2014). Hydrothermal liquefaction of microalgae for biocrude production: improving the biocrude properties with vacuum distillation. *Bioresource Technology*, 174, 212-221.
- ❖ Ekpo, U., Ross, A. B., Camargo-Valero, M. A., Fletcher, L. A. (2016). Influence of pH on hydrothermal treatment of swine manure: impact on extraction of nitrogen and phosphorus in process water. *Bioresource Technology*, 214, 637-644.
- ❖ Elliott, D. C., Biller, P., Ross, A. B., Schmidt, A. J., Jones, S. B. (2015). Hydrothermal liquefaction of biomass: developments from batch to continuous process. *Bioresource Technology*, 178, 147-156.
- ❖ Evans, C. T., Ratledge, C. (1983). A comparison of the oleaginous yeast, *Candida curvata*, grown on different carbon sources in continuous and batch culture. *Lipids*, 18 (9), 623-629.
- ❖ Yaopo, F., Jusi, W., Zhaochun, J. (1997). Treatment of petrochemical waste water with a membrane bioreactor, *Acta Scientiae Circumstantiae*. 1, 68-74.
- ❖ Fakas, S., Galiotou-Panayotou, M., Papanikolaou, S., Komaitis, M., Aggelis, G. (2007). Compositional shifts in lipid fractions during lipid turnover in *Cunninghamella echinulata*. *Enzyme and Microbial Technology*, 40 (5), 1321-1327.
- ❖ Fakas, S., Papanikolaou, S., Batsos, A., Galiotou-Panayotou, M., Mallouchos, A., Aggelis, G. (2009). Evaluating renewable carbon sources as substrates for single cell oil production by *Cunninghamella echinulata* and *Mortierella isabellina*. *Biomass and Bioenergy*, 33 (4), 573-580.

- ❖ Feng, G. D., Zhang, F., Cheng, L. H., Xu, X. H., Zhang, L., Chen, H. L. (2013). Evaluation of FT-IR and Nile Red methods for microalgal lipid characterization and biomass composition determination. *Bioresource Technology*, 128, 107-112.
- ❖ Feng, Y., Li, C., Zhang, D. (2011). Lipid production of *Chlorella vulgaris* cultured in artificial wastewater medium. *Bioresource Technology*, 102, 101-105.
- ❖ Fini, E. H., Al-Qadi, I. L., You, Z., Zada, B., Mills-Beale, J. (2012). Partial replacement of asphalt binder with bio-binder: characterisation and modification. *International Journal of Pavement Engineering*, 13 (6), 515-522.
- ❖ Fonts, I., Gea, G., Azuara, M., Abrego, J., Arauzo, J. (2012). Sewage sludge pyrolysis for liquid production: a review. *Renewable and Sustainable Energy Reviews*, 16 (5), 2781-2805.
- ❖ Fulekar, M. H., Pathak, B. (2019). *Bioremediation Technology: Hazardous Waste Management*. CRC Press.
- ❖ Gao, C., Zhai, Y., Ding, Y., Wu, Q. (2010). Application of sweet sorghum for biodiesel production by heterotrophic microalga *Chlorella protothecoides*. *Applied Energy*, 87 (3), 756-761.
- ❖ Gao, D., Zeng, J., Zheng, Y., Yu, X., Chen, S. (2013). Microbial lipid production from xylose by *Mortierella isabellina*. *Bioresource Technology*, 133, 315-321.
- ❖ Garcia-Nunez, J. A., Ramirez-Contreras, N. E., Rodriguez, D. T., Silva-Lora, E., Frear, C. S., Stockle, C., Garcia-Perez, M. (2016). Evolution of palm oil mills into bio-refineries: literature review on current and potential uses of residual biomass and effluents. *Resources, Conservation and Recycling*, 110, 99-114.
- ❖ Gasparovic, L., Korenova, Z., Jelemensky, L. (2010). Kinetic study of wood chips decomposition by TGA. *Chemical Papers*. 64, 174-181.
- ❖ Gielen, D., Boshell, F., Saygin, D., Bazilian, M. D., Wagner, N., Gorini, R. (2019). The role of renewable energy in the global energy transformation. *Energy Strategy Reviews*, 24, 38-50.
- ❖ Gollakota, A. R. K., Kishore, N., Gu, S. (2018). A review on hydrothermal liquefaction of biomass. *Renewable and Sustainable Energy Reviews*, 81, 1378-1392.
- ❖ Gonzalez, R., Treasure, T., Phillips, R., Jameel, H., Saloni, D., Abt, R., Wright, J. (2011). Converting Eucalyptus biomass into ethanol: Financial and sensitivity analysis in a co-current dilute acid process. *Biomass and Bioenergy*, 35 (2), 767-772.
- ❖ Gordillo, F. J., Goutx, M., Figueroa, F. L., Niell, F. X. (1998). Effects of light intensity, CO<sub>2</sub> and nitrogen supply on lipid class composition of *Dunaliella viridis*. *Journal of Applied Phycology*, 10 (2), 135-144.
- ❖ Goshadrou, A., Karimi, K., Taherzadeh, M. J. (2011). Bioethanol production from sweet sorghum bagasse by *Mucor hiemalis*. *Industrial Crops and Products*, 34 (1), 1219-1225.
- ❖ Goswami, L., Kumar, R. V., Manikandan, N. A., Pakshirajan, K., Pugazhenth, G. (2017a). Simultaneous polycyclic aromatic hydrocarbon degradation and lipid accumulation by *Rhodococcus opacus* for potential biodiesel production. *Journal of Water Process Engineering*, 17, 1-10.
- ❖ Goswami, L., Manikandan, N. A., Dolman, B., Pakshirajan, K., Pugazhenth, G. (2018). Biological treatment of wastewater containing a mixture of polycyclic aromatic hydrocarbons using the oleaginous bacterium *Rhodococcus opacus*. *Journal of Cleaner Production*, 196, 1282-1291.
- ❖ Goswami, L., Namboodiri, M. T., Kumar, R. V., Pakshirajan, K., Pugazhenth, G. (2017b). Biodiesel production potential of oleaginous *Rhodococcus opacus* grown on biomass gasification wastewater. *Renewable Energy*, 105, 400-406.
- ❖ Gouda, M. K., Omar, S. H., Aouad, L. M. (2008). Single cell oil production by *Gordonia* sp. DG using agro-industrial wastes. *World Journal of Microbiology and Biotechnology*, 24 (9), 1703.
- ❖ Goudriaan, F., Van de Beld, B., Boerefijn, F. R., Bos, G. M., Naber, J. E., Van der Wal, S., Zeevalkink, J. A. (2000). Thermal efficiency of the HTU process for biomass liquefaction, *Progress in thermochemical biomass conversion*. 2.
- ❖ Gouveia, L., Neves, C., Sebastião, D., Nobre, B. P., Matos, C. T. (2014). Effect of light on the production of bioelectricity and added-value microalgae biomass in a photosynthetic alga microbial fuel cell. *Bioresource Technology*, 154, 171-177.

- ❖ Gouveia, L., Oliveira, A. C. (2009). Microalgae as a raw material for biofuels production. *Journal of Industrial Microbiology and Biotechnology*, 36 (2), 269-274.
- ❖ Goyal, H. B., Seal, D., Saxena, R. C. (2008). Bio-fuels from thermochemical conversion of renewable resources: a review. *Renewable and Sustainable Energy Reviews*, 12 (2), 504-517.
- ❖ Guo, Y., Yeh, T., Song, W., Xu, D., Wang, S. (2015). A review of bio-oil production from hydrothermal liquefaction of algae. *Renewable and Sustainable Energy Reviews*, 48, 776-790.
- ❖ Guschina, I. A., Harwood, J. L. (2006). Lipids and lipid metabolism in eukaryotic algae. *Progress in Lipid Research*, 45 (2), 160-186.
- ❖ Janßen, H. J., Ibrahim, M. H., Bröker, D., Steinbüchel, A. (2013). Optimization of macroelement concentrations, pH and osmolarity for triacylglycerol accumulation in *Rhodococcus opacus* strain PD630. *AMB express*, 3(1), 1-8.
- ❖ Liu, H., Ma, M., & Xie, X. A. (2017). New materials from solid residues for investigation the mechanism of biomass hydrothermal liquefaction. *Industrial Crops and Products*, 108, 63-71.
- ❖ Alvarez, H. M., Kalscheuer, R., Steinbüchel, A. (2000). Accumulation and mobilization of storage lipids by *Rhodococcus opacus* PD630 and *Rhodococcus ruber* NCIMB 40126. *Applied Microbiology and Biotechnology*, 54(2), 218-223.
- ❖ Xu, H., Miao, X., Wu, Q. (2006). High quality biodiesel production from a microalga *Chlorella protothecoides* by heterotrophic growth in fermenters. *Journal of Biotechnology*, 126(4), 499-507.
- ❖ Hadhoun, L., Balistrout, M., Burnens, G., Loubar, K., Tazerout, M. (2016). Hydrothermal liquefaction of oil mill wastewater for bio-oil production in subcritical conditions. *Bioresource Technology*, 218, 9-17.
- ❖ Hao, H., Liu, Z., Zhao, F., Ren, J., Chang, S., Rong, K., Du, J., (2018). Biofuel for vehicle use in China: Current status, future potential and policy implications. *Renewable and Sustainable Energy Reviews*, 82, 645-653.
- ❖ Hao, X. D., Wang, Q. L., Zhu, J. Y., & Van Loosdrecht, M. C. (2010). Microbiological endogenous processes in biological wastewater treatment systems. *Critical Reviews in Environmental Science and Technology*, 40(3), 239-265
- ❖ Hassan, M., Blanc, P. J., Granger, L. M., Pareilleux, A., Goma, G. (1996). Influence of nitrogen and iron limitations on lipid production by *Cryptococcus curvatus* grown in batch and fed-batch culture. *Process Biochemistry*, 31 (4), 355-361.
- ❖ He, B. J., Zhang, Y., Funk, T. L., Riskowski, G. L., Yin, Y. (2000). Thermochemical conversion of swine manure: an alternative process for waste treatment and renewable energy production. *Transactions of the ASAE*, 43 (6), 1827.
- ❖ He, W., Li, G., Kong, L., Wang, H., Huang, J., Xu, J. (2008). Application of hydrothermal reaction in resource recovery of organic wastes. *Resources, Conservation and Recycling*, 52 (5), 691-699.
- ❖ Hena, S., Fatimah, S., Tabassum, S. (2015). Cultivation of algae consortium in a dairy farm wastewater for biodiesel production. *Water Resources and Industry*, 10, 1-14.
- ❖ Heng, K. S., Hatti-Kaul, R., Adam, F., Fukui, T., Sudesh, K. (2017). Conversion of rice husks to polyhydroxyalkanoates (PHA) via a three-step process: optimized alkaline pretreatment, enzymatic hydrolysis, and biosynthesis by *Burkholderia cepacia* USM (JCM 15050). *Journal of Chemical Technology and Biotechnology*, 92 (1), 100-108.
- ❖ Hesami, S. M., Zilouei, H., Karimi, K., Asadinezhad, A. (2015). Enhanced biogas production from sunflower stalks using hydrothermal and organosolv pretreatment. *Industrial Crops and Products*, 76, 449-455.
- ❖ Hsieh, C. H., Wu, W. T. (2009). Cultivation of microalgae for oil production with a cultivation strategy of urea limitation. *Bioresource Technology*, 100 (17), 3921-3926.
- ❖ Hu, G., Cateto, C., Pu, Y., Samuel, R., Ragauskas, A. J. (2011). Structural characterization of switchgrass lignin after ethanol organosolv pretreatment. *Energy and Fuels*, 26 (1), 740-745.
- ❖ Hu, G., Li, J., Zeng, G. (2013). Recent development in the treatment of oily sludge from petroleum industry: a review. *Journal of Hazardous Materials*, 261, 470-490.

- ❖ Hu, Y., Gong, M., Feng, S., Xu, C. C., Bassi, A. (2019). A review of recent developments of pre-treatment technologies and hydrothermal liquefaction of microalgae for bio-crude oil production. *Renewable and Sustainable Energy Reviews*, 101, 476-492.
- ❖ Hu, Y., Qi, L., Feng, S., Bassi, A., Xu, C. C. (2019). Comparative studies on liquefaction of low-lipid microalgae into bio-crude oil using varying reaction media. *Fuel*, 238, 240-247.
- ❖ Huang, C., Chen, X. F., Xiong, L., Yang, X. Y., Ma, L. L., Chen, Y. (2013). Microbial oil production from corn cob acid hydrolysate by oleaginous yeast *Trichosporon coremiiforme*. *Biomass and Bioenergy*, 49, 273-278.
- ❖ Huerlimann, R., De Nys, R., Heimann, K. (2010). Growth, lipid content, productivity, and fatty acid composition of tropical microalgae for scale-up production. *Biotechnology and Bioengineering*, 107 (2), 245-257.
- ❖ Muniraj, I. K., Xiao, L., Hu, Z., Zhan, X., & Shi, J. (2013). Microbial lipid production from potato processing wastewater using oleaginous filamentous fungi *Aspergillus oryzae*. *Water Research*, 47(10), 3477-3483.
- ❖ Isa, Y. M., Ganda, E. T. (2018). Bio-oil as a potential source of petroleum range fuels. *Renewable and Sustainable Energy Reviews*, 81, 69-75.
- ❖ Isa, Y. M., Ganda, E. T., 2018. Bio-oil as a potential source of petroleum range fuels. *Renewable and Sustainable Energy Reviews*. 81, 69-75.
- ❖ Fargione, J., Hill, J., Tilman, D., Polasky, S., Hawthorne, P. (2008). Land clearing and the biofuel carbon debt. *Science*, 319 (5867), 1235-1238.
- ❖ Saien, J., Shahrezaei, F. (2012). Organic pollutants removal from petroleum refinery wastewater with nanotitania photocatalyst and UV light emission. *International Journal of Photoenergy*.
- ❖ Tang, J., Zhu, W., Kookana, R., Katayama, A. (2013). Characteristics of biochar and its application in remediation of contaminated soil. *Journal of Bioscience and Bioengineering*, 116 (6), 653-659.
- ❖ Wiszniowski, J., Ziemińska, A., Ciesielski, S. (2011). Removal of petroleum pollutants and monitoring of bacterial community structure in a membrane bioreactor. *Chemosphere*, 83 (1), 49-56.
- ❖ Zhong, J., Sun, X., Wang, C. (2003). Treatment of oily wastewater produced from refinery processes using flocculation and ceramic membrane filtration. *Separation and Purification Technology*, 32(1-3), 93-98.
- ❖ Kim, J. H., Jung, J. M., Cho, S. H., Tsang, Y. F., Wang, C. H., Lee, J., Kwon, E. E. (2019). Upgrading bio-heavy oil via esterification of fatty acids and glycerol. *Journal of Cleaner Production*, 217, 633-638.
- ❖ Jacobson, K., Maheria, K. C., Dalai, A. K. (2013). Bio-oil valorization: a review. *Renewable and Sustainable Energy Reviews*, 23, 91-106.
- ❖ Jahirul, M.I., Rasul, M.G., Chowdhury, A.A., Ashwath, N. (2012). Biofuels production through biomass pyrolysis—a technological review. *Energies*, 5 (12), 4952-5001.
- ❖ Jazrawi, C., Biller, P., He, Y., Montoya, A., Ross, A. B., Maschmeyer, T., Haynes, B. S. (2015). Two-stage hydrothermal liquefaction of a high-protein microalga. *Algal Research*, 8, 15-22.
- ❖ Jazrawi, C., Biller, P., Ross, A. B., Montoya, A., Maschmeyer, T., Haynes, B. S. (2013). Pilot plant testing of continuous hydrothermal liquefaction of microalgae. *Algal Research*, 2 (3), 268-277.
- ❖ Jena, U., Das, K. C., Kastner, J. R. (2011). Effect of operating conditions of thermochemical liquefaction on biocrude production from *Spirulina platensis*. *Bioresource Technology*, 102 (10), 6221-6229.
- ❖ Jinkerson, R. E., Subramanian, V., Posewitz, M. C. (2011). Improving biofuel production in phototrophic microorganisms with systems biology. *Biofuels*, 2 (2), 125-144.
- ❖ Kalscheuer, R., Luftmann, H., Steinbuchel, A. (2004). Synthesis of novel lipids in *Saccharomyces cerevisiae* by heterologous expression of an unspecific bacterial acyltransferase. *Applied Environmental Microbiology*, 70 (12), 7119-7125.
- ❖ Kalscheuer, R., Steinbuchel, A. (2003). A novel bifunctional wax ester synthase/acyl-CoA: diacylglycerol acyltransferase mediates wax ester and triacylglycerol biosynthesis in *Acinetobacter calcoaceticus* ADP1. *Journal of Biological Chemistry*, 278 (10), 8075-8082.
- ❖ Kamat, S., Khot, M., Zinjarde, S., RaviKumar, A., Gade, W. N. (2013). Coupled production of single cell oil as biodiesel feedstock, xylitol and xylanase from sugarcane bagasse in a biorefinery concept using fungi from the tropical mangrove wetlands. *Bioresource Technology*, 135, 246-253.

- ❖ Kang, S., Yu, J. (2015). Hydrophobic organic compounds from hydrothermal liquefaction of bacterial biomass. *Biomass and Bioenergy*, 74, 92-95.
- ❖ Katsimpouras, C., Christakopoulos, P., Topakas, E. (2016). Acetic acid-catalyzed hydrothermal pretreatment of corn stover for the production of bioethanol at high-solids content. *Bioprocess and Biosystems Engineering*, 39 (9), 1415-1423.
- ❖ Kim, G. Y., Yun, Y. M., Shin, H. S., Kim, H. S., Han, J. I. (2015). *Scenedesmus*-based treatment of nitrogen and phosphorus from effluent of anaerobic digester and bio-oil production. *Bioresource Technology*, 196, 235-240.
- ❖ Kim, J. H., Jung, J. M., Cho, S. H., Tsang, Y. F., Wang, C. H., Lee, J., Kwon, E. E. (2019). Upgrading bio-heavy oil via esterification of fatty acids and glycerol. *Journal of Cleaner Production*. 217, 633-638.
- ❖ Kucerova, V., Vybohova, E., Canova, I., Durkovic, J. (2016). The effects of both insoluble lignin and the macromolecular traits of cellulose on the content of saccharides within solids during hydrothermal pretreatment of hybrid poplar wood. *Industrial Crops and Products*, 91, 22-31.
- ❖ Kumar, S., Gupta, N., Pakshirajan, K. (2015). Simultaneous lipid production and dairy wastewater treatment using *Rhodococcus opacus* in a batch bioreactor for potential biodiesel application. *Journal of Environmental Chemical Engineering*, 3, 1630-1636.
- ❖ Alba, L. G., Torri, C., Fabbri, D., Kersten, S. R., & Brilman, D. W. W. (2013). Microalgae growth on the aqueous phase from hydrothermal liquefaction of the same microalgae. *Chemical Engineering Journal*, 228, 214-223.
- ❖ Goswami, L., Namboodiri, M. T., Kumar, R. V., Pakshirajan, K., Pugazhenth, G. (2017). Biodiesel production potential of oleaginous *Rhodococcus opacus* grown on biomass gasification wastewater. *Renewable Energy*, 105, 400-406.
- ❖ Goswami, L., Manikandan, N. A., Dolman, B., Pakshirajan, K., Pugazhenth, G. (2018). Biological treatment of wastewater containing a mixture of polycyclic aromatic hydrocarbons using the oleaginous bacterium *Rhodococcus opacus*. *Journal of Cleaner Production*, 196, 1282-1291.
- ❖ Goswami, L., Manikandan, N. A., Taube, J. C. R., Pakshirajan, K., Pugazhenth, G. (2019). Novel waste-derived biochar from biomass gasification effluent: preparation, characterization, cost estimation, and application in polycyclic aromatic hydrocarbon biodegradation and lipid accumulation by *Rhodococcus opacus*. *Environmental Science and Pollution Research*, 26(24), 25154-25166.
- ❖ Goswami, L., Kumar, R. V., Manikandan, N. A., Pakshirajan, K., Pugazhenth, G. (2017). Simultaneous polycyclic aromatic hydrocarbon degradation and lipid accumulation by *Rhodococcus opacus* for potential biodiesel production. *Journal of Water Process Engineering*, 17, 1-10.
- ❖ Goswami, L., Kumar, R. V., Manikandan, N. A., Pakshirajan, K., Pugazhenth, G. (2017). Anthracene biodegradation by oleaginous *Rhodococcus opacus* for biodiesel production and its characterization. *Polycyclic Aromatic Compounds*, 39(3), 207-219.
- ❖ Martínková, L., Uhnáková, B., Pátek, M., Nešvera, J., & Křen, V. (2009). Biodegradation potential of the genus *Rhodococcus*. *Environment international*, 35(1), 162-177.
- ❖ Martínková, L., Uhnáková, B., Pátek, M., Nešvera, J., Křen, V. (2009). Biodegradation potential of the genus *Rhodococcus*. *Environment International*, 35(1), 162-177.
- ❖ Wei, L., Liang, S., Guho, N. M., Hanson, A. J., Smith, M. W., Garcia-Perez, M., McDonald, A. G. (2015). Production and characterization of bio-oil and biochar from the pyrolysis of residual bacterial biomass from a polyhydroxyalkanoate production process. *Journal of Analytical and Applied Pyrolysis*, 115, 268-278.
- ❖ Lai, Y. S., De Francesco, F., Aguinaga, A., Parameswaran, P., Rittmann, B. E. (2016). Improving lipid recovery from *Scenedesmus* wet biomass by surfactant-assisted disruption. *Green Chemistry*, 18(5), 1319-1326.
- ❖ Lavanya, M., Meenakshisundaram, A., Renganathan, S., Chinnasamy, S., Lewis, D. M., Nallasivam, J., Bhaskar, S. (2016). Hydrothermal liquefaction of freshwater and marine algal biomass: a novel approach to produce distillate fuel fractions through blending and co-processing of biocrude with petrocruide. *Bioresource Technology*, 203, 228-235.
- ❖ Lei, H., Ren, S., Wang, L., Bu, Q., Julson, J., Holladay, J., Ruan, R. (2011). Microwave pyrolysis of distillers dried grain with solubles (DDGS) for biofuel production. *Bioresource Technology*, 102 (10), 6208-6213.

- ❖ Leng, L., Li, J., Wen, Z., Zhou, W. (2018). Use of microalgae to recycle nutrients in aqueous phase derived from hydrothermal liquefaction process. *Bioresource Technology*, 256, 529-542.
- ❖ Li, H., Liu, Z., Zhang, Y., Li, B., Lu, H., Duan, N., Si, B. (2014). Conversion efficiency and oil quality of low-lipid high-protein and high-lipid low-protein microalgae via hydrothermal liquefaction. *Bioresource Technology*, 154, 322-329.
- ❖ Li, Y., Han, D., Sommerfeld, M., Hu, Q. (2011). Photosynthetic carbon partitioning and lipid production in the oleaginous microalga *Pseudochlorococcum* sp. (Chlorophyceae) under nitrogen-limited conditions. *Bioresource Technology*, 102 (1), 123-129.
- ❖ Li, Y., Horsman, M., Wang, B., Wu, N., Lan, C. Q. (2008). Effects of nitrogen sources on cell growth and lipid accumulation of green alga *Neochloris oleoabundans*. *Applied Microbiology and Biotechnology*, 81 (4), 629-636.
- ❖ Li, Y., Zhao, Z. K., Bai, F. (2007). High-density cultivation of oleaginous yeast *Rhodospiridium toruloides* Y4 in fed-batch culture. *Enzyme and Microbial Technology*, 41 (3), 312-317.
- ❖ Liu, H. M., Wang, F. Y., Liu, Y. L. (2014). Alkaline pretreatment and hydrothermal liquefaction of cypress for high yield bio-oil production. *Journal of Analytical and Applied Pyrolysis*, 108, 136-142.
- ❖ Liu, Z., Zhang, F. S. (2008). Effects of various solvents on the liquefaction of biomass to produce fuels and chemical feedstocks. *Energy Conversion and Management*, 49 (12), 3498-3504.
- ❖ Ahmad, M., Ahmad, M., Usman, A. R., Al-Faraj, A. S., Abduljabbar, A., Ok, Y. S., Al-Wabel, M. I. (2019). Date palm waste-derived biochar composites with silica and zeolite: synthesis, characterization and implication for carbon stability and recalcitrant potential. *Environmental Geochemistry and Health*, 41(4), 1687-1704.
- ❖ Iqbal, M., Nisar, J., Adil, M., Abbas, M., Riaz, M., Tahir, M. A., Shahid, M. (2017). Mutagenicity and cytotoxicity evaluation of photo-catalytically treated petroleum refinery wastewater using an array of bioassays. *Chemosphere*, 168, 590-598.
- ❖ Parsa, M., Nourani, M., Baghdadi, M., Hosseinzadeh, M., & Pejman, M. (2019). Biochars derived from marine macroalgae as a mesoporous by-product of hydrothermal liquefaction process: characterization and application in wastewater treatment. *Journal of Water Process Engineering*, 32, 100942.
- ❖ Saber, M., Nakhshiniev, B., Yoshikawa, K. (2016). A review of production and upgrading of algal bio-oil. *Renewable and Sustainable Energy Reviews*, 58, 918-930.
- ❖ Saisriyoot, M., Sahaya, T., Thanapimmetha, A., Chisti, Y., & Srinophakun, P. (2016). Production of potential fuel oils by *Rhodococcus opacus* grown on petroleum processing wastewaters. *Journal of Renewable and Sustainable Energy*, 8(6), 063106.
- ❖ Waszak, M., & Gryta, M. (2016). The ultrafiltration ceramic membrane used for broth separation in membrane bioreactor. *Chemical Engineering Journal*, 305, 129-135.
- ❖ Cortes, M.A.L.R.M., de Carvalho, C.C.C.R. (2015). Effect of carbon sources on lipid accumulation in *Rhodococcus* cells, *Biochemical Engineering Journal*, 94, 100-105.
- ❖ Maeda, R. N., Serpa, V. I., Rocha, V. A. L., Mesquita, R. A. A., Santa Anna, L. M. M., De Castro, A. M., Polikarpov, I. (2011). Enzymatic hydrolysis of pretreated sugar cane bagasse using *Penicillium funiculosum* and *Trichoderma harzianum* cellulases. *Process Biochemistry*, 46 (5), 1196-1201.
- ❖ Malins, K., Kampars, V., Brinks, J., Neibolte, I., Murnieks, R., Kampare, R. (2015). Bio-oil from thermo-chemical hydro-liquefaction of wet sewage sludge. *Bioresource Technology*, 187, 23-29.
- ❖ Mansour, M. P., Volkman, J. K., Blackburn, S. I. (2003). The effect of growth phase on the lipid class, fatty acid and sterol composition in the marine dinoflagellate, *Gymnodinium* sp. in batch culture. *Phytochemistry*, 63 (2), 145-153.
- ❖ Mathimani, T., Mallick, N., 2019. A review on hydrothermal processing of microalgal biomass to bio-oil- Knowledge gaps, and recent advances towards sustainable fuel production. *Journal of Cleaner Production*, 217, 69-84.
- ❖ Mehrabadi, A., Craggs, R., Farid, M. M. (2015). Wastewater treatment high rate algal ponds (WWT HRAP) for low-cost biofuel production. *Bioresource Technology*, 184, 202-214.

- ❖ Mehrabadi, A., Craggs, R., Farid, M. M. (2017). Wastewater treatment high rate algal pond biomass for bio-crude oil production. *Bioresource Technology*, 224, 255-264.
- ❖ Meireles, L. A., Guedes, A. C., Malcata, F. X. (2003). Increase of the yields of eicosapentaenoic and docosahexaenoic acids by the microalga *Pavlova lutheri* following random mutagenesis. *Biotechnology and Bioengineering*, 81 (1), 50-55.
- ❖ Meryemoglu, B., Hasanoglu, A., Irmak, S., Erbatur, O. (2014). Biofuel production by liquefaction of kenaf (*Hibiscus cannabinus* L.) biomass. *Bioresource Technology*, 151, 278-283.
- ❖ Merzari, F., Langone, M., Andreottola, G., Fiori, L. (2019). Methane production from process water of sewage sludge hydrothermal carbonization. A review. Valorizing sludge through hydrothermal carbonization. *Critical Reviews in Environmental Science and Technology*, 49(11), 947-988.
- ❖ Metzger, P., Largeau, C. (2005). *Botryococcus braunii*: a rich source for hydrocarbons and related ether lipids. *Applied Microbiology and Biotechnology*, 66 (5), 486-496.
- ❖ Miao, X., Wu, Q. (2004). High yield bio-oil production from fast pyrolysis by metabolic controlling of *Chlorella protothecoides*. *Journal of Biotechnology*, 110 (1), 85-93.
- ❖ Milbrandt, A., Seiple, T., Heimiller, D., Skaggs, R., Coleman, A. (2018). Wet waste-to-energy resources in the United States. *Resources, Conservation and Recycling*, 137, 32-47.
- ❖ Miller, N. (2012). Process design and modeling for the production of triacylglycerols (TAGs) in *Rhodococcus opacus* PD630 (Doctoral dissertation, Massachusetts Institute of Technology).
- ❖ Minowa, T., Kondo, T., Sudirjo, S. T. (1998). Thermochemical liquefaction of Indonesian biomass residues. *Biomass and Bioenergy*, 14 (5-6), 517-524.
- ❖ Minowa, T., Murakami, M., Dote, Y., Ogi, T., Yokoyama, S. Y. (1995). Oil production from garbage by thermochemical liquefaction. *Biomass and Bioenergy*, 8 (2), 117-120.
- ❖ Montella, S., Balan, V., da Costa Sousa, L., Gunawan, C., Giacobbe, S., Pepe, O., Faraco, V. (2016). Saccharification of newspaper waste after ammonia fiber expansion or extractive ammonia. *AMB Express*, 6 (1), 18.
- ❖ Moussa, D. T., El-Naas, M. H., Nasser, M., Al-Marri, M. J. (2017). A comprehensive review of electrocoagulation for water treatment: Potentials and challenges. *Journal of Environmental Management*. 186, 24-41.
- ❖ Gupta, N., Manikandan, N. A., Pakshirajan, K. (2018). Real-time lipid production and dairy wastewater treatment using *Rhodococcus opacus* in a bioreactor under fed-batch, continuous and continuous cell recycling modes for potential biodiesel application. *Biofuels*, 9 (2), 239-245.
- ❖ Ocfemia, K. S., Zhang, Y., Funk, T. (2006). Hydrothermal processing of swine manure into oil using a continuous reactor system: Development and testing. *Transactions of the ASABE*, 49 (2), 533-541.
- ❖ Goswami, L., Kumar, R. V., Pakshirajan, K., Pugazhenthii, G. (2019). A novel integrated biodegradation—microfiltration system for sustainable wastewater treatment and energy recovery. *Journal of Hazardous Materials*, 365, 707-715.
- ❖ Biller, P., Ross, A. B. (2011). Potential yields and properties of oil from the hydrothermal liquefaction of microalgae with different biochemical content. *Bioresource Technology*, 102(1), 215-225.
- ❖ Saikia, P., Gupta, U. N., Barman, R. S., Katak, R., Chutia, R. S., Baruah, B. P. (2015). Production and characterization of bio-oil produced from *Ipomoea carnea* bio-weed. *BioEnergy Research*, 8(3), 1212-1223.
- ❖ Saravanan, P., Pakshirajan, K., Saha, P. (2011). Biodegradation kinetics of phenol by predominantly *Pseudomonas* sp. in a batch shake flask. *Desalination and Water Treatment*, 36(1-3), 99-104.
- ❖ Papanikolaou, S., Aggelis, G. (2002). Lipid production by *Yarrowia lipolytica* growing on industrial glycerol in a single-stage continuous culture. *Bioresource Technology*, 82 (1), 43-49.
- ❖ Papanikolaou, S., Komaitis, M., Aggelis, G. (2004). Single cell oil (SCO) production by *Mortierella isabellina* grown on high-sugar content media. *Bioresource Technology*, 95 (3), 287-291.
- ❖ Pasangulapati, V., Ramachandriya, K. D., Kumar, A., Wilkins, M. R., Jones, C. L., Huhnke, R. L. (2012). Effects of cellulose, hemicellulose and lignin on thermochemical conversion characteristics of the selected biomass. *Bioresource Technology*, 114, 663-669.

- ❖ Pati Patil, P. D., Gude, V. G., Mannarswamy, A., Cooke, P., Munson-McGee, S., Nirmalakhandan, N. Deng, S. , (2011). Optimization of microwave-assisted transesterification of dry algal biomass using response surface methodology. *Bioresource Technology*, 102, 1399-1405.
- ❖ Pedersen, T. H., Grigoras, I. F., Hoffmann, J., Toor, S. S., Daraban, I. M., Jensen, C. U., Nielsen, R. P. (2016). Continuous hydrothermal co-liquefaction of aspen wood and glycerol with water phase recirculation. *Applied Energy*, 162, 1034-1041.
- ❖ Peng, L., Chen, Y. (2011). Conversion of paper sludge to ethanol by separate hydrolysis and fermentation (SHF) using *Saccharomyces cerevisiae*. *Biomass and Bioenergy*, 35 (4), 1600-1606.
- ❖ Perez-Garcia, O., Bashan, Y. (2015). Microalgal heterotrophic and mixotrophic culturing for bio-refining: from metabolic routes to techno-economics. In *Algal biorefinerie*, Springer, Cham, 61-131.
- ❖ Peterson, A. A., Vogel, F., Lachance, R. P., Fröling, M., Antal Jr, M. J., Tester, J. W. (2008). Thermochemical biofuel production in hydrothermal media: a review of sub-and supercritical water technologies. *Energy and Environmental Science*, 1, 32-65.
- ❖ Phukan, M. M., Chutia, R. S., Konwar, B. K., Kataki, R. (2011). Microalgae *Chlorella* as a potential bio-energy feedstock. *Applied Energy*, 88 (10), 3307-3312.
- ❖ Praveenkumar, R., Johny, K., MubarakAli, D., Vijayan, D., Thajuddin, N., Gunasekaran, M. (2012). Demonstration of increased lipid accumulation potential of *Stigeoclonium* sp., Kutz. BUM11007 under nitrogen starved regime: A new source of lipids for biodiesel production. *Journal of Biobased Materials and Bioenergy*, 6 (2), 209-213.
- ❖ Fei Q., Wewetzer S.J., Kurosawa K., Rha C., Sinskey A.J., (2015). High-cell-density cultivation of an engineered *Rhodococcus opacus* strain for lipid production via co-fermentation of glucose and xylose, *Process Biochemistry*, 50, 500–506.
- ❖ Qadeer, S., Khalid, A., Mahmood, S., Anjum, M., Ahmad, Z. (2017). Utilizing oleaginous bacteria and fungi for cleaner energy production. *Journal of Cleaner Production*, 168, 917-928.
- ❖ Qin, Z., Zhuang, Q., Cai, X., He, Y., Huang, Y., Jiang, D., Wang, M. Q. (2018). Biomass and biofuels in China: Toward bioenergy resource potentials and their impacts on the environment. *Renewable and Sustainable Energy Reviews*, 82, 2387-2400.
- ❖ Mitra, R., Chaudhuri, S., Dutta, D. (2017). Modelling the growth kinetics of *Kocuria marina* DAGII as a function of single and binary substrate during batch production of B-Cryptoxanthin, *Bioprocess Biosystem Engineering*, 40, 99–113.
- ❖ Kumar, R. V., Ghoshal, A. K., Pugazhenth, G. (2015). Elaboration of novel tubular ceramic membrane from inexpensive raw materials by extrusion method and its performance in microfiltration of synthetic oily wastewater treatment, *Journal of Membrane Science*, 490, 92-102.
- ❖ Raikova, S., Smith-Baedorf, H., Bransgrove, R., Barlow, O., Santomauro, F., Wagner, J. L., Chuck, C. J. (2016). Assessing hydrothermal liquefaction for the production of bio-oil and enhanced metal recovery from microalgae cultivated on acid mine drainage. *Fuel Processing Technology*, 142, 219-227.
- ❖ Ramos-Tercero, E. A., Bertuccio, A., Brilman, D. W. F. (2015). Process water recycle in hydrothermal liquefaction of microalgae to enhance bio-oil yield. *Energy and fuels*, 29, 2422-2430.
- ❖ Ratledge, C., Botham, P. A. (1977). Pathways of glucose metabolism in *Candida* 107, a lipid-accumulating yeast. *Microbiology*, 102 (2), 391-395.
- ❖ Reddy, H. K., Muppaneni, T., Ponnusamy, S., Sudasinghe, N., Pegallapati, A., Selvaratnam, T., Holguin, F. O., (2016). Temperature effect on hydrothermal liquefaction of *Nannochloropsis gaditana* and *Chlorella* sp. *Applied Energy*, 165, 943-951.
- ❖ Ren, H. Y., Liu, B. F., Kong, F., Zhao, L., Xie, G. J., Ren, N. Q. (2014). Enhanced lipid accumulation of green microalga *Scenedesmus* sp. by metal ions and EDTA addition. *Bioresource Technology*, 169, 763-767.
- ❖ Roberts, G. W., Fortier, M. O. P., Sturm, B. S., Stagg-Williams, S. M. (2013). Promising pathway for algal biofuels through wastewater cultivation and hydrothermal conversion. *Energy and Fuels*, 27 (2), 857-867.

- ❖ Rodolfi, L., Chini Zittelli, G., Bassi, N., Padovani, G., Biondi, N., Bonini, G., Tredici, M. R. (2009). Microalgae for oil: Strain selection, induction of lipid synthesis and outdoor mass cultivation in a low-cost photobioreactor. *Biotechnology and Bioengineering*, 102 (1), 100-112.
- ❖ Ross, A. B., Biller, P., Kubacki, M. L., Li, H., Lea-Langton, A., Jones, J. M. (2010). Hydrothermal processing of microalgae using alkali and organic acids. *Fuel*, 89 (9), 2234-2243.
- ❖ Roy, A.S., Chingkheibunba, A., Pakshirajan, K. (2016). An Overview of Production, Properties, and Uses of Biodiesel from Vegetable Oil. In *Green Fuels Technology*. Springer, Cham. 83-105.
- ❖ Ruiz, H. A., Ruzene, D. S., Silva, D. P., Quintas, M. A., Vicente, A. A., Teixeira, J. A. (2011). Evaluation of a hydrothermal process for pretreatment of wheat straw-effect of particle size and process conditions. *Journal of Chemical Technology and Biotechnology*, 86 (1), 88-94.
- ❖ Amara, S., Seghezzi, N., Otani, H., Diaz-Salazar, C., Liu, J., & Eltis, L. D. (2016). Characterization of key triacylglycerol biosynthesis processes in *Rhodococci*. *Scientific reports*, 6(1), 1-13.
- ❖ Divyapriya, S., Dimi, D., Deepthi, K. P. (2014). Biochemical effect of industrial effluence on germinating seeds of *Cicer arietinum*. *International Journal of Pharmacy and Pharmaceutical Sciences*, 6(2), 538-542.
- ❖ Agarry, S. E., Solomon, B. O., & Audu, T. O. K. (2010). Substrate utilization and inhibition kinetics: Batch degradation of phenol by indigenous monoculture of *Pseudomonas aeruginosa*. *International Journal of Biotechnology and Molecular Biology Research*, 1(2), 22-30.
- ❖ González, S., Petrovic, M., & Barceló, D. (2007). Removal of a broad range of surfactants from municipal wastewater—comparison between membrane bioreactor and conventional activated sludge treatment. *Chemosphere*, 67(2), 335-343.
- ❖ Ishak, S., Malakahmad, A., & Isa, M. H. (2012). Refinery wastewater biological treatment: A short review.
- ❖ Kumar, S., Gupta, N., Pakshirajan, K. (2015). Simultaneous lipid production and dairy wastewater treatment using *Rhodococcus opacus* in a batch bioreactor for potential biodiesel application. *Journal of Environmental Chemical Engineering*, 3(3), 1630-1636.
- ❖ Zou, S., Wu, Y., Yang, M., Li, C., & Tong, J. (2010). Bio-oil production from sub-and supercritical water liquefaction of microalgae *Dunaliella tertiolecta* and related properties. *Energy and Environmental Science*, 3(8), 1073-1078.
- ❖ Davis, S. C., Boddey, R. M., Alves, B. J., Cowie, A. L., George, B. H., Ogle, S. M., van Wijk, M. T. (2013). Management swing potential for bioenergy crops. *Gcb Bioenergy*, 5(6), 623-638.
- ❖ Shariati, S. R. P., Bonakdarpour, B., Zare, N., & Ashtiani, F. Z. (2011). The effect of hydraulic retention time on the performance and fouling characteristics of membrane sequencing batch reactors used for the treatment of synthetic petroleum refinery wastewater. *Bioresource Technology*, 102(17), 7692-7699.
- ❖ Joshi, S. S., Dhopeswarkar, R., Jadhav, U., Jadhav, R., D'souza, L., Dixit, J. (2001). Continuous ethanol production by fermentation of waste banana peels using flocculating yeast, 8(3), 153-156.
- ❖ Chiu, S.Y., Kao, C.Y., Chen, T.Y., Bin Chang, Y., Kuo, C.M., Lin C.S. (2015). Cultivation of microalgal *Chlorella* for biomass and lipid production using wastewater as nutrient resource, *Bioresource Technology*, 184, 179–189.
- ❖ Saber, M., Nakhshiniev, B., Yoshikawa, K. (2016). A review of production and upgrading of algal bio-oil. *Renewable and Sustainable Energy Reviews*, 58, 918-930.
- ❖ Saikia, P., Gupta, U. N., Barman, R. S., Katak, R., Chutia, R. S., Baruah, B. P. (2015). Production and characterization of bio-oil produced from *Ipomoea carnea* bio-weed. *BioEnergy Research*. 8, 1212-1223.
- ❖ Sankaran, S., Khanal, S. K., Jasti, N., Jin, B., Pometto III, A. L., Van Leeuwen, J. H. (2010). Use of filamentous fungi for wastewater treatment and production of high value fungal byproducts: a review. *Critical Reviews in Environmental Science and Technology*, 40(5), 400-449.
- ❖ Santala, S., Efimova, E., Kivinen, V., Larjo, A., Aho, T., Karp, M., Santala, V. (2011). Improved triacylglycerol production in *Acinetobacter baylyi* ADP1 by metabolic engineering. *Microbial cell factories*, 10 (1), 36.
- ❖ Sasaki, M., Adschiri, T., Arai, K. (2003). Production of cellulose II from native cellulose by near-and supercritical water solubilization. *Journal of Agricultural and Food Chemistry*, 51 (18), 5376-5381.

- ❖ Sawangkeaw, R., Ngamprasertsith, S. (2013). A review of lipid-based biomasses as feedstocks for biofuels production. *Renewable and Sustainable Energy Reviews*, 25, 97-108.
- ❖ Scott, E., Peter, F., Sanders, J. (2007). Biomass in the manufacture of industrial products—the use of proteins and amino acids. *Applied Microbiology and Biotechnology*, 75 (4), 751-762.
- ❖ Selvaratnam, T., Henkanatte-Gedera, S. M., Muppaneni, T., Nirmalakhandan, N., Deng, S., Lammers, P. J. (2016). Maximizing recovery of energy and nutrients from urban wastewaters. *Energy*, 104, 16-23.
- ❖ Shafiei, M., Karimi, K., Taherzadeh, M. J. (2010). Pretreatment of spruce and oak by N-methylmorpholine-N-oxide (NMMO) for efficient conversion of their cellulose to ethanol. *Bioresource Technology*, 101 (13), 4914-4918.
- ❖ Shakya, R., Adhikari, S., Mahadevan, R., Dempster, T. A. (2018). Catalytic upgrading of bio-oil produced from hydrothermal liquefaction of *Nannochloropsis* sp. *Bioresource Technology*, 252, 28-36.
- ❖ Shakya, R., Whelen, J., Adhikari, S., Mahadevan, R., Neupane, S. (2015). Effect of temperature and Na<sub>2</sub>CO<sub>3</sub> catalyst on hydrothermal liquefaction of algae. *Algal Research*, 12, 80-90.
- ❖ Shao, J., Yuan, X., Leng, L., Huang, H., Jiang, L., Wang, H., Zeng, G. (2015). The comparison of the migration and transformation behavior of heavy metals during pyrolysis and liquefaction of municipal sewage sludge, paper mill sludge, and slaughterhouse sludge. *Bioresource Technology*, 198, 16-22.
- ❖ Sharifzadeh, M., Sadeqzadeh, M., Guo, M., Borhani, T. N., Konda, N. M., Garcia, M. C., Shah, N. (2019). The multi-scale challenges of biomass fast pyrolysis and bio-oil upgrading: Review of the state of art and future research directions. *Progress in Energy and Combustion Science*, 71, 1-80.
- ❖ Shen, Y., Yu, S., Ge, S., Chen, X., Ge, X., Chen, M. (2017). Hydrothermal carbonization of medical wastes and lignocellulosic biomass for solid fuel production from lab-scale to pilot-scale. *Energy*, 118, 312-323.
- ❖ Shruthi, P., Rajeshwari, T., Mrunalini, B. R., Girish, V., Girisha, S. T. (2014). Evaluation of oleaginous bacteria for potential biofuel. *International Journal of Current Microbiology and Applied Sciences*, 3, 47-57.
- ❖ Shuping, Z., Yulong, W., Mingde, Y., Kaleem, I., Chun, L., Tong, J. (2010). Production and characterization of bio-oil from hydrothermal liquefaction of microalgae *Dunaliella tertiolecta* cake. *Energy*, 35 (12), 5406-5411.
- ❖ Singh, A., Nigam, P. S., Murphy, J. D. (2011). Renewable fuels from algae: an answer to debatable land based fuels. *Bioresource Technology*, 102 (1), 10-16.
- ❖ Singh, R., Balagurumurthy, B., Prakash, A., Bhaskar, T. (2015). Catalytic hydrothermal liquefaction of water hyacinth. *Bioresource Technology*, 178, 157-165.
- ❖ Skaggs, R.L., Coleman, A.M., Seiple, T.E., Milbrandt, A.R. (2018). Waste-to-Energy biofuel production potential for selected feedstocks in the conterminous United States. *Renewable and Sustainable Energy Reviews*, 82, 2640-2651.
- ❖ Song, W., Wang, S., Guo, Y., Xu, D (2017). Bio-oil production from hydrothermal liquefaction of waste *Cyanophyta* biomass: Influence of process variables and their interactions on the product distributions. *International Journal of Hydrogen Energy*, 42 (31), 20361-20374.
- ❖ Sriwongchai, S., Pokethitiyook, P., Pugkaew, W., Kruatrachue, M., Lee, H. (2012). Optimization of lipid production in the oleaginous bacterium *Rhodococcus erythropolis* growing on glycerol as the sole carbon source. *African Journal of Biotechnology*, 11 (79), 14440-14447.
- ❖ Standard Methods for the Examination of Water and Wastewater. (twentieth ed.), American Public Health Association, Washington. DC (1998).
- ❖ Subhadra, B. (2011). Algal biorefinery-based industry: an approach to address fuel and food insecurity for a carbon-smart world. *Journal of the Science of Food and Agriculture*, 91 (1), 2-13.
- ❖ Sudasinghe, N., Dungan, B., Lammers, P., Albrecht, K., Elliott, D., Hallen, R., Schaub, T. (2014). High resolution FT-ICR mass spectral analysis of bio-oil and residual water soluble organics produced by hydrothermal liquefaction of the marine microalga *Nannochloropsis salina*. *Fuel*, 119, 47-56.
- ❖ Sun, P., Heng, M., Sun, S., Chen, J. (2010). Direct liquefaction of paulownia in hot compressed water: Influence of catalysts. *Energy*, 35 (12), 5421-5429.

- ❖ Sun, X. F., Jing, Z., Fowler, P., Wu, Y., Rajaratnam, M. (2011). Structural characterization and isolation of lignin and hemicelluloses from barley straw. *Industrial Crops and Products*, 33 (3), 588-598.
- ❖ Vo, T. K., Lee, O. K., Lee, E. Y., Kim, C. H., Seo, J. W., Kim, J., & Kim, S. S. (2016). Kinetics study of the hydrothermal liquefaction of the microalga *Aurantiochytrium* sp. KRS101. *Chemical Engineering Journal*, 306, 763-771.
- ❖ Mathimani, T., & Mallick, N. (2019). A review on the hydrothermal processing of microalgal biomass to bio-oil- Knowledge gaps and recent advances. *Journal of Cleaner Production*, 217, 69-84.
- ❖ Takeno, S., Sakuradani, E., Murata, S., Inohara-Ochiai, M., Kawashima, H., Ashikari, T., Shimizu, S. (2005). Molecular evidence that the rate-limiting step for the biosynthesis of arachidonic acid in *Mortierella alpina* is at the level of an elongase. *Lipids*, 40 (1), 25-30.
- ❖ Tekin, K., Karagöz, S., Bektaş, S. (2014). A review of hydrothermal biomass processing. *Renewable and Sustainable Energy Reviews*, 40, 673-687.
- ❖ Tian, C., Liu, Z., Zhang, Y., Li, B., Cao, W., Lu, H., Zhang, T. (2015). Hydrothermal liquefaction of harvested high-ash low-lipid algal biomass from Dianchi Lake: effects of operational parameters and relations of products. *Bioresource Technology*, 184, 336-343.
- ❖ Tian, S., Zhu, W., Gleisner, R., Pan, X. J., Zhu, J. Y. (2011). Comparisons of SPORL and dilute acid pretreatments for sugar and ethanol productions from aspen. *Biotechnology Progress*, 27 (2), 419-427.
- ❖ Togarcheti, S. C., kumar Mediboyina, M., Chauhan, V. S., Mukherji, S., Ravi, S., Mudliar, S. N. (2017). Life cycle assessment of microalgae based biodiesel production to evaluate the impact of biomass productivity and energy source. *Resources, Conservation and Recycling*, 122, 286-294.
- ❖ Valdez, P. J., Tocco, V. J., Savage, P. E. (2014). A general kinetic model for the hydrothermal liquefaction of microalgae. *Bioresource Technology*, 163, 123-127.
- ❖ Vardon, D. R., Sharma, B. K., Blazina, G. V., Rajagopalan, K., Strathmann, T. J. (2012). Thermochemical conversion of raw and defatted algal biomass via hydrothermal liquefaction and slow pyrolysis. *Bioresource Technology*, 109, 178-187.
- ❖ Vardon, D. R., Sharma, B. K., Scott, J., Yu, G., Wang, Z., Schideman, L., Strathmann, T. J. (2011). Chemical properties of biocrude oil from the hydrothermal liquefaction of *Spirulina* algae, swine manure, and digested anaerobic sludge. *Bioresource Technology*, 102 (17), 8295-8303.
- ❖ Viell, J., Inouye, H., Szekely, N. K., Frielinghaus, H., Marks, C., Wang, Y., Makowski, L. (2016). Multi-scale processes of beech wood disintegration and pretreatment with 1-ethyl-3-methylimidazolium acetate/water mixtures. *Biotechnology for Biofuels*, 9 (1), 7.
- ❖ Vo, H. N. P., Ngo, H. H., Guo, W., Chang, S. W., Nguyen, D. D., Chen, Z., Zhang, X. (2020). Microalgae for saline wastewater treatment: a critical review. *Critical Reviews in Environmental Science and Technology*, 50(12), 1224-1265.
- ❖ Voloshin, R. A., Rodionova, M. V., Zharmukhamedov, S. K., Veziroglu, T. N., Allakhverdiev, S. I. (2016). Biofuel production from plant and algal biomass. *International Journal of Hydrogen Energy*, 41 (39), 17257-17273.
- ❖ Gwenzi, W., Chaukura, N., Noubactep, C., & Mukome, F. N. (2017). Biochar-based water treatment systems as a potential low-cost and sustainable technology for clean water provision. *Journal of environmental management*, 197, 732-749.
- ❖ Finnerty, W. R. (1992). The biology and genetics of the genus *Rhodococcus*. *Annual review of microbiology*, 46(1), 193-218.
- ❖ Wądrzyk, M., Janus, R., Vos, M. P., Brilman, D. W. F. (2018). Effect of process conditions on bio-oil obtained through continuous hydrothermal liquefaction of *Scenedesmus* sp. microalgae. *Journal of Analytical and Applied Pyrolysis*, 134, 415-426.
- ❖ Wagner, J., Bransgrove, R., Beacham, T.A., Allen, M.J., Meixner, K., Drosig, B., Ting, V.P., Chuck, C.J. (2016). Co-production of bio-oil and propylene through the hydrothermal liquefaction of polyhydroxybutyrate producing cyanobacteria. *Bioresource Technology*, 207, 166-174.

- ❖ Wang, B., Karpouk, A., Yeager, D., Amirian, J., Litovsky, S., Smalling, R., Emelianov, S. (2012). In vivo intravascular ultrasound-guided photoacoustic imaging of lipid in plaques using an animal model of atherosclerosis. *Ultrasound in Medicine and Biology*, 38 (12), 2098-2103.
- ❖ Wang, C., Pan, J., Li, J., Yang, Z. (2008). Comparative studies of products produced from four different biomass samples via deoxy-liquefaction. *Bioresource Technology*, 99 (8), 2778-2786.
- ❖ Wang, L., Shahbazi, A., Hanna, M. A. (2011). Characterization of corn stover, distiller grains and cattle manure for thermochemical conversion. *Biomass and Bioenergy*, 35 (1), 171-178.
- ❖ Wang, X., Sheng, L., Yang, X. (2017). Pyrolysis characteristics and pathways of protein, lipid and carbohydrate isolated from microalgae *Nannochloropsis* sp. *Bioresource Technology*, 229, 119-125.
- ❖ Wang, Y., Wang, H., Lin, H., Zheng, Y., Zhao, J., Pelletier, A., Li, K. (2013). Effects of solvents and catalysts in liquefaction of pinewood sawdust for the production of bio-oils. *Biomass and Bioenergy*, 59, 158-167.
- ❖ Wang, Z., Keshwani, D. R., Redding, A. P., Cheng, J. J. (2010). Sodium hydroxide pretreatment and enzymatic hydrolysis of coastal Bermuda grass. *Bioresource Technology*, 101 (10), 3583-3585.
- ❖ Watanabe, H., Li, D., Nakagawa, Y., Tomishige, K., Kaya, K., Watanabe, M. M. (2014). Characterization of oil-extracted residue biomass of *Botryococcus braunii* as a biofuel feedstock and its pyrolytic behavior. *Applied Energy*, 132, 475-484.
- ❖ Wei, L., Liang, S., Coats, E. R., McDonald, A. G. (2015a). Valorization of residual bacterial biomass waste after polyhydroxyalkanoate isolation by hydrothermal treatment. *Bioresource Technology*, 198, 739-745.
- ❖ Wei, L., Liang, S., Guho, N. M., Hanson, A. J., Smith, M. W., Garcia-Perez, M., McDonald, A. G. (2015b). Production and characterization of bio-oil and biochar from the pyrolysis of residual bacterial biomass from a polyhydroxyalkanoate production process. *Journal of Analytical and Applied Pyrolysis*, 115, 268-278.
- ❖ Wei, N., Via, B. K., Wang, Y., McDonald, T., Auad, M. L. (2014). Liquefaction and substitution of switchgrass (*Panicum virgatum*) based bio-oil into epoxy resins. *Industrial Crops and Products*, 57, 116-123.
- ❖ Williams, P. T., Slaney, E. (2007). Analysis of products from the pyrolysis and liquefaction of single plastics and waste plastic mixtures. *Resources, Conservation and Recycling*, 51 (4), 754-769.
- ❖ Wu, S., Zhao, X., Shen, H., Wang, Q., Zhao, Z. K. (2011). Microbial lipid production by *Rhodospiridium toruloides* under sulfate-limited conditions. *Bioresource Technology*, 102 (2), 1803-1807.
- ❖ Wu, X., Jiang, S., Liu, M., Pan, L., Zheng, Z., Luo, S. (2011). Production of L-lactic acid by *Rhizopus oryzae* using semicontinuous fermentation in bioreactor. *Journal of Industrial Microbiology and Biotechnology*, 38 (4), 565-571.
- ❖ Xiu, S., Shahbazi, A. (2012). Bio-oil production and upgrading research: A review. *Renewable and Sustainable Energy Reviews*, 16 (7), 4406-4414.
- ❖ Xiu, S., Shahbazi, A., Shirley, V., Cheng, D. (2010). Hydrothermal pyrolysis of swine manure to bio-oil: effects of operating parameters on products yield and characterization of bio-oil. *Journal of Analytical and Applied Pyrolysis*, 88 (1), 73-79.
- ❖ Xu, C., Etcheverry, T. (2008). Hydro-liquefaction of woody biomass in sub- and super-critical ethanol with iron-based catalysts. *Fuel*, 87 (3), 335-345.
- ❖ Xu, C., Lancaster, J. (2008). Conversion of secondary pulp/paper sludge powder to liquid oil products for energy recovery by direct liquefaction in hot-compressed water. *Water Research*, 42 (6-7), 1571-1582.
- ❖ Xu, D., Lin, G., Guo, S., Wang, S., Guo, Y., Jing, Z. (2018). Catalytic hydrothermal liquefaction of algae and upgrading of biocrude: A critical review. *Renewable and Sustainable Energy Reviews*, 97, 103-118.
- ❖ Xu, D., Savage, P. E. (2017). Effect of temperature, water loading, and Ru/C catalyst on water-insoluble and water-soluble biocrude fractions from hydrothermal liquefaction of algae. *Bioresource Technology*, 239, 1-6.
- ❖ Xu, J., Zhao, X., Wang, W., Du, W., Liu, D. (2012). Microbial conversion of biodiesel byproduct glycerol to triacylglycerols by oleaginous yeast *Rhodospiridium toruloides* and the individual effect of some impurities on lipid production. *Biochemical Engineering Journal*, 65, 30-36.
- ❖ Xu, Y., Zheng, X., Yu, H., Hu, X. (2014). Hydrothermal liquefaction of *Chlorella pyrenoidosa* for bio-oil production over Ce/HZSM-5. *Bioresource Technology*, 156, 1-5.

- ❖ Xue, F., Miao, J., Zhang, X., Luo, H., Tan, T. (2008). Studies on lipid production by *Rhodotorula glutinis* fermentation using monosodium glutamate wastewater as culture medium. *Bioresource Technology*, 99 (13), 5923-5927.
- ❖ Xue, Y., Chen, H., Zhao, W., Yang, C., Ma, P., Han, S. (2016). A review on the operating conditions of producing bio-oil from hydrothermal liquefaction of biomass. *International Journal of Energy Research*, 40 (7), 865-877.
- ❖ Gao, Y., Wang, X. H., Yang, H. P., Chen, H. P. (2012). Characterization of products from hydrothermal treatments of cellulose. *Energy*, 42(1), 457-465.
- ❖ Ma, Y., Wang, Q., Sun, X., Wang, X. (2015). A novel magnetic biochar from spent shiitake substrate: characterization and analysis of pyrolysis process. *Biomass Conversion and Biorefinery*, 5(4), 339-346.
- ❖ Isa, Y. M., Ganda, E. T. (2018). Bio-oil as a potential source of petroleum range fuels. *Renewable and Sustainable Energy Reviews*, 81, 69-75.
- ❖ Mu, Y., Yu, H. Q., Wang, G. (2007). A kinetic approach to anaerobic hydrogen-producing process. *Water Research*, 41(5), 1152-1160.
- ❖ Sun, Y., Zhang, J. P., Wen, C., Zhang, L. (2016). An enhanced approach for biochar preparation using fluidized bed and its application for H<sub>2</sub>S removal. *Chemical Engineering and Processing: Process Intensification*, 104, 1-12.
- ❖ Zhang, Y., Brown, T. R., Hu, G., Brown, R. C. (2013). Techno-economic analysis of two bio-oil upgrading pathways. *Chemical Engineering Journal*, 225, 895-904.
- ❖ Yan, Y., Xu, J., Li, T., Ren, Z. (1999). Liquefaction of sawdust for liquid fuel. *Fuel Processing Technology*, 60 (2), 135-143.
- ❖ Yang, H., Yan, R., Chen, H., Lee, D. H., Zheng, C. (2007). Characteristics of hemicellulose, cellulose and lignin pyrolysis. *Fuel*, 86, 12-13. 1781-1788.
- ❖ Yang, L., Si, B., Tan, X., Chu, H., Zhou, X., Zhang, Y., Zhao, F. (2018). Integrated anaerobic digestion and algae cultivation for energy recovery and nutrient supply from post-hydrothermal liquefaction wastewater. *Bioresource Technology*, 266, 349-356.
- ❖ Yang, W., Li, X., Li, Z., Tong, C., Feng, L. (2015). Understanding low-lipid algae hydrothermal liquefaction characteristics and pathways through hydrothermal liquefaction of algal major components: crude polysaccharides, crude proteins and their binary mixtures. *Bioresource Technology*, 196, 99-108.
- ❖ Ye, L., Zhang, J., Zhao, J., Tu, S. (2014). Liquefaction of bamboo shoot shell for the production of polyols. *Bioresource Technology*, 153, 147-153.
- ❖ Yin, S., Dolan, R., Harris, M., Tan, Z. (2010). Subcritical hydrothermal liquefaction of cattle manure to bio-oil: effects of conversion parameters on bio-oil yield and characterization of bio-oil. *Bioresource Technology*, 101 (10), 3657-3664.
- ❖ Yu, G., Zhang, Y., Schideman, L., Funk, T., Wang, Z. (2011). Distributions of carbon and nitrogen in the products from hydrothermal liquefaction of low-lipid microalgae. *Energy and Environmental Science*, 4 (11), 4587-4595.
- ❖ Yuzgeç, U., Palazoglu, A., Romagnoli, J. A. (2010). Refinery scheduling of crude oil unloading, storage and processing using a model predictive control strategy. *Computers and Chemical Engineering*. 34, 1671-1686.
- ❖ Shuping, Z., Yulong, W., Mingde, Y., Kaleem, I., Chun, L., Tong, J. (2010). Production and characterization of bio-oil from hydrothermal liquefaction of microalgae *Dunaliella tertiolecta* cake. *Energy*, 35(12), 5406-5411.
- ❖ Zhai, Y., Chen, H., Xu, B., Xiang, B., Chen, Z., Li, C., Zeng, G. (2014). Influence of sewage sludge-based activated carbon and temperature on the liquefaction of sewage sludge: yield and composition of bio-oil, immobilization and risk assessment of heavy metals. *Bioresource Technology*, 159, 72-79.
- ❖ Zhang, B., Feng, H., He, Z., Wang, S. Chen, H. (2018). Bio-oil production from hydrothermal liquefaction of ultrasonic pre-treated *Spirulina platensis*. *Energy Conversion and Management*, 159, 204-212.
- ❖ Zhang, B., von Keitz, M., Valentas, K. (2008). Thermal effects on hydrothermal biomass liquefaction. *Biotechnology for Fuels and Chemicals*, 511-518.
- ❖ Zhang, F., Ouellet, M., Bath, T. S., Adams, P. D., Petzold, C. J., Mukhopadhyay, A., Keasling, J. D. (2012). Enhancing fatty acid production by the expression of the regulatory transcription factor FadR. *Metabolic Engineering*, 14 (6), 653-660.

- ❖ Zhang, L., You, T., Zhou, T., Zhang, L., Xu, F. (2016). Synergistic effect of white-rot fungi and alkaline pretreatments for improving enzymatic hydrolysis of poplar wood. *Industrial Crops and Products*, 86, 155-162.
- ❖ Zhang, R. H., Li, Z. G., Liu, X. D., Wang, B. C., Zhou, G. L., Huang, X. X., Brooks, M. (2017). Immobilization and bioavailability of heavy metals in greenhouse soils amended with rice straw-derived biochar. *Ecological Engineering*, 98, 183-188.
- ❖ Zhang, Y. M., Chen, H., He, C. L., Wang, Q. (2013). Nitrogen starvation induced oxidative stress in an oil-producing green alga *Chlorella sorokiniana* C3. *PloS one*, 8, (7)
- ❖ Zhao, C. H., Cui, W., Liu, X. Y., Chi, Z. M., Madzak, C. (2010). Expression of inulinase gene in the oleaginous yeast *Yarrowia lipolytica* and single cell oil production from insulin-containing materials. *Metabolic Engineering*, 12 (6), 510-517.
- ❖ Zhao, X., Kong, X., Hua, Y., Feng, B., Zhao, Z. (2008). Medium optimization for lipid production through co-fermentation of glucose and xylose by the oleaginous yeast *Lipomyces starkeyi*. *European Journal of Lipid Science and Technology*, 110 (5), 405-412.
- ❖ Zhong, C., Wei, X. (2004). A comparative experimental study on the liquefaction of wood. *Energy*, 29 (11), 1731-1741.
- ❖ Zhou, D., Zhang, L., Zhang, S., Fu, H., Chen, J. (2010). Hydrothermal liquefaction of macroalgae *Enteromorpha prolifera* to bio-oil. *Energy and Fuels*, 24 (7), 4054-4061.
- ❖ Zhu, G., Zhu, X., Fan, Q., Wan, X. (2010). Recovery of biomass wastes by hydrolysis in sub-critical water. *Resources, Conservation and Recycling*, 55(4), 409-416.
- ❖ Zhu, L. Y., Zong, M. H., Wu, H. (2008). Efficient lipid production with *Trichosporon fermentans* and its use for biodiesel preparation. *Bioresource Technology*, 99 (16), 7881-7885.
- ❖ Zou, S., Wu, Y., Yang, M., Li, C., Tong, J. (2009). Thermochemical catalytic liquefaction of the marine microalgae *Dunaliella Tertiolecta* and characterization of bio-oils. *Energy and Fuels*, 23 (7), 3753-3758.
- ❖ Zucconi, F. (1981). Evaluating toxicity of immature compost. *Biocycle*. 22, 54-57.

**Table** Simple cost estimation of bio-oil production from *R. opacus* biomass treating refinery wastewater in a CSTR

<b>Single time investment (Instruments cost) (a)</b>	<b>Cost (\$)</b>
Peristaltic pump (2)	~1062.69
Aeration pump (1)	~10.73
Workman cost	~180.55
Hydrothermal vessel	~147.58
<b>Raw material cost (b)</b>	
PVC pipe \ perspex tube	~80.66
Silicon tubings	~70.42
Cylinder and other materials	~115.87
<b>Operation and maintenance costs (c)</b>	
Power consumption 7.5/- unit for connected load more than 5 KW during the operation of the reactor (2 Peristaltic pump, 1 agitator, 2 aeration pump) for reactor and hot air oven for HTL for 2 hours	~9.12
Consumables: Media , Milli Q water, trace element solution, chemicals ( DCM) etc.	~98.79
<b>Total (a+b+c)</b>	<b>~1776.41</b>



---

**List of Publications Based on This Research Work****Referred International Journals**

- ✓ Paul, T., Baskaran, D., Pakshirajan, K., Pugazhenth, G., Rajamanickam, R. (2020). Bio-oil production by hydrothermal liquefaction of *Rhodococcus opacus* biomass utilizing refinery wastewater: Biomass valorization and process optimization. Environmental Technology and Innovation, 101326. (<https://doi.org/10.1016/j.eti.2020.101326>)
- ✓ Paul, T., Baskaran, D., Pakshirajan, K., Pugazhenth, G (2020). Valorization of refinery wastewater for lipid-rich biomass production by *Rhodococcus opacus* in batch system: a kinetic approach. Biomass and Bioenergy, 143, 105867. (<https://doi.org/10.1016/j.biombioe.2020.105867>)
- ✓ Paul, T., Sinharoy, A., Baskaran, D., Pakshirajan, K., Pugazhenth, G., Lens, P. N. (2020). Bio-oil production from oleaginous microorganisms using hydrothermal liquefaction: A biorefinery approach. Critical Reviews in Environmental Science and Technology, 1-39. (<https://doi.org/10.1080/10643389.2020.1820803>)
- ✓ Paul, T., Sinharoy, A., Pakshirajan, K., Pugazhenth, G. (2020). Lipid-rich bacterial biomass production using refinery wastewater in a bubble column bioreactor for bio-oil conversion by hydrothermal liquefaction. Journal of Water Process Engineering, 37, 101462. (<https://doi.org/10.1016/j.jwpe.2020.101462>)
- ✓ Paul, T., Baskaran, D., Pakshirajan, K., Pugazhenth, G. (2019). Continuous bioreactor with cell-recycle using tubular ceramic membrane for simultaneous wastewater treatment and bio-oil production by oleaginous *Rhodococcus opacus*. Chemical Engineering Journal 367, 76–85. (<https://doi.org/10.1016/j.cej.2019.02.050>)
- ✓ Paul, T., Iyyappan, J., Manikandan, N. A., Pakshirajan, K., Pugazhenth, G., Girisa, S., Kunnumakkara, A.B. Toxicity assessment and reuse potential of petroleum refinery

wastewater treated using a high performance two-stage submerged tubular membrane bioreactor with the oleaginous hydrocarbonoclastic bacterium *Rhodococcus opacus* (**Under review**)

✓ Tanushree Paul, Iyyappan J, Kannan Pakshirajan, G. Pugazhenth. Novel and hybrid/integrated reactor configurations for the removal of recalcitrant organics from petroleum refinery wastewater. (**Under preparation**)

#### **National and International conferences**

- ✓ Tanushree Paul, Iyyappan J, Kannan Pakshirajan and G. Pugazhenth. Biological treatment of refinery wastewater using a submerged tubular membrane bioreactor. International Conference on Recent Advancements in Chemical, Energy & Environmental Engineering (**RACEEE-2020**), February 13-14, 2020, SSN College of Engineering, Chennai, India.
- ✓ Tanushree Paul, Kannan Pakshirajan and G. Pugazhenth. Bio-oil production from oleaginous *Rhodococcus opacus* biomass treating refinery wastewater in a bioreactor under fed-batch operation mode. International Conference on Energy and Sustainable Development (**ICESD-2020**), February 14-15, 2020, Jadavpur University, Kolkata, India.
- ✓ Tanushree Paul, Kannan Pakshirajan and G. Pugazhenth. Valorization of *Rhodococcus opacus* biomass cultivated using refinery wastewater by hydrothermal liquefaction. National Conference on “Issues & Challenges in Water Treatment and Allied Research for Sustainable Environment” (**WATER 2020**), January 23-25, 2020, IIT Guwahati, Guwahati, India.
- ✓ Tanushree Paul, Kannan Pakshirajan and G. Pugazhenth. Eco-toxicity analysis of biologically treated refinery wastewater following cell recycle with tubular membrane. International Conference on Nutraceuticals and Chronic Diseases (**INCD-2019**), September 23-25, 2019, IIT Guwahati, Guwahati, India.

- ✓ Tanushree Paul, Kannan Pakshirajan and G. Pugazhenth. Refinery wastewater treatment using the oleaginous *Rhodococcus opacus* and bio-oil production from the lipid-rich bacterial biomass by hydrothermal liquefaction. **Research Conclave 2019**, March 14-17, 2019, IIT Guwahati, Guwahati, India
- ✓ Tanushree Paul, DivyaBaskaran, Kannan Pakshirajan and G. Pugazhenth. Bioreactor strategies for refinery wastewater treatment using *Rhodococcus opacus* and bio-oil production by hydrothermal liquefaction. International Conference on Bioprocess for Sustainable Environment and Energy (**ICBSEE-2018**), December 6-7, 2018, NIT Rourkela, India.
- ✓ Tanushree Paul, Kannan Pakshirajan and G. Pugazhenth. Optimization of micro-nutrients and process parameters for treatment of refinery wastewater by oleaginous *Rhodococcus opacus* for potential bio-oil production. **Research Conclave 2018**, March 8-11, 2018, IIT Guwahati, Guwahati, India.
- ✓ Tanushree Paul, Kannan Pakshirajan and G. Pugazhenth. Biological treatment of refinery wastewater using oleaginous/hydrocarbonoclastic *Rhodococcus opacus* for potential triacylglycerol (TAG) production. International Conference on Waste Management (**RECYCLE 2018**), February 22-24, 2018, IIT Guwahati, Guwahati, India.
- ✓ Tanushree Paul, Kannan Pakshirajan and G. Pugazhenth. Optimization of media and process conditions for high biomass production of *Rhodococcus opacus* from refinery wastewater for potential bio-oil production. Indo-Japan Bilateral Symposium on Future Perspective of Bio-resource Utilization “In North-Eastern Region” (**IJBS-2018**), February 1-4, 2018, IIT Guwahati, Guwahati, India.
- ✓ Tanushree Paul, LalitGoswami, Kannan Pakshirajan and G. Pugazhenth. Optimization of micro-nutrients and process parameters for treatment of refinery wastewater by oleaginous *Rhodococcus opacus* for potential triacylglycerol (TAG) production. 5<sup>th</sup> Annual

conference on Recent Trends in Bio-processing for Healthcare, Energy and Environment (**BPI-2017**), December 9-11, 2017, IIT Guwahati, Guwahati, India.

- ✓ Tanushree Paul, Kannan Pakshirajan and G. Pugazhenth. Treatment of refinery wastewater using oleaginous *Rhodococcus opacus* for potential bio-oil production. One day symposium on Recent Advancements in Environmental Research (**RAER-2017**), June 5, 2017, IIT Guwahati, Guwahati, India.

